3-21-2013

Experimental Characterization of the Structural Dynamics and Aero-Structural Sensitivity of a Hawkmoth Wing Toward the Development of Design Rules for Flapping Wing Micro Air Vehicles

Aaron G. Norris

Follow this and additional works at: https://scholar.afit.edu/etd

   Part of the Aerospace Engineering Commons

**EXPERIMENTAL CHARACTERIZATION OF THE STRUCTURAL DYNAMICS
AND AERO-STRUCTURAL SENSITIVITY OF A HAWKMOTH WING
TOWARD THE DEVELOPMENT OF DESIGN RULES FOR
FLAPPING-WING MICRO AIR VEHICLES**

DISSERTATION

Aaron G. Norris, Lieutenant Colonel, USAF

AFIT-ENY-DS-13-M-40

DEPARTMENT OF THE AIR FORCE
AIR UNIVERSITY

AIR FORCE INSTITUTE OF TECHNOLOGY

WRIGHT-PATTERSON AIR FORCE BASE, OHIO

AFIT-ENY-DS-13-M-40

EXPERIMENTAL CHARACTERIZATION OF THE STRUCTURAL DYNAMICS
AND AERO-STRUCTURAL SENSITIVITY OF A HAWKMOTH WING
TOWARD THE DEVELOPMENT OF DESIGN RULES FOR
FLAPPING-WING MICRO AIR VEHICLES

DISSERTATION

Presented to the Faculty

Graduate School of Engineering and Management

Air Force Institute of Technology

Air University

Air Education and Training Command

In Partial Fulfillment of the Requirements for the

Degree of Doctor of Philosophy

Aaron G. Norris, B.S.A.E., M.S.A.E.

Lieutenant Colonel, USAF

March 2013

APPROVED FOR PUBLIC RELEASE; DISTRIBUTION UNLIMITED

EXPERIMENTAL CHARACTERIZATION OF THE STRUCTURAL DYNAMICS AND AERO-STRUCTURAL SENSITIVITY OF A HAWKMOTH WING TOWARD THE DEVELOPMENT OF DESIGN RULES FOR FLAPPING-WING MICRO AIR VEHICLES

Aaron G. Norris, B.S.A.E., M.S.A.E.

Lieutenant Colonel, USAF

Approved:

_____
Dr. Anthony N. Palazotto (Chairman)

5 Mar 13
Date

_____
Dr. Richard G. Cobb (Member)

5 MAR 13
Date

_____
Dr. William P. Baker (Member)

5 Mar 2013
Date

Accepted:

_____
HEIDI R. RIES, Ph.D.
Interim Dean, Graduate School of
Engineering and Management

13 Mar 2013
Date

Abstract

A review of research trends in the area of micro air vehicles (MAV) reveals a strong affinity toward biologically inspired flapping-wing designs. A case is made for why the structures discipline must take on a more central role, especially if research trends continue toward insect-sized and flexible wing designs. In making the case, the eigenstructure of the wing emerges as a key structural metric for consideration. But with virtually no structural dynamic data available for actual insect wings, both engineered and computational wing models that have been inspired by biological analogs have no structural truth models to which they can be anchored. An experimental framework is therefore developed herein for performing system identification testing on the wings of insects. This framework is then utilized to characterize the structural dynamics of the forewing of a large sample of hawkmoth (*Manduca Sexta*) for future design and research consideration. Single wing samples of four other species of insect are also investigated and reveal uncanny structural dynamic resemblance to the hawkmoth and each other, raising the possibility for a universal design rule. The research also weighs-in on a decade-long debate as to the relative contributions that the inertial and fluid dynamic forces acting on a flapping insect wing have on its deformation (expression) during flight. The most often cited evidence suggests that fluid dynamic forces play such a minor role that they can be neglected, allowing for the aerodynamic analysis of the flexible flapping-wing to be aeroelastically decoupled. The research performed herein, employing a similar but higher fidelity experimental approach determines that fluid dynamic forces do have *significant* influence on wing expression, calling into question the previous work.

To my children - finish what you start

Acknowledgements

Table of Contents

List of Figures

List of Tables

EXPERIMENTAL CHARACTERIZATION OF THE STRUCTURAL DYNAMICS
AND AERO-STRUCTURAL SENSITIVITY OF A HAWKMOTH WING
TOWARD THE DEVELOPMENT OF DESIGN RULES FOR
FLAPPING-WING MICRO AIR VEHICLES

I. Overview

We have a habit in writing articles published in scientific journals to make the work as finished as possible, to cover all the tracks, to not worry about the blind alleys or to describe how you had the wrong idea first, and so on. So there isn't any place to publish, in a dignified manner, what you actually did…

Richard P. Feynman [38]

Anyone who has ever endeavored to conduct research can probably attest to Dr. Feynman's opening remarks delivered during his Nobel acceptance speech in December, 1965. The work described herein is no exception. To have documented every *blind alley, wrong idea* or *false start* would have easily filled a volume five times longer than what follows. Nonetheless, the lessons learned by these detours have proved immeasurably valuable in arriving at the final results and conclusions presented herein. Indeed, the process of discovery throughout this research was neither as linear nor sanitary as this final polished paper may convey.

Because the term is used rather loosely when referring to the smaller class of unmanned air vehicles (UAVs), this chapter begins by providing *the* definition of a micro air vehicle (MAV) as it was originally conceived and as it is viewed for purposes of this research. It also describes where the MAV fits, or rather will someday fit, within the

broader class of the unmanned aerial systems (UAS) across the Department of Defense (DOD). Since this research was made possible by Air Force resources, a brief exploration of the potential applications that MAV promises is presented and serves as a motivation for conducting this and other MAV-related research. And, right or wrong, since all research is ultimately critiqued, or at least its value measured through the prism of its relevancy to existing or emerging challenges within its sphere of application, a brief discussion of the current defense climate and how it affects MAV development is presented. Finally, the chapter concludes by providing the research objectives and a roadmap for how the rest of the document is organized.

1.1 The MAV Defined

Many have their own conception about what a MAV is, or what it is not, either based off their own experience or gained second hand. It would be tough convincing the Airmen, Seamen, Soldiers, or Marines who have been remotely piloting Wasps or Ravens (Figure 1) that their platforms are not MAVs. At one time their individual Service or Commands referenced these platforms as such and so did the principal contractors who build the systems.

The DOD now classifies UASs according to Table 1, with the Air Force classifying small unmanned aerial systems (S-UAS) as those comprising Group 1 through Group 3 [3]. By any reasonable definition or conception of them, MAVs are certainly members of the S-UAS family. Operators currently associate MAVs with platforms that are man-packable (lightweight, collapsible, and stowable) and able to be hand-launched and recovered without the need for a runway. Since trying to hurl an airframe weighing

Figure 1:   An RQ-11Raven (top) [27] and Wasp III (bottom) UAS being hand-launched in the field. Bottom image provided courtesy of Aerovironment Inc.

more than 20 pounds into the air is a stretch even for the most fit of operators, nobody would argue that MAVs are exclusively members of Group 1.   But the current *operational* airframes that occupy Group 1 are virtually all the size of hobby-class R/C aircraft with the smallest platforms having wingspans of around two feet. To be precise, the research herein is *not* focused on these sized aircraft. Instead it is focused on a UAV that will actually fit in the palm of the average adult hand (e.g. Figure 2). Specifically the research in this paper is directly inspired by the definition of a MAV proposed by the Defense Advanced Research Projects Agency (DARPA) over fifteen years ago:

The term, Micro Air Vehicle, may be somewhat misleading if interpreted too literally. We tend to think of flying model aircraft as "miniature", so the term "micro" now alludes to a class of significantly smaller vehicles. But MAVs are not small versions of larger aircraft. They are affordable, fully functional, militarily capable, small flight vehicles in a class of their own. The definition employed in DARPA's program limits these craft to a size less than 15 cm (about 6 inches) in length, width or height. This physical size puts this class of vehicle at least an order of magnitude smaller than any missionized UAV developed to date.

McMichael and Francis, 1997 [67]

Beyond the limitation that no dimension shall exceed approximately 6 inches, they further state that a MAV will weigh up to 50 grams and be able to carry up to 20 grams of payload, have approximate endurance and range of 60 minutes and 10 kilometers respectively at airspeeds between 10 and 20 meters per second (22-45 mph).

Table 1: DOD UAS classification based on weight, operating altitude, and airspeed. Note that Group1includes lighter than air vehicles hence the zero entry under weight. A MAV, by definition, falls into Group 1, but not all Group 1 UAS's are MAVs. [26]
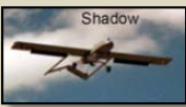
UAS Groups	Maximum Weight (lbs) (MGTOW)	Normal Operating Altitude (ft)	Speed (kts)	Representative UAS	
Group 1	0 – 20	<1200 AGL	100	Raven (RQ-11), WASP	Raven
Group 2	21 – 55	<3500 AGL	< 250	ScanEagle	ScanEagle
Group 3	< 1320	< FL 180		Shadow (RQ-7B), Tier II / STUAS	Shadow
Group 4	>1320		Any Airspeed	Fire Scout (MQ-8B, RQ-8B), Predator (MQ-1A/B), Sky Warrior ERMP (MQ-1C)	MQ-1/Predator
Group 5		> FL 180		Reaper (MQ-9A), Global Hawk (RQ-4), BAMS (RQ-4N)	RQ-4/Global Hawk

Figure 2: The "Hummingbird" developed by Aerovironment under contract with DARPA. Weighing-in at 19 grams with a 6.5 inch wingspan, even this prototype UAS is slightly larger than the DARPA definition for a MAV, though it embodies the essence of how MAVs were originally conceived. Image provided courtesy of Aerovironment Inc.

They also imbue the MAV with qualities that should allow it to perch, operate in windy conditions, and be able to traverse through urban canyons and even indoors through complex corridors and passageways (e.g. a maze of hallways in a building). And, in some cases, perform while maintaining a high degree of stealth, or "hiding in plain sight" as it has come to be known. According to this definition of a MAV, there are exactly zero operational MAVs in any of the Services' inventories to date. And, while there have been developmental MAVs that meet, or come close to meeting this definition (Figure 2), each has been technologically immature, requiring much more research and development across multiple disciplines in order to approach realization of DARPA's original vision.

In essence, McMichael and Francis' description of a MAV is a flying machine capable of the performance of *small birds* or *large flying insects* and in some cases even

mimicking their appearance. It is the latter of these, *large flying insects*, that this research concerns itself with; specifically the hawkmoth (*Manduca Sexta*).

1.2   MAVs Many Applications

The future uses of MAVs will undoubtedly have limitations due to the very nature of the size that makes them so exceptional for certain applications. For instance, juxtaposing the MAV against other airborne platforms suited for such missions as close air support, long range strike, or rapid global mobility seems paradoxical at best. Nonetheless, sooner or later the MAV will figure prominently alongside other military systems, both manned and unmanned, within future battlespaces. It will be their size primarily, coupled with their inherent maneuverability and unique ability to *hide in plain sight* that will ultimately determine their future roles in military as well as civil applications. The following passage does an exceptionally good job of painting an image for the promise of the MAV.

> *The small speck in the sky approaches in virtual silence, unnoticed by the large gathering of soldiers below. In flight, its tiny size and considerable agility evade all but happenstance recognition. After hovering for a few short seconds, it perches on a fifth floor window sill, observing the flow of men and machines on the streets below. Several kilometers away, the platoon leader watches the action on his wrist monitor. He sees his target and sends the signal. The tiny craft swoops down on the vehicle, alighting momentarily on the roof. It senses the trace of a suspected chemical agent and deploys a small tagging device, attaching it to the vehicle. Just seconds later it is back in the sky, vanishing down a narrow alley. Mission accomplished....*

> McMichael and Francis, 1997 [67]

The brief but illustrative passage above speaks volumes about the expected capability and military utility of the MAV. Similar virtues of the MAV are told by a host of other authors [72,74,88,93]. It will be small and agile, capable of moving through tight spaces while remaining virtually undetectable due to its ability to blend in with the natural surroundings (i.e. hiding in plain sight). Perhaps it will look like a small bird, butterfly, or dragonfly. No matter its form, it will eventually look and behave as a natural flier or will be too small and quiet to bring attention to itself. Its capability of hovering will allow it to persist over its target long enough to collect data with its sensing payload. Hovering will allow the MAV to transition to a perch whereby it is able to save energy or even recharge itself via the sun, surrounding power lines, or absorption of thermal and vibrational energy. Perching will also allow it to lie-in-wait until it is remotely commanded or its onboard sensing algorithm commands it to spring into action. After it has performed its mission, it will return to its base, possibly the shoulder pack of a foot soldier, or the cargo hold of a larger, loitering UAV, once again undetected by the enemy.

The descriptions above align well with the urban warfare environment for which the MAV is ideally suited. But, the MAV is suited for other environments as well, including desert, jungle, maritime, mountain and arctic [74]. The MAV is also perfectly suited for the concept of swarming [13] where hundreds, if not thousands, of these small, autonomous vehicles working in unison could overwhelm enemy radar, communication or power systems by flying to and landing on specified locations of the system, thereby disrupting transmission or even shorting circuitry. MAVs could also be used to infiltrate tunnels, hard and deeply buried targets (HDBT), or other enemy infrastructures that are otherwise inaccessible to the DOD's most capable arsenal of penetrating weapons. They

would gain access through "soft spots" such as ventilation shafts or small but temporary breaches (e.g. opened doors) and defeat the target from within by detonating incendiary payloads. One author even talks about administering what amounts to immunizations on the battlefield or even delivery of microscopic weapons through needle-wielding MAVs [47]. Another author envisions MAVs being able to neutralize enemy jet aircraft by extinguishing their engines before ever taking off as hundreds of them fly into and clog engine inlets [54]. And the list of other uses could go on ad nauseam.

From a military point-of-view, while there are obvious limitations to their uses, the options that the MAV presents seem literally endless. And, the role of the MAV is not exclusive to military applications, as others have identified civilian applications as well, including roles for police and fire departments, news and entertainment production, environmental, meteorological and more [88,89]. In short, there are many valuable applications of the MAV that make any research in the area a worthwhile investment.

1.3   Has the MAV Ship Sailed?

For all intents and purposes, this research was conducted between mid-2008 and the end of 2009. During this period, and for several years prior, the notion of the MAV was very much popular across the DOD's research enterprise, including the Air Force Research Laboratory (AFRL), Army Research Laboratory (ARL), Naval Research Laboratory (NRL), Air Force Office of Scientific Research (AFOSR), Office of Naval Research (ONR), and DARPA to name the most prominent organizations with active MAV research and development investments. There was not a question of *if* MAV research and development would continue, but *when* MAVs would be ready for

operational use. In fact, in 2005 the Air Force drew a line in the sand announcing that

bird-sized operational MAVs would be in the inventory by 2015 followed by insect-sized

in 2030 [63]. While certainly a lofty goal, there were at least three reasons that many

were optimistic that the goal would be reached.

First, their larger UAV ancestors like Global Hawks and Predators, as well as

their small, but still larger predecessors like the Raven and the Wasp (Figure 1) had

already enjoyed, and were continuing to enjoy widespread use and praise among the

operational warfighting communities.   Since the start of the Global War on

Terror (GWOT) in 2001, the almost insatiable and exponential desire for intelligence,

surveillance, and reconnaissance (ISR) to aid in man-hunting and improvised explosive

device (IED) detection missions kept UAS and S-UAS platforms in a constant state of

demand among theater commanders (Figure 3). There were certainly grounds to think
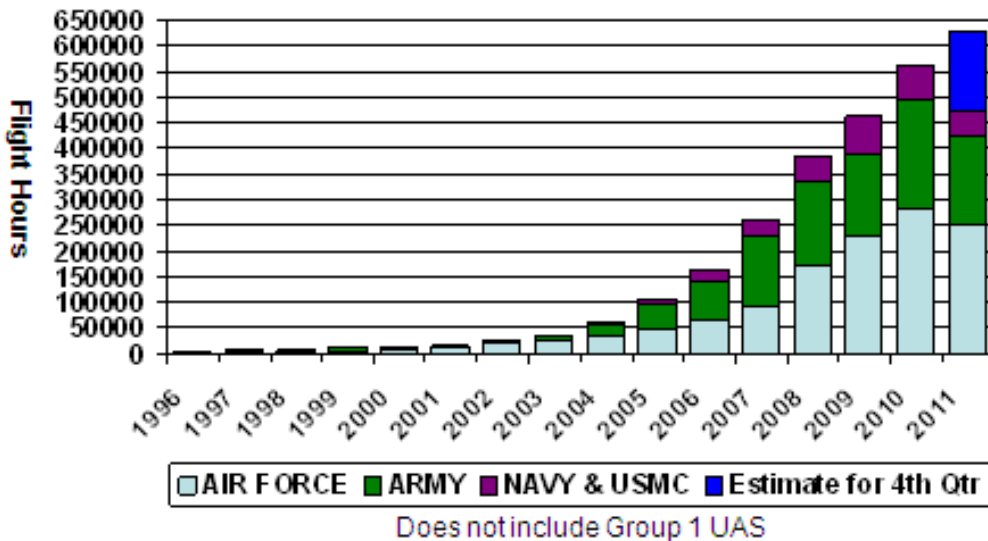
Figure 3   The number of UAS hours flown by the DOD from 1996-2011[28] The Air
Force accounted for nearly half of all flight hours of all Services combined. Note the
exponential increase since 2001, underscoring the demand for the UAS during the
GWOT.

US National Defense Spending

Source: Department of Defense (DoD) Greenbook, CSBA using DoD data
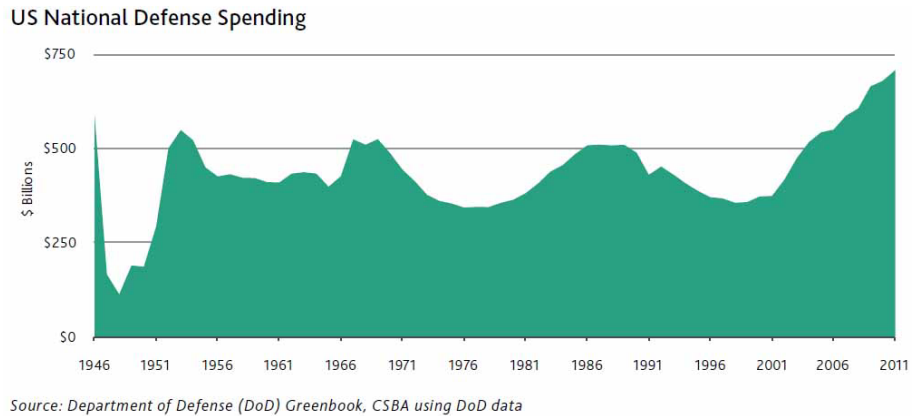
Figure 4:   Department of Defense spending from 1946-2011[25]. Note the significant increase in spending starting in 2001, marking the beginning of the US involvement in the longest war period in its history.

that an operational MAV would be ushered along atop the shoulders of its successful predecessors.

Second, despite America's ailing economic environment at the time, the DOD was one of the few departments of government "enjoying" significant increases in its budget. In fact, defense spending nearly doubled between 2001 and 2011 (Figure 4). Granted, the nation was fighting two wars abroad in Afghanistan and Iraq and had been for most of the decade, but the years were decidedly marked by massive budgets and the research and development community (Air Force and DOD) was aptly resourced with the research, development, test and evaluation (RDT&E) budgets nearly doubling from 2001-2010 (Figure 5). In fact, a steady stream of MAV-related research was published, and a host of S-UAS systems acquired since 2001, with no sign of slowing down by 2009.

Third, Osama bin Laden (OBL), the proclaimed leader of the global terrorist network Al Qaeda and mastermind behind the September 11, 2001 attacks on the Pentagon and New York's World Trade Center was still at-large. Given that two

10
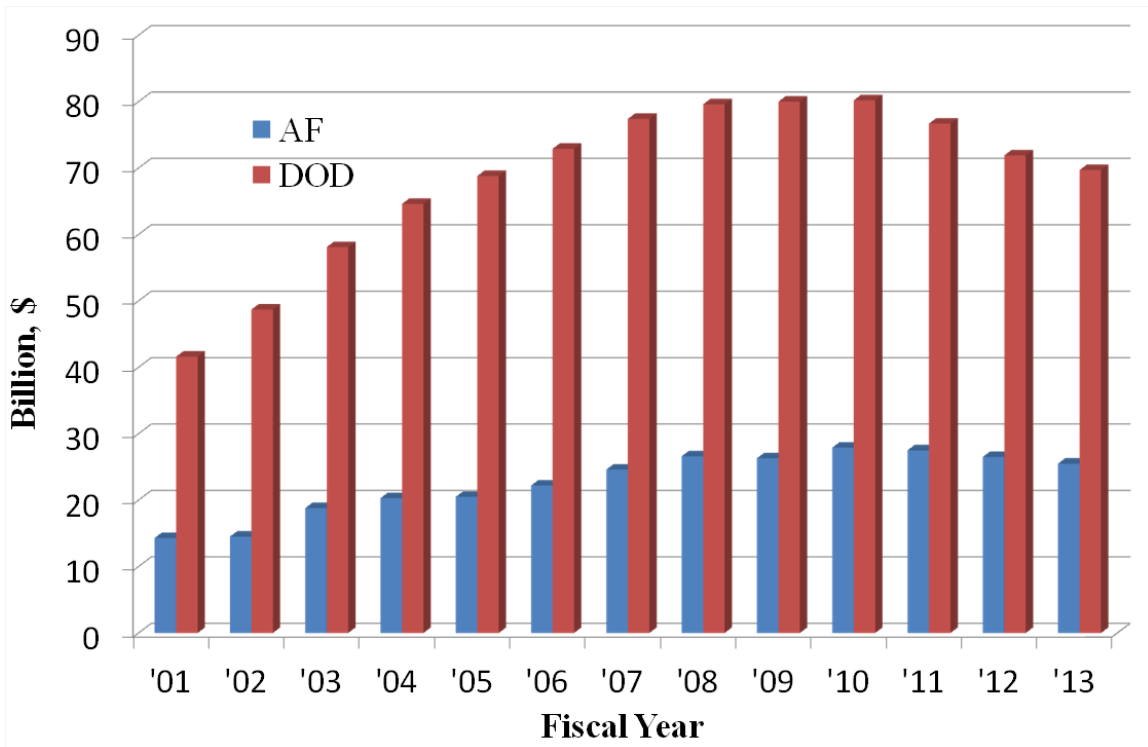
Figure 5:   The RDT&E budget from 2001-2013. The DOD and the Air Force saw the research, development, test and evaluation (RDT&E) budget nearly double between 2001 and 2010. Derived from data taken from the DoD *Greenbook* [25].

consecutive presidential administrations and supportive congresses had declared that no cost would be spared in order to bring this criminal to justice, it was a safe bet that resources would continue to flow to the DOD until OBL was either caught or killed. The longer the manhunt went on, and the more intelligence that suggested he was hiding in a cave in Afghanistan, Pakistan, or somewhere on the border between, the more likely it seemed that a less conventional technique or platform for collecting ISR would be needed to ferret him out. Of course, that line of reasoning boded well for MAV technology development, since the notion of the MAV is anything but conventional.

Fast forward to December, 2012 at the time this paper is being written. After successful operations spanning more than 8.5 years, American troops withdrew from Iraq

in December, 2011. Osama bin Laden was killed by American forces in Pakistan in May, 2011 ending the longest and most extensive and expensive manhunt in American history. The President has announced the end of operations in Afghanistan by the end of 2014 with a transition starting in mid-2013. America's economy, and to a larger extent the global economy, is still reeling from the financial meltdown of late 2008. The news wires are dominated by talks of mandatory budget cuts, or "sequestration" as it is known. Furloughs and personnel cuts, hiring freezes, and possible government shutdowns are being seriously discussed as budget cuts loom. From a fiscal perspective the outlook for the DOD budget for the foreseeable future is grim even through the lens of an optimist.

Budget woes aside, as much or more of a concern for the future of MAV development are the shifting defense priorities due to the developing worldwide threat environment   A shift is well underway from the more asymmetric, unconventional warfare that has dominated the last decade towards more conventional engagements with near-peer adversaries and other state actors. Some of the Air Force's top priorities include: arming its 5th and 6th generation of fighters and bombers with more capable munitions; developing long range, high speed strike platforms capable of delivering strategic blows to the enemy within hours, virtually anywhere on the globe; and developing survivable penetrating munitions capable of defeating emerging HDBT threats. And all of these priorities must be addressed within environments of heavily contested airspace where GPS and communications links will be either degraded or denied, demanding hefty research and development investments all its own. Granted, there exist some novel concepts for MAVs that could and have been considered in the

trade space of solutions for meeting some of these challenges. But for the most part they are not being seriously considered for these applications or others.

At this point in time the 2015 and 2030 "lines in the sand" referenced earlier have virtually faded from memory. The AFRL technical team (incidentally once led by the author) charged with leading, inventing, maturing and integrating the technologies for achieving the Air Force's stated goals of bird and insect-sized operational MAVs has disbanded, largely as a direct result of cuts in and redirection of research funds toward technologies aimed at more conventional uses and with much more near-term payoffs for the warfighter. Many researchers within the Air Force are convinced that the MAV has become a "four letter word" among senior leaders who are (appropriately so) addressing the emerging and higher priorities of the warfighting community.

Admittedly, the above narrative may seem peculiar given that it runs counter to motivating MAV-related research at-hand. But in the current climate, to promote the virtues and relevancy of MAVs and any associated research without providing some caveat based on the current state of things would seem disingenuous and like trying to put the proverbial "lipstick on a pig". With that said, the notion of the MAV is out of the bag. Or, as Peter Singer, Brookings Institute scholar and author of *Wired for War* [93] aptly noted, "…they [drones] are here to stay, and the boom has barely begun. We are at the Wright Brothers Flier stage of this [9]." So the answer to the question posed by the title of this section is decidedly "no", the MAV ship has not sailed, but its impending departure has been delayed.

1.4 Document Organization and Research Objectives

<u>Research Objective 1</u>

By using existing system identification tools and techniques, develop an experimental framework that can be used to determine the underlying structural dynamic features of insect wings and then characterize for future study those features for the forewing of a hawkmoth.

<u>Research Objective 2</u>

Determine if fluid dynamic forces significantly influence the expression of a flexible flapping insect wing by comparing the expressions between a hawkmoth's forewing undergoing pure inertial excitation (flapping in vacuum) and coupled inertial-aero excitation (flapping in air).

In the spirit of providing the "bottom line up front" the research objectives are posed above without development. Chapter II provides the full context for how these objectives were ultimately settled upon through an exhaustive survey and review of existing literature. Chapter III focuses on the first research objective by first reviewing, in detail, previous related research and then describing the experimental framework developed for extracting the structural system identification parameters of insect wings. It then provides the results and discussion for both primary and secondary research findings. Chapter IV follows and is organized in the same fashion as Chapter III but is focused on the second research objective. Finally, Chapter V provides the conclusions of the research and summarizes the major contributions offered to the flapping-wing MAV research community.

II.   Survey and Objectives

Research is to see what everybody else has seen, and to think what nobody else has thought.

Albert Szent-Gyorgyi

Realization of the full potential that MAVs have to offer can point research vectors down any number of directions within and across the many diverse disciplines of mathematics, science, and engineering. With so many options available, both within and across disciplines, it can be a daunting undertaking just to narrow the field to a few that are both relevant and of benefit to the broader research community. The winding path to settling on research objectives is an important part of the research in its own right. So, the purpose of this chapter is to provide a context for how the research objectives were settled on. In doing so, this chapter presents a natural segue to the heart of the research that follows in the remainder of the document.

2.1   AFIT's MAV History

Prior to approximately 2007, MAV-related aerodynamics research at the Air Force Institute of Technology (AFIT), specifically in the Department of Aeronautics and Astronautics, was exclusively focused on the class of small UAVs consistent with Group 1 of the DOD UAS classification system (Table 1). Virtually all of the research at

AFIT up to that timeframe was geared toward small, flexible, fixed-wing platforms [21,22,40,51,69,81,82,96,103,108] like those shown in Figure 6. Incidentally, AFIT is adherence to a definition of "MAV" that was inconsistent with DARPA's was not intentional, but more an artifact of remaining consistent with the terminology used by their research sponsoring organizations.

In the 2007-2008 academic year, just before the present research began to take shape, three students and their advisors began to shift their research focus toward platforms more aligned with those meeting the DARPA definition for a MAV [17,66,99]. Not entirely coincidental, it was also during this timeframe that the Air Force had "drawn the line in the sand", as previously mentioned (section 1.3), for developing bird-sized and insect-sized MAVs by 2015 and 2030 respectively. The AFRL had begun to make significant investments in both in-house MAV test infrastructure [59] and allocation of

Figure 6:   Typical subjects of "MAV" studies at AFIT prior to 2007 [21].

basic research funds to MAV technology development and was actively engaging AFIT to perform related research. The present research was motivated by this effective *call to action*, but since this was a brand new research vector for AFIT, there was no obvious "next link" in a research chain from which to reference as a point for departure. Therefore, a more extensive review of the research outside the walls of the Institute was undertaken to guide the direction that this research would ultimately take.

2.2   MAV Research – Trends, Controversies, and Gaps

Penn State suggests that a literature review should review the available and relevant literature for active areas of study in order to determine research areas and *trends* while specifically looking for those areas where "*issues, gaps in knowledge, or controversies*" have been cited by researchers in the field [80]. To that end a large sample (nearly 700 articles) of MAV-related research was retrieved from across more than twenty individual archival journals, conference proceedings, books, and periodicals, each being reviewed at least at a cursory level, with a smaller subset reviewed in greater depth. From that review, three trends, one controversy, and one knowledge gap emerged.

2.2.1   Trend 1: Flapping is the Answer

First, a trend toward flapping-winged MAV's was almost immediately clear. To gain some semblance of an objective measure of this trend, a simple survey using the American Institute of Aeronautics and Astronautics (AIAA) online papers database [2] was performed with details and results shown in Figure 7. While it is true that MAV related research is not exclusively published by the AIAA (not even close) it is a fair

assessment that the AIAA publications database presents a representative sample of the research trends in the broader aerospace community as a whole and at any given time throughout its history.

The results of this survey, not surprisingly, showed that MAV-related research was not apparent before the 1993-1997 timeframe. While McMichael and Francis are largely credited with first coining the term "MAV" and with its first working definition in 1997, the notion of the MAV emerged at least five to ten years earlier [55,39,16]. But wherever the starting line is drawn for MAVs, what's clear is that it was not until after 1997 that MAV-related research exploded within the aerospace community and with it an accompanying interest in flapping-wing flight. Figure 7 also underscores a dearth of any relevant flapping-wing research throughout the aeronautical community up until the period when MAVs emerged. To be exact, in the 30 year period from 1963 to 1992, only 10 papers were published by the AIAA that related to "flapping" in any way [11,41,42,43,44,45,52,57,71,109]. However, these papers dealt primarily with rotary wing dynamics and in particular with stability considerations due to unsteady wake effects and atmospheric turbulence. None of them dealt with the complexities of flapping-wing flight as related to Nature's fliers or of bioinspired design.

Prior to the emergence of the MAV, flapping-wing flight research was exclusively the domain of biologists like Weis-Fogh, Dudley, Ellington, and Azuma to name only a few of the most prominent researchers in the early days of the *biology-of-flight* community. And the details of their research were primarily published within biological circles. Virtually no attention was being paid to flapping-wing flight within the aeronautical community until MAVs emerged. While the results of this simplified survey

Number of Papers Published by AIAA

Flapping
MAV
Flapping & MAV

140
120
100
80
60
40
20
0

1963-1967 1966-1972 1973-1977 1978-1982 1983-1987 1988-1992 1993-1997 1998-2002 2003-2007 2008 (1Q)
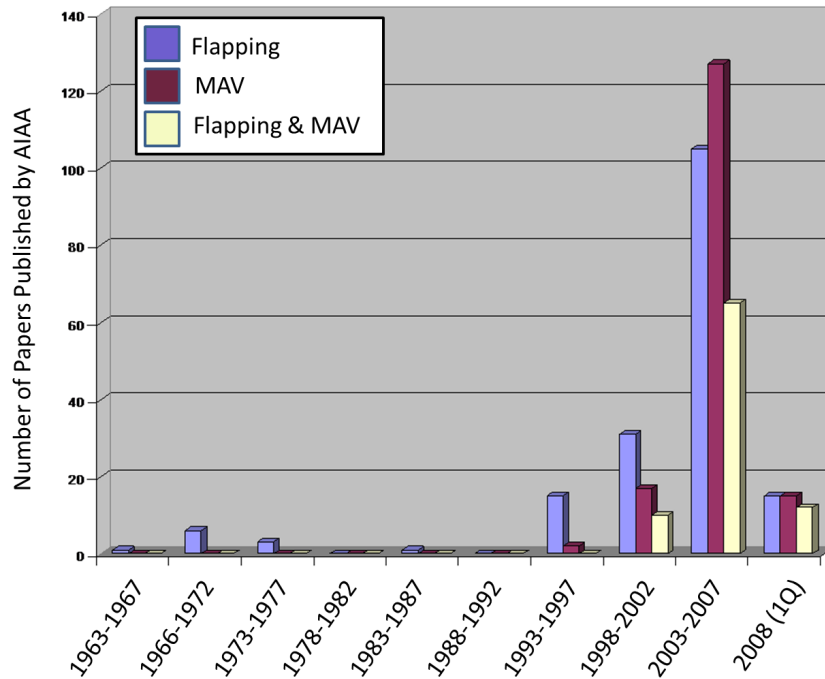
Figure 7:   Results of a February 2008 survey of literature from the AIAA online data base clearly show a dramatic increase not just in MAV-related research but in flapping-wing research after MAVs started to gain traction in the early 1990's. The database query returned the number of articles containing "Flapping", "MAV", and "Flapping and MAV" in their titles or abstracts. Both "MAV" and "Micros Air Vehicle" were queried.

do not include trends prior to 1963 (before the AIAA was founded), it is likely safe to say that little or no interest was paid to flapping-wing flight within the aeronautical community prior to that time either. The community was engaged in the larger ventures of jet and rocket powered flight, supersonics, and commercial airline development to name just a few.

2.2.1.1 *Why Flap?* It is neither immediately obvious nor intuitive as to why the aeronautics community quickly migrated toward flapping-wings as the

19

preferred design choice for future MAVs versus fixed or rotary designs. But, Michelson

and Reece [72] do a commendable job of summing up why a MAV should flap:

> *Fixed wing solutions are immediately discounted because they require either high forward speed, large wings, or a method for creating circulation over the wings in the absence of fuselage translation. High speed is not conducive to indoor operations because it results in reduced reaction time, especially when autonomously navigating through unbriefed corridors or amid obstacles. When indoors, slower is better. If, on the other hand, the wings are enlarged to decrease wing loading to accommodate slower flight, the vehicle soon loses its distinction as a "micro" air vehicle. A significant advantage of a flapping-wing over a rotor is the rigidity of the wider chord wing relative to the high aspect ratio of a narrow rotor blade, and the fact that it can be fixed relative to the fuselage (e.g., nonflapping glide) to reclaim potential energy more efficiently than an autorotating rotor. There is also a stealth advantage of a flapping implementation over a comparably sized rotor design in that the acoustic signature will be less because the average audible energy imparted to the surrounding air by the beating wing is much less than that of a rotor. The amplitude of vortices shed from the tips of the beating wing grows, and then diminishes to zero as the wing goes through its cyclical beat, whereas the rotor tip vortices (which are the primary high frequency sound generator) are constant and of higher local energy. The sound spectrum of a flapping-wing will be distributed over a wider frequency band with less energy occurring at any particular frequency, thereby making it less noticeable to the human ear. All the energy of the rotor spectrum will be concentrated in a narrow band that is proportional to the constant rotor tip velocity. As the diameter of a rotor system decreases with the size of the air vehicle design, it will become less efficient since the velocity at the tips will decrease while the useless center portion becomes a larger percentage of the entire rotor disk.*

Notwithstanding the possible benefits that leveraging Nature's already successful and

flightworthy designs could have (which will be touched on later), it seems that arguments

of efficiency, the benefit of slow speed flight, and maintaining stealth from both a visual

and audible point of view have compelled the community toward flapping-wing designs.

2.2.2   Trend 2: Fluids-Dominated Research

To be sure, there are a host of disciplines and research areas that must be involved in the development of fully operational MAVs. They include but are not limited to research in fluid dynamics, structures and structural dynamics, landing systems, navigation systems, power systems, communication systems, operator-in-the-loop architectures, flight controls, autonomous control and collision avoidance, and of course the systems integration of all disciplines into a single MAV package. But many, if not all of these discipline areas are not exclusive to MAV development. For instance, to use just one example, decreasing the size and weight and increasing the power density of batteries or solar cells (critical and enabling technologies for MAVs) is certainly an area that many other technology development programs throughout the DOD and many civilian sectors are constantly researching and will greatly benefit from. However, in using the AIAA publications database to conduct this survey, there is no evidence of any research being done in this area for MAVs. This is not evidence that power systems research isn't underway; it most certainly is. Articles relating to power systems, however, are more likely (and more appropriately) to be published/presented in journals/conferences where the readership/membership is more aligned with that discipline. For this reason, the AIAA survey of literature that revealed approximately 400 MAV related papers in the past decade is a *gross* underestimate of the larger scope of MAV research. It is, by design, more heavily weighted toward the classical disciplines of aeronautics (fluids, structures, and guidance, navigation and controls) due to its source and even then it is only a statistical subset of the overall volume of research in those disciplines. With this

in mind, it is still revealing to consider the relative concentration of research of this survey.

An estimate for the relative volume of research in the classical disciplines of aeronautics was determined by randomly selecting 100 papers from the population of approximately 400 papers that constitute the data of Figure 7. Papers were separated by thrust into 3 bins; fluids, structures, and guidance, navigation and controls (GN&C). The results are visually presented in Figure 8 and show that fluids is by far the most researched area (70%), followed by GN&C (20%) and finally structures (10%). The structures discipline is likely even inflated as many of the papers written on structures deal with fluid-structure interaction (FSI) and could have been easily, if not more appropriately, placed in the fluids bin.
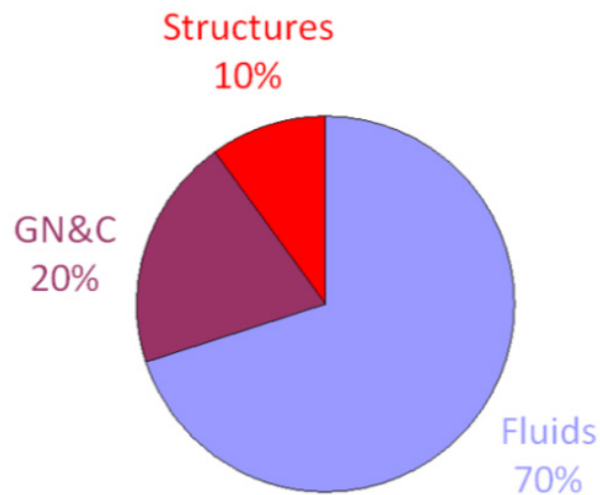
Figure 8: Relative percentage of MAV research across the classical disciplines of aeronautics from 1993 through February 2008. Data derived from the AIAA publications database [2].

2.2.3   Trend 3: Biomimicked Wing Design

A third and final trend observed was the affinity by most researchers toward bioinspired wing designs, whether their research is computational or experimental in nature. In the case of computational studies, it is quite common for researchers to borrow designs or features from Nature (often inspired by the Hummingbird, dragonfly or hawkmoth) replicating anything from just wing planform, to the full network of the wing battens (veins or bones), to just about anything in between. The degree to which the structure is modeled (e.g. simplifying assumptions) varies widely as well.

Recent advancements in rapid prototyping, laser etching and micro machining, has allowed for the engineering of small biologically inspired wings with, in some cases, uncanny resemblance (at least in form) to their biological analogs. These bioinspired engineered wing specimens are being studied in earnest by hundreds of researchers worldwide. Since 2008, the fidelity of wings being produced has increased by an order of magnitude. This review of literature revealed that Harvard's Microrobotics Laboratory is arguably the world's leading pioneer in this area and the wing prototypes that they produce is nothing short of remarkable [90,95,100]. AFIT has recently leveraged Harvard's expertise and within the last year has developed a similar wing prototyping capability [4,5,20,78,79]. Figure 9 and Figure 10 show examples of engineered wings from both institutions.
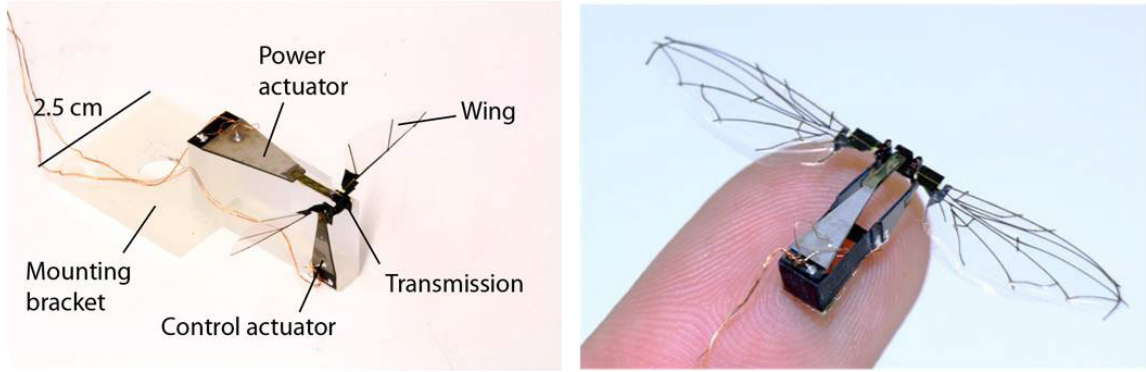
Figure 9: Example of a biomimetic insect wing and flapper [79]. Hardware and original image credited to Harvard's Microrobotics Laboratory.
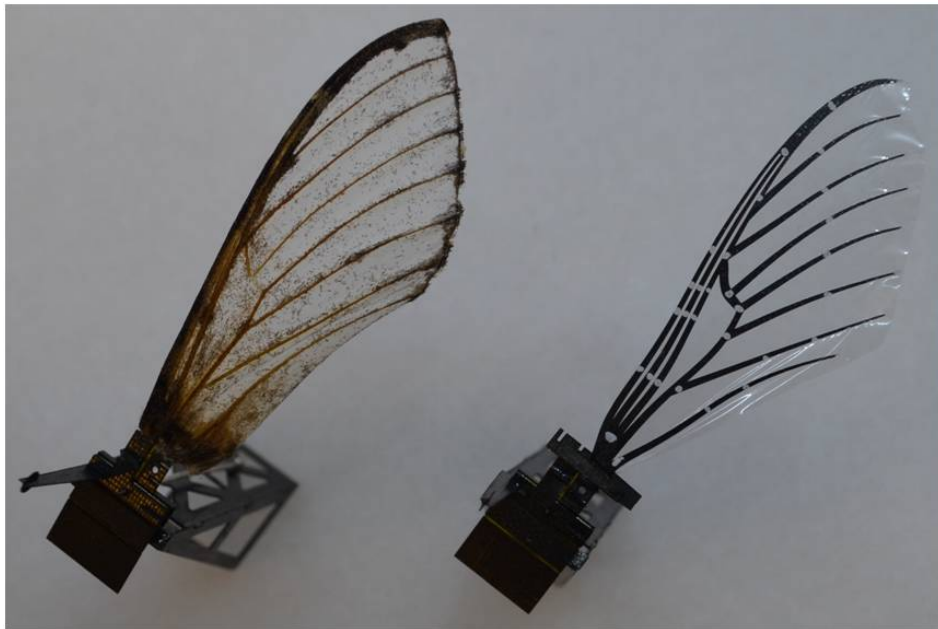
Figure 10: Image of an actual hawkmoth wing with its scales removed (left) compared to its engineered counterpart (right) [79].

2.2.4   Knowledge Gap: Beneficial Flexibility

Several questions that have been posed by biologists who have been studying insect flight for many years relates to the large scale, in-flight deformations seen in the wings of larger species of flying insects [8,18].   Are these deformations, and more specifically the underlying flexibility that permits them, beneficial to flight?   Might flexibility even be necessary for flight of these larger species? Despite several studies in this area the answer to these questions are generally unknown. Even more confounding, is that many of these studies, both experimental and computational, have presented evidence that contradict one another. So, despite all of the research to date, the jury is still largely out on the benefits (or detriments) that wing flexibility implies to the flight of insects.

2.2.5   Controversy: The Aeroelastic Debate

The flow around and the forces imparted on a thin, flexible structure (like an insect wing) subjected to an oscillating angle of attack and freestream velocity is determined by highly coupled fluid-structure interaction. This statement, or ones like it, although not taken word-for-word from any particular source, is not uncommon within the aerodynamics literature related to flapping-wing flight. Because fifty or more sources could easily be cited that would make similar claims, there is no need to single out or prescribe it to one specifically. In fact, most aeronautical engineers will likely accept this claim without argument or debate. In the words of many engineering professors, "it is obvious." But is it accurate? And, is it a claim or is it a fact?

One particular study that is cited frequently in flapping-wing research, perhaps more than any other single source, suggests that the statement above is *false*. And not just for the insect wing that served as the specimen for their study, but apparently for all passively deforming flexible structures articulated in air. Combes and Daniel (C&D) concluded from their carefully crafted experiment that the fluid dynamic forces acting on an insect's flapping-wing (or any lightweight flexible structure for that matter) provide negligible contribution to the instantaneous deformed state of the wing (sometimes called instantaneous wing shape, expression[1], or posture) throughout its wing beat cycle [14]. In fact, many flapping-wing aerodynamics researchers predicate their own findings and conclusions on C&D's findings that a flexible, flapping-wing's expression during flight is determined solely by the wing's inertial-elastic properties; aeroelastic effects being "relatively unimportant" according to their study. By accepting C&D's conclusion, researchers can effectively disregard the affect that the surrounding air has on deforming the wing, reducing the problem of solving for the flowfield around and hence the aerodynamic forces on, a flexible flapping-wing to an uncoupled, *non-aeroelastic* analysis.

Whether or not some researchers truly buy-in to C&D's conclusion, or instead invoke it for expedience sake is not clear. While many researchers have and still invoke their findings, many others do not. Others seem either unaware of C&D's findings (unlikely) or pay no mind to them asserting, as fact, their intuition that the flow around a

---

[1] Expression will be used hereafter to mean the instantaneous deformed state of the wing during flapping-wing flight.

flexible flapping-wing is aeroelastic in nature. Still, others will acknowledge the "debate" and either proceed to invoke C&D in their own analysis or, in some cases not. What is clear is that C&D were the only researchers at the time that the current research was being formulated (2008) that had any experimental evidence to make a case either way. And their evidence was, and still is, counter to the intuition of most aerodynamicists.

2.3 Survey Analysis – Narrowing the Scope

This section offers an analysis of each trend, knowledge gap, and controversy discussed above and naturally leads to stating the primary objectives of this research. Each section below provides an analysis of the respective section from above. In other words, section 2.3.1 analyzes the findings discussed in section 2.2.1, section 2.3.2 analyzes the findings of section 2.2.2, and so on and so forth.

2.3.1 Flapping Makes Sense

As enumerated by Michelson and Reece above (section 2.2.1.1) there are compelling physical arguments to reject more conventional designs. But perhaps as compelling of a reason to consider flapping-wing designs for MAVs is the unlikelihood of mankind conceiving a design capable of rivaling the elegance, and maybe even the efficiency, of the flapping-wing solution that Nature has already designed for flight at small scale. Nature has essentially "given the answer at the back of the book" so it seems reasonable to leverage the hundreds of millions of years of design trades already performed in the laboratory of Nature. That said, as discussed more thoroughly later, due

caution is warranted as mimicry of Nature certainly carries with it some limitations and pitfalls.

2.3.2   So Many Fluids, So Few Structures

Given that the current conventional wisdom is leaning toward flapping-wing designs, the relative lack of research in the structures discipline provides some reason for pause. The "division of labor" among the classical disciplines of aeronautics cited by the survey above is arguably historically consistent with the development of conventional air vehicles. But flapping-wing vehicles will be anything but conventional and could very well demand an approach favoring a more centered role for the structures discipline area. To understand why, consider the following discussion.

Most who have viewed an airplane's wing in flight from the safety of a fuselage or cockpit window can attest to its flexibility as the wings bounce, usually gently, up and down during flight. But this bouncing or "flapping" motion compared with Nature's flapping-wing is quite different. From the aerodynamicist's perspective, a fixed-wing aircraft's wing is generally classified as a rigid structure. Wing flapping is not required for flight and is generally undesirable. Of course, small flapping-like excursions from an otherwise rigid wing are expected, due to the inherent finite nature of material properties and are ultimately considered by the aircraft designer from a structural (static and dynamic), aerodynamic, and controls point of view. From the structural engineer's perspective, the challenge of fixed-wing aircraft wing design as it relates to aerodynamics (there are a host of other challenges) can simply be summarized as designing a wing structure that is stiff enough to preserve the designer's intended aerodynamic moldline.

That is to say, the underlying structure of the wing is not responsible for *determining* the geometry of the wing; that's the designer's job. Rather, the wing's structure is responsible for *preserving* the geometry of the wing during flight. The conventional wing design process is fairly straightforward and linear. Namely, the designer determines the wing's moldline based on performance requirements and the structural engineer, in-turn, designs a structure capable of preserving this moldline during flight. This process stands in sharp contrast with how flexible flapping-wings will have to be designed for achieving specific aerodynamic performance goals.

Unlike the wings of conventional fixed-wing aircraft, the flapping motion of an animal's wings during flight is vital. Not only is wing flapping responsible for creating the lift required to support the weight of the animal, but also for producing propulsive and control/maneuver forces. Since insect wings are widely accepted as being passively deforming structures during flight [29], then no matter where the chips fall on the "Aeroelastic Debate", its structure (its inertial-elastic properties) is indelibly entangled with its expression, which along with flapping kinematics determines its aerodynamic performance. If C&D have it wrong, then there is another layer of coupling in that the aerodynamics (loads) also influence the wing's expression in conjunction with the its inertial-elastic properties. Either way, the challenge for the structural engineer is to design a wing whose structure deforms in a manner that achieves wing expressions (throughout the flapping cycle) that the designer determines as necessary to achieve aerodynamic performance. One method of doing so would be to include an array of sensors and actuators that actively work to control wing expression. This method presents hurdles of feasibility and complexity at these small scales as well as weight

penalties that translate to performance penalties. The other method is to borrow from Nature's example by developing a wing structure that appears to have "encoded" just the right structural properties (distributions of mass and stiffness) so that the wing will express under load (inertial and possibly fluid dynamic) in such a way throughout its wingbeat cycle that the intended aerodynamic performance is achieved. This is an incredibly challenging problem and requires design methods and tools that are far beyond the conventional design process of the fixed-wing aircraft. Nonetheless it appears to be the way the community is headed, and therefore *structures must take on a more central, if not <u>the</u> central role in the space of flapping-wing design*.

2.3.3   The "Intent" of Bioinspired Design

Practically since the dawn of recorded history, Nature has inspired mankind's quest for flight. From legends of Greek mythology (Figure 11) and drawings by Da Vinci, to the gliders of Chanute and Lilienthal, to the dozens of aviation pioneers like the Wright Brothers who risked life, limb, and treasure to be the first to conquer powered flight. Just as early attempts of human flight looked to animals for inspiration, apparently so are the early attempts of developing flying machines at hummingbird and insect scales.

But students of human flight history are keenly aware that its path is littered with cautionary tales of failed attempts that sought no more than to mimic the mechanics and form of animal flight in order to leap skyward. A quick internet search (keyphrase: "early flight movies") will reveal vintage film footage of a handful of these early attempts. While arguably humorous to watch, many early attempts at human flight were made by pioneers that learned the difficult and often tragic lessons of trying to blindly

Figure 11: A statue of Icarus in front of AFIT that reminds onlookers of both the childlike curiosity that Icarus had for flight as well as Daedalus' use of Nature's design to "slip the surly bonds of earth".

mimic Nature's fliers. As is often the case with having the luxury of hindsight, not to mention the benefit of centuries of scientific discovery and achievement, it is easy to look back and see the fallacy of these early attempts. Luckily, the stakes for the MAV pioneers are not as high as those of early manned flight pioneers.

Most will concede that in all research and design endeavors, aerospace or otherwise, when existing or previous designs, whether engineered, natural, or biological, are considered as a basis of inheritance or inspiration, the intent of any feature of the original should be known and thoroughly understood. Admittedly, this statement seems obvious and yet the history (and to some degree the present) of flight is littered with examples that run counter to this apparent truth. While undoubtedly there is much that can and arguably should be learned and leveraged from the hundreds of millions of years

of design trade studies in the laboratory of Nature, due caution is warranted. In considering Nature's designs, determining *intent* is not as simple as consulting the original designer, engineering drawings, or design pedigree. In fact, in most, or arguably all cases of animal morphology, *intent* is not known or is at best a reasoned hypothesis with "proof" subject to an incomplete fossil record. To complicate matters further, Nature often confounds its designs by shrouding *intent* in apparent complexity.

As any undergraduate biology textbook will attest, animal morphology is a product of *competing* demands for *survival of the species*. According to Darwin's generally accepted theory, an animal's form is the result of a *natural* process that *selects* for individual traits - whether behavioral or physical - among a field of other traits that *collectively* tend toward enhancement of the overall *fitness of the species*. His theory does not guarantee optimization of any single trait toward a specific function. To the contrary, Darwin's theory would more likely argue against optimization of any single trait when viewed among a sea of competing fitness demands. So, while many engineers and researchers may intuitively argue the flight efficiency of Nature's fliers and therefore take comfort in their bioinspired or biomimicked designs, biologists will counter that the natural flier is not necessarily, and more unlikely to be, an efficient design from the point of view of flight alone. In fact, the design could be quite far from optimal.

2.3.3.1 The Fine Print As one simple but appropriate example, consider the wing of a moth. It is certainly hard to argue against the *intent* of the wing as an appendage for locomotion. But to blindly mimic any or every feature of the moth's wing carries the potential of inheriting artifacts that may adversely, or at least non-

optimally, affect flight. The competing demands of thermal regulation, ornamentation for attracting mates, or camouflaging from predators, to name only a few other wing functions [29], may sub optimize the wing's design away from the exclusive function of flight. Admittedly, because of the enormous energy demands of flight, the morphology of any animal must be quite tuned for its given set of competing traits [76]. That is to say, that a given animal is probably as good a flier as it can be given the constraints placed on its collective morphology by other competing fitness demands. But this does *not* imply an efficient design for flight - just an efficient design for overall fitness.

So, if bioinspired flapping-wing design was to have a "fine print" disclaimer, and maybe it should, it would read something like "Designers Beware: Potential hidden traits may sub optimize flight performance." With that said, the current trend of mimicking biological wings is a little troubling, although admittedly it is likely the right starting point. But with so many options to pick from in Nature where does one start? Why, for instance, would a researcher or designer choose one wing planform or venation pattern over another? Are planform and/or venation somehow optimally matched to the flapping kinematics that a given insect imparts to its wings? What are the structural differences between the wings of hovering and non-hovering insects? What are the structural differences between wing designs of insects known to fly long distances (measured in miles) versus those that are short distance fliers (measured in yards)? How about structural differences between the wings of "fast" versus "slow" flying insects? If there are differences in the structural features of these wing designs, what are they, how can they be quantified, and how might they be varied so that parametric studies can be carried out that lead to a broader understanding of what attributes of the wing (particularly its

structure) are critical or beneficial for flight? Of course these questions, and ones like them, just begin to scratch at the surface and are not easily answered but they are at the heart of developing designs for flapping-wings. And yet the lack of answers to questions like these has not slowed the pace of the researchers who churn out analyses of arbitrarily chosen wing designs often extrapolating their results to flapping-wings as a whole.

2.3.3.2 A Need for Metrics With all the design variations seen in larger aircraft (manned or unmanned) tailored to their specific missions, it can be said with reasonable certainly that someday there will be a wide array of MAV designs with no "one size fits all" wing design. Wing designs will likely be as varied as the MAV missions themselves. So, even as successful flapping-wing designs begin to emerge, an understanding of how to tailor them toward another application or to optimize one design toward specific performance parameters given a unique set of constraints will be essential, just as with conventional aircraft design.

One particularly telling encounter with the project leader and chief engineer for the DARPA Hummingbird Program (Figure 2) revealed that his team iterated on their design over 100 times before settling on a final wing design. When asked if his team had learned anything about wing design that would allow them to tailor it toward another set of requirements (e.g. 30% increased range, or 50% increased speed) he was very clear that theirs was a point design and that if they had new requirements they would have to virtually start from scratch [58]. So, four years and five million dollars later, not a single design rule came out of that program. This anecdotal case is not meant as an attack or to belittle their work. By all measures, the team was successful at meeting the requirements

given to them by DARPA. It is, however, offered as a shining example of what appears to be the status quo in the MAV aerodynamic research community. As is often the case, and as the Aerovironment's team confirmed, if enough ideas are "thrown at the wall" something is bound to stick.

The more important message from this narrative is to underscore the need for *metrics*. It is well known that the Wright Brothers were successful because they paid attention to the *metrics of design* rather than, as many competitors of their time had, the design itself. While their competitors were building and testing one full-scale glider after the next, the Wrights studied the flight of large gliding birds, and systematically studied over two hundred scaled airfoil shapes varying camber, angle-of-attack, and freestream velocities through a massive parametric study [75]. They were able to focus on the truly important metrics of the wing's aerodynamic design. As the Smithsonian puts it, "The genius of Wilbur and Orville lay not only in the singular act of getting a flying machine into the air, but also in the approach they evolved and employed to create the technology of flight" [94]. So, in light of the discussion in section2.3.2 that underscored the need for more focus on the structures discipline in flapping-wing design, and taking a lesson from the Wrights on a more metric-centered approach, what structural metric(s) might be lurking in the natural design of insect wing's that may be important, if not required for flight?

2.3.3.3 The Dilemma An obvious question is how does one know, among all the diversity found in insect wings [65], which traits are the important ones to inherit or mimic? Unfortunately posing that question is easier than answering it. The

trivial answer is simply to *not* mimic any trait (attribute) whose function is not understood in order to avoid the possibility of inheriting a useless, or worse, detrimental trait. Of course, that is neither particularly satisfying nor instructive since the function of any particular wing attribute can be speculative at best, or worse, not understood at all.

Returning to the wing of a moth for a moment, consider the possible function of the tiny hairs and scales found on their wings as shown in Figure 12. Some biologists think that they serve, at least in part, to attenuate bat sonar thereby making them more invisible to bats [7]. One exchange with a practicing biologist [111] also suggested that they might well serve as an escape mechanism from the webs of spiders or as irritating agents for would be predators. Aerodynamicists undoubtedly may propose that they serve some aerodynamic benefit by adding drag-reducing surface roughness. Maybe their primary intent is to serve as an insulating mechanism to aid in thermal regulation? Unfortunately, nobody can know with certainty and to some degree each hypothesis may hold some merit. But the degree to which any plays in the overall fitness of the species – to include flight – is likely unknowable. So this puts the MAV flight researcher looking to nature for bioinspired wing designs in a bit of a dilemma. On the one hand they should strive to avoid traits that aren't fully understood but on the other hand there appears to be no way to do that when the function of any particular attribute is either entirely unknown, fuzzy at best, or coupled with one or more other attributes, the extent which is likely unknown.
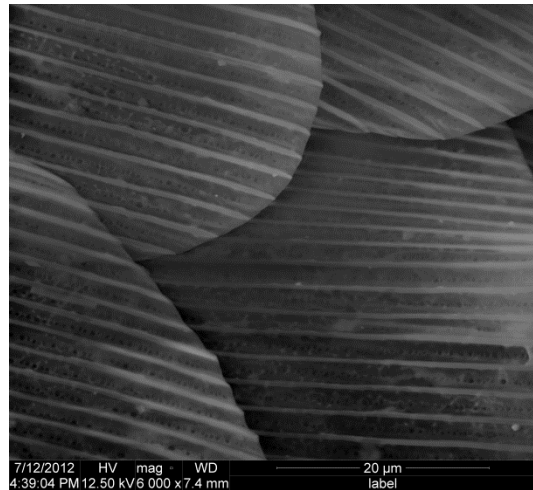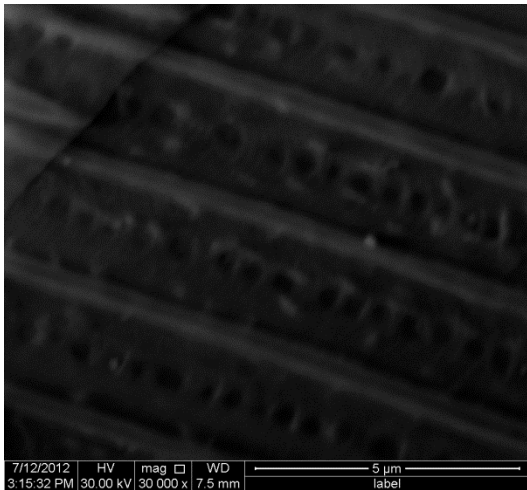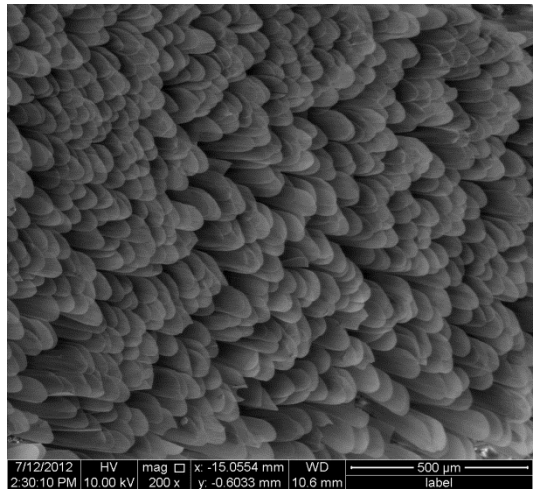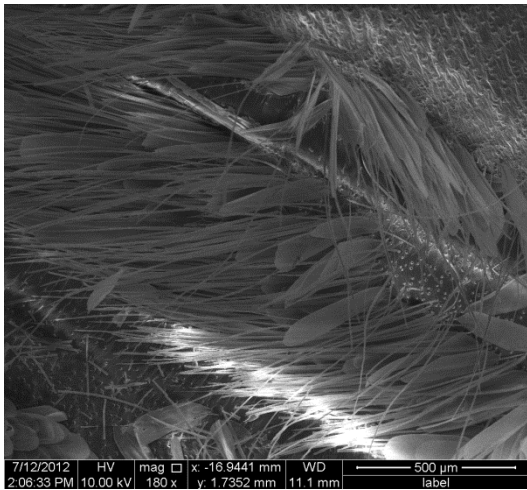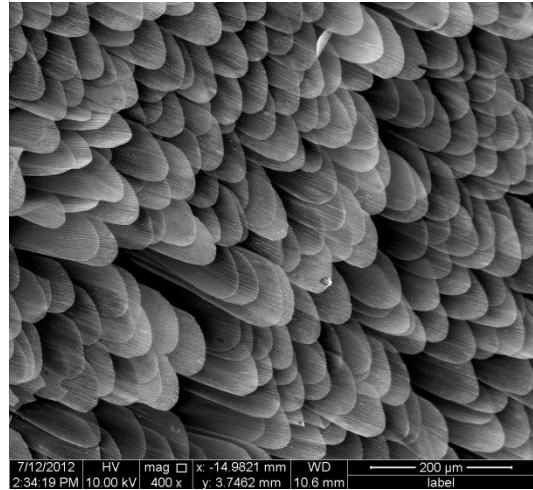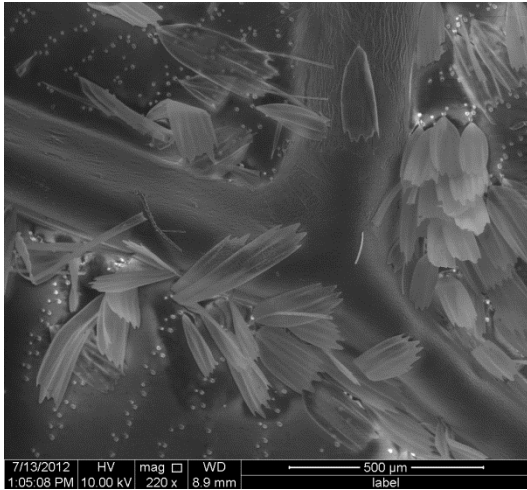
Figure 12:   Scanning electronic microscope images of the scales on the wings of the hawkmoth.   Images courtesy of Dr. Heath Misak (AFIT/ENY).

2.3.3.4 Mimic What? In terms of insect wings, features such as size, ornamentation, and planform are nearly as varied as the species themselves [65]. While some flying insects have two wings others have four. Some wings are covered in scales or hairs - or "butter" as the layperson may say - while others have none, or at least comparatively few. Some have complex networks of "veins" that are seemingly too many to count while others have just a few. And to go one step beyond, wing flapping kinematics are arguably all over the map, not only across but even within species. With all of this variability that just scratches at the surface, how does one make any sense about which wing attributes are relevant or even required for flight? Again, and alarmingly, uncertainty of the answer to this question has not slowed the pace of research. Without citing any specifically, there is no shortage of examples in MAV-related research where bioinspired or biomimicked designs have been established, virtually arbitrarily, as departure points for study. More alarmingly, the pace of study is only increasing as the computational tools of the aerodynamics trade have advanced so far that turning out one solution after another has become almost trivial. But without being able to justify the features of the design used for study - whether planform, vein patterns (venation), number of wings, wing beat kinematic, etc. - how is this path any different than that traversed by some early flight pioneers who sought no more than to mimic Nature? If the stakes for the MAV flight researcher were life or limb, how many casualties would have already been suffered?

In fairness, a great many researchers, a number of them biologists and animal physiologists with particular affinities toward aerodynamics, have elucidated the nature of flapping-wing flight, and in particular the flight of insects. The exhaustive works of

Ellington [30-35] stand out amongst many other noteworthy researchers. Even more recently, Dickinson [23] and Dickson [24] together have arguably gone further than any other to broaden the understanding of flapping-wing flight. While their work and that of many others have made giant strides toward a deeper understanding of insect wing kinematics and the ensuing aerodynamic mechanisms of delayed stall, wake capture, and rotational circulation, those strides have been made without specific attention to which attributes of the wing structure make the intricate, and possibly aeroelastic "dance" of insect flight possible. Some recent research suggests that wing flexibility, a hallmark of insect wings and in particular larger species of flying insect, is likely an important attribute for flapping flight [48,66]. Robustness and efficiency may very well demand it. But with wing flexibility covering the waterfront, from the more rigid paddle-like wing structures of small flies (whose deformations in flight are reported to amount to more than about 5% of wing length [31]), to the moderately flexible wings of dragonflies, to the more supple and compliant wings of moths and butterflies, the nature and magnitude of what constitutes beneficial flexibility is still at-large. So, again the question is asked of what attributes of the insect's wing are important, if not required for flapping insect flight? The following section proposes a possible way forward.

2.3.3.5 Universal Attributes The answer offered here to the last question posed above is admittedly simple. *Focus only on what is universal among flying insects.* With all of their variability and diversity, it turns out that the only *truly common* attribute across them is that they all achieve aerial locomotion through a *set of structures* (wings) that they articulate through some sort of *dynamic excitation* (flapping)

originating at their root/base (basal excitation). Furthermore, these wing structures are all common in that they all lack muscular and skeletal features. Unlike birds and bats that are equipped with these systems, allowing them to actively control wing shape through muscular flexure and actuation of joints, insect wings reportedly *respond passively* to forcing [29]. Considering the insect wing through this *universal lens* naturally leads us to a structural dynamic feature worthy of more attention.

2.3.3.6 Eigenstructure = Wingprint A review of basic vibration theory [68] will confirm that any *passive structure* that is *dynamically excited*, whether through direct forcing (e.g. basal excitation) or indirect forcing (e.g. resulting aerodynamic loading) will respond in a manner that relates back to its *eigenstructure*. So, along with its rigid body wing kinematics originating from its base, the wing will *act on* and *react to* the surrounding air as dictated by its eigenstructure. Therefore, the eigenstructure of the insect wing must be indelibly intertwined with the wing's aerodynamic response and hence directly with the overall flight worthiness of the insect wing design.

Recall that eigenstructure, or a system's natural frequencies and corresponding modeshapes (i.e. its system identification), is *independent of applied loading*, being completely determined by the system's mass and stiffness distributions; functions in continuous form or matrices in discrete form. They are a property or identifying feature of the system. The eigenstructure can therefore be thought of as a sort of "fingerprint" of the system, or more appropriately for the current discussion of insect wings, a "wingprint". Because of the insect wing's extreme complexity, not to mention its

diversity and variation even within the same species of insect, continuous functional forms or discrete matrix representations of its mass and stiffness arrays would prove both troublesome and elusive. But system identification offers a quantifiable way of "measuring" the mass and stiffness matrices without necessarily knowing their element-by-element compositions. Much as the concepts of linear algebra enable a conceptual view of n-dimensional space, system identification enables one to measure the resultant "structure" of the mass and stiffness distributions of the wing taken together. A thorough development on the theory and application of system identification is available from many sources [15].

With their eigenstructure revealed, comparative metrics between the wings of different species of insect can begin to be made. Examination of underlying eigenstructure may reveal commonalities shared across orders, families, and species of flying insect, potentially identifying features that may be either required or desirable for flapping-wing flight or envelopes of flight such as hovering. With modern aeroelastic computer codes, structural models that isolate or extract specific modes from the overall eigenstructure of the wing can be developed and analyzed for a variety of basal excitations in order to understand how specific modes participate in the overall aero-structural response of the wing. Is it possible that one particular structural mode or a unique coupling between multiple modes could provide the mechanism for passive wing response that aids in the development and control of a flapping-wing's leading edge vortex that is critical for the aerodynamic mechanism of delayed stall? Might parametric studies that vary the natural frequency/frequencies of mode(s) reveal that insect wings tend to favor some particular ratio of modes? Answers to questions like this could help to

form a foundation necessary for eventually understanding what structural properties (both mass and stiffness distributions) of the wing are truly important, or even allow for "designing out" sub-optimal or even degenerate structural features that may be present in biological entities. Ideally, focusing on the eigenstructure of the wing may begin to pave the way for formulating a basis of design rules/metrics for how to exploit flexibility (or possibly write it off) in flapping-wing designs. But that journey begins by first revealing the eigenstructure of insect wings which leads to the *first objective* of this research:

> *By using existing system identification tools and techniques, develop an experimental framework that can be used to determine the underlying structural dynamic features of insect wings and then characterize for future study those features for the forewing of a hawkmoth.*

2.3.4 Flexibility Benefits are "TBD"

Judging by the methodologies of the handful of papers published on the subject of flexibility of flapping-wings, when MAV researchers use the term "wing flexibility" they mean the relative ease by which the flapping-wing deforms (from one design to the next) as opposed to the more formal definition of flexibility as the inverse of stiffness or the stiffness matrix. In this sense, wing flexibility is necessarily tied to both its stiffness *and* mass distributions, and hence eigenstructure, since the flexible flapping-wing is ultimately subjected to dynamic loading which implies inertial influences that potentially have softening (or hardening) effects on the wing; particularly when the wing (presuming it is lightly damped like most structures) is excited near structural modes. Computational or simplified experimental studies that have investigated flapping-wing flexibility have typically varied the single parameter (primarily) of the wing's material modulus of elasticity. While this can readily be done in computational modeling without affecting

other material properties, in experimental studies this is done by selecting an alternate material for the wing's main structural elements which compel other variations in material properties (e.g. Poisson ratio, material density). These types of studies, in effect, scale the stiffness and/or the mass properties (matrices in a discrete sense), thereby leaving the underlying eigenvectors of the wing undisturbed but likely changing modes (natural frequencies). However no parametric studies have been noted to date that have studied the sensitivity of the wing's structural response to modal frequencies or to varying modeshapes. Achieving the research objective above will provide a baseline measurement for the "flexibility" of a successful flapping-wing design produced by Nature, enabling future researchers to tweak, tune or de-tune their computational or engineered wing models and run parametric studies showing how structural dynamic properties – the metrics for "flexibility" - manifest themselves in aerodynamic performance. Until extensive parametric studies like these are accomplished, the benefits of flexibility will remain as "to be determined" (TBD).

2.3.5   Aeroelastic Wing Response - To Be or Not To Be

There is no question that C&D's finding of what is essentially a "non-aeroelastic" wing response has incredible implications, especially if they're right and more so if their finding, as they claim, extrapolates to insect wings in general. If right, not only does it greatly reduce the complexity and cost of analyzing flapping-wings or, as they state, makes "…an integrative model of insect flight that incorporates passive wing flexibility…easier to develop…", but more importantly it would offer tremendous insight into how Nature might have "solved" the challenges of flexible flapping-wing flight.

If C&D are right, one possibility for a wing that behaves aeroelastically is that Nature could have invented a workaround that avoided the coupled aeroelastic problem altogether. In effect, Nature would have had to select against any structural trait of the wing that coupled its structural response to aerodynamic forcing acting on it, or selected in favor of some other trait (or traits) that produced this apparent serendipitous uncoupled side-effect. Either way, from a structural point of view Nature would have had to imbue the flapping insect wing with just the right flexibility (or combination of mass and stiffness distributions), to make it structurally impervious to the fluid dynamic loading via the surrounding air medium, yet simultaneously make it compliant enough (in just the right way) to permit deformations by inertial loading.

From a survival of the species perspective, one could make the argument that such a wing trait would have made flying insects less susceptible to changes in the composition of the air in earth's "early" atmosphere (200 million years ago). As these changes occurred throughout history, insects with wings that were virtually impervious to the surrounding air medium would have likely fared better than those with wings structurally "tuned" for a specific air composition that would have suffered from aerodynamic efficiency losses "costing" them more energy to take flight. The loss in efficiency would, in turn, have made it more demanding for the insect to forage for food and find mates that ensured survival of its traits. While intellectually stimulating to consider, or maybe even mathematically plausible, is such a structural trait physically possible?

By focusing for now only on wing structure, a *flexible* flapping-wing that exhibits such a non-aeroelastic characteristic would have, from a discrete mathematical

perspective, either distributions of mass and stiffness that implied (1) infinite stiffnesses along the set of eigenvectors that fluid dynamic forces ultimately act, or (2) eigenvectors that somehow would be orthogonal to fluid dynamic forces. Provided they could exist in the physical domain, each case would result in fluid forces *not* contributing to wing expression and hence result in a non-aeroelastic wing response when subjected to fluid dynamic and inertial loading.

The first case of infinite stiffness is obviously a degenerate one that cannot physically exist, but what about cases of sufficiently large stiffness? Could a wing have directional stiffness such that inertial forces could readily deform it but comparable fluid dynamic forces could not, or at least only minimally? Suppose for a moment, that the eigenspace of the wing's structure could be decomposed into two sets of eigenvectors. One set only fluid dynamic forces could stretch and the other set only inertial forces could stretch. If the wing's stiffness in the directions of the eigenvectors that only *fluid dynamic forces* stretch was *sufficiently* greater (orders of magnitude more) than in the directions of the eigenvectors that only *inertial forces* stretch, then the wing would express primarily by inertial forces, as C&D observed, when subjected to a combination of comparable fluid dynamic and inertial forces. The problem of course, is that this fictitious case cannot exist physically. Every eigenvector making up the eigenspace of the wing structure is determined (along with its elastic properties) by its inertial properties, so that every eigenvector must be stretchable by inertial (and restorative elastic) forces. So the eigenvectors that fluid dynamic forces stretch would also be stretched by inertial forces. Therefore, there exists no physical way of stiffening the wing that would on the one hand virtually completely resist fluid forces while on the other be

45

compliant to comparable inertial forces. The wing cannot, at least in the physical domain, artificially discriminate between the forces acting on it.

The second case would violate Newton's Third Law of action and reaction. If the fluid dynamic forces, that must be present to sustain flight, acted orthogonal to the wing's eigenvectors then there would be no other physical mechanism for the wing to resist/react to these forces and hence no way for the insect to sustain its weight or create maneuver and control forces. But insects are able to fly so the assumption of orthogonality must be a non-physical assumption as well.

The discussion above leads to the conclusion that Nature could not (without violating its own laws) have somehow cleverly evolved a flapping-wing structure that decoupled the effects of inertial and fluid dynamic forces acting on the wing. If it could, Newton would roll in his grave. Therefore, the only possible explanation[2] for Nature's flapping-wing to exhibit *what appears* to be a non-aeroelastic response is for *fluid dynamic forces to be subdominant to inertial forces*. In fact, that is precisely the argument made by C&D. Although they concluded this from their experimental evidence, which will be more closely examined in the Chapter IV, this finding seems, at least on the surface, to be counterintuitive with how Nature might naturally have evolved wing design. Granted, Nature can be complex and not necessarily intuitive as discussed in section 2.3.3, but it seems fairly logical to think that over hundreds of millions of years of evolution that Nature would tend to favor the lightest possible wing structure (it takes

---

[2] Beyond the wing being actively deformed or the wing being so stiff that it effectively behaves so rigidly that neither inertial nor fluid dynamic force could significantly deform it. Neither case is consistent with observations of large flying insects in nature.

energy, and hence more food to flap those appendages) for a given insect which would drive down the inertial forces acting on the wing.[3] It also seems logical that inertial forces acting on the wing would be dependent on the position of the wing (in time) within its wing beat cycle. As the wing abruptly switches directions (during supination and pronation [29]) one would naturally expect inertial loads to be highest then, thereby taking on a more pronounced role in wing expression. Fluid loads on the other hand, at least the resultant load, would have to remain fairly constant to permit steady flight. So the relative dominance of inertial-to-fluid forces or vice versa could indeed change even throughout the wing beat cycle of any given insect. So the wing's expression may be dominated by inertial forces at one time and aerodynamic at another.

The only thing that is certain in all of this discussion is that the community of researchers participating in flapping-wing MAV design would benefit greatly by a second, independent assessment of the contribution that fluid dynamic forces have on the expression of the flexible flapping-wing of an insect. If a second and arguably higher fidelity investigation could conclude the same as C&D, then their case for developing more simplified, uncoupled models of flapping-wings would be considerably bolstered. To that end the second objective of the research is arrived at:

> *Determine if fluid dynamic forces significantly influence the expression of a flexible flapping insect wing by comparing the expressions between a hawkmoth's forewing undergoing pure inertial excitation (flapping in vacuum) and coupled inertial-aero excitation (flapping in air).*
> .

---

[3] Of course competing demands for robustness could drive wing mass and hence inertial forces in the opposite sense.

2.3.6   Why the Hawkmoth?

As the title suggests, the experimental specimens of this research were hawkmoth wings. One may legitimately inquire why the hawkmoth was selected. In truth, any larger flying insect would have done. Pragmatically though, the hawkmoth's size alone made it both a convenient and attractive subject for MAV study. As Figure 13 illustrates, even with readily available consumer technology, useful payloads could be reasonably integrated onto a MAV at the scale of a hawkmoth which makes it that much more intriguing to a user community. The same could not be said for insects at the scale of the fruit fly, whose relative size can also be seen (barely) on the head of the dime in Figure 13. Not to mention, the wings of smaller insect are reported to behave much more rigidly and which are less interesting from a flexibility and structural dynamic sense [32].

Of course there are many other species of larger flying insect with similar scale to the hawkmoth. In fact, if the choice were based on size, performance, and/or visual appeal then the dragonfly, widely accepted as the king of the flying insects for its aerial maneuverability, would likely top the list. But the life cycle of the dragonfly, potentially up to 5 years long from egg to nymph and then adult, make using it as a controlled subject difficult, particularly when there are no known captive colonies in the United States. On the other hand, butterflies and moths are readily available as most major universities with biology or entomology departments maintain active colonies. What's more, a large variety of butterfly and moth pupae (cocoons) may even be purchased from online vendors and shipped to most addresses in the US.

A drawback of butterflies and moths is that they are, in general, considered to be clumsy fliers, so turning to them for design inspiration may carry with it some scrutiny.

The hawkmoth is an exception to this generalization. It is an incredibly agile flier, having the ability to perform a variety of aerial maneuvers including hovering, backward, and inverted flight. In fact, when seen flying toward dusk hours it is frequently confused with a hummingbird. From a performance perspective, any MAV researcher should be happy to call this "bug" their biological inspiration. What's more, the Daniel Lab at the University of Washington confirms that hawkmoths are capable of sustained and controlled flight with their hind wings removed, making the forewing alone a flight worthy design and thereby eliminating the complexities associated with structural and/or fluidic interactions of tandem or overlapping wings. Furthermore, its relatively short, 2 to 3 month lifecycle from egg, to larvae, to pupae, and then adult makes it an ideal candidate for study. The hawkmoth is also, in the words of one behavioral biologist, the "white lab rat" of the insect world making it the subject of a wealth of other research and a "comfort specimen" among scholars. Therefore the likelihood of this research reaching a broader audience is improved by selecting the hawkmoth. And finally, the work by C&D on the aeroelastic nature of insect wings was performed on a hawkmoth's forewing. So, while the first objective of this research could have used any large insect with flexible wings, for comparative purposes with the work of C&D the hawkmoth made most sense.
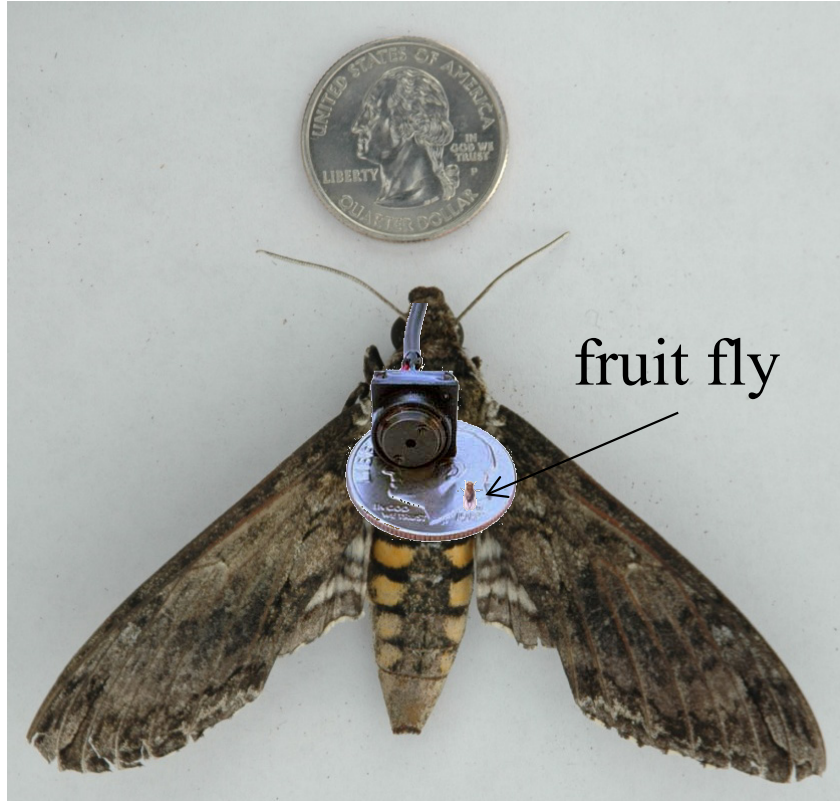
Figure 13: Top view of the hawkmoth as compared with as US quarter, noting its relative size to the fruit fly and a small commercially available 1-megapixel digital video camera.

III. Structural Dynamics

An experiment is a question which science poses to Nature, and a measurement is the recording of Nature's answer.

Max Planck [83]

As discussed in the previous chapter, while many bioinspired flapping-wing micro air vehicle wing designs continue to be conceived and studied in earnest, a general consensus of which physical attributes of the biological entity are important for flight is still at-large. An argument was also made for why the eigenstructure of the wing should figure prominently among rigorous engineering metrics for guiding flapping-wing micro air vehicle wing designs at the scales of large insects. This chapter starts with brief background of the basic principle of structural dynamics and then provides a brief overview of insect wing morphology to provide an appreciation for the complexity of an insect wing's structure. An examination of two previous research efforts that investigated insect wing structural dynamics is then offered that leads to the ultimate conclusion that virtually no *compelling* previous work had been accomplished prior to the start of this research in 2008 and up to the point that initial results of this research were published in 2010 [77]. Finally, the methods and results of system identification tests for the forewings of a representative sample of hawkmoth (*Manduca Sexta*) are presented, revealing the underlying structural nature of this incredibly agile flier's wings. Despite their inherent biological variability, these wings show very little variability in eigenstructure. Finally, the wings of four other insect species are briefly examined and

show remarkable similarity with the hawkmoth wing's eigenstructure, potentially suggesting it as a flight-critical structural feature. Finally, several secondary observations made through the course of the research are discussed that may be of interest and potentially useful to future development by MAV wing designers.

3.1   Structural Dynamics Primer

From an analytical point of view, the structure of an insect wing is no different than any other engineered or natural structure/system. Indeed, it is a natural mechanical system all of its own. And, as any introductory course or text on mechanical vibrations reveals, any general mechanical system subjected to arbitrary loading can be modeled as a second order system of masses, springs, and dampers and is classically formulated in discrete notation as

$$[M]\{\ddot{D}\} + [C]\{\dot{D}\} + [K]\{D\} = \{R\} \tag{1}$$

where, [M], [C], and [K] represent the mass, damping, and stiffness matrices of the system, subjected to externally applied loading $\{R\}$ with the displacement, velocity and acceleration degrees of freedom (DOF) represented by $\{D\}$, $\{\dot{D}\}$, $\{\ddot{D}\}$ respectively. Equation (1) is really no more than Newton's Second Law of Motion and is merely a statement of equilibrium between the externally applied, inertial, and elastic restorative forces of the system. Despite its apparent simplicity, it is posed here in general enough form that the parameters may be time and/or spatially dependent with no assumptions of linearity or homogeneity implied. From a static point of view, the equation is simply reduced to the familiar form [K]{D} = {R} whose solution yields the displaced state of

the system (relative to a reference state) under static load. Incidentally, the only time this reduced form yields the posture of an insect wing is when the insect is perched at rest in zero wind which is not of any particular interest. But the flapping of an insect wing clearly does not occur statically which suggests that more than stiffness is needed to describe a wing subjected to the dynamics of flapping motion.

In following the development found in Cook [15], Eq. (1) can be rewritten in its undamped, free vibration form as

$$([K] - \omega^2[M])\{\bar{D}\} = \{0\} \tag{2}$$

which is just a generalized eigenproblem, where ω^2 is an eigenvalue, whose square root ω can be shown to physically represent one of the natural frequencies (modes) of the system. Incidentally, $([K] - \omega^2[M])$ is commonly referred to as the dynamic stiffness of the system [15]. For a given mode of vibration, $\{\bar{D}\}$ is the corresponding eigenvector that physically represents the modeshape, or displaced state, of the system in which inertial forces are exactly balanced by elastic resistive forces. The beauty of modeshapes is that they represent the prime building blocks of the response of a structural system to loading. In mathematical parlance they form a basis for the response of the system. That is to say, the response of a system to arbitrary loading can be decomposed into a combination of its modeshapes and in the case of linear response, a superposition of the modeshapes. But even a nonlinear response, which is the likely scenario for a flapping insect wing, is a combination of these modes, albeit a much more complex and coupled combination, yet a combination nonetheless. What's more, it is often the case that only a

small subset of modeshapes, at the lower end of the eigenspectrum, is needed to accurately approximate the response of the system.

It is important to note that the eigenpairs (natural frequencies and corresponding modeshapes) are independent of applied loading, being completely determined by the mass and stiffness distributions (matrices in discrete form) of the system. In other words, they are a property or identifying feature of the system, hence the process of determining these features is widely known as system identification. The eigenstructure can therefore be thought of as a sort of "fingerprint", or more appropriately for the current case, as mentioned earlier, a "wingprint" of a structural system. Because of their extreme complexity and variation even within the same family of insect, continuous forms or discrete representations of an insect wing's mass and stiffness arrays would prove both troublesome and elusive. However, system identification offers a quantifiable way of "measuring" the mass and stiffness matrices without necessarily knowing their element-by-element compositions and can be done without dissecting the wing piece by piece. Lastly, Eq. (2) implies, in general, that altering the mass and/or stiffness *distribution* of the system necessarily changes its modes and corresponding modeshapes. Scaling either matrix does not change distributions so while eigenvalues will change with scaling, eigenvectors will not. Hence, only systems with identical mass and stiffness distributions will share the same underlying eigenstructure.
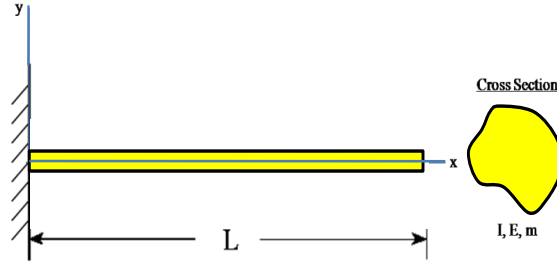
Figure 14: Schematic of a cantilevered, isotropic and prismatic beam. Note the arbitrary cross section. Slenderness is such that Euler-Bernoulli assumptions are valid.

3.1.1   System ID – A Simplified Analytic Example

As a simple example, consider the motion in the x-y plane of an isotropic cantilever Euler-Bernoulli beam with arbitrary but constant cross section (prismatic) as shown in Figure 14. The parameters L, I, E, and m are its length, cross sectional area moment of inertia, material modulus of elasticity, and mass per unit length respectively. Following the development by Meirovitch [68], it can be shown that the natural frequencies (modes) of the beam are given by Eq. (3), where the first three modes (i=1,2,3) have values of $C_1 = 3.5160$, $C_2 = 22.0345$, and $C_3 = 61.6972$.

$$\omega_i = C_i \sqrt{\frac{EI}{mL^4}} \tag{3}$$

The corresponding modeshapes are

$$Y_i(x) = A_i \left[\sin \beta_i x - \sinh \beta_i x - \frac{\sin \beta_i L + \sinh \beta_i L}{\cos \beta_i L + \cosh \beta_i L} (\cos \beta_i x - \cosh \beta_i x) \right] \tag{4}$$

where

55

$$\beta_i = \sqrt[4]{\frac{\omega_i{}^2 m}{EI}} \tag{5}$$

and A_i is an arbitrary constant of integration. Visualizations of the modeshapes are given in Figure 15. While a structure's natural frequencies themselves are dependent on its material and geometric properties, it is also worth noting that the ratios of the modes (frequencies)

$$\frac{\omega_2}{\omega_1} = 6.267 \ and \ \frac{\omega_3}{\omega_1} = 17.548 \tag{6}$$

are invariant. So, any isotropic, prismatic, cantilevered beam must satisfy Eq.(6). That said, it is certainly within the realm of possibility that a completely different structure could share these ratios of its first few modes, so they alone cannot completely identify the structure. Indeed, dynamically similar structures must also share the same modeshapes.

In all of structural mechanics, there are surprisingly few structures with associated boundary conditions that have closed-form mathematical expressions for their modes and modeshapes like the cantilevered beam. Even those that do exist are primarily elemental structures (e.g. rods, beams, cables, plates, shells) that are typically only parts of larger assemblages. So, not surprisingly, the eigenstructure for the vast majority of engineered structures must be determined either computationally, by methods such as FEA, or experimentally. Biological entities, like insect wings are no different and require the same techniques. Scaled models or in many cases full scale structures can be determined through experimental methods so that computational models can be validated and

anchored. Unfortunately, due to their light weight and delicate structure, only with the relatively recent emergence of truly non-contact system identification techniques and equipment has it been possible to experimentally perform system identification on structures such as the wings of insects.

The remainder of the chapter is devoted to the discussion of the experimental characterization of insect wings by both past attempts and the one accomplished through the current research. A detailed discussion of the theory and variety of techniques of experimental system identification, whether contact or non-contact, as well as the variety of computational techniques used in FEA are beyond the scope of the current research. The readers should consult the wealth of sources available on the subject for more information. An overview of the theory of experimental laser vibrometry used in the research that follows can be found in [84].
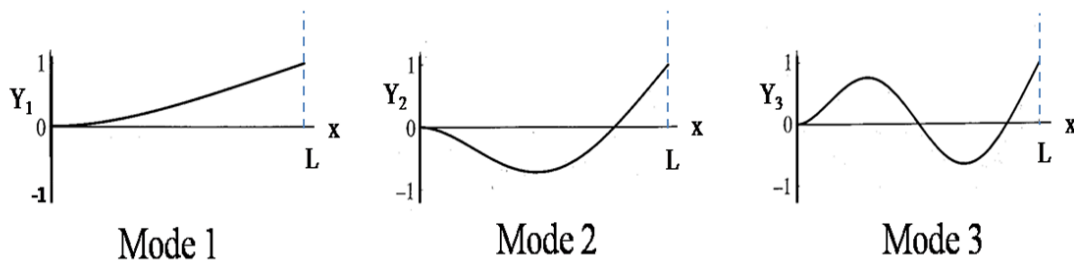
Figure 15: Plot of the first three bending modeshapes of a cantilevered, isotropic, and prismatic Euler-Bernoulli beam. Note that they are normalized so that each has a maximum value of unity.
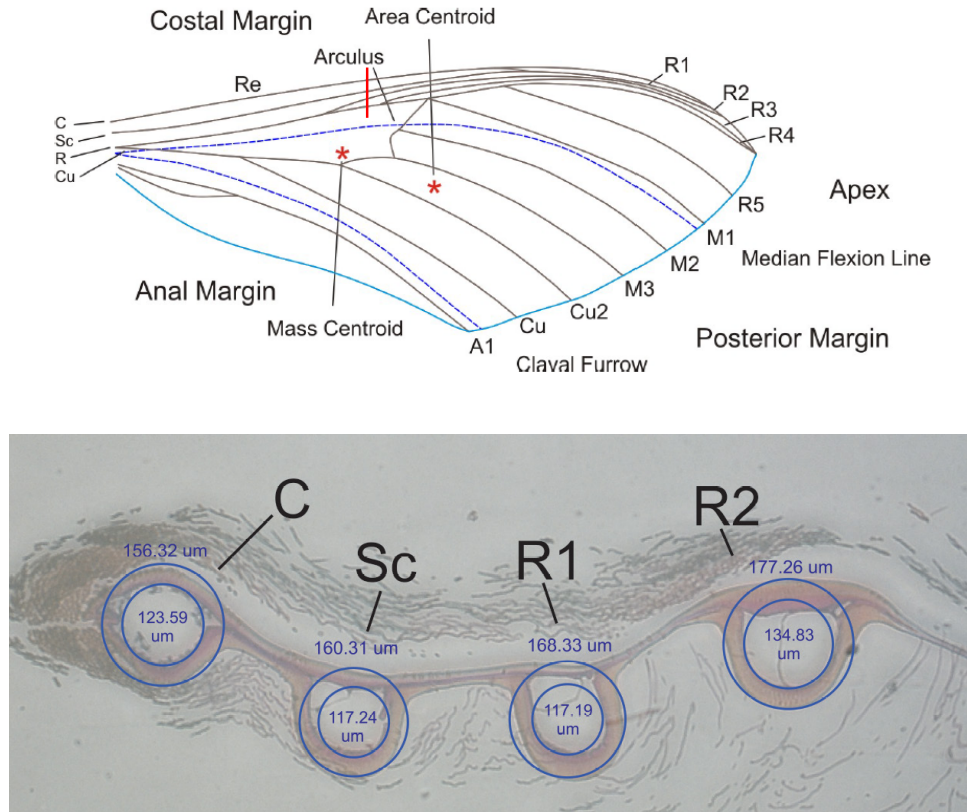
Figure 16: Top: Typical wing venation of the *Manduca Sexta*. Bottom: A cross section of the wing (taken at the location represented by the vertical red line in the image above it) showing the geometric complexity of the vein cross sections. Circular annuli that would give rise to similar rigidity are superposed over the image [79].

3.2   Structural Complexity

If the close-up images of the wing scales of a hawkmoth shown in Figure 12 do not espouse some sense of awe as to the intricacy of the insect wing then nothing will. For the hawkmoth, the scales account for nearly 20%-30% of total wing mass [78] so they cannot be neglected from a structural dynamics point of view. While they are not generally considered to be structural elements since they do not resist loads, the scales cannot be neglected (at least for the hawkmoth wing) since as the wing is excited

dynamically through flapping, the mass of the scales will contribute from 20 to 30 percent of the wing's total inertial loading.

The venation pattern and a partial cross section of a hawkmoth wing is shown in Figure 16. It demonstrates the tremendous complexity of the underlying wing structure. Generally speaking, the hawkmoth wing's venation is simple when compared to other orders and families of insect. Consider, for instance the venation of the dragonfly wing shown later (Figure 18). Insect wings are as complex as they are diverse [65].
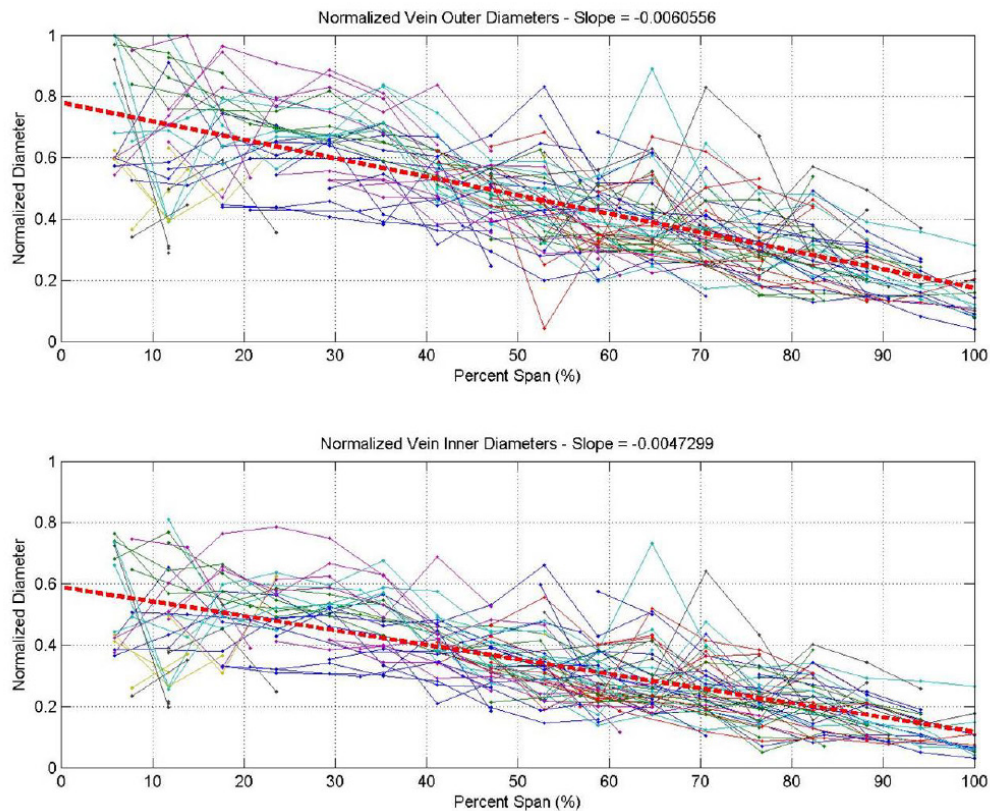
Figure 17: Results of a study that measured the inner and outer cross sectional diameters of veins at spanwise locations across the wing. The diameters were normalized to the largest vein cross section which corresponded to the costal vein at the wing's root (marked "C" in Figure 16). The vein diameters taper from root to tip on average according to the dotted red trend lines [78].

Wing cross section varies widely as it branches out across the planform, with vein wall thicknesses generally tapering from root to tip [29]. Figure 17 shows the relative tapering effect but also shows the fair amount of variability among just five hawkmoth specimens. The fine details of the insect wing's structure are so intricate that trying to mimic its form challenges even the most advanced micromachining techniques.

To be sure, lifetimes have been spent and books have been written [29] that reference hundreds of other books and research articles on the subject of insect wing morphology. The intent of this discussion has been to give a small appreciation for the complexity of insect wing structure and to underscore once more the need to understand what is common among them all. There is no doubt that microscopic features of the wing such as material properties and fine details of cross sectional geometry ultimately determine the wing's structural dynamics and hence how it responds to both inertial and fluid dynamic loads generated by flapping. Untold volumes of research have been written toward documenting these features. But with so many features having such variability, not just across orders, families and species of insects but even within the same insect [29], it can be hard to separate the proverbial "wheat from the chaff". To use an admittedly poor analogy, studying a single drop of water will do little to clarify an understanding of tidal forces and ocean currents. At some point a broader, more macroscopic view has to be taken. The more global properties of a wing's eigenstructure that take into account the manifestations of its microscopic properties could largely be of help. There is no question that more attention can be paid in this direction as the next section highlights.

3.3   Previous Related Work

Only two previous attempts at experimentally revealing the modes and modeshapes of an insect wing could be found before 2008 conducted by two independent researchers and both considered the wings of dragonflies [12,98]. Each missed however, or at least failed to communicate satisfactorily, the potential significance that eigenstructure may play in insect wing design and flight. And each were limited in providing reliable estimates of modal frequencies and/or resolved estimates of modeshapes due to limitations of their experimental apparatuses, especially when compared to the state-of-the-art in laser vibrometry used in the present research. Details of their specific methodologies and results are described and examined below. Despite the limitations of their experimental apparatuses and hence their findings, it was their work, at least in part, that helped to develop the current research methodology.

3.3.1   Chen, Chen and Chou [12]

Remarkably, the research performed in 2007 by this group of researchers from Taiwan was actually intended toward refuting the findings made by C&D in their frequently cited paper [14]. The specific motivation for their research and how it ties to structural dynamics will be discussed in the next chapter. Suffice to say for now that this group of researchers performed what appears to be the first detailed attempt to experimentally characterize the structural dynamic features of an insect's wing. In that regard, given the limitations of their equipment they did a commendable job.

3.3.1.1 Experiment Both the hindwings and forewings of two species of dragonfly were investigated by this study. An image of a dragonfly's detached hindwing is shown in Figure 18. This was not the sample they used but is provided for illustrative purposes. In order to measure the frequency response at multiple points on the wing's surface, their specific methodology required that reflective model paint be applied at 25 distinct locations across the wing planform shown by yellow dots superposed over the wing in Figure 18. The paint was reported to add approximately 30% to the overall mass of the wing. Over the course of a 24 hour period non-contact system identification testing (via photonic probing) was performed by measuring the frequency response of each of the painted markers as the wing was subjected to low amplitude transverse basal excitation (via a sine sweeping) by use of a small shaker head (Figure 19). The wing was attached at its root/base to the shaker head with an adhesive agent. After collecting the wing's frequency response at each measurement location, the frequency response function (FRF) for each point was computed and curve fitting techniques employed to provide estimates of modes (natural frequencies), mode shapes and structural damping. A free response test was also performed that traced the deflection history of the wing tip following imposition of an initial transverse bending displacement. This test was used to verify the fundamental frequency and damping estimates. These procedures were repeated for each of 21 wing samples tested.

Figure 18: Examples of unmarked and marked dragonfly hindwings consistent with the way in which Chen, et al. [12] marked their wing samples. The yellow dots represent typical sizes and locations of where reflective model paint was applied to enable measurement of the wing's frequency response with a photonic "probe". The paint increased the overall mass of the wing by 30% and affected stiffness by an unknown quantity.
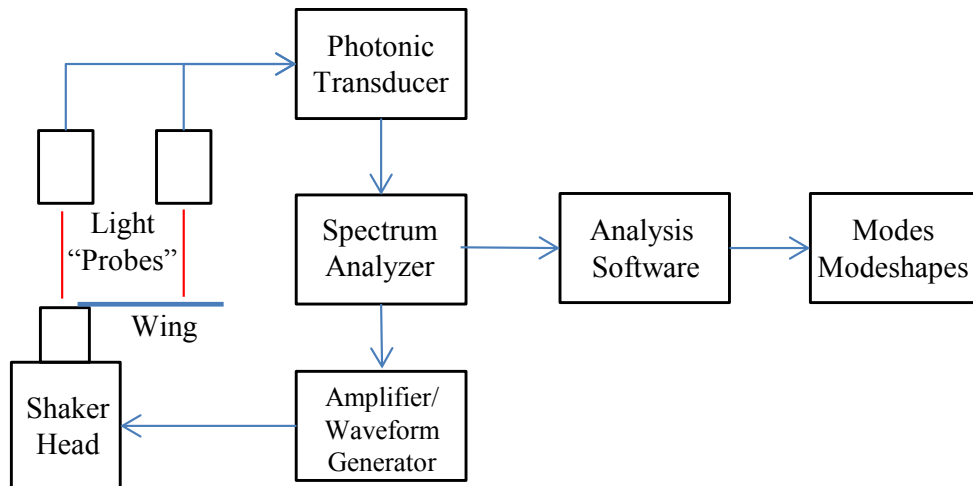
Figure 19: Schematic of the system identification experimental arrangement used by the team from Taiwan. Schematic derived from original paper [12].

3.3.1.2 Results System ID testing concluded that the wings had four natural modes between 100 Hz and 500 Hz. Differences in natural frequencies between species or between left and right wings were not observed. Damping was reported as an average of 5% across all modes. The natural frequency of the first mode for the forewing and hindwings was approximately 150 Hz with a sample standard deviation of 15% (23 Hz). By adjusting the frequencies for the added mass of the painted markers they estimated that the frequency of the first mode of an unpainted wing would be approximately 15% higher, or about 170Hz. They reported the ratio of the natural frequencies of the first three modes with the frequency of the first mode as 1:1.7:2.3 for the forewings and 1:1.4:2.0 for the hindwings. The geometric nature of modeshapes was extremely difficult to discern due to the coarseness of the measurement grid and they reported several discrepancies were observed between wing samples. Attempting to reconstruct them here for visual purposes would be futile since they do not elucidate the shapes anyway. The reader is encouraged to consult the original paper to draw their own conclusions.

3.3.1.3 Critique While a commendable effort given their experimental equipment, multiple issues cloud their results. First, the painted markers on the wings virtually defeat the purpose of the non-contact methodology employed in the rest of their experiment. While they do account for the added mass of the paint, it is via a simplifying assumption that is only consistent with a distributed mass loading which is clearly not the case here. While an added mass of just a few percent may have been acceptable even with a distributed assumption, 30 percent is too large by any measure.

Furthermore, the paint spots themselves have stiffness (like paint chips would) and therefore add stiffness to the wing in an unpredictable fashion and in this case exactly at the locations where the measurements are taken. As the authors state themselves "…natural frequencies should be interpreted with caution."

Second, the authors rightly note that there is an added mass effect due to the surrounding air that could be quite large in comparison to this lightweight structure and suggest that the testing would be better suited to vacuum. It would have been good to have the results both in and out of vacuum for comparative purposes since, as they state, insects do fly in air and results in air versus vacuum would be of value. All good advice but vacuum results here would not have helped to overcome the other deficiencies noted and so the same cautionary statement would apply.

Third, the coarseness of the measurement grid provides little value to visualizing the modeshapes. Granted that more points in this case would have further mass loaded the structure and further skewed the results from the intended purposes of extracting the eigenstructure of an untreated wing. That said, it is clear that a measurement grid numbering in the hundreds of points is likely necessary to glean useful information about the geometry of the modeshapes. The authors could have added the same cautionary statement about modeshapes that they used to caveat their reported natural frequencies.

Finally, the duration of testing is exorbitantly long. Undoubtedly the wing structure will undergo changes once removed from the insect due to desiccation. It will likely lose mass and gain stiffness as it dries out. Points on the wing measured closer in time to wing liberation would be less affected by this but the extent would be unknown. In effect with a 24 hour test time as the authors cite here, each measurement could

represent a slightly different wing in terms of stiffness and mass distributions. There is some likelihood that the inconsistencies they report in their overly faceted modeshapes were due to this aging/drying effect.

Unfortunately, the reported results for natural frequencies are tenuous at best and their highly faceted modeshapes do little to elucidate their geometric nature. So there is little value that can be placed on the results. Luckily, all of the deficiencies cited above can and have been fixed in the current research that exploited the current state-of-the-art equipment. One of the strengths of their research was the idea of the ratio of modal frequencies that they cite. Because even the same species of insect can vary significantly in size and weight, one should expect accompanying dispersions of its wing's natural frequencies. The ratio of frequencies on the other hand should have less dispersion based on allometric considerations. Their results, despite the obvious shortcomings, indicate this fact and one might expect it to hold, even more so, once those deficiencies are rectified.

3.3.2   Sunada, Zeng and Kawachi [98]

Completed in 1998 by a team from Japan, this research was actually two-fold. Its first goal was to determine the effect that wing corrugation had on torsional rigidity and the second, of specific interest to the current research, was to determine the natural frequency of the wing's torsional mode. With respect to the second goal, their specific interest was to compare the natural frequency of a dragonfly wing's torsional mode to its typical in-flight flapping frequency and thereby make the argument for whether or not the insect might be exploiting resonance (i.e. operating its wing at or near one of its natural

frequencies - torsion in this case - to produce an amplified response for a given excitation). It has long been assumed, though not proved, that insects might exploit resonance during flight.

This research appears to be an extension of the team's previous work from 1995, where they developed a non-contact methodology for extracting the natural frequencies from transparent structural specimens [116]. In that work they provide the results of testing on the forewing of a dragonfly. While that paper provides the specifics of the non-contact methodology, it does not do a good job of detailing the specifics of how the wing was actually tested and so that work is not examined here. Presumably, their more recent work, examined below, was an attempt to fill in the gaps left by their previous paper.
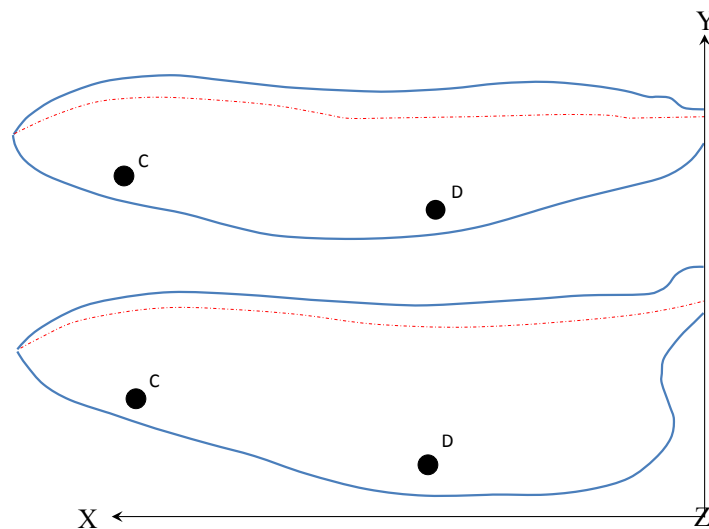
Figure 20: Outlines of the dragonfly forewing and hindwing planforms that Sunada, et al. [98] used in their research. The dots indicate the points at which the wing was initially excited by applying and then rapidly removing an applied force (e.g. a quick flick). The red dotted line represents what they determined to be the wing's torsional axis.

67

3.3.2.1 Experiment Both the hindwings and forewings of four different species of dragonfly were examined by this research. Subsequent to a wing's liberation from the thorax of the insect, the wing was attached at its base to a rigid "wall" using instant adhesive. An external force was then applied at one of two points (C or D) on the wings surface (Figure 20). These points were chosen to not lie on the torsional axis which had been carefully determined in a previous torsional rigidity study and shown as dotted red curves in Figure 20. Furthermore, they state that the torsion axis was not bent while the load was applied to the wing, so that only torsional deformations were imparted to the wing, presumably to imply that only the torsion mode was excited. Once the applied load was abruptly removed the motion of the free vibration of the wing was captured at the point at which the load was applied with the non-contact measurement system detailed in their previous paper [116]. Though significantly different in physical principle, the non-contact measurement system used was functionally similar to that described in Figure 19. In essence, a laser "probe" captured the time history of wing response and that response signal was processed through a spectrum analyzer that computed the FRF for the given measurement point. Of course, the novelty of this system was that the wing did not need to be treated with reflective markers. Except for one species of dragonfly (Species A) where the FRF was computed at two points (Points C and D), the wings were only measured at Point C (see Figure 20).

Table 2:   Results of system identification testing performed by Sunada, et al. on multiple species of dragonfly. Derived from their original paper [98].

Species	Insect Mass (mg)	Wingbeat Frequency Ω, (Hz)	Natural Frequency ω, (Hz)	Measurement Location (--)	Ω/ω (--)
A	670	27	75/120	C/D	0.4/0.2
B	27	41	133	C	0.3
C	191	31	67	C	0.5
D	245	15	48	C	0.3

3.3.2.2 Results   The results of their research are summarized in Table 2.   They deduce that for each species of dragonfly tested, resonance is not exploited since the natural frequency of the torsion mode for each is only 20 to 50 percent of the respective species' typical wing flapping frequency.

3.3.2.3 Critique   Provided the frequencies they compute are indicative of the wing's actual torsional mode, then the species of dragonfly tested, although not operating on top of a frequency do gain some added deformation (10 to 30 percent) assuming the wing is lightly damped (less than 10 percent); see Figure 21. Whether or not 30% is significant is subjective and while the authors tend to think it is not, if the added deformations are beneficial to the wing's aerodynamics then 30 percent probably translates to more efficient flight and hence improved survival.

Because each wing is effectively only sampled at a single point on the wing there is no way to ascertain modeshapes. While this is troublesome to would-be-designers looking to the dragonfly for design inspiration, it is more alarming that there is no way for the researchers here to guarantee that the frequencies being reported are for the

torsional mode. They assume they are reporting on the torsion mode because they are careful to imply that they are only exciting the wing about its torsional axis. But with all of the complexity in the structure of these wings, with venation running wildly across the planform, to assume that one mode could be excited freely of all others is speculative and probably wishful thinking. Even if the initial displacement appeared to be just torsional, which is unlikely based on their methodology, the modes are likely coupled so that as the torsion wave moves about the wing it will excite both chordwise and spanwise bending and vice versa. So, whether or not the reported frequencies are torsion is suspect.

$$DAF = \{ (1-\beta^2)^2 + (2\xi\beta)^2 \}^{-1/2}$$
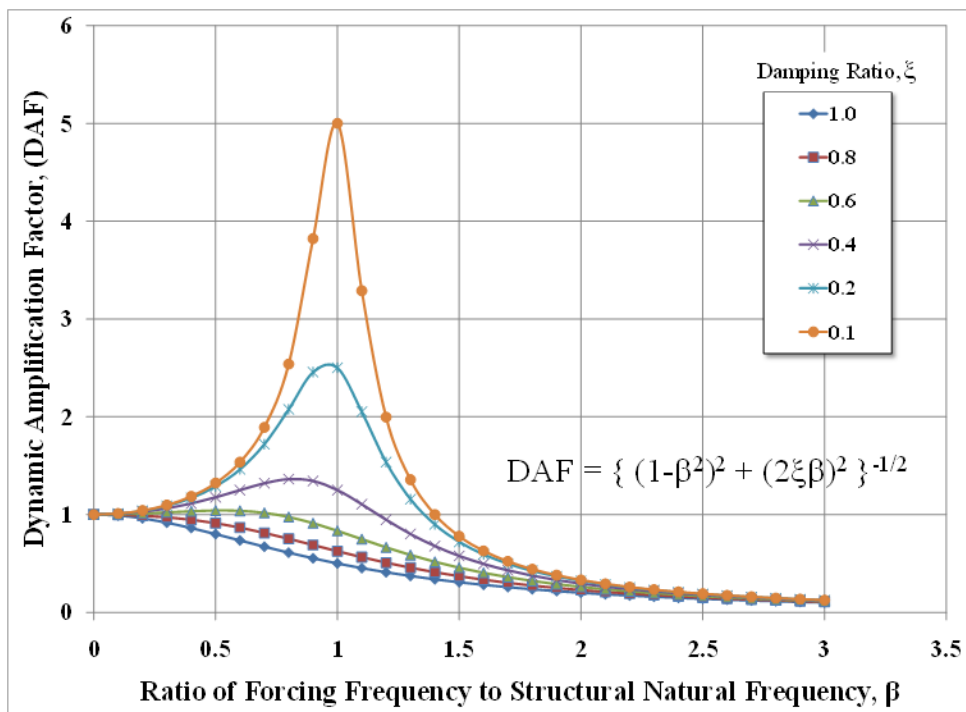
Figure 21: Dynamic Amplification Factor as a function of β. For systems with moderately low damping and forced at or near resonance ($\beta = 1$) system response is dramatically accentuated. The last column in Table 2 is defined as β in this figure. β is simply the ratio between forcing frequency (flapping frequency for purposes of this paper) and a system's natural frequency.

Perhaps the most curious observation of their findings is that they report two values for the natural frequency for Species A. Their results indicate that when they apply and abruptly remove a load at one point (C) and measure the frequency response at that point, that the natural frequency is different from the value computed when they accomplish the same task at a different point (D); see Table 2 and Figure 20. This is absolutely consistent with the discussion in the previous paragraph. Because point C is further removed from the wing's root than point D, when a load is applied and removed at Point C versus Point D it is more likely to induce a spanwise bending mode of the wing. So it is not surprising that the mode they are reporting when exciting the wing from there is lower frequency because it is more likely the spanwise bending mode. That said, without modeshapes it is difficult to rely on any of the data and therefore conclusions of this research.

3.4   Experimental Methodology

With lessons learned and deficiencies cited, a methodology employing equipment and procedures that negated every deficiency cited in previous research was developed to perform system identification on a large sample of hawkmoth wings. This section provides a detailed discussion of the equipment employed and procedures utilized to accomplish testing. Because biological specimens already have inherent variability, every effort was made to select, handle, and prepare wing specimens in a way that did not add to that variability. Mishandling or not accounting for certain variability could invite criticism and taint the findings so an effort is made in this section to provide as much detail as possible to minimize those legitimate concerns.

3.4.1 Experimental Equipment

3.4.1.1 Scanning Laser Vibrometer

The lightweight and delicate nature of insect wings demands that a non-contact system identification technique be employed. As such, Polytec's PSV-400-3D scanning laser vibrometer was utilized to extract the natural frequencies and corresponding modeshapes from specimens of hawkmoth forewings. As mentioned earlier, the specific details of the system and the methodology it employs to perform system identification are outside the scope of this research but can be referred to by visiting the Polytec website [84].
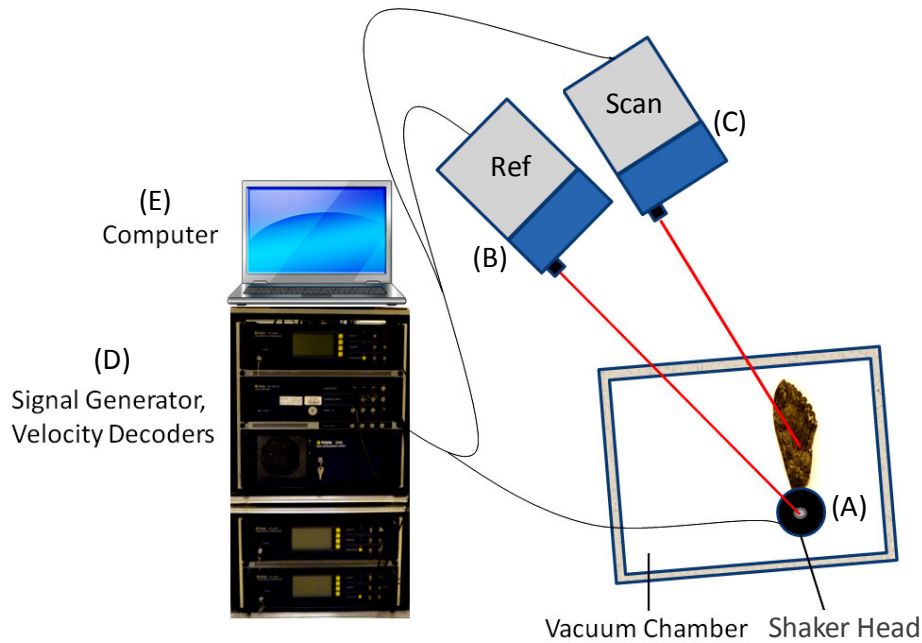
Figure 22: Schematic of the key components of the experimental apparatus used for system identification testing in this research. Note that the laser vibrometer heads were situated in such a way that the beams intersected the vacuum chamber's acrylic panes at oblique angles.

72
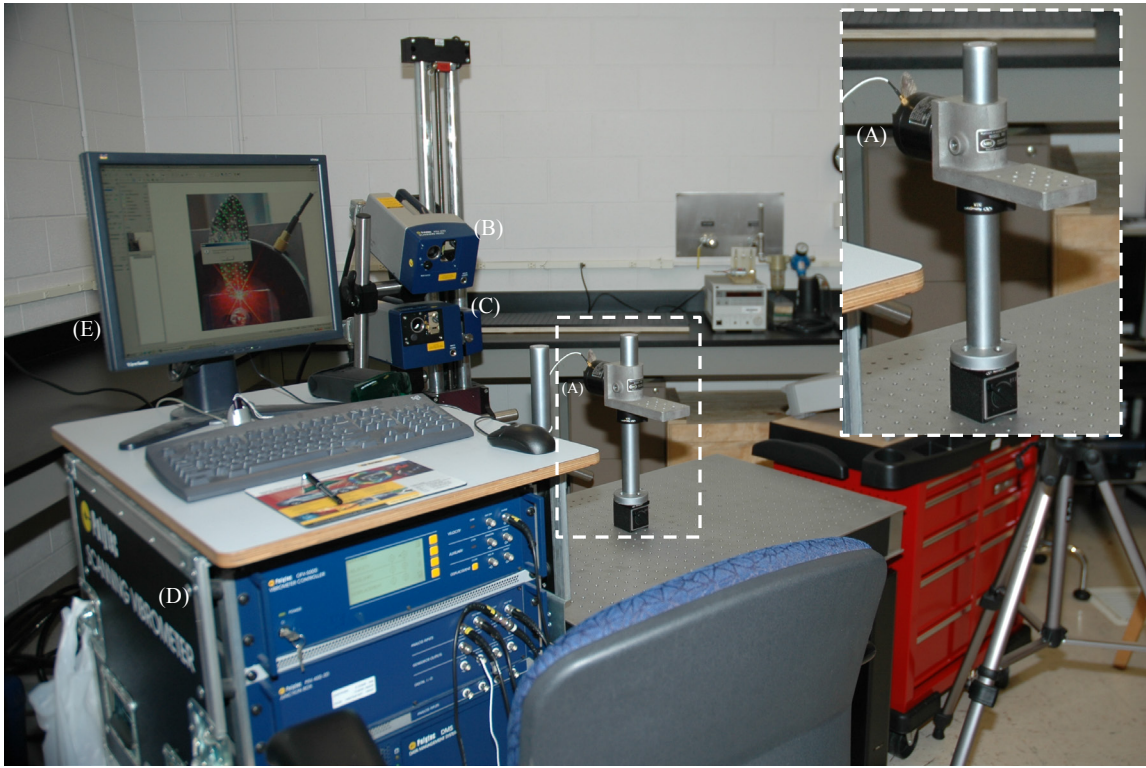
Figure 23: A photograph of the system identification experimental apparatus and arrangement shown without the vacuum chamber. Though slightly obscured by a pop-up menu, a front view of the wing and shaker (Appendix A) as seen from the laser scanning head can be seen on the computer's monitor.

The basic schematic of the experimental arrangement used in this research is shown in Figure 22, and is comprised of a shaker head (A) that excites the wing's vibrational modes via transverse basal forcing; a reference laser vibrometer (B) to measure the actual velocity output of the shaker head; a scanning laser vibrometer (C) that measures the velocity response of the wing at hundreds of predefined locations on the wing called scan points; and a control unit (D) composed of velocity decoders and a waveform generator that enable setting operating parameters for the vibrometer as well as the excitation signal waveforms for the shaker head. Polytec's interface computer (E)

and accompanying software was an integral part of the setup and served as the primary user interface for interacting with each hardware component, defining test parameters, triggering test execution, and visualizing results. A photograph of the actual equipment and physical arrangement is shown (without the vacuum chamber) in Figure 23.

3.4.1.2 *Vacuum Chamber* Because of their lightweight and delicate nature, it was surmised that the affects of an added air mass could have a pronounced effect on the wing's structural dynamic character compared to more massive and stiff structures where the affect can most often be ignored. Of course, this added air mass also complicates the ability to anchor future structural models, so it would be nice to dispense with it altogether. In order to do so, a custom vacuum chamber (Figure 24) was designed and built so that the system identification testing could be performed in vacuum. Detailed engineering drawings are included in Appendix C.

The 24-inch cubical chamber was made of stainless steel and incorporated large optical quality acrylic panes that were over 2-inches thick, designed to deflect no more than 0.003 inches at their centers. Only the shaker head with wing attached was placed within the chamber during testing. Preliminary tests confirmed that the acrylic pane of the vacuum chamber *did not* contribute to any shift in system identification results (Figure 25), provided the lasers were aligned so that they passed through the pane at oblique angles. If the laser was positioned perpendicular, or nearly perpendicular to the pane then the response of the acrylic pane (negligible for the relatively small forcing used) was measured and not the wing. This effect was readily apparent (Figure 26) and easily corrected for by slightly angling the laser heads. The vacuum pump and plumbing
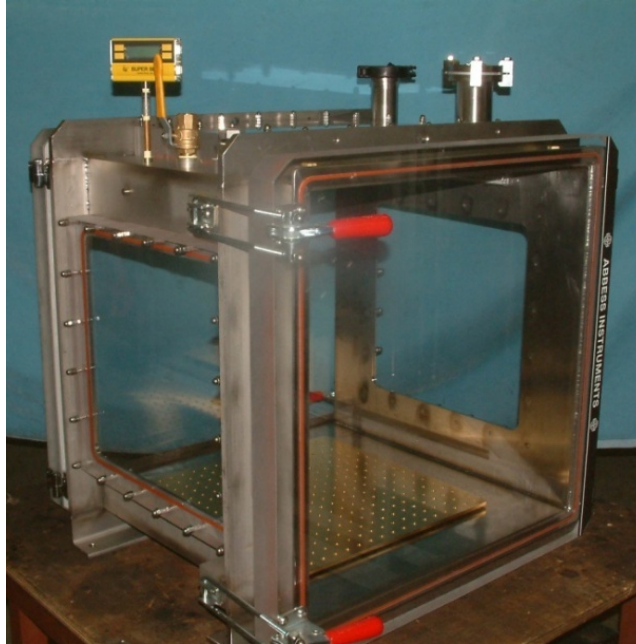
Figure 24: The 24-inch cubicle stainless steel vacuum chamber with 2-inch thick optical quality acrylic viewing panes used in this research. The pane thickness was designed to deflect no more than 3 mils (0.003 inches) at the panes' centers while subjected to hard vacuum.
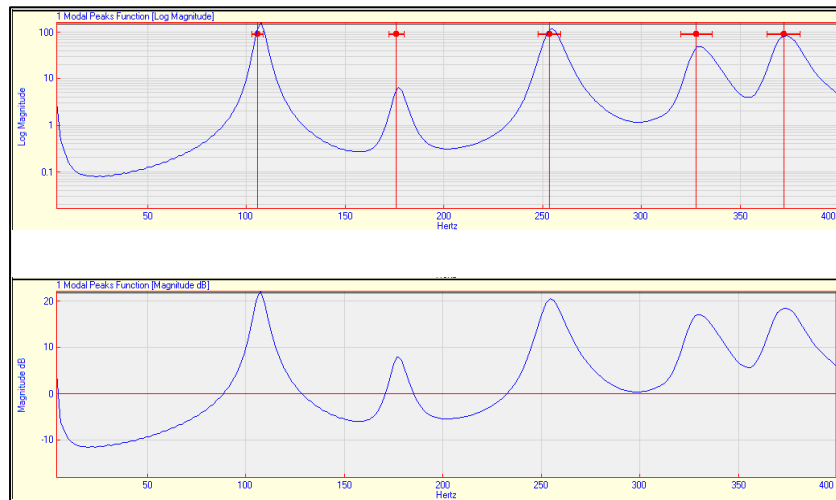
Figure 25: Shown are average frequency response functions (Modal Peaks Functions from *ME Scope*) for a dried out sample of a hawkmoth wing in air. The top plot is for a system identification test conducted with the wing placed behind an acrylic pane positioned at an oblique angle to the laser vibrometer heads. The bottom shows results with no pane. Results concluded that testing behind acrylic (required for vacuum testing) would not artificially shift measured natural frequencies.
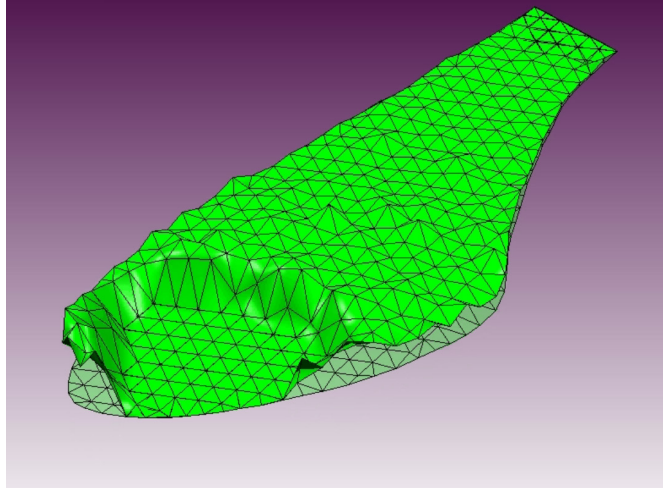
Figure 26: A view of the influence that the acrylic panes of the vacuum chamber could appear to have on the modeshapes of the wing. The unnatural appearance of no deformation in part of the wing was a sure sign that the panes of the vacuum chamber were not at oblique enough angles to the scanning laser. In this case the laser vibrometer system measures the response of the acrylic pane which was effectively zero. This was easily fixed by slightly angling the chamber.

fixtures were procured commercially off-the-shelf (COTS) and are not shown here. The vacuum pump was capable of drawing down the chamber to less than 1 Torr in ten minutes or less.

3.4.1.3 Clamping Assembly and Shaker Head
A custom made clamp assembly was used to attach the wing to the shaker head. The clamp was functionally composed of two rigid plates, each with a layer of one eighth inch hobby foam affixed to one side. As illustrated in Figure 27 B-C, the sides with foam faced each other and served to sandwich the root of the wing when the plates were drawn together with a small securing bolt and locknut. The same bolt secured the clamp to a threaded hole on the shaker head. For illustration purposes, the one eighth inch (at most) of the wing's root that was actually clamped during testing is grossly exaggerated in

Figure 27B. This "sandwiching" technique ensured a snug fit of the wing, approximating a clamped boundary condition. Early trial tests revealed that using rigid plates without cushioning foam damaged the veins at the wing root and also induced deformation throughout the wing by forcing the veins at the root to unnaturally lie in a plane, effectively "squeezing" the natural camber out of the wing root that propagated through the entire planform (discussed further in section 3.8). Incidentally, gluing the wing's root to the shaker head or clamp would induce the same phenomenon and was therefore abandoned as an option.

(A)   (B)   (C)
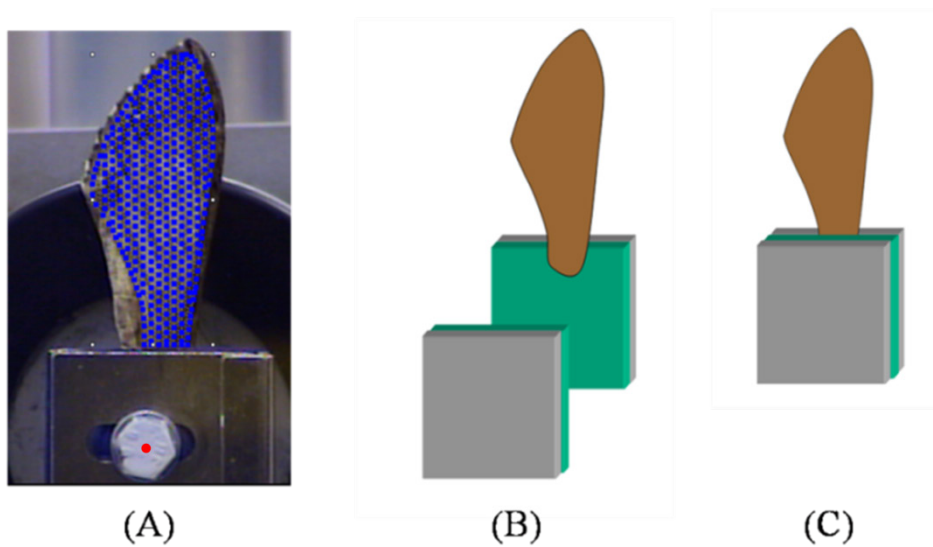
Figure 27: Shown is a typical measurement grid (A) and schematics of an exploded (B) and clamped (C) view of the custom wing clamping assembly. The amount of wing shown being clamped is grossly exaggerated. Less than one eighth of an inch of the wing root was clamped for all specimens. The reference laser was always focused on the head of the bold artificially marked in (A) by a small red dot for illustration only. Typical measurement grids consisted of approximately 200-250 points.
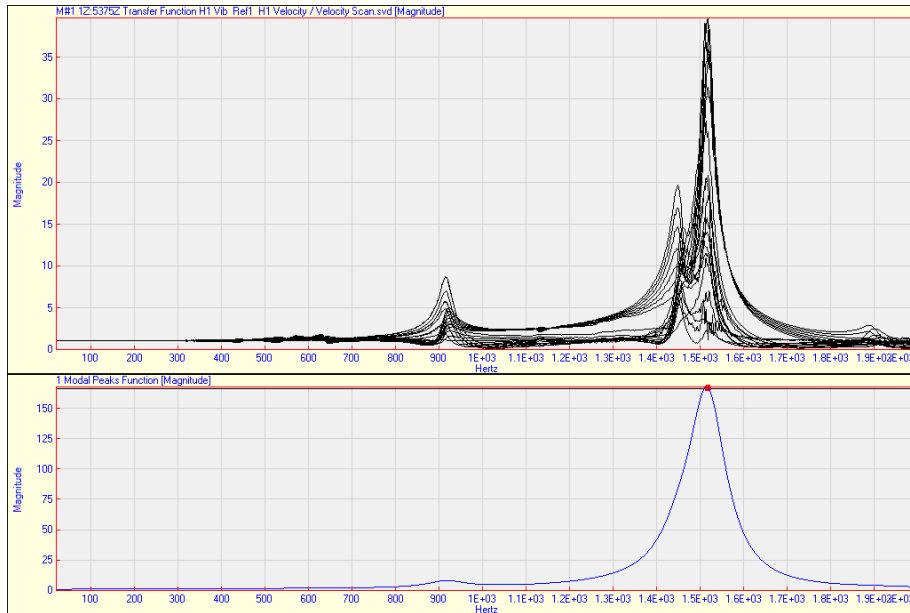
Figure 28:   The results of system identification of the primary clamping assembly used in this research. Below 900 Hz the clamp was effectively quiescent and therefore suitable as a clamping mechanism. The top plot is FRF overlays of every point measured on the clamp (approximately 20 points) and the bottom is a plot of the Modal Peaks Function (essentially a mean-squared sum of all FRFs) computed by *MEScope*.

Because the reference laser that measures the motion imparted to the wing by the shaker head was focused on the bolt head, rather than the more flexible plates that made up the clamp a shown in Figure 27A, there was some chance that the modes of the clamping plates could contribute to the measured response of the wing. In that case, the measured eigenstructure of the wing could actually be that of the clamp/wing combination. In order to verify that the measured response was that of the wing alone, the clamping assembly was independently tested for its system identification. The results showed that the lowest modes of the clamp occurred at 900 Hz and 1500 Hz (Figure 28). Because the modes of the moth wings exist at considerably lower frequencies, as the results will show later, the measured response of the wings below 900 Hz was free of any clamp dynamics and hence the clamp was suitable for its purpose.
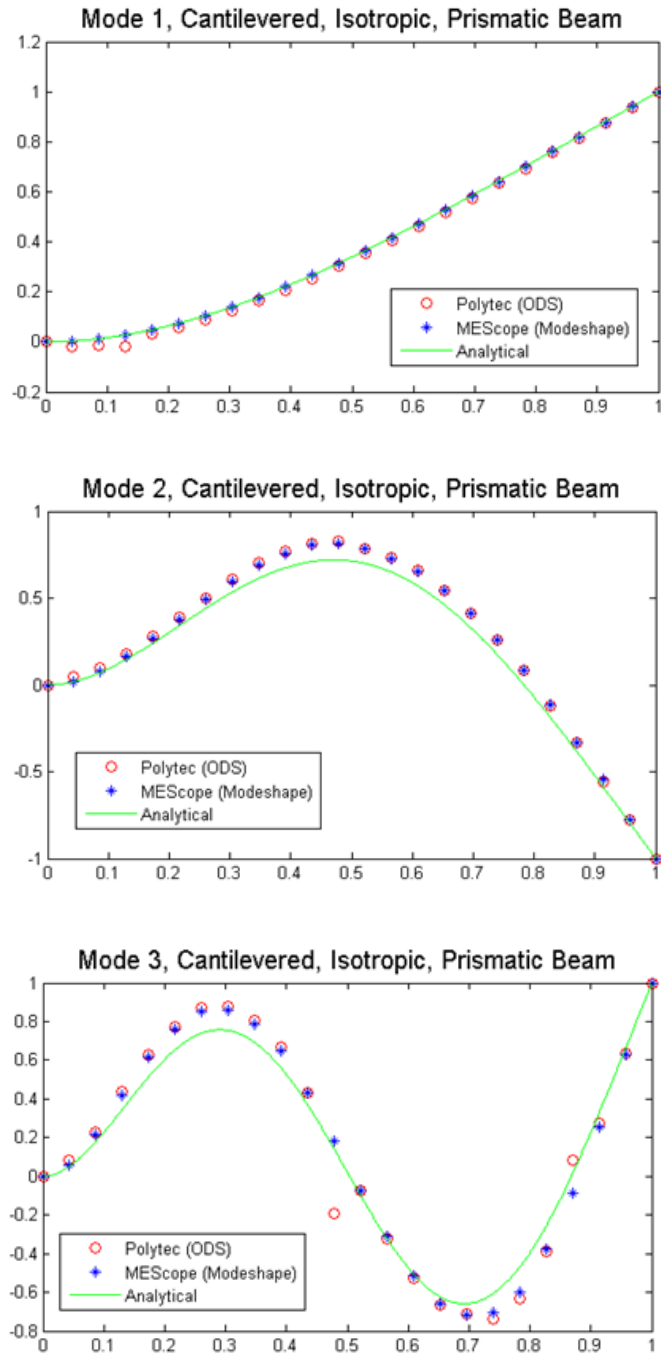
Figure 29: The modes of a paper strip mounted in the clamp assembly verifying that it does a very good job of enforcing a cantilever condition. The slight differences with theory are likely more related to the paper not being truly isotropic than the clamping condition. The differences in Polytec (ODS) and MEScope (Modeshapes) is discussed in section 3.4.2.4.

To further validate use of the clamp assembly, a small strip of standard printer paper approximating a thin, lightweight beam was tested exactly as the wings were tested for system identification as described in the next section. The paper "beam" had the properties shown in Table 3. The test was initially accomplished in air and then again in vacuum. The results of system identification are shown in Figure 29 and Table 4. The modeshapes were identical in air and vacuum and the natural frequencies increased, as expected, in vacuum by 22, 17, and 13 percent respectively for the first three modes. The natural frequency ratios in vacuum compare remarkably well to the theoretical model of a cantilevered beam discussed in section 3.1.1. The clamp obviously does a good job of enforcing a clamped boundary condition and the paper, even though not an isotropic material does a reasonably good job of approximating the properties of a beam.

The slight variations in the modeshapes were thought to be more the result of non-uniform material properties of the paper than the clamped condition. Paper, after all is not isotropic. Although a simple tensile test cannot determine where non-uniformity exists in a material, it does provide for a measure of its elastic modulus (Young's) that can then be compared to the results backed out of the system identification tests and hence provides another way to build confidence in the use of the clamping assembly. As such, a simple tensile test using one of AFIT's extensometer machines (Figure 30) was performed on a sample of paper taken from the same sheet from which the paper "beam" was cut. The test resulted in a stress strain curve shown in Figure 31 which indicated a Young's modulus of approximately 3 GPa which is consistent with paper (Figure 32). By substituting the properties of the paper beam from this study into Eq. (3) and considering the natural frequencies determined experimentally the results for Young's

modulus were approximately 4 GPa or 6 GPa (still within the range of paper) using the results from air and vacuum respectively. The differences were not completely surprising based on the fact that paper absorbs moisture from the air readily and its properties are heavily determined by its moisture content [64]. The more moisture content paper has the lower its modulus. Because the system identification vacuum test evacuated the surrounding air and all of the moisture in it, the paper in vacuum would have had less moisture content than it had during the same test in air which would account for at least some of the shift in natural frequencies in addition to an effect of added air mass. Likewise, the tensile test of the paper beam was accomplished during summertime in a warm machine shop open to the outside environment where humidity was extremely high. So the differences in results of Young's Modulus by the multiple methods and test conditions are not completely surprising and more importantly are consistent with what should be expected given the nature of the tests. Hence, every indication is that the clamping assembly provides an appropriate method for clamping the wings. Incidentally, another clamp design was fabricated and used in later test (as discussed later). In order to validate it, a similar paper beam was constructed and tested for system identification and the same conclusion made that it was viable for use as a wing clamping assembly.

Table 3:   Properties of the paper beam used in the clamp validation study.

Cantilever length	29.3 mm
Thickness	0.0889 mm
Width	8.3 mm
Mass per Length	0.00063 g/mm

Table 4: A comparison of the experimentally derived and theoretical natural frequencies of a simple cantilevered paper beam.

Mode, i	Air		Vac		Theoretical
	ω_i	ω_i/ω_1	ω_i	ω_i/ω_1	ω_i/ω_1
1	36	1	44	1	1
2	242	6.7	284	6.5	6.3
3	682	18.9	768	17.5	17.5

Figure 30: Extensometer machine like the one used to characterize Young's Modulus for the paper beam, clamp validation study.
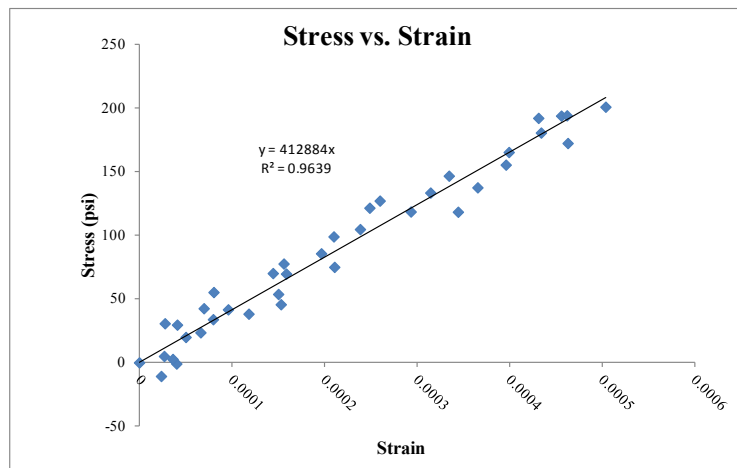
Figure 31: Stress-Strain curve of a sample of paper used in the paper beam, clamp validation study. The test determined a Modulus of Elasticity, E, of approximately 3 GPa.
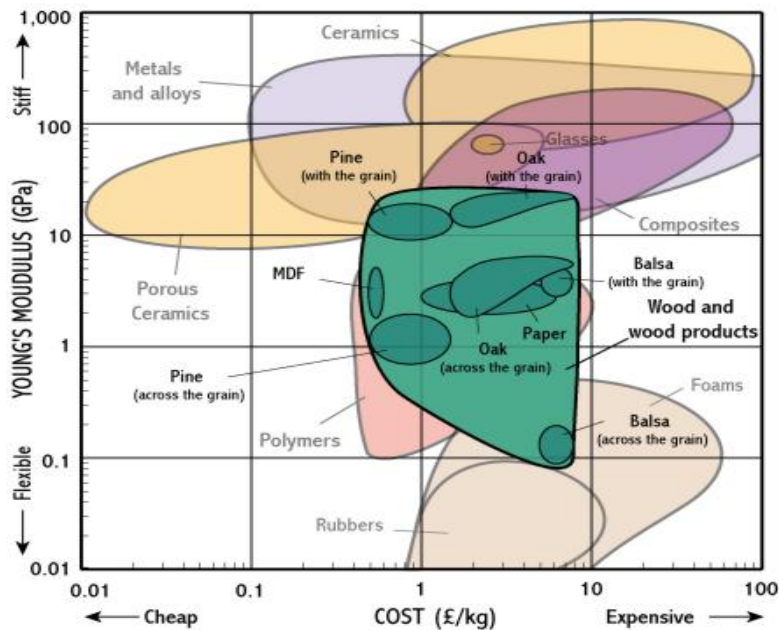
Figure 32: Typical properties of common materials, including paper [105].

3.4.2 Experimental Procedure

The hawkmoth (*Manduca Sexta*) used in this research were female members of a captive colony maintained at the Willis Lab at Case Western Reserve University in Cleveland, Ohio. Technicians hand-picked each pupae (see life cycle, Figure 33) specimens for gender and shipped them, usually 5 to 10 at a time, overnight to the Air Force Institute of Technology in Dayton, Ohio. Only females were selected to avoid any potential added variability due to a gender bias. The pupae were typically received 3 to 10 days prior to eclosing, or "hatching" from their "cocoon" to use laymen terms. Once received, the pupae were immediately transferred to an emergence chamber where they were kept at room temperature conditions from 70°F to 75°F and on a natural light-dark cycle by keeping them in a room with an external window. Failure to keep them on a

natural light-dark cycle would result in their death before eclosing; a lesson painfully learned. The emergence chamber amounted to a small cardboard box lined with paper towels and covered with a screened top. The moths emerged from their pupae with very moist and crumpled wings. Within minutes of emergence, they climbed up the paper towel-lined vertical sides of the chamber and hung upside down from the screened top where they inflated their wings with hemolymph (insect blood) and air, allowing their wings to dry in a fully expanded state. If the moths failed to make the vertical trek in a timely fashion their wings would dry in a crumpled state and render them useless for both flight and testing purposes.

Recently emerged moths with fully expressed wings were marked on their abdomen with a small dot of colored paint to identify "birth date" which was then recorded on an electronic data sheet. Twelve to twenty-four hours later they were transferred to a terrarium (Figure 34) where they were housed until commencing system identification testing 5 to 7 days later, consistent with the typical timeline when the Willis Lab normally performed behavioral flight tests. To keep the moths from damaging their wings against the boundaries of the enclosure, the terrarium was place in a room on a full light cycle to keep them from flying. Since the hawkmoth is nocturnal, it only flies when the ambient light is dimmed or dark. Preventing flight was the best measure from keeping their wings in a pristine state and avoiding the added variability of an unknown quantity of wing fatigue or damage. On two occasions, multiple moths were lost to broken or tattered wings due to the light cycle being interrupted by other laboratory workers.

Figure 33: A view of the life cycle of the *Manduca Sexta* set against the backdrop of the caterpillar's favorite food, the tobacco leaf *[49]*. Clockwise starting from the adult moth are the egg, larval (caterpillar), and pupal (cocoon) stages of life. Case Western's Willis Lab supplied specimens at the late (dark brown) pupal stage. The presence of the giant leaf in the images can be deceptive. This moth would nearly cover the expanse of the average adult palm.

Figure 34: Hawkmoth habitat used to house moths prior to testing. Note the screened container for water. The smaller container with a small funnel protruding is filled with a sugar water solution. It was used in early setup trials but the moths did not appear to drink. Furthermore, it quickly became a haven for bacteria so it was eventually removed.

The moths were initially provided a source of nourishment through a sugar water receptacle placed in the enclosure. However, after prolonged observation indicated they were not consuming, the source was removed. The Willis Lab's technician stated in all of the years she has cared for her colonies she has never witnessed them drink. Nonetheless, pure water was kept in the enclosure in a screened plastic container that helped to maintain humidity in the enclosure and to offer a hydration source, although the moths were never observed to drink throughout the course of this research either.

3.4.2.1 Wing Specimen Preparation   The experimental specimens were not the hawkmoths themselves, but their wings. In order to liberate their wings in a humane fashion, the moths were placed by hand into a sealed plastic bag and then into a small freezer where they were cooled for 15 to 20 minutes and then removed in an anesthetized state. The full mass of the moth was then measured by placing it on a highly sensitive scientific scale (Figure 35, far right) capable of measuring to one ten thousandth of a gram. The anesthetized moth was then moved to a dissection station (Figure 35, middle) where its forewing was then detached from its thorax using small surgical scissors and a teasing needle. Careful attention was made to clip the wing as close to the moth's thorax as possible and as consistent as possible between wings and moths. The forewing was then weighed and its mass recorded on an electronic data sheet, along with liberation time and total refrigeration time. The moth was then put back in the refrigerator with only one of its forewings removed. Only the forewing was liberated and subsequently tested. Once the system identification testing was complete for the liberated wing (procedure described later) the wing's mass was measured once

more so that the mass loss during testing due to handling and moisture loss could be recorded. The host moth was then taken back out of the refrigerator and the same process repeated for its other forewing, excluding measuring total bug mass.

Figure 35: Image showing the moth terrarium, dissection station and high sensitivity scale use to weigh the moths and their liberated wing specimens. The freezer (not shown) was just to the right of this station. All handling and testing occurred within a ten foot radius.

3.4.2.2 System Identification Testing in Air Immediately following wing liberation as described above, the wing was clamped at its base with the clamping assembly that was then secured to the shaker head. Well before wing liberation, the laser vibrometer system was setup and cued, so that once the wing was mounted into the clamp and shaker head, testing commenced almost immediately. It took only a few minutes to interactively create a grid of approximately 250 measurement (scan) points mapped to the wing's surface (Figure 27A), fine tune the system's operating parameters that yielded the highest possible signal-to-noise ratio (i.e. optimize coherence) and take a photo of the wing used to record dimensional details. A ruler was placed in the scene just adjacent to the wing (Figure 36) in order to calibrate the image in future dimensional post processing. With these steps complete, the Polytec system was manually triggered and its software orchestrated the collection of frequency response data at each scan point defined in the measurement grid. Scans of a single wing took place in less than 15 minutes. Therefore, the time from wing liberation to completion of system identification testing was normally completed in less than 30 minutes for every wing in the study. In all, 42 individual hawkmoth forewings were tested in this way.

3.4.2.3 System Identification in Vacuum After the first 42 wing specimens were tested for system identification, a good sense of the wing's eigenstructure in air was in-hand. Only 12 remaining wings were tested for system identification in both air *and* vacuum. This was primarily due to the delay in the delivery of the vacuum equipment and not by original planning. By the time the vacuum chamber was available (several months following the initial 42 specimens were tested in air) a new

clamp assembly had been fabricated that could be used in the second half of the research; the aero-structural investigation as presented in Chapter IV. Therefore, remaining system identification tests were completed using this new clamp. This clamp was also tested for system identification and its lowest mode was just over 400 Hz. There was some initial concern that if the frequencies of the wing shifted appreciably enough in vacuum that this may pose a problem. As the results will show, the wing frequencies did shift in vacuum, as expected, but not enough that the new clamp's dynamics presented a concern. The new clamp assembly is shown in Figure 36 (right).

All vacuum tests were conducted in air first and then vacuum. No change in the setup of the apparatus was required between testing in air and vacuum. The wing was clamped in place to the shaker head and then placed in the vacuum chamber. The acrylic door was closed and testing commenced in ambient conditions first. Once complete, the chamber's pressure was drawn down to vacuum (< 1 Torr) and system identification testing was repeated. There was some concern initially that subjecting the wings to vacuum may impart damage or introduce a drying or brittling effect on the wing, thereby making it difficult or impossible to associate any shift in structural dynamic properties to a true added mass effect. To address this concern, system identification tests were performed in air immediately before and after the vacuum testing for the first 3 of 12 wings tested in both air and vacuum. No apparent differences were noted between pre-vacuum and post-vacuum system identification results and so it was concluded that the vacuum did not introduce any deleterious effect on the wing's structure. All system identification tests performed in vacuum were initiated at pressures of approximately 1 Torr with the vacuum pump turned off to avoid any other source of vibration. Because

pressure was not actively controlled, and since all vacuum chambers have a finite leak rate, the pressure at the end of each test varied between 2-3 Torr.

For all system identification testing (air *and* vacuum), a pseudo random waveform was provided to the shaker head, subjecting the wing to broadband transverse basal excitation from 0 to 800 Hz. Since a hawkmoth's maximum wingbeat frequency is near 40 Hz (during hover), it is unlikely that modes over 400 Hz, or approximately 10 times the max wingbeat frequency, participate substantially in the wing's forced response. Nonetheless, frequency response in excess of 20 times the maximum wing beat frequency of a hawkmoth was considered. Response above 400 Hz for the tests using the revised clamp (Figure 36, right) was not considered. In actuality, any response above 200 Hz was not considered since the discernible modes of the hawkmoth wing existed below 200 Hz as discussed in section 3.5.
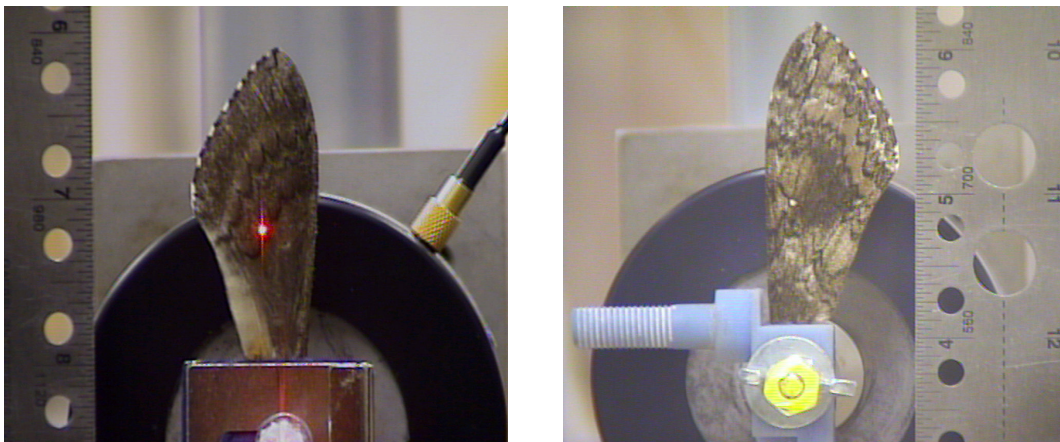
Figure 36: A photo of the wing in its clamped configurations taken just before the start of every system identification test. The ruler was placed in the plane of the wing and was used to calibrate the scene so that wing dimensions could later be measured. The clamping assembly on the left was used for the first 42 wing specimens tested in air only while the one to right was used for the 12 wing specimens tested in both air and vacuum and during in flapping assembly discussed in Chapter IV.

3.4.2.4 Post Processing   Strictly speaking, the Polytec system returns the *operating deflection shape* (ODS) of the wing at a given frequency. Very often, when the Polytec software is used to animate "modeshapes" they can appear to "walk" which could be indicative of complex modes or modal interactions. In order to determine whether or not a given mode was a normal mode (versus a complex mode or coupled response), the frequency response data from the Polytec system was exported and analyzed in Vibrant Technology's *MEScope* software analysis package.   Among other functions and visualization tools for picking out modes and modeshapes buried in the frequency response data, this software employs modal curve fitting techniques whereby the frequency response function (FRF) of all measurement points are fitted with a series of orthogonal basis functions so that the requirement of orthogonality (normality) between modes, as established by the expansion theorem [68], is satisfied. A plethora of references on the methods that the software incorporates are available through the Vibrant Technology (developer of *MEScope*) website [106].

As an example of what *MEScope* does in the normalization process, consider the modes that were determined for the paper beam that were presented in section 3.4.1.3. During testing, as in virtually every test of every wing throughout the course of this research, when the "modes" were animated using the Polytec software a slight walking of the "modes" was evident.   In this case the frequency response data was exported to *MEScope.*   One way to visualize the normalization that *MEScope* accomplishes is through use of the complexity plot which plots the magnitude and phase response of each measurement point. On a complexity plot (or "shot gun" plot as they're sometime called) normal modes will be evident by all points collapsing to a line which indicates that all

91
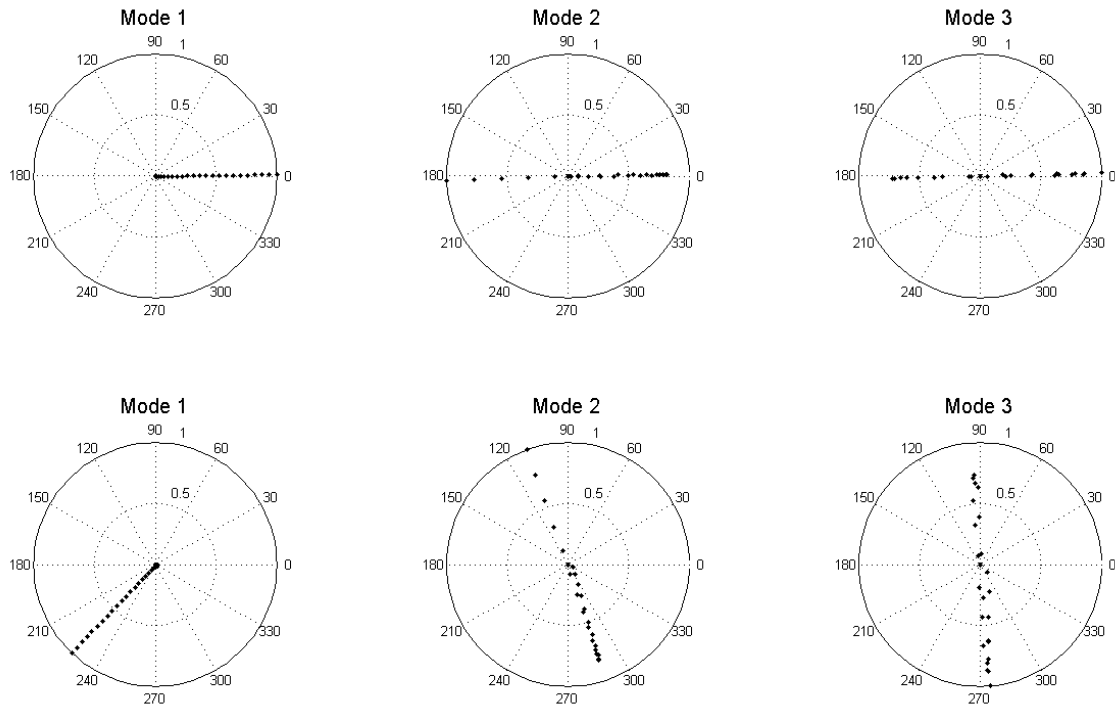
Figure 37: Complexity plots of the modes of the paper beam example discussed in section 3.4.1.3. Comparing the top row (post-*MEScope*) with the bottom row (pre-*MEScope*) shows how MEScope, through the use of curve fitting techniques, is able to extract only normal modes that essentially collapse to a line on a complexity plot.

points are either moving in phase with one another or exactly 180 degrees out of phase since a mode is essentially a standing wave where all degrees of freedom oscillate in unison. Figure 37 provides a visual comparison between the data for the paper wing modes both pre and post normalization. Every wing in the study was post-processed using *MEScope* to ensure only normal (orthogonal) modes were extracted.

After determining that a particular response at a given frequency was truly a normal mode, which in practice was typically done by animating a mode in *MEScope* following user aided normalization and verifying that no, or at least minimal walking was evident. Once that was accomplished a variety of plotting aids were available within the

92

software enabling determination of the exact frequency of a given mode. In some cases more than one plotting/visualization tool was used. The most commonly used tool was *MEScope's* Modal Peaks Function which is essentially a weighted average of all frequency responses for every point in a measurement grid. Figure 38 provides an example of one of these plots. This particular plot is for that of a small butterfly forewing tested in vacuum and is discussed further in section 3.6.1. The top half of the plot shows the FRFs (magnitude vs. frequency) for each of the scan points in the measurement grid. The bottom half of the plot shows a Modal Peaks Function (log magnitude vs. frequency) which, again, amounts to a mean-squared sum of all FRFs measured over the entire wing and assists in more precisely locating modes. Once a possible mode was identified its corresponding modeshape was plotted for final identification.
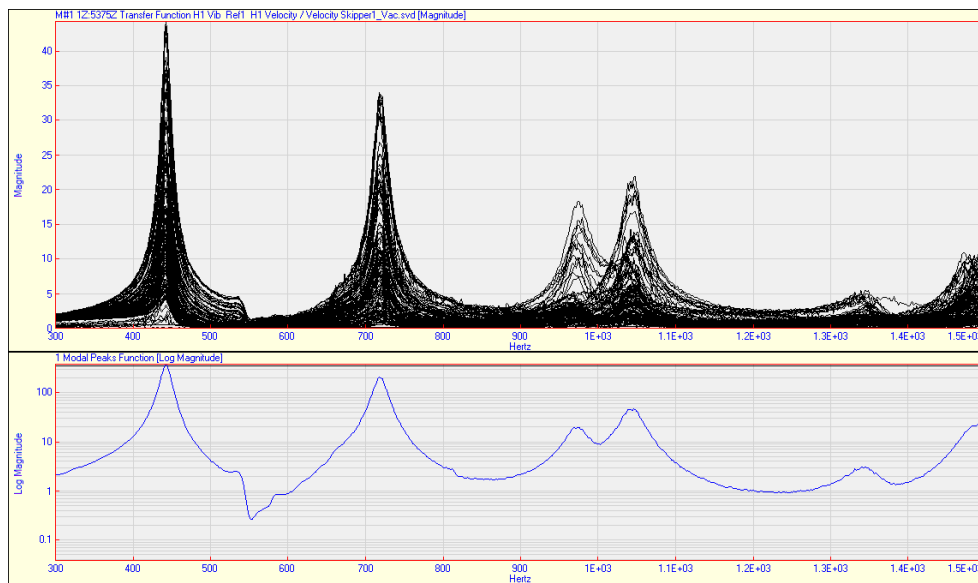
Figure 38: A typical frequency response overlay plot (top) and Modal Peaks Function plot (bottom) output by *MEScope* used for locating the frequencies of the natural modes of the clamped wing. This particular plot was generated for the forewing of the skipper butterfly tested later in the research as discussed in section 3.6.

The process of testing and interactive analysis with *MEScope* yielded estimates of modes, modeshapes, and damping for each wing and was completed for every one of the 54 wings in the sample population (n=54). The natural frequencies, damping estimates, and modeshape descriptors were then recorded in an electronic data sheet where they were later used in a statistical analysis to determine the average structural dynamics characteristics of the sample of wings tested.

3.5   Experimental Results

3.5.1   Eigenvectors (Modeshapes)

The first four modeshapes of the hawkmoth's forewings were revealed as a first spanwise bending, first spanwise torsion, first chordwise bending and second chordwise bending as shown, in Figure 39 and Figure 40. They're coined here for the first time as the *flap, feather, saddle,* and *bisaddle* modes respectively, in order of ascending frequency (mode). The bisaddle mode was the highest consistently discernible mode to be observed and was typically found at frequencies 4-8 times higher than normal hawkmoth wingbeat frequencies of 25 Hz to 40 Hz. Some evidence of higher-order modes was noted, but appeared to be localized phenomenon (e.g. membrane modes between adjacent veins or along the wing's trailing edge fringe) that made it difficult to distinguish from noise. These local modes seemed to be more pronounced in vacuum and it is likely that is due to the affects of air damping suppressing the higher modes. The first four modeshapes themselves were consistent across all wings in the study, in both air and vacuum, showing virtually no differences despite the presence of implicit biological and test-to-test variation. The feather mode was least excitable for the method

of transverse basal excitation employed, and was not apparent in about 20% of the wings tested. Each of these wings had slightly higher than average aspect ratios making them more slender and therefore less excitable in torsion/feather. In hindsight, forcing these wings slightly more vigorously would likely have excited their feather mode more readily.

It is noteworthy to point out that of the 42 wings tested in only air that the excitation method employed stimulated the feather modes of 83 percent of them. Contrast that with testing in vacuum where excitation was only able to stimulate the feather mode of only 6 of the 12 wings tested. Of these same wings that were tested in vacuum, 9 of the 12 feather modes were excited when tested in air. Even at the small amplitudes of vibration for system identification test, the air loading on the wing is able to manifest itself. This observation alone supports the possibility that aerodynamic loading cannot be neglected in determining wing expression.

3.5.2   Eigenvalues (Modes/Natural Frequencies)

Because of variations in the sizes of wing specimens in the sample population tested, one should expect a variation in modal frequencies. Just like the cantilevered beam example discussed earlier (section 3.1.1), while the natural frequency of any particular mode can take on any value, the ratio of frequencies is invariant. Accordingly, the natural frequencies of the hawkmoth wing by themselves are likely to indicate more about the overall mass and/or dimensional aspects of the wing than of any underlying structural dynamic feature. But, taken with their accompanying modeshapes, the ratio of
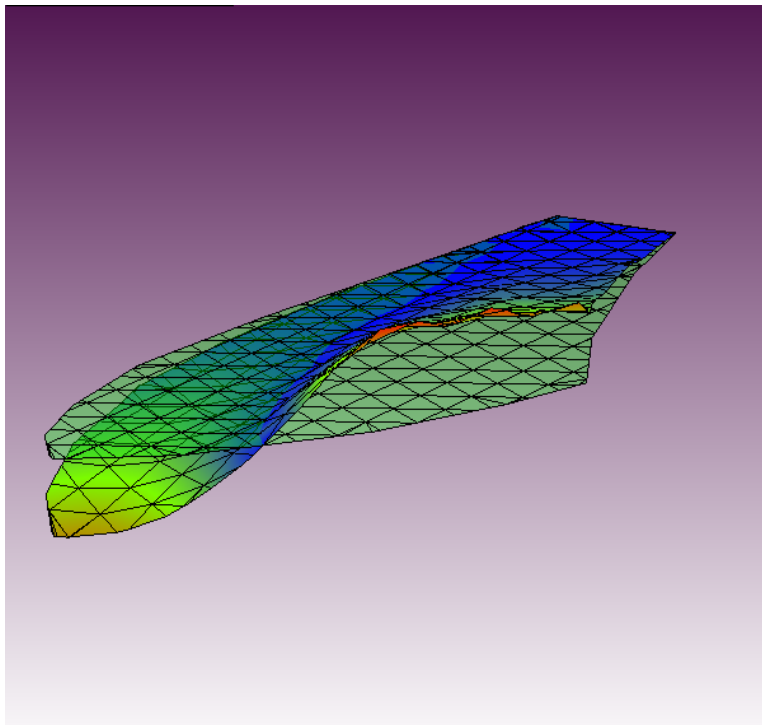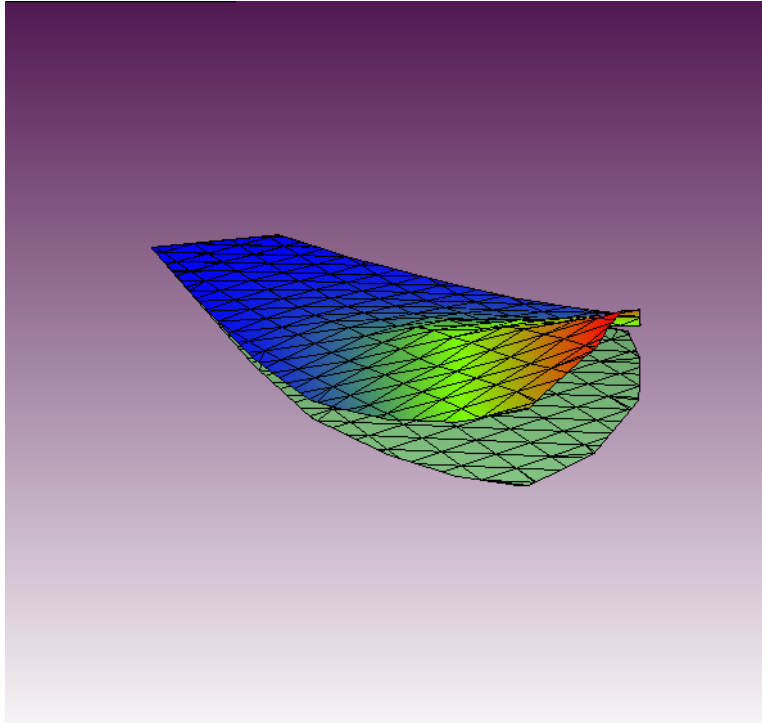
Figure 39:   The first two structural modes of the hawkmoth *Manduca Sexta* forewing; the first spanwise bending or "flap" mode (top) and the first torsion or "feather" mode (bottom).
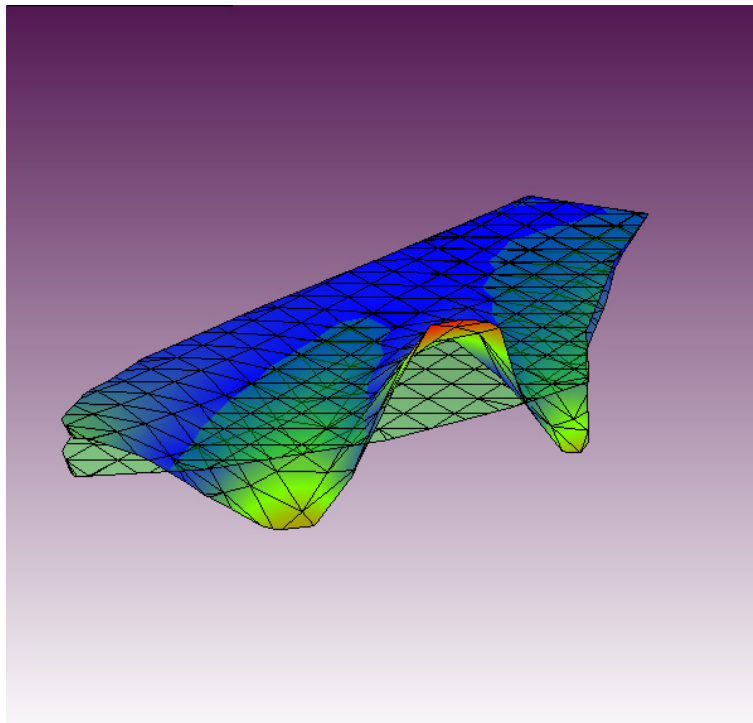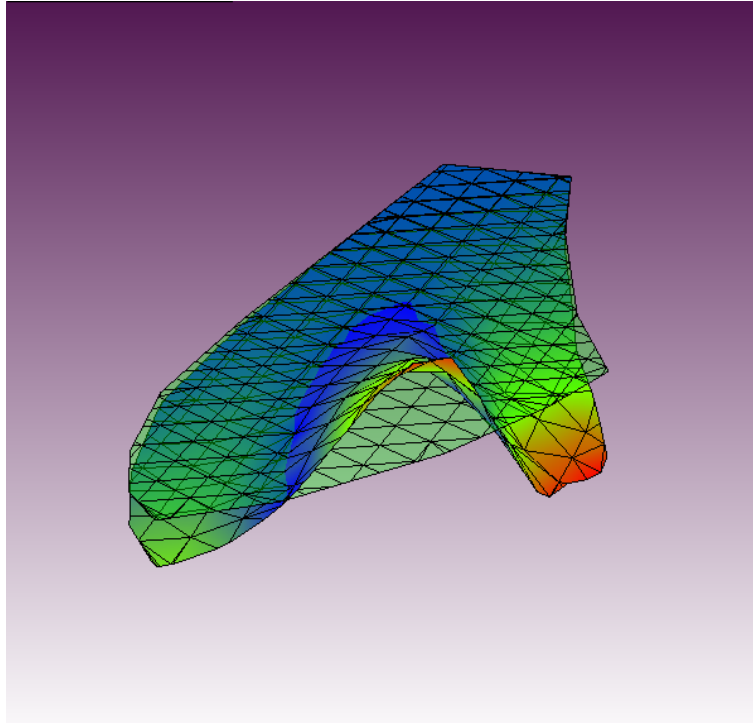
Figure 40: The second and third modes of the hawkmoth *Manduca Sexta* forewing; the first chordwise bending or "saddle" mode (top) and the second chordwise bending or "bisaddle" mode (bottom).

the wing's natural frequencies (referred to as modal ratios hereafter) should also be distinguishing features that identify them as a hawkmoth wings. These ratios, in effect, represent the relative *dynamic stiffness* [15] of each mode of vibration. Even though no such simple relations like those in Eq. (3) through (6) exist for insect wings, or for any but the most basic structures for that matter, it should follow within some expected variation that similar structures will share similar modal ratios. Insect wings should be no exception. In fact, this is exactly what the results have confirmed for hawkmoths. As summarized with their other structural dynamic characteristics in Table 5, the average feather-to-flap, saddle-to-flap, and bisaddle-to-flap modal ratios (MR), in air, were approximately 1.4, 1.8, and 2.4 respectively. In vacuum the modal ratios decreased by an average of 10% across modes, largely due to the wing's first mode being more sensitive to the added mass effect of the surrounding air than its higher modes. When compared to their values in air, the modal frequencies of the wing in vacuum increased by an average of 26 Hz across modes, with a relative increase of 40, 25, 30, and 20 percent respectively in ascending order of modes. The modal ratios were normally distributed (Figure 41) with 95% confidence intervals amounting to no more than approximately 2% of each of their arithmetic means (Table 5), indicating these modal ratios to be tightly controlled parameters. Of course, arithmetic mean is one measure of central tendency, but perhaps a more useful metric is a "fit" of modal ratios over the range of observations. To that end Figure 42 includes linear fits (all with R^2 values greater than 0.75) of the modal ratios observed in air and vacuum. Note that the slopes of each of the straight line equations are not exactly equivalent to the modal ratios since the lines were not constrained to pass through the origin; no physically good reason was determined to enforce that constraint.

The data indicates that the modes of hawkmoth forewings reside in a fairly narrow band of natural frequencies, as depicted by the grey shaded regions also shown in Figure 42, and when plotted against their first fundamental mode fit a linear model quite well.

3.5.3 *Air Damping vs. Structural Damping*[4]

Wing structural damping was also considered and estimated using the half power bandwidth method employed by *MEScope*. Damping of the wing in air was determined to be approximately 5%. Tests in vacuum revealed structural damping of 2.5%. Therefore, half of the wing's damping in air was attributable to the presence of air, and the other half to structural damping. This damping value is surprisingly consistent with many engineered structures and is often used as a typical "rule of thumb" in design and analysis when the actual damping is unknown.

Table 5: Structural dynamic features of an "average" hawkmoth wing are presented with its modal ratios (MR) provided as 95% confidence intervals.

Mode	Name	Description	In Air			In Vacuum		
			Freq, Hz	MR	Damp, %	Freq, Hz	MR	Damp, %
1	Flap	First Spanwise Bending	60	1.0	5.0	85	1.0	2.5
2	Feather	First Spanwise Torsion	84	1.41 ± 0.02	5.0	105	1.30 ± 0.02	2.5
3	Saddle	First Chordwise Bending	107	1.83 ± 0.03	5.0	138	1.62 ± 0.03	2.5
4	Bisaddle	Second Chordwise Bending	142	2.43 ± 0.05	5.0	170	2.21 ± 0.05	2.5

---

[4] Some authors use "structural damping" to specifically mean *hysteresis* damping. The use of the term heretofore is only to contrast it with the damping of the wing also provided by the surrounding air medium. The wing's structural damping estimates provided herein include all sources of damping (e.g. hysteresis, viscous, Coulomb, etc.) but specifically exclude the contribution from the surrounding air mass.
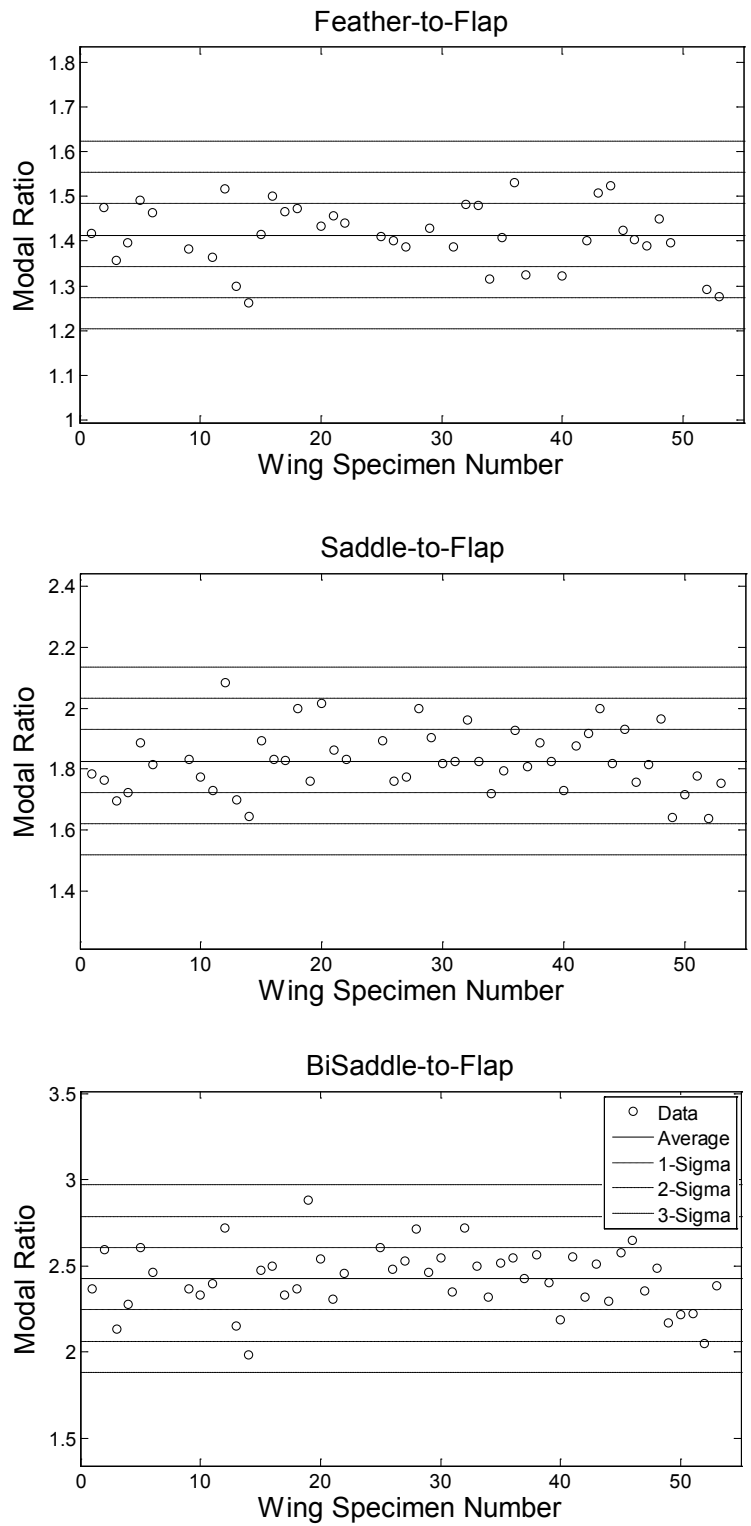
Figure 41: Modal ratio data for all hawkmoth wing specimens indicate they are normally distributed about a mean.
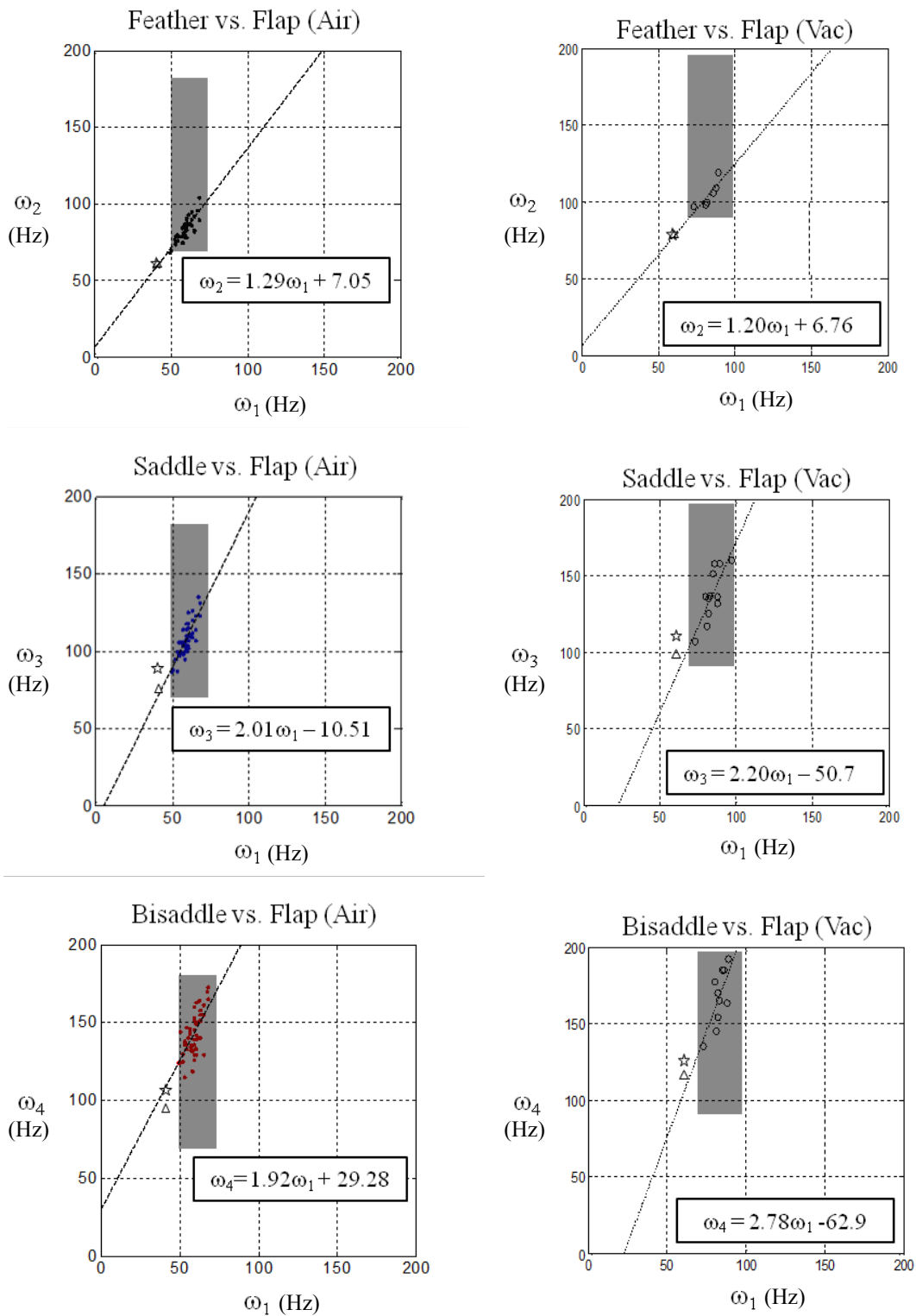
Figure 42: Plots of the feather, saddle, and bisaddle modal frequencies of each wing against its flap mode frequency and fitted with straight lines. Triangle and star symbols represent results for monarch and swallowtail butterflies discussed in section 3.6.

101

3.5.4   Age Sensitivity Testing

Some degree of skepticism, rightfully so, concerning the quality of data was anticipated due to the inherent "shelf life" of biological entities. Indeed, the wings began to desiccate virtually from the moment they were detached from the host moth. A simple time sensitivity study of a hawkmoth's forewing was conducted in order to bound the effect of drying on eigenstructure. Using the same procedures previously described, a wing was prepped and tested for system identification in air. At the conclusion of the initial test, approximately 20 minutes after wing liberation, the wing was left undisturbed, in the clamped configuration, and subsequently tested at 1, 2, 12, 24, 36, 48 and 72 hours later. This test series was repeated for two wings to verify repeatability. The results (Figure 43) showed that dramatic changes in modes and modal ratios occurred over the first 36 hours and then stabilized. Damping also fell from 5.0% to 2.5% and then stabilized after 36 hours, indicating that half of the wing's damping is due to its moisture content. The results showed that by limiting the time between wing liberation and conclusion of system identification testing to one hour, no more than a 3% increase in any given frequency (mode) or modal ratio should be expected as well as no measureable change in damping.   The results also indicated that modeshapes were virtually impervious to drying, indicating that wing desiccation is a fairly homogeneous process that does not disrupt the balance between mass and stiffness distribution within the wing; that bodes well for an aging moth. One implication of this finding suggests that one could legitimately perform system identification of preserved insect wings (e.g. insect collections) and glean relevant modeshapes, although the modes and modal ratios would not be indicative of "fresh" wings. For purposes of accurate and complete system
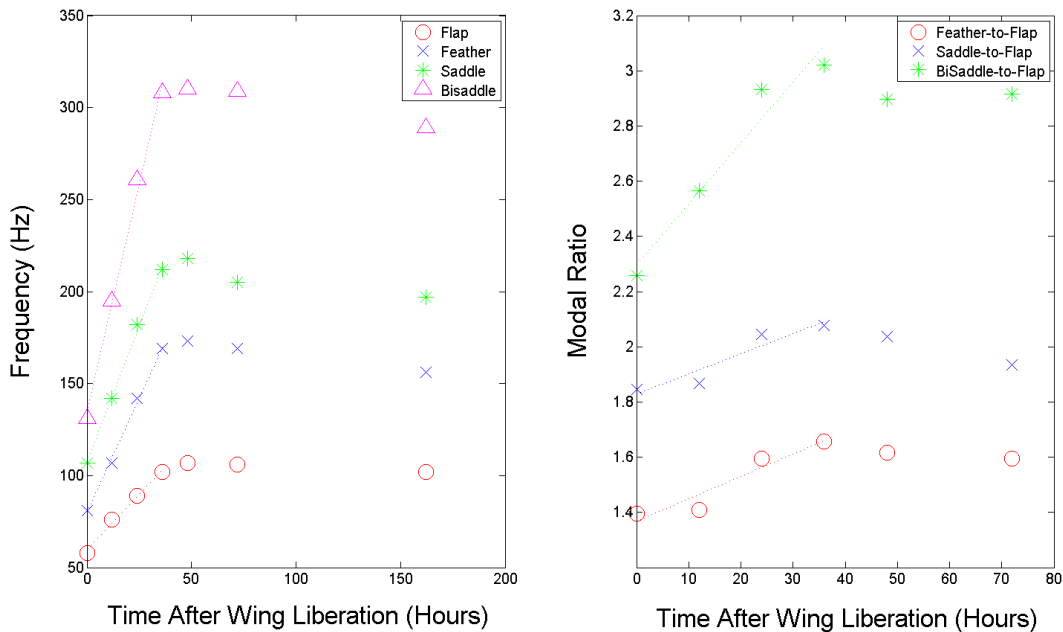
Figure 43: Results of a time sensitivity study showed that by limiting the time between wing liberation and conclusion of system identification testing (to 1 hour or less) that no more than a 3 percent increase in any frequency or modal ratio was expected.

identification testing, a fresh wing is one that has been removed from its host for no more than about an hour. A more qualitative yet ingenious test by Tubbs (104) came to the same conclusion.

3.6 The Possibility of a Golden Design Rule

3.6.1 Butterfly Wings

During a break in hawkmoth testing, pure intellectual curiosity led to performing system identification on the forewings of three butterflies. In biological terms each butterfly considered, a monarch, swallowtail, and skipper (Figure 44) resides in the insect order *Lepidoptera,* just as the hawkmoth does. As Figure 45 depicts, while their wings share some geometric similarity, their planforms all differ from the hawkmoth and the

skipper is even an order of magnitude smaller in scale (based on area). What make their wings even more unique are their distinct venation patterns. The monarch and swallowtail are arguably similar but differ significantly from the hawkmoth and skipper. By virtue of their unique venation patterns alone, not to mention the differences in vein and membrane thicknesses that attribute to overall differences in wing mass, one would reasonably expect to see differences, perhaps dramatic, in the eigenstructure of their wings.
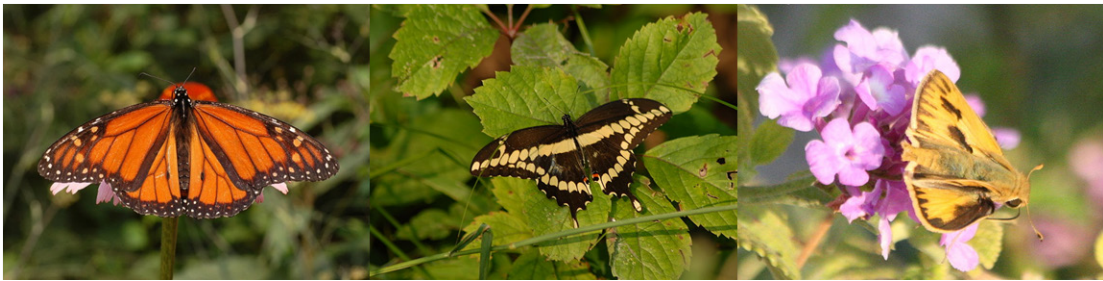
Figure 44: Images of butterfly species also considered for system identifications. Shown from left to right are the monarch [87], swallowtail [86], and skipper [102].

Figure 45: Shown from left to right, at ~70% actual size are the forewings of the hawkmoth, monarch, swallowtail, and skipper with graphical overlays of venation pattern. Skipper venation is set to the far right and enlarged to show detail.

The monarch and swallowtail wings (~0.02 grams) were less than half the mass of an average hawkmoth forewing (~0.04 grams) and the skipper (~0.001 grams) was an order of magnitude lighter. Nonetheless, the results showed that the modeshapes of all of these butterflies to be virtually identical with the hawkmoth and with each other (Figure 46). Moreover, the modal ratios were found to be quite consistent with the fit of hawkmoth modes. A meticulous reader may have noticed the addition of two data points outside the lower left hand side of the gray shaded regions in Figure 42. The triangle and star represent the results for the monarch and swallowtail respectively. Not shown on the plots due to scaling are the skipper forewing's flap, saddle, and bisaddle modes which were respectively 300, 539, and 774 Hz in air and 446, 720, and 1050 Hz in vacuum. Incidentally, the FRF overlay plot shown earlier in Figure 38 are the results of vacuum testing on the skipper's wing. Inspection of this FRF suggests some likelihood that the feather mode resides at approximately 550 Hz which would fit the hawkmoth mode data (modal ratio) within 2%, but the modeshape could not be confirmed by the data. While not directly observed in this single sample, its feather mode likely exists but the method of transverse basal excitation, as discussed before, did not excite it as readily as the bending modes. Its observed modes in air and vacuum were within an average of 18% of the linear fit of hawkmoth mode data (Figure 47).

The similarities observed with these closely related insects naturally begged the question of what about more distant relatives in the larger space of flying insects? To that end, the forewings of three more insects were tested for system identification; a dragonfly, damselfly and bumble bee. Unfortunately, the data of the dragonfly and
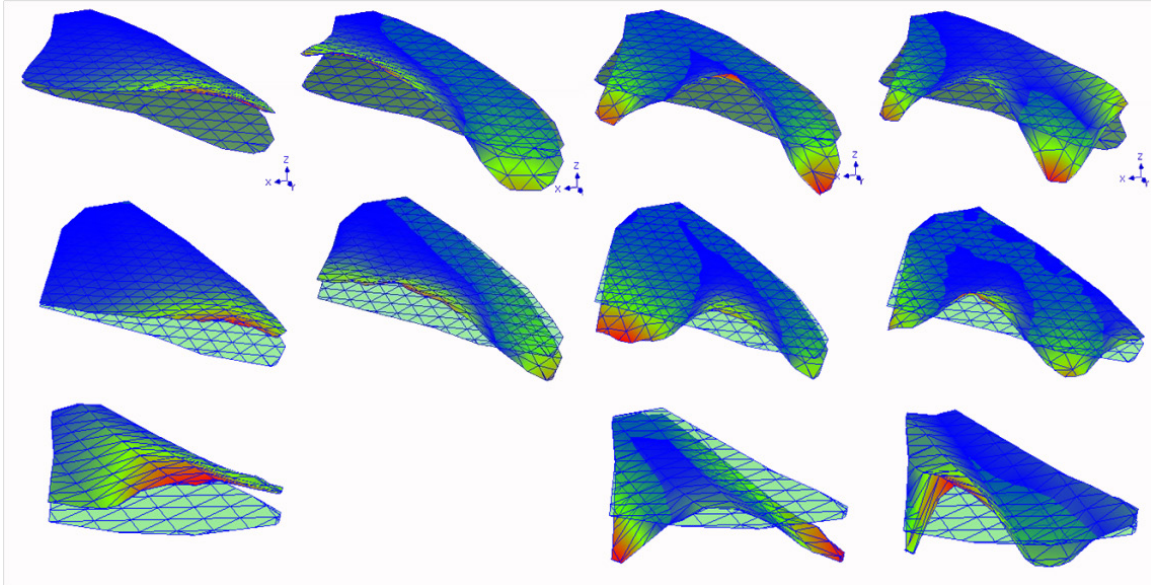
Figure 46: Shown from top to bottom are the first four modeshapes for the forewings of the monarch, swallowtail, and skipper butterflies relative to their undeformed planforms. Despite their differences in planform, venation, and scale their modeshapes are remarkably similar with each other and the hawkmoth indicating that they all share the same underlying mass and stiffness distributions.
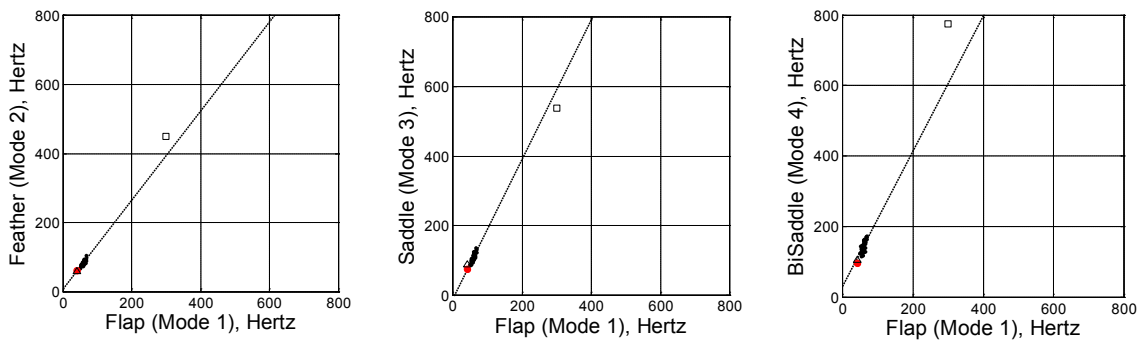
Figure 47: Plots of the feather, saddle, and bisaddle modal frequencies of each wing sample against its flap mode frequency in vacuum. The hawkmoth, swallowtail and monarch are clustered toward the bottom left of each plot while the skipper is indicated by the small square. Despite its scale and very different venation pattern it shares not only similar modeshape but even similar modal ratios. The skipper wing's FRF (Figure 38) indicates the presence of the feather mode.

damselfly, while absolutely suggesting the presence of the characteristic modes reported above, was sufficiently noisy to preclude positive identification. Several other modes may also have been present in their wings but the frequency response data was too noisy to glean conclusive results and therefore results are not reported here. The transparent nature of these wings allowed much of the laser's energy to pass through the wing rather than be reflected back to the vibrometer. Even with a light powder coating, coherence of the laser return was tenuous at best. The bumble bee wing on the other hand (Figure 48), while slightly opaque, did permit testing with just a slight powder coating of Magnaflux Spotcheck applied to it. This treatment added 0.0001 grams to the wing's overall mass, effectively adding a 10% distributed mass load, so the untreated wing's modes would be higher than those observed. This distributed load which represented only a scaling of the mass matrix leaves stiffness undisturbed, rendering the modeshapes and modal ratios of the treated wings valid representations of the untreated wings. Its feather-to-flap, saddle-to-flap, and bisaddle-to-flap modal ratios were 2.4, 4.8 and 5.8 Hz in air, and 2.3, 4.3, and 5.3 in vacuum respectively which do not compare well with the hawkmoth. However, as Figure 49 shows, the similarities of its first four modeshapes with all other insect wings tested in this study is indisputable, despite the obvious differences in venation pattern highlighted by Figure 48.
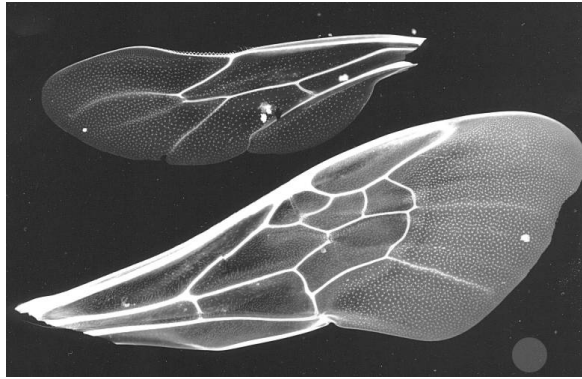
Figure 48: Enlarged photographic negative image of a bumble bee forewing (lower) and hind (upper) wings. Note the dramatic difference in venation compared with other wing specimens tested in this study [101].
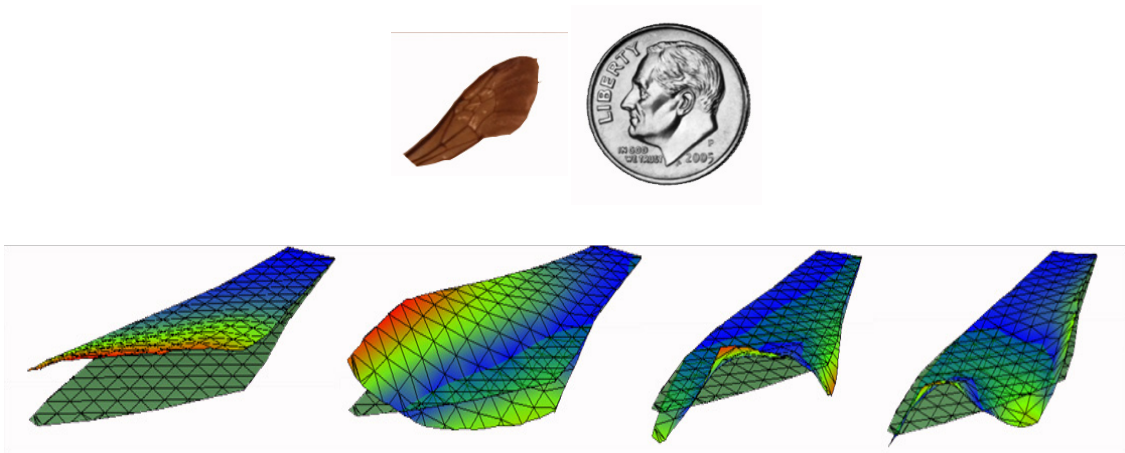
Figure 49: An image of the bumble bee forewing tested in this study in comparison with a dime, shown above its first four modeshapes relative to its undeformed planform. The bumblebee shares the same underlying eigenstructure with the other insects considered in this research despite its dramatically different venation.

3.6.2   *Paper Wing Stencil* After observing the dramatic similarities

between eigenstructures of different species of winged insect, naturally a question of any irregularity in test setup was posed. After all, how could such apparently different structures share such common underlying eigenstructures? As a sanity check, system identification testing was performed on a paper stencil of a hawkmoth forewing. A photocopied image of one of the hawkmoth wings used in the study was carefully cut out and then tested exactly as all other biological wings had been in the study. As Figure 50 indicates, other than having the spanwise bending (flap) and torsion (feather) modes that should be expected in cantilevered structures, the paper wing bore no resemblance to the biological entity. Its feather-to-flap modal ratio of nearly 5 was dramatically different from all insect wings tested. In fact, the modeshapes of the paper wing were much more consistent with plate behavior, having no indication of saddle or bisaddle modes. A finite element analysis using plate elements confirmed with great accuracy the experimental results of the paper wing. With this corroborating evidence, a high degree of confidence in the results throughout this study is warranted and concludes a clear commonality between all insects successfully tested.
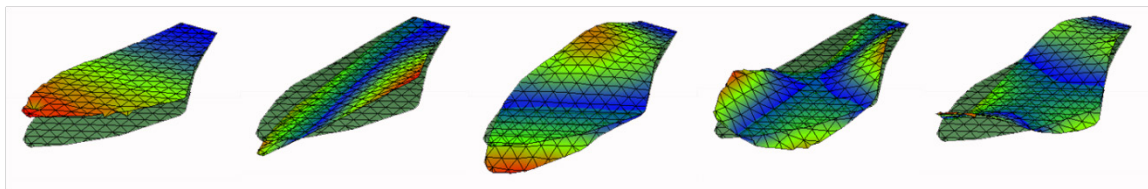
Figure 50: The first five modeshapes of a paper stencil of a hawkmoth forewing planform relative to its undeformed state. Judging by the third, fourth, and fifth modes which share an eigenstructure more consistent with a flat plate, if follows that the insect wings considered in this research are markedly different in mass and stiffness distribution from a flat plate.

3.6.3 Dimensional Trends

Some effort was made to identify dimensional trends in the hawkmoth wing data. For instance, borrowing from the knowledge of beam and plate behaviors, it seems likely that the flap and feather modes should correlate inversely with wing length. Likewise, the feather, saddle, and bisaddle modes should correlate inversely with chord length. As Figure 51 shows, these expected trends generally held true, but with a fair amount of scatter. Furthermore, trying to find some non-dimensional correlation, such as modal ratio versus wing aspect ratio, proved futile. The apparent lack of strong trends and the relative scatter of data suggest the possibility of strongly coupled dimensional relationships (e.g. internal structure such as vein diameters) that merits future study. Or, it might suggest a fairly robust wing design where "close is good enough" for flight worthy wings. For instance, a wing falling within some locus of parameters bounded by some parameter space/region, like the grey shaded regions of Figure 42, may be a viable wing design. From a survival point of view, this "robustness" trait could be of value so that slightly damaged wings, presumably with slightly shifted eigenstructure, could still continue to function. All said, while thought provoking, this line of reasoning is speculative. The dimensional data along with all modal parameters collected in this portion of the research are tabulated in Appendix B in what has been previously referenced as the "electronic data sheet". Future researchers may find it of some use. A schematic showing how dimensions were defined is provided in (Figure 52). The *ImageJ* software suite was used to extract physical dimensions from the digital images taken of each wing just before system identification commenced.
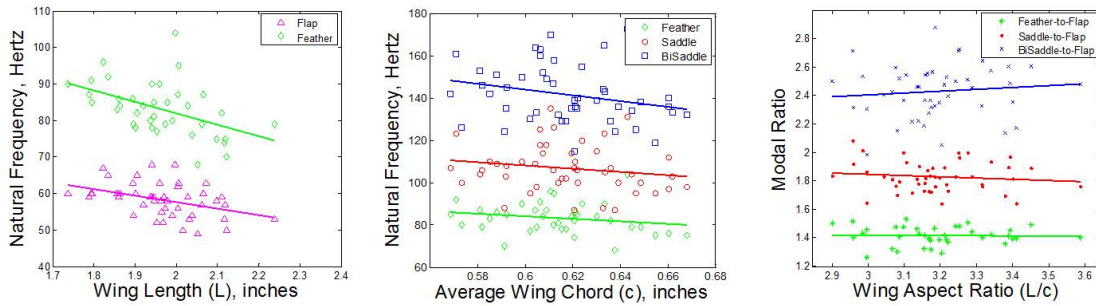
Figure 51: In general, dimensional trends for the hawkmoth wings were in the expected direction. Since flap and feather modes are spanwise modes they should exhibit some dimensional sensitivity with wing span/length. Likewise, the feather, saddle and bisaddle modes should exhibit dimensional sensitivity to chord. Modal ratios trends, particularly feather-to-flap and saddle-to-flap exhibit only slight sensitivity to wing aspect ratio (slenderness).

$L = AB$
$b = BD$
Tip Chord $(C\_tip) = BC$
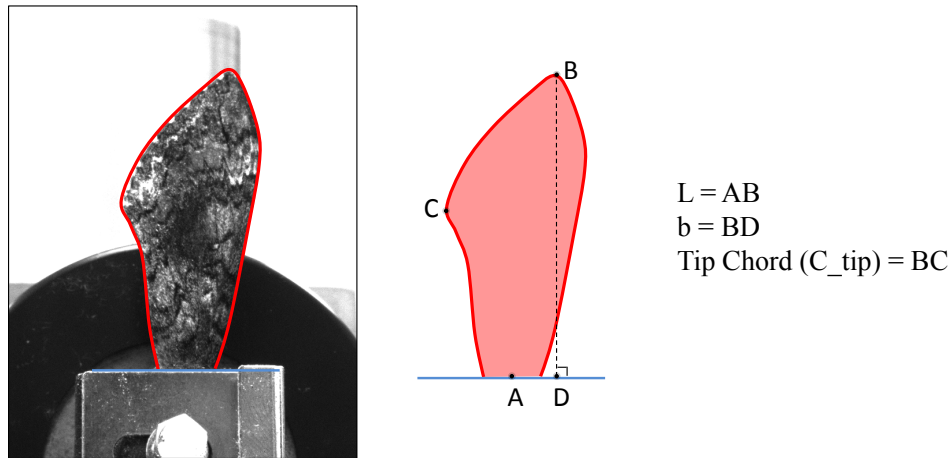
Figure 52: A schematic showing how dimensions were defined for the dimensional study. A table of all wing specimen dimensional data is provide in Appendix B which also includes the experimental modal parameters collected for all hawkmoth wing specimens.

3.7 Finite Element Modeling – An Initial Cut

As discussed in Chapter II, parametric studies are going to be crucial for exploring the entirety of the flapping wing design space. Ultimately the intent of this research is to provide the structural dynamic metrics that can be used to anchor structural models. While not part of the original research focus or objectives, the resources of a graduate student were employed and guided toward construction of a wing model in an attempt to anchor it to the structural dynamic metrics provided by this research. The intent of this section is not to give a full account of every detail of model development, but an overview of the process and the lessons learned from it. A detailed account is offered by [91,92]. With the explosion in the popularity and availability of commercial structural finite element analysis (FEA) software, and with no shortage of FEA models of insect and MAV wings in the open literature, the absence of reporting on wing eigenstructure is surprising. Once a FEM has been developed there is no additional cost to the user, and little computational expense to extract modal parameters. Nonetheless, at the time this research commenced, not a single eigenanalysis of an insect wing model could be found. One paper [70] was published as the current research wrapped up in 2009. The observation is likely due to the dearth of experimental data in existence with which to compare computational models. That is no longer the case, at least for the hawkmoth since its structural dynamic character has now been revealed.

3.7.1 Geometric Modeling

Of course the first step to a FEA is to construct the geometry of the structure. By far the best means of obtaining high fidelity measures of the underlying geometries of the

hawkmoth wing is to take the slice-by-slice approach as used by O'hara [79]. Once again, Figure 16 shows a single cross section of the wing using that approach. Of course hundreds of these sections are needed to reconstruct the geometry which is a tedious undertaking to say the least, requiring hundreds of hours of dissection under a microscope. Another technique, used here, is through the use of computed tomography (CT) scanning, which essentially amounts to a performing a three dimensional x-ray. For this, the capability of the AFRL Materials and Manufacturing Directorate was leveraged. They typically use their CT machine (Figure 53) for investigating debonds within composite materials, so this was definitely a departure for them and outside their expertise. Initial scanning of a dry wing proved quite troublesome. Coating the wing in iodine was one helpful technique used during trial tests. The drawback of iodine treatments was that it tended to crinkle the wing as it dried and induced pronounced corrugation within the wing. As more experience was gained with using the machine and

Figure 53: AFRL's computed tomography (CT) machine employed to obtain the three dimensional geometry, with internal vein features of a hawkmoth wing.

113

its accompanying post processing software, a "sweet spot" of parameters (e.g. beam intensity, target distance, sweep time, resolution) was determined. In the end, iodine coatings were not required as the moisture content of fresh wings aided in arriving at a high quality scan. A full scan took approximately 20 minutes from the time the wing specimen was secured on the scanning pedestal. The wing, which was firmly secured in the same clamp assembly used for system identification and subsequently used during flapping tests (detailed in Chapter IV), was adhered to the scanning pedestal by a small clump of clay.

Figure 54: Example of a wing cross section produced through CT scanning. Hundreds or thousands (depending on resolution of the scan) of these images are created as part of the scanning process. These scans are used to determine vein and membrane thicknesses at locations throughout the wing that are used in the FEM.

A close-up of a wing's cross section created during a CT scan is shown in Figure 54. Several other views of are also shown in Figure 55. During CT scanning setup the user selects a reference length in the scan scene which, in this case was the width of the clamp assembly so that the final three dimensional model and each of its two dimensional "sliced" images that compose it are scaled to physical dimensions. Of course, the real work comes in final post-processing. The model is oriented and cross sections of the wing, like the one show in Figure 54, are examined for dimensional details of vein diameters and wall thicknesses as well as membrane thickness. The cross

114
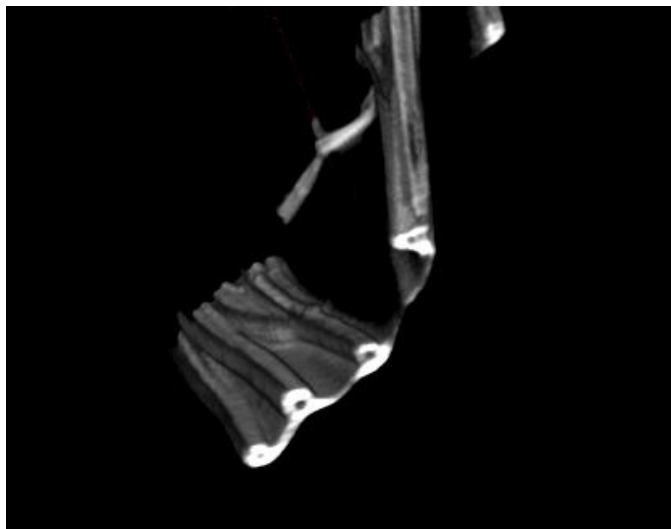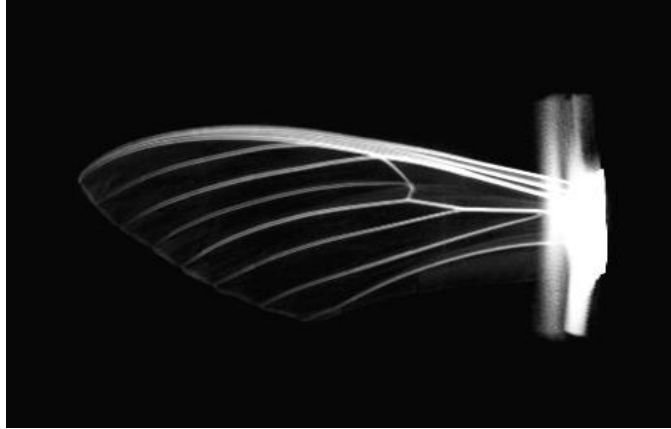
Figure 55: Computed tomography (CT) scans of a hawkmoth wing. The views from top to bottom are the wing's planform, local surface topology, and mid-span cross section. Note the corrugated nature of the wing camber shown in the bottom image. This particular wing was several weeks old accentuating the actual corrugation and camber evident in freshly liberated wings.

sections are examined at carefully chosen stations along the wing's span where natural branch points occur (e.g. where veins converge or bifurcate) as well as at points where vein thickness appears to change abruptly. This process of dimensioning follows exactly as the physical one referenced above, only it is done here with the aid of a computer, not a microscope, and the physical specimen is not involved after scanning. Figure 56 is provided for reference and shows a typical cross section of an insect wing vein and comparing it with the vein cross section shown in Figure 54 confirms that the hawkmoth's veins are decidedly typical.

The relative positioning of veins with each other and over the wing's planform is accomplished by tracing over a CT scan of the planform in the FEA tool (ABAQUS in this case) as shown in Figure 57. From there, cross sectional properties, both dimensional and material, are assigned to each vein element, many of which are divided into several separate elements in order to allow for varying cross sectional properties along the span and chordwise directions as observed in the natural wing. This method of geometric modeling produces a planar finite element, absent the camber seen in the natural wing.

3.7.2 Material Properties

At the time this research was being carried out, material properties specific to the *Manduca Sexta* had not been investigated. O'hara would later accomplish this [79]. Researchers will often use the properties of chitin, which is a very common protein in insect wings, when modeling insect wings. In this case the material properties for the Cicada (*Tibicen Canicularis*) were used as a baseline [70], with the Young's Modulus
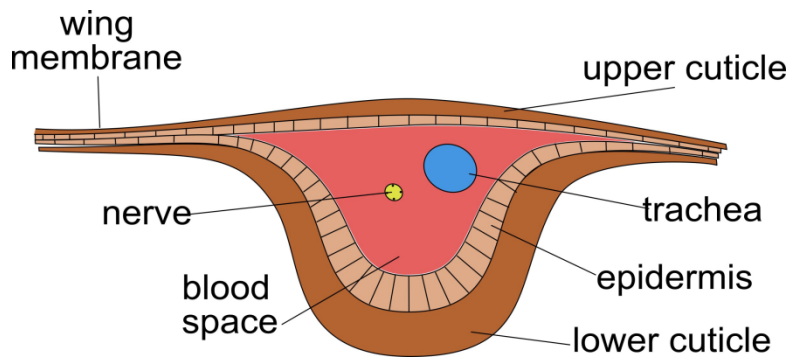
Figure 56: A typical cross section of an insect wing vein. Note that not all wing veins are the same. As Wooton [114] points out, some veins may not contain hemolymph (blood), nerves, or both. The trachea is a small orifice confined to the base of the wing and it is used during initial expression (inflation) of the wing to inflate the wing with air. Image attributed to Caffarilla [10].
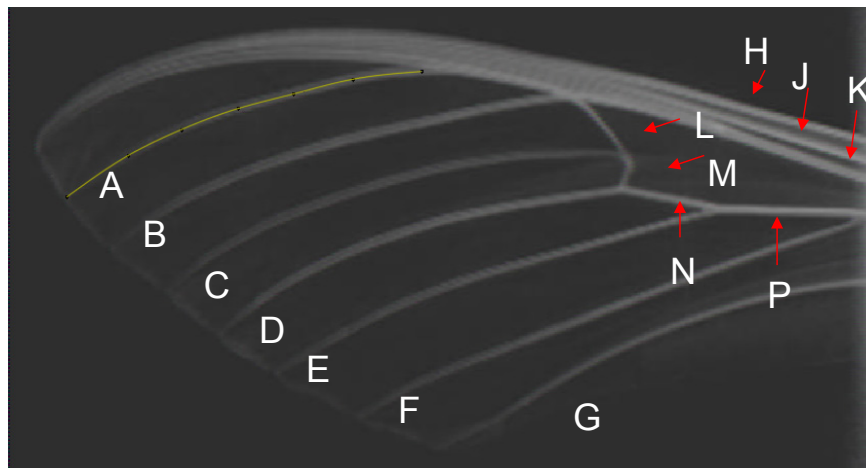
Figure 57: The CT scan of the wing serves as the underlying image for which the vein pattern is then traced in the FEA tool. Careful consideration is given to ensure the dimensions are kept. Once traced, and elements selected, cross sectional properties are assigned to each. Only a single vein (A) is shown traced.

Table 6:   Material properties used in the fourth and final FEM developed in this study. The properties are based on those derived by Mengesha, et al. [70] for a Cicada, with the Modulus of Elasticity of the veins slightly (7.5 percent) increased.

	Units	Vein	Membrane
Density	g/cm^3	2.30	2.30
Moduls of Elasticity	GPa	4.00	1.90
Poisson's Ratio	--	0.495	0.495
Membrane thickness	μm	--	12

of the vein material being increased by 7.5 percent. The final properties settled on are tabulated in Table 6.

3.7.3   Results

Throughout this process, multiple FEMs were constructed using a variety of finite elements and permutations of the material properties in Table 6. With each iteration, a higher level of fidelity than the next was achieved in an effort to ultimately tune a structural model to the experimentally determined structural dynamic parameters documented in section 3.5. Already, as discussed in section 3.6.2, an FEM of the paper wing stencil that matched the experimental results of the paper wing in vacuum had confirmed that the hawkmoth wing had much different mass and stiffness distributions than an isotropic wing analog. Other than the first two modes resembling bending and torsion (Figure 50), its higher modes were more plate-like in behavior and the feather-to-flap ratio of 5 was very different from average hawkmoth ratio of 1.31. A second FEM,

still using isotropic properties but imbuing the wing stencil with camber similar to that observed in the natural wing was developed. The results indicated the flap and feather modes but their frequencies were practically on top of each other with a feather-to-flap ratio of less than 1.09 (compared to 1.31 for the natural wing). A third extraneous mode, resembling more plate-like features than saddle-like was also evident. A third FEM was assembled that effectively amounted to tying vein members to the flat stencil wing having material properties of the membrane. But this model was still planar as the geometric modeling process described it above. With vein elements modeled as beams and dimensioned per the findings of the CT scan, this was by far the most realistic model yet, lacking only the camber of the natural wing. This model also exhibited an extraneous, second spanwise bending mode between the feather and saddle modes with feather-to-flap and saddle-to-flap modal ratios of 2.2 and 7.5 respectively which were markedly different from the natural wing.
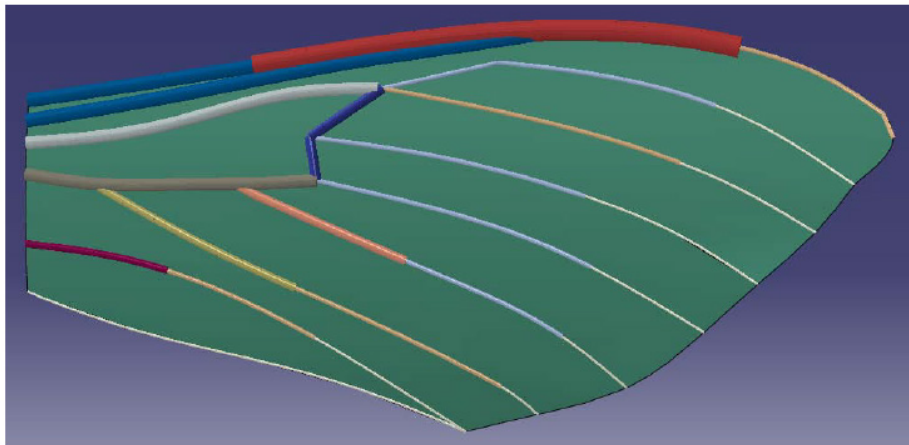
Figure 58: A planform view of the FEM of the hawkmoth wing showing the relative cross sectional dimensions of the veins. ABAQUS did not permit smooth tapering of beam elements.

Finally, a fourth FEM was developed, adding constant camber (15% of mean chord) to the previous model having veins. The specifics of how camber was modeled can be found in [91]. Essentially, the outline of the wing with veins was projected onto a cylindrical surface having a constant radius of curvature. Suffice it to say that it did not capture the true three dimensional detail of the wing. This model, like the others, was developed in ABAQUS. While the other models experimented with various elements, this one utilized the three-noded quadratic beam and four-noded, doubly y-curved shell elements to model the veins and membrane respectively. The material properties from Table 6 were also used. While the cross sections of the beams were sized according to the measurements determined by the CT scan, some creative license was taken since ABAQUS did not permit tapering beam elements. So the natural vein tapering observed in the wing was stepwise tapered. This feature is illustrated in Figure 58. The number of elements in the model was varied from 250 to 80,000 to ensure convergence was achieved. Only modal analysis, employing the Lanczos methodology, was accomplished in order to extract natural frequencies and modeshapes. The experimentally-determined natural frequencies and modal ratios of a hawkmoth are compared side by side with the FEM results in Table 7. It should be noted that the experimental values are for a wing specimen (Moth ID = 54, Appendix B) and not the average parameters reported by Table 5. The modeshapes determined by the final FEM are shown in Figure 59. The most likely reason for the differences in the saddle-to-flap ratio is the simplified approximation of the wing's natural and variable camber. This was clearly a good start for the first two modes but larger error in the third mode persisted. Clearly, more geometric and material model fidelity is needed to better anchor the model.

Table 7:   A comparison between the experimentally determined natural frequencies and modal ratios of a hawkmoth wing specimen with its finite element model.

Mode	Experimental		FEM	
	ω_i	ω_i/ω_1	ω_i	ω_i/ω_1
1	86	1	85	1
2	106	1.23	106	1.25
3	155	1.80	318	3.74
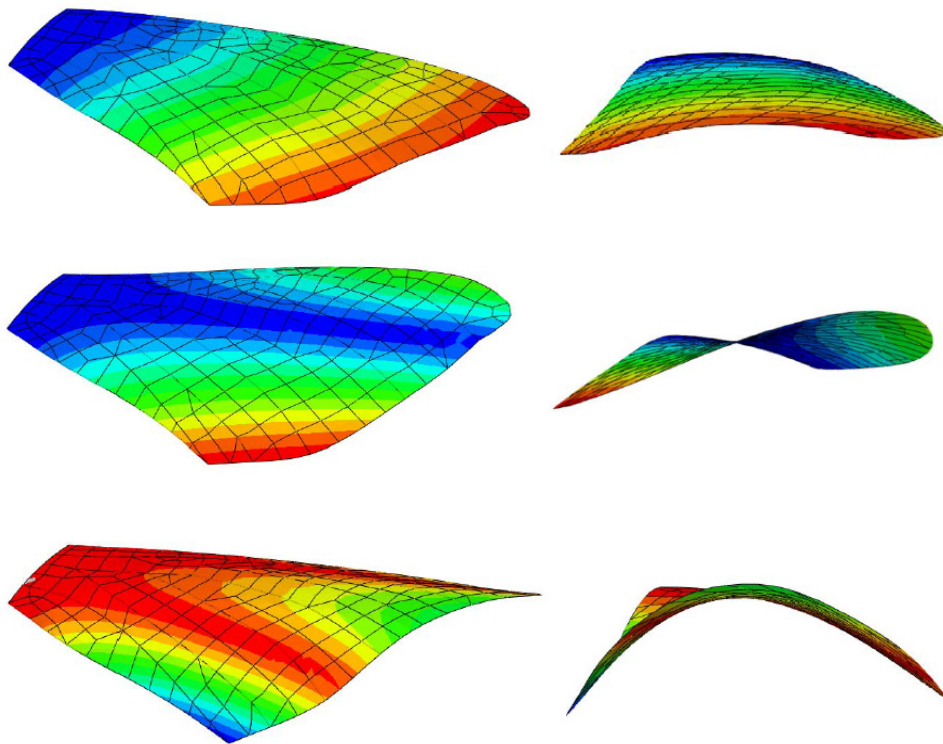
Figure 59: Isometric (left) and front (right) views of the modeshapes generated by the hawkmoth wing FEM. The flap, feather, and saddle modes are shown from top to bottom respectively.

3.8 Secondary Observations

It is virtually impossible to work in a laboratory for nearly two years and not make observations that occasionally challenge one's way of thinking. The following is not meant to be a treatise or to stand up to the absolutes of scientific certainty or scrutiny. What follows are not research claims, just observations and should be taken as such. The reader is free to read into these observations as much, or as little, as they will permit themselves. As Dr. Feynman's words noted at the start of Chapter I, there doesn't seem to be any good place to record such observations in the archival literature, and yet they are at least noteworthy since they bolster or challenge at least a couple of widely held beliefs.

3.8.1 Wing Flapping and Resonance

Most researchers of flapping-wing flight believe that insects exploit structural resonance during flight. Some of that belief no doubt is intuition-based following from the logic that flight is extremely demanding energetically so that Nature must have had a way to offset those demands on the insect, otherwise they might all be crawling. There are some studies that anecdotally suggest resonance [29], but none with concrete proof since nobody has yet been able to point to *the* structure that is resonating. From a preponderance of evidence standard, the findings of this research would seem to favor the resonance belief.

It is widely known that the hawkmoth flaps its wings in hover at approximately 40 Hz and at 25 Hz during traversing flight. The system identification results found that the lowest natural frequency of the wing was for its flap mode which had a sample

population average of 62 Hz with a 95% confidence interval of [53 Hz, 72 Hz]. This implies that the average hawkmoth flaps its wing anywhere from around 60 to 75 percent of resonance during hover, which is the most energetically demanding mode of flight. By referring to Figure 21 and recalling that in air the wing has 5 percent damping, the insect is realizing an amplification factor of around 1.5 to 2.3. That may very well be the "sweet spot" for this particular bug. It is possible that the increased response (deformations) of the wing operating even closer to resonance could drive the wing to a point where the effect may become deleterious. This last point is pure speculation and certainly merits further study. But to the point of operating on resonance, there is no doubt that the wing is operating near (60 to 75 percent) resonance in air while at hover. While not as dramatic of an effect during traversing flight the wing is still operating between approximately 35 to 50 percent of resonance which amounts to dynamic amplification of 1.14 to 1.28. If the relationship between structural efficiency and aerodynamic efficiency is directly proportional then the moth still benefits around 15 to 30 percent more than it would otherwise, which is at least in the direction of goodness for survival.

Some may rightfully point out that only the forewing has been tested here but in actuality the hawkmoth wing acts in conjunction with and literally in contact with its hindwing. That point is true, which would likely drive down the natural frequency of the wing combination even closer to its flapping frequencies, potentially allowing the combined wing to achieve even more benefit. Again that's speculation that only future experimentation could determine.

Finally, there was one moth (Moth ID = 4, Appendix B) that was tested for system ID when it was only a day old. Recall all others were three or more days old. This moth was inadvertently dropped while transferring it from its emergence chamber to the terrarium. Fearing that it may die and faced with the possibility of losing its wing specimens, the decision was made to test it early. It was tested like any other specimen but its natural frequencies were found to be much lower, with its flap mode at 23 Hz. When the moth was retrieved to test its second wing, a droplet of bright green hemolymph (blood) was observed coming from its clipped wing root. Realizing that there may have been blood remaining in the wings, which had never been seen before and not since, the wing was "roller pinned" in a direction from its tip to its root squeezing blood from it. It was quite astonishing how much blood it contained. In fact this wing weighed about 3 times more than the average wing. While at that time an "average" wing was not known as far as modal parameters, it was later determined that this wing, despite being filled with blood was an "average" wing as far as modal ratios were concerned. The feather-to-flap ratio could not be determined because the feather mode, being more difficult to excite in general, was also not excited for this more massive wing.

So where does this all lead to? The question is this: was it accidental that the first natural frequency of this day old moth was 23 Hz, which is nearly exactly the flapping frequency of forward flight *and not hover*? Generally speaking, a newly emerged moth will not take flight for 2 to 3 days while it fully expresses its wings and keeps them inflated with blood and air while the outer layer of cuticle in its wings' veins hardens. During this time they would seem to be the proverbial "sitting duck". But if confronted with a predator and they had to fly (which apparently they can [111]) then the young

moth with its wings weighing three times more than its elders would likely benefit from a resonance at a wingbeat frequency made for traversing flight; and it apparently does. Incidentally, resonating at 40 Hz would not do much good since hover does not move it very fast away from predators. If it is accidental that the newly emerged moth wing has a resonant frequency at its natural traversing wingbeat frequency, then it seems even less likely that it would also share the same ratio of modes with its elders since its wings are full of blood. And yet, somehow that's exactly the case. Both of these points provide further anecdotal evidence that hawkmoths may exploit wing resonance and that the ratio of modes may be a sweet spot for their flight.

3.8.2   A Case Against Passive Wing Response

It is generally accepted, and has been stated numerous times throughout this document, that the wings of insects are passive structures. Lacking any muscles or joints within the wing planform that would allow for articulation, the wing is essentially along for the ride, driven by the aerodynamic and inertial forces that are induced by the kinematic motion imparted at its base. In fact, the whole premise of this research virtually relies on the wing being passive. If it were actively controlled then the passive response might even be irrelevant. But could the insect use a combination of both passive and active structural control?

Early in the research while options were being explored for how to clamp the wing, a wing specimen was placed in a small desktop vice. As the vice was tightened down on the root of the wing a wave of twisting and deforming was observed throughout the wing. As the vice was tightened and loosened the camber in the wing was clearly

125

changing throughout in a fairly predictable manner. Eventually, by cushioning the faces of the vice with compliant foam that molded itself around the more rigid veins at the root of the wing, a suitable clamping assembly was fashioned. As the FEM analysis showed, the wing's structural dynamics are fairly sensitive to cambering effects. Could the insect be exploiting this sensitivity by employing a method of articulating the base of individual or combinations of veins and thereby be controlling wing camber, and hence stiffness actively? Even if it can be shown that they do not or physiologically cannot, might engineered flapping wing designs be able to incorporate such a method of active control?

3.8.3 Blood Pressure Regulated Wing Stiffness/Control

On multiple occasions throughout the course of this research both questions and comments have come from engineers and biologists alike, about the possibility that insects might actively control wing stiffness through blood pressure. In effect this gets back to the passive versus active wing structure argument above. Admittedly this seems like a plausible idea. However the observations made throughout this research suggest that it is *unlikely*, at least for hawkmoths.

Other than the single moth that was tested at 1-day old and observed to have blood in its wings, no other moth was ever observed to have any trace of blood in their wings, despite the numerous attempts to actively express blood from them through a pressing process. It was also reported by the Willis Lab's technician that she has never observed a wing to bleed despite tens of hundreds of tests where she has removed wings, many times without even anesthetizing the moths. Furthermore, on two occasions during this research the full light cycle of the laboratory where the moths were kept after

emerging was disrupted, causing the moths to take flight in the confines of a their small enclosure. In both cases the moths severely tattered their wing fringes but there was absolutely no evidence of blood "sprays" on the sides of the enclosure despite the fact that the veins had clearly been broken at their tips, which would have allowed for blood to freely exit the wing. Furthermore, if blood were in their veins, especially in the amounts that would be needed to pressurize them, the moths that had damaged their wings should have bled out and died, but they did not. In fact they could still fly effectively with the damage. In reality the wing veins are not "veins" in a cardiovascular sense. The "blood space" is only filled with blood in the 2 to 3 days following emergence to keep the wings inflated while the wing cuticle (see Figure 56) hardens. The wing is nourished and kept "fresh" throughout the moth's short life via transport of nutrients through the softer epidermis tissue [29]. All said, even if hawkmoths (or insects in general) do not actively control wing stiffness it does not mean that engineered wings could not employ it through design, though it seems to add unnecessary complexity.

3.8.4   Vacuum Induced Wing Damage

Prior to this research, no research could be found regarding the affects that vacuum conditions had on insect wings. Of course, other than performing system identification on such light-weight structures, it is not clear what other reasons there might be to expose them to vacuum. Furthermore, neither of the two previous attempts at experimental system identification on insect wings had collected any data in vacuum. So this may have marked the first time that insect wings were, at least purposefully, exposed to vacuum conditions. There was some speculation that the wings might undergo

127

structural changes as a result of moisture within the wing's tissue transitioning to a gaseous state which could potentially disrupt the distribution of mass in the wing or even upset stiffness distribution as the transition could damage the wing's microstructure. But speculation was put to rest when it was confirmed through three separate tests (as discussed in section 3.4.2.3) that the wings' structural dynamic properties did not shift from their pre-vacuum test state following exposure to vacuum. In essence, the exposure to vacuum will accelerate the "aging" effects (Figure 43) by drying the wing out faster. But for the relatively short time (less than a half hour) it took to draw vacuum and complete system identification the effects were negligible. Future researchers performing system identification on insect wings in vacuum should have reasonable confidence that exposure to vacuum will not pose deleterious effects on the wing. That said, effects of accelerated aging should be explored in order to account for their impact and to ensure test procedures and timelines are devised that avoid or account for the effects.

IV. Aero-Structural Sensitivity

False facts are highly injurious to the progress of science, for they often long endure; but false views, if supported by some evidence, do little harm, as everyone takes a salutary pleasure in proving their falseness; and when this is done, one path towards error is closed and the road to truth is often at the same time opened.

Charles Darwin [19]

This chapter starts out with a quick primer on the fundamentals of flapping-wing kinematics only to acquaint the reader with some basic terminology and to highlight the complexity of the flapping-wing flowfield responsible for generating fluid forces on the wing. With that in hand, a brief review of previous related research is provided with the work of C&D being more thoroughly considered and examined since its scope was virtually the same as the current research. From there an overview of the kinematics that the wing specimen in this study is subjected to in both air and vacuum will be discussed, showing how it relates to the parameters of a four bar mechanism and then how it differs from the kinematics C&D imposed on their wing specimen. The remainder of the chapter dedicates itself to describing the experimental methodology, from apparatus and procedures to post processing of data and results. The chapter concludes with a discussion of why the results presented here conflict with those of C&D that have, up until now, been the only compelling experimental evidence to indicate a subdominant role of fluid dynamics on wing expression.

4.1 Basics of Insect Wing Kinematics

The flowfield around a flapping insect wing is enormously complex. Of course it is this flowfield, governed by the famous Navier Stokes equations that produce the pressure and viscous forces that act over the surface of the wing ultimately allowing the insect to take flight. Contrast the flowfield over the flapping and rigid rectangular wings shown in Figure 60 with that of the well known and comparatively smooth flow over a well designed rigid airfoil in low to moderate angle-of-attack flows. The differences are night and day to say the least. But in terms of aerodynamic forces whether flapping, rotary, or fixed wing designs, the fluid dynamic forces acting are proportional to the square of the velocity acting over them. The difficulty, of course, arises from knowing that velocity field. In fixed wing, and to a large extent even rotary wing aerodynamics, the velocity is just that of a predictable freestream and the forces can be determined by the well established theory of airfoils (1). But what is the velocity acting over a flapping wing like the one shown in Figure 60?
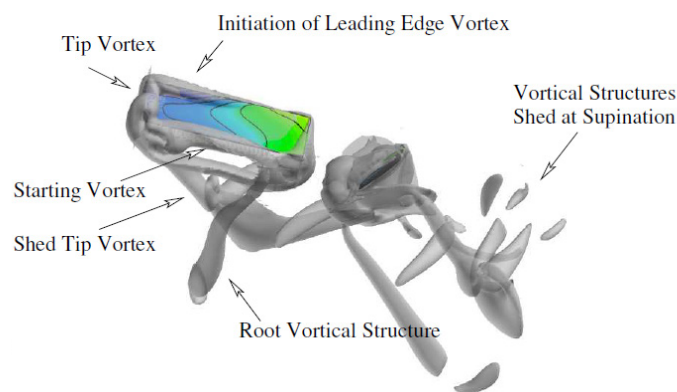
Figure 60: The complex vortical flowfield engulfing two rigid rectangular flapping plates underscores the complexity of the flowfield. Any assumptions of velocity distributions around the wing are tenuous at best. Graphics attributed to McClung [66].

In the case of traversing flight the velocity is at least partly determined by a freestream condition. But it is also setup by the local "stirring" of the surrounding air as the wing heaves and rotates to and fro in three dimensions. As is exclusively the case in hovering flight where there is no freestream, the velocity is also determined by the flowfield setup in the previous wing stroke(s). The wing effectively penetrates its own wake from wing stroke to wing stroke. And, since the wing is the bounding surface that the flow acts over, any changes to its shape (no longer restricting it to the rigid wing of Figure 60) due to inertial and/or aerodynamic loading will work in coupled concert with wing kinematics to setup the flowfield that ultimately determines the velocity field. So the aerodynamic and inertial forces acting on an insect's wing are determined by its structural response, which is inherently tied to its structural makeup and to the flapping kinematics prescribed to it. The kinematics are briefly discussed below.

Researchers have spent decades studying the kinematics of insect flight. What they have found is that flapping kinematics are practically as diverse as the insects themselves. One of the most common, if not the current standard way of describing insect wing flapping kinematics is presented by Willmott and Ellington [112]. Figure 61 provides a pictorial that describes the basic kinematic parameters of sweep, feather, and elevation which are all functions of time and termed $\phi(t)$, $\alpha(t)$, and $\theta(t)$ respectively. Each is a measure that the wing axis (a line connecting a point on its root with a point on its tip) makes with an arbitrary, but conveniently placed inertial coordinate system defined by the stroke plane and the right hand rule. Sweep is the major rotational motion of the wing in the stroke plane and the one that most laymen would call the flapping motion. It is essentially the rotation of the wing about its root chord. Feather is the

rotational motion of the wing *about* its axis. It gets its name from the way in which propeller driven aircraft "feather" their props to reduce drag in an engine out condition. Elevation is rotational motion of the wing axis out of the stroke plane. To make an imperfect analogy, by likening these motions to the more familiar set of fixed wing aircraft motions, sweep, feather and elevation are the rotational motions of the wing about the aircraft's roll, pitch, and yaw axes respectively.

Since insect flapping frequencies vary wildly, from tens of Hertz to more than five hundred, it is very common and convenient to describe the wing's motion in non-dimensional time, τ, by dividing time by the period of the wingbeat. In this way the flapping kinematics of multiple insects can be compared on the same plot. A complete wingbeat is defined as one complete upstroke (beginning with wing supination) and one complete downstroke (beginning with wing pronation) which ends just before the next supination (Figure 62). Pronation and supination are nothing more than the wing feathering (again, rotating about its axis) in a direction that turns the leading edge into the direction of motion of the wing. The wing stroke amplitude (or just wing stroke) is the sum of the maximum sweep angles during upstroke and downstroke. The mid-stroke is generally defined at $\tau = 0.5$ and can technically be at any "position" in the wingbeat. Authors vary on how they define the start of the wingbeat ($\tau = 0$), therefore the position of the wing at the mid-stroke can vary from one author to the next. Many other sources are widely available on the subject of insect wing kinematics that can be consulted. Dudley [29] has a full bibliographic index of nearly 2000 sources with at least two dozen focused on kinematics of insect wings. Suffice to say that this brief introduction to the terminology is more than enough for what follows.
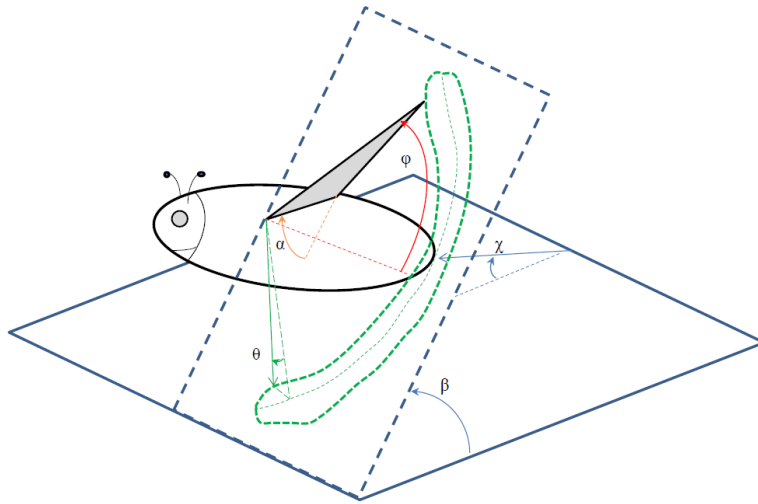
Figure 61: Insect wing kinematic parameters as defined by Willmott and Ellington [112]. The wing's sweep, feather, and elevation angles are denoted by ϕ, α, and θ respectively. β is the wing stroke plane angle and is referenced to the horizontal. Graphic attributed to [4].
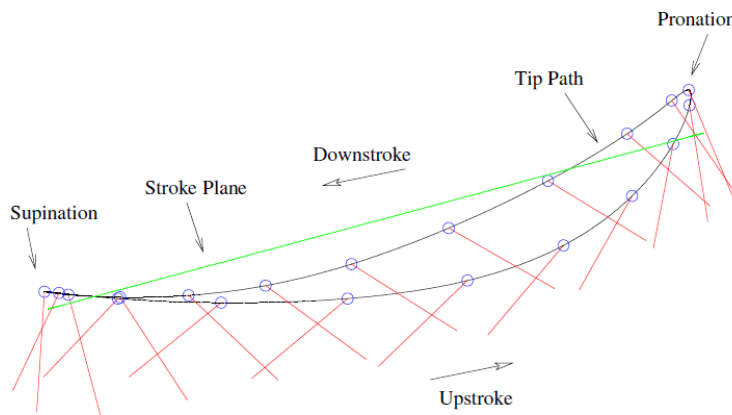
Figure 62: Side view of a flapping-wing chordline illustrating how the wing flips direction (supination and pronation) at the beginning and end of its wing stroke. It is the wing's non-zero elevation angle, $\theta(t)$, that causes the orbital motion of the wing tip. If elevation is zero, then the orbit collapses to a line in this view. Schematic derived from [66].

4.2   Previous Related Work

Prior to the work published by C&D virtually no other research specifically addressing the question of the sensitivity of wing expression to fluid dynamic and inertial loading could be found in archival sources.   While several researchers have sought to determine the relative magnitudes of inertial and fluid dynamic forces in flapping wing flight, none of these works specifically addressed the relative contribution of either to wing expression [36,60,97,107,110,115].   Curiously, but not surprisingly, their results as to which forces are dominant were conflicting.   Arguably, the real value of determining whether fluid dynamic or inertial forces are dominant is to determine if the two can be decoupled so that aerodynamic analysis can be simplified, just as C&D suggested.

While previous researchers had only focused on the forcing side of the equations of motion, which is only half the problem, C&D experimentally considered both the forcing and the resultant structural response.   One researcher team [46] whose conclusions sided with C&D also considered the problem from both sides, but from a computational point of view.   However, their simplifying assumptions largely overshadowed their results and the authors even cited some spurious results in their data, ultimately citing their findings as *preliminary*. So those will not be examined here. Only one other piece of research could be found that directly commented on the contribution that fluid dynamic and inertial forces had on the expression of the flapping wing of an insect. That research was accomplished by a familiar team and along with the work of C&D will be more closely examined next.

4.2.1 Chen, Chen and Chou [12]

This research was thoroughly reviewed in section 3.3.1. As briefly alluded to then, even though their research was centered around extracting the eigenstructure of dragonfly wings their primary motivation was to specifically take on the experimentally derived conclusion by C&D that the forces acting on flapping insect wings are dominated by inertial forces and hence fluid dynamic forces can essentially be neglected in determining wing expression during flight. This team of researchers asserts just the opposite and goes as far as stating that the "conjecture" made by C&D is patently false.

4.2.1.1 Critique
Since the details of their research have already been thoroughly discussed previously an immediate examination of their conclusion is offered now. To quote them directly:

> *Therefore, we conclude that inertial force of the wing is negligible compared to the elastic force during flapping flight. In other words, the wing deformation observed during insect flight is solely due to the balance between the external aerodynamic force and the elastic force of the wing structure. It is noted that this observation is contrary to the conjecture made [by Combes and Daniel].*

Clearly, the authors do not mince their words. But how did they arrive at this conclusion having only studied the structural dynamics of a dragonfly wing? Their conclusion follows directly from what they cited by their system identification results. Specifically, because the natural frequencies they determined for the wing were so much higher than the normal wing beat frequency of the dragonfly that the wing was not operating "near" structural resonance. The authors essentially discard inertial loading completely because the wing is not operating on a resonance. But that conclusion is unfortunately misguided.

If a structure, say for instance an insect wing, were to be placed in vacuum and excited/flapped (research presented in Chapter III proves it can be done without defying any natural laws) would it behave as if it were rigid and exhibiting no expression? To follow the authors' logic leads one to have to accept that it would act rigidly. But that cannot be the case. The affect that acceleration has on mass does not cease to exist in vacuum. To cite Figure 21 one last time, the implication of operating well away from resonance is not to imply that forcing becomes zero. It only implies that the stiffness of the system does not exhibit an inertial "softening" (or potential hardening if forcing frequency is sufficiently high) as it would near a resonance. In fact, in the case of an insect wing being flapped at its base in vacuum the only resulting forces acting on the wing are inertial. It appears that the authors made a simple error in logic. If so, then the findings of C&D stand virtually unopposed.

4.2.2   *Combes and Daniel [14]*

Combes and Daniel (C&D) has been cited in this paper already over two dozen times. When "Combes and Daniel, Into Thin Air" was queried by *Google Scholar* in mid-February 2013, nearly nine thousand (8,890) "hits" were returned. Like the initial survey of literature using the AIAA online database, the metric is not perfect but it lends some credence to the fact that their work is cited by hundreds, if not thousands, of other pieces of research. For that reason alone C&D's work is an important piece of research. But what did they do in their experiment and how did they arrive at their conclusion? This section will provide an overview and critique of their work.

4.2.2.1 Experiment A freshly severed hawkmoth forewing was mounted by glue to the shaft of an electric motor and placed into a cubicle acrylic chamber (Figure 63). The wing was then flapped at 26 Hz sinusoidally at approximately +/-50° sweep angles. As the wing flapped back and forth, high speed cameras positioned 90° apart recorded the motion of the wing that had been marked with small dots of reflective paint. The test was accomplished in air first and then in a helium rich environment measured at greater than 95% concentration (or 15% equivalent air density). A custom *Matlab* routine was then used to analyze individual video frames in order to measure the positions of the reflective points in angular degrees from the center of rotation of the motor axis. The points were tracked for three consecutive wingbeats.
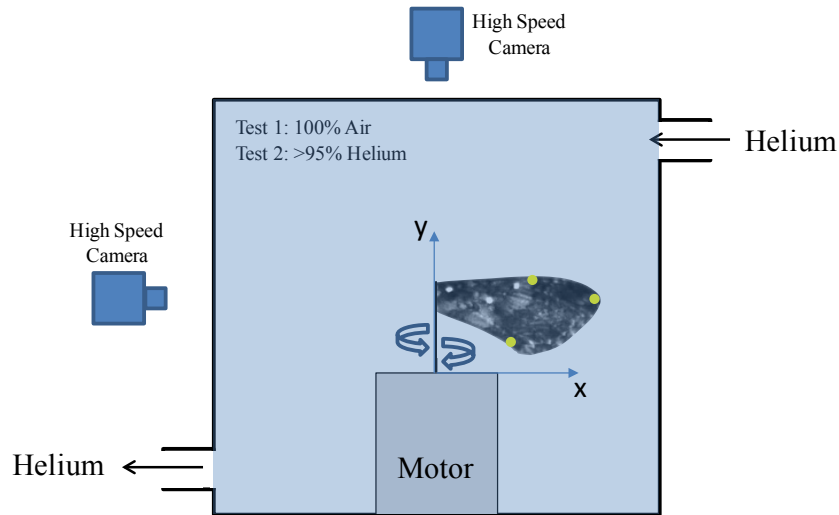
Figure 63: Functional schematic of the apparatus used by C&D. A cubicle acrylic chamber housed a flapping motor with shaft that a hawkmoth forewing was glued to at its root. The wing was marked with 3 reflective paint dots on its leading and trialing edges and at the wing tip. Tests were accomplished in 100% air and >95% helium. High speed cameras positioned 90 apart captured the motion of the wing as it flapped at 26 Hz at +/-50° sweep angles. Graphic derived from original paper [14].

4.2.2.2   Results   The traces of each of the marked points of the wing are plotted in Figure 64 which were digitized from their original paper and presented here for convenience. As part of their experiment C&D also filmed the wing (in air) as it was slowly rotated (at 2 Hz) to establish a "non-deformed" baseline wing with which to compare the deformed flapping wing in both air and vacuum. Since that data is largely redundant and argues the same point it is has been excluded here. They also provide results of a hawkmoth forewing FEM they developed and an oversimplified analytic assessment of the ratio between the magnitude of aerodynamic and inertial loads on the wing. Both are too simplified to significantly corroborate their findings so they too are excluded here. If their evidence compels one way or the other, it is their experimental results alone. Readers are encouraged to consult the original paper for those secondary details.

Since the traces of the points (actually angles) on the wing in both air and helium matched rather well, C&D concluded that the effects of fluid dynamic forces on wing posture were negligible. This followed from their argument that the helium environment, having only 15 percent the density of air, would yield aerodynamic forces only 15 percent of those in air since aerodynamic loads are directly proportional to density. With dramatically different fluid dynamic loads acting on the wing one should expect different deformation patterns (expression). But since the expressions, at least as measured by 3 dots on the wing, were not substantially different they concluded that fluid dynamic forces must be negligible as compared to inertial forces as far as their overall contributions to wing expression.
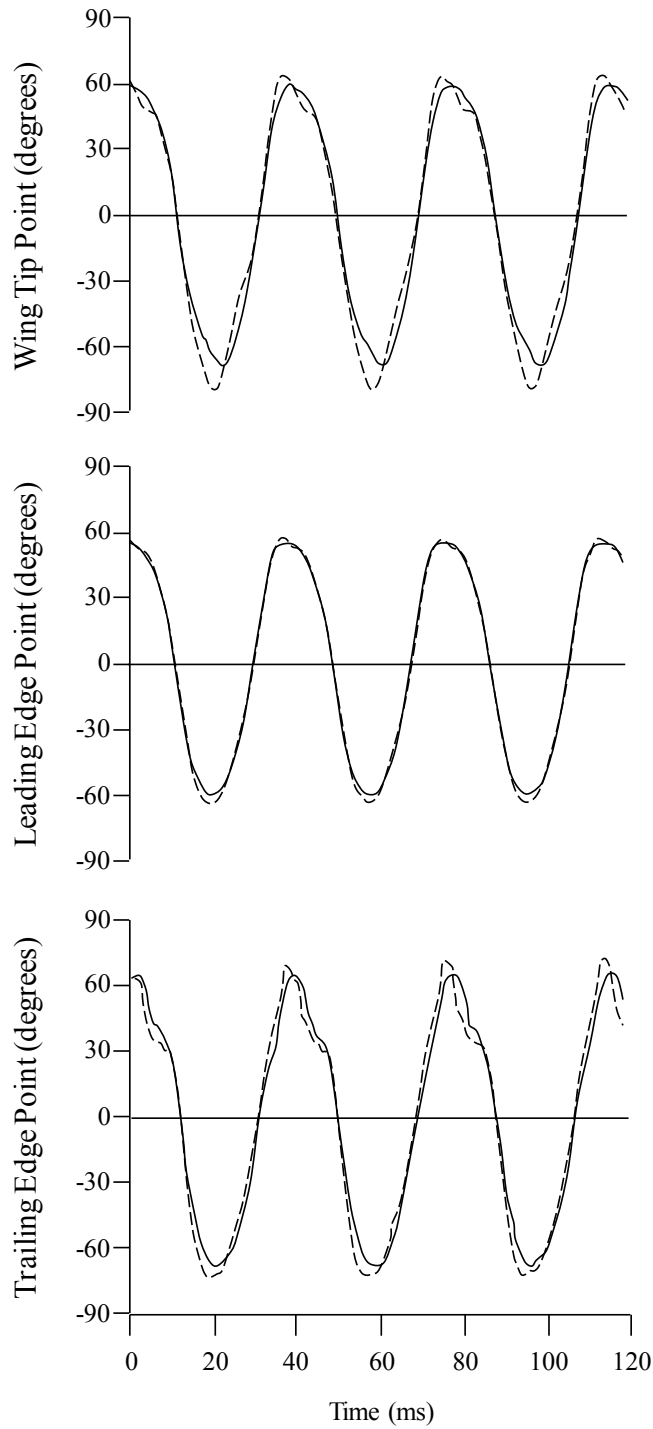
Figure 64: Traces of the angular positions of three distinct points on the severed forewing of a hawkmoth over three wing beat cycles. The points were measured from frames of two high speed cameras that filmed the wing while it flapped in air (solid line) and helium (dotted line) at 26 Hz. Plots derived/digitized from Combes and Daniel [14].

4.2.2.3 Critique One may legitimately argue that a more accurate kinematic representation of wing motion (which will be discussed in the next section) would make a stronger case. However, the fluid dynamic loads that C&D imposed on their hawkmoth wing (in air) may likely have exceeded what an actual wing experiences during flight since they prescribed a pure sweep kinematic whereas an actual hawkmoth would tend to reduce load on its wing by streamlining itself with the oncoming flow through active feathering. So, it would appear that C&D have tested for a worst case which bolsters their argument. Their results would have also been bolstered by eliminating the presence of any aerodynamic loads by operating the wing in vacuum.

By far, the single greatest issue with their experimental approach, perhaps even its Achilles heel, is in the metric they use to measure expression. In tracking the three points on the wing, they only consider the relative angle that each point's position vector makes with its projection onto the x-z plane as defined by Figure 63. This approach effectively "squeezes" out the other two dimensions/coordinates needed to describe a point in three dimensions and can be potentially misleading. In fact, further examination of their own video footage that they have made available to the public [73] suggests the possibility that their metric is flawed since the video seems to show stark differences in bending patterns between the wing operating in air and helium. Admittedly, the quality of the web-based video is poor, so it is difficult to draw definitive conclusions based on it. But the almost obvious finding from the video suggests a much different conclusion than C&D have asserted. Figure 65 and Figure 66 both show raw frames at two instances in the wingbeat cycle in the wing's upstroke and downstroke respectively. Below each raw frame is the same frame annotated with the approximate shape of the wing's leading edge
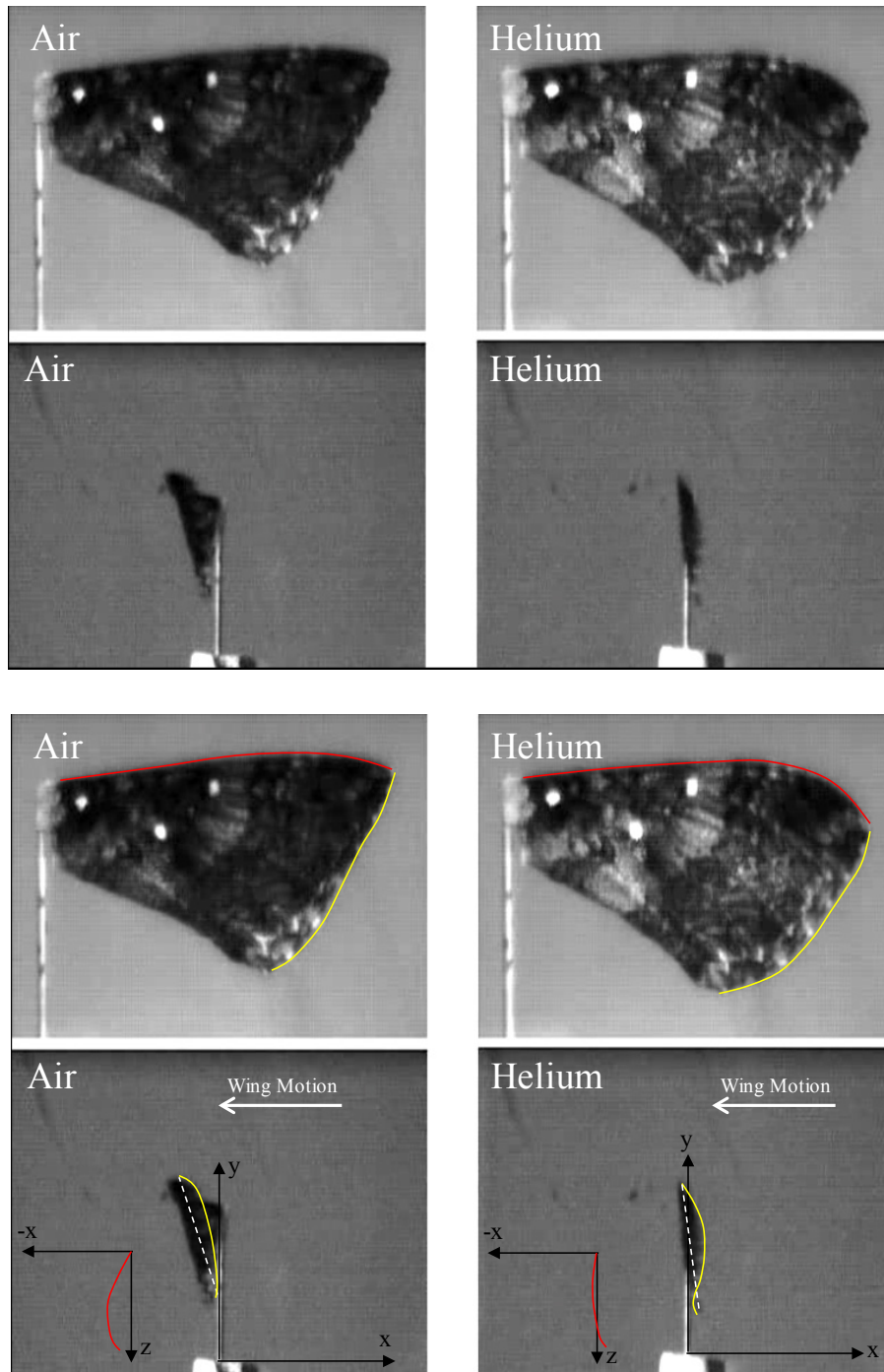
Figure 65: Top: Raw frames from high speed video footage captured by C&D of a hawkmoth forewing flapping in air and helium. Bottom: An estimate of the shape of the wing's leading edge and tip and its tip chordline based off observations of the actual video. Images derived from archived video [73].
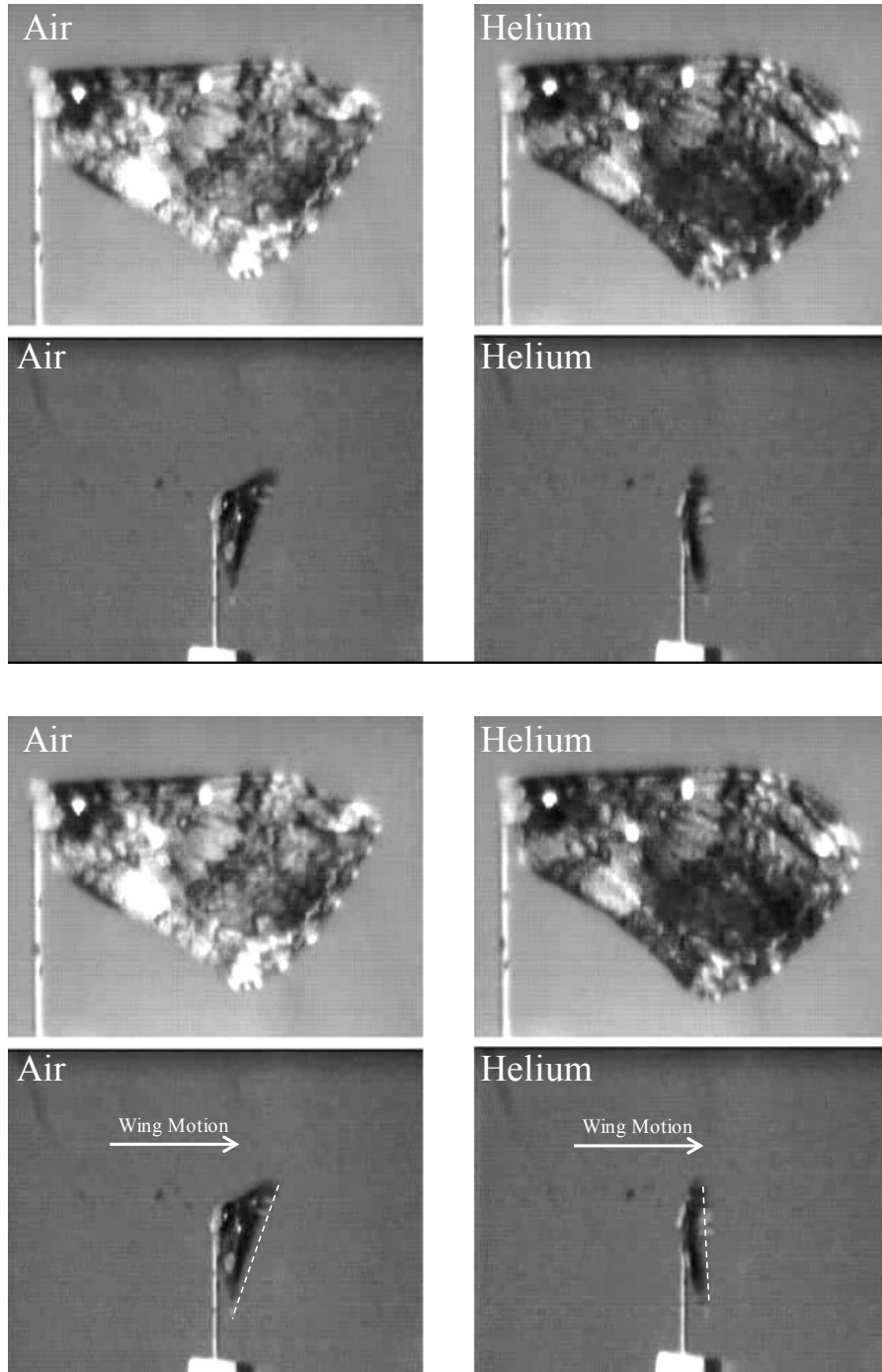
Figure 66: Top: Raw frames from high speed video footage captured by C&D of a hawkmoth forewing flapping in air and helium. Bottom: An estimate of the tip chordline based off observations of the actual video. Images derived from archived video [73].

and chordline near its tip. Multiple subjects were asked to independently review the video footage and each came to the same conclusion that there appears, at least qualitatively, to be dramatic differences in the wing expression between flapping in air and helium. The problem of determining differences between two relatively complex shapes in space really requires a field of point data (or point cloud). Many more points are needed to gain confidence that the shapes are in fact similar.

This critique is not meant to minimize the work of C&D at all. In fact their work was extremely novel and has caught and held the interest and adulation of many aerodynamicists who have been inclined to cite their results. But clearly there are grounds to take another look and either corroborate their findings or refute them by using more state of the art methodologies. In fact, both of the weaknesses of C&D's research that were largely imposed by limitations of their equipment can and will be rectified in the current research.

4.2.3   Hawkmoth-Specific Wing Kinematics

Before providing the wing kinematics of the hawkmoth it is worth describing how they are determined. In his book, Dudley cites three primary ways that insects kinematics can be determined; free flying, tethered, and captive [29]. All methods require a way to record synchronous images at high speeds from multiple cameras at various angles so that they may be analyzed by one of many photogrammetric methods in order to ascertain meaningful wing position and angular details throughout the insect's wingbeat cycle. It turns out these may be the least of all challenges. Trying to derive meaningful data from an uncooperative bug can be next to impossible.

The free flight method is certainly the preferred method for quality of the data but the logistics of following an insect around make it virtually impossible not to mention there is no ability to control test parameters (like wind speed, heading, etc.) as the insect strays about. About the only useful data that can be collected this way is flight trajectory. So, not surprisingly, virtually no insect wing kinematic data exists from this method. Tethered flight is exactly that. The insect is constrained physically by a thread or other device attached to its abdomen so that it cannot fly freely. As one might imagine, this is the best way to ensure high quality imagery by keeping the subject in focus at all times but the results are tainted by an insect that may be operating under great stress. Many researchers in fact will pay little mind to the results gleaned from this collection process. Finally, the balance between the two previous methods are to limit the volume in which the insect can fly by an enclosure and entice it or hope that it flies into the field of view of multiple cameras for long enough durations to gather imagery. Even then, the nature of high speed camera usage demands the subject be flooded with light which is known to disorient insects. Of course even in these tests insects that would not otherwise be in this environment must be induced to fly rather than by choosing to do so through free will. Dudley quotes two French biologists (Magnan and Planiol) who have studied insect flight and wing kinematics and they had this to say (translated):

> *In effect, the majority of insects are endowed with a temperament that seems to the operator to be essentially capricious, their actions generally unforeseen, weird and discouraging.*

Many other researchers have shared similar frustrations by the lack of consistency of wing kinematics not just within species of an insect, but even with the same insect

specimen during the same test. This discussion is specifically offered before providing the actual kinematics of the hawkmoth in order to clarify that all insect wing kinematic data must be approached with some caution. In many respects its gathering is more an art than a science. In general, however, there are certain features of the wing kinematic of an insect that are shared across the species. In the case of the hawkmoth, the wingbeat frequency during hover is about 40 Hz and around 25Hz to 27 Hz for forward/traversing flight. Furthermore wing stroke is around 100° with a slightly larger sweep angle on the upstroke. It has a slight out of plane motion (elevation) but comparatively flat when compared to other insects and a fairly dramatic but symmetric feathering motion during upstroke and downstroke. Figure 67 and Figure 68 show top and side views of a hawkmoth in hovering flight at three different points within its upstroke and downstroke. Figure 69 provides a qualitative view of the degree to which bending occurs in the wing during flight. It should be noted again, that the hawkmoth has a forewing and hindwing and these images are shown with all wings in-tact. Finally, Figure 70 describes the kinematics of *a* hawkmoth wing as derived by Willmott and Ellington [112,113] which were determined through a captive method; even though they refer to it as "free flight". The next section describes the overall experimental methodology employed including the kinematic that the wing specimen in this study was subjected to and the approach for achieving it.

$t/\tau = 1/6$

$t/\tau = 2/6$

$t/\tau = 3/6$
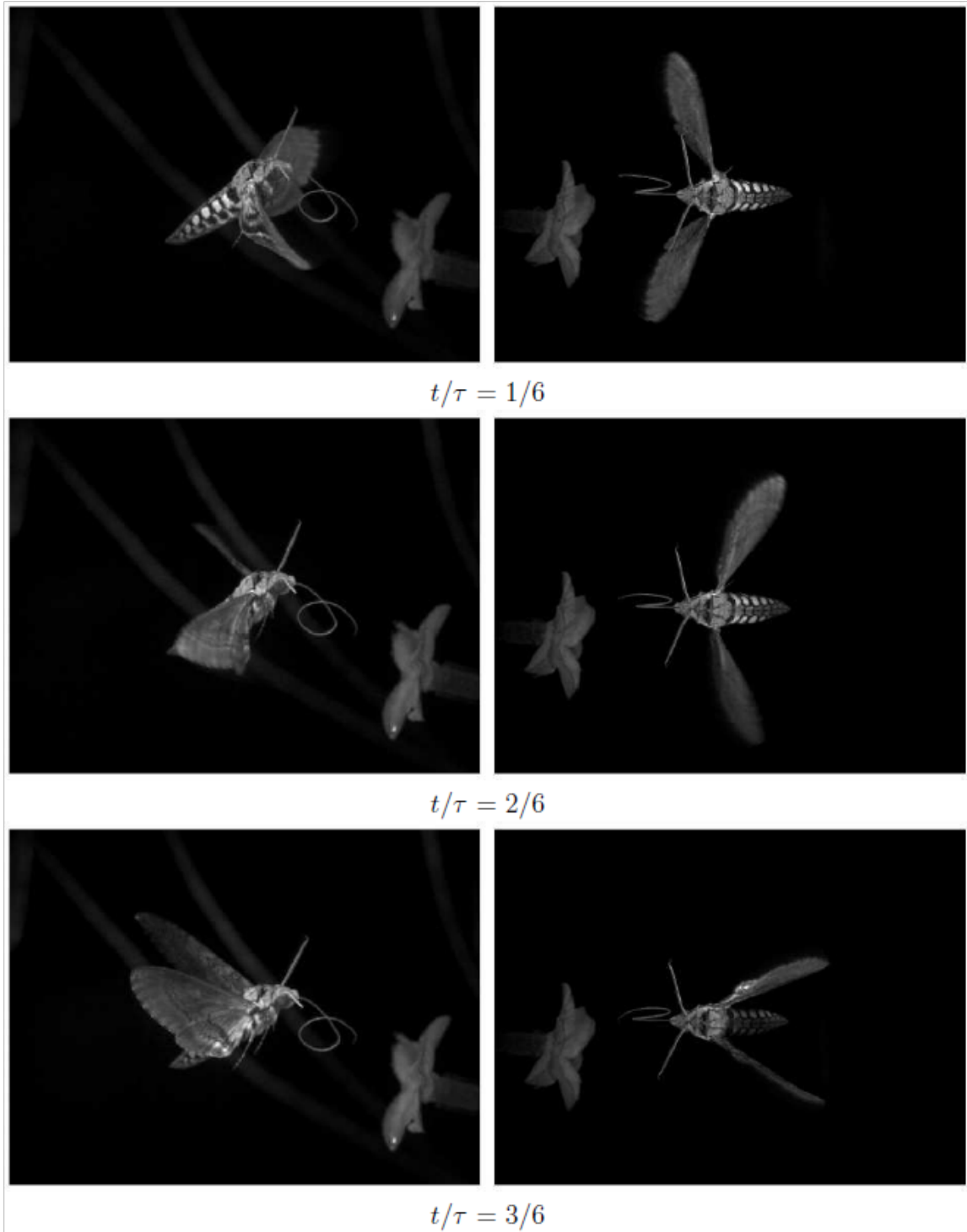
Figure 67: Snapshots of the side view (left column) and top view (right column) of a hawkmoth in hover at three distinct positions in the wing *upstroke* [66]. Each image represents a frame extracted from high-speed video footage captured by Hedrick [50] for use in extracting kinematic data.

$$t/\tau = 4/6$$

$$t/\tau = 5/6$$

$$t/\tau = 6/6$$
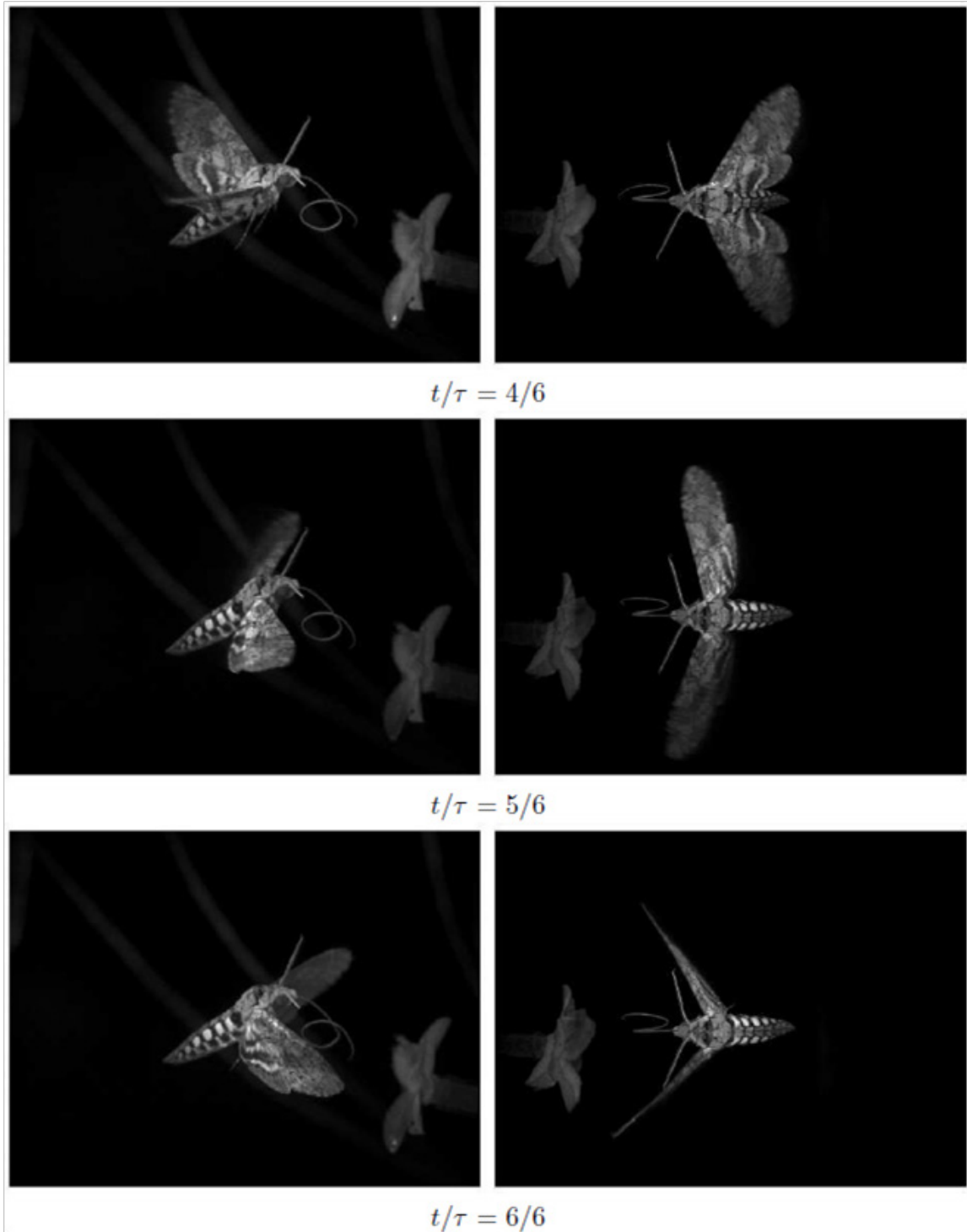
Figure 68: Snapshots of the side view (left column) and top view (right column) of a hawkmoth in hover at three distinct positions in the wing *downstroke* [66]. Each image represents a frame extracted from high-speed video footage captured by Hedrick [50] for use in extracting kinematic data.
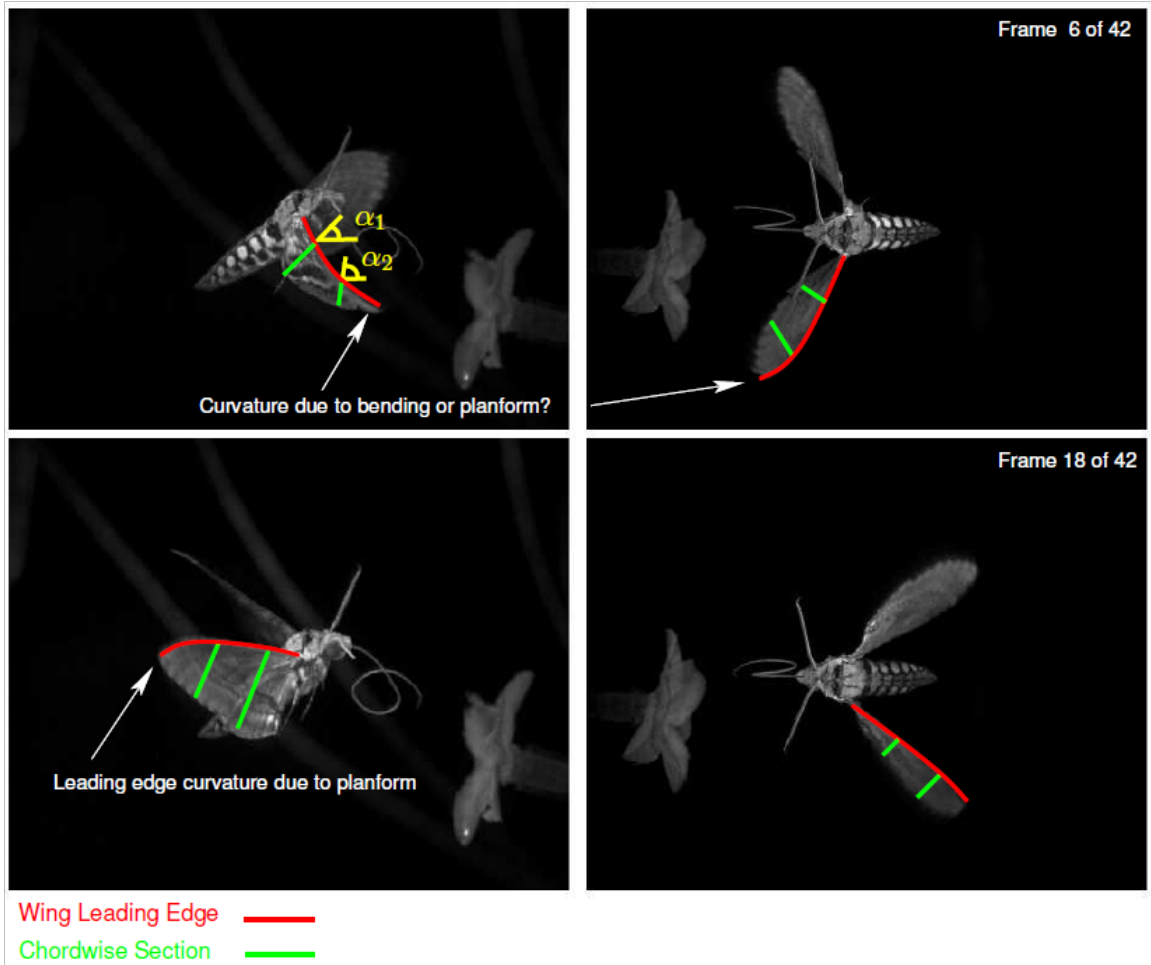
Figure 69: Side and top views of the hawkmoth during hover. The images underscore the difficulty and even subjectivity of extracting wing deformation data from the frames of high speed video. However, qualitatively significant wing deformations are apparent. Image attributed to [66] derived by Hedrick [50].
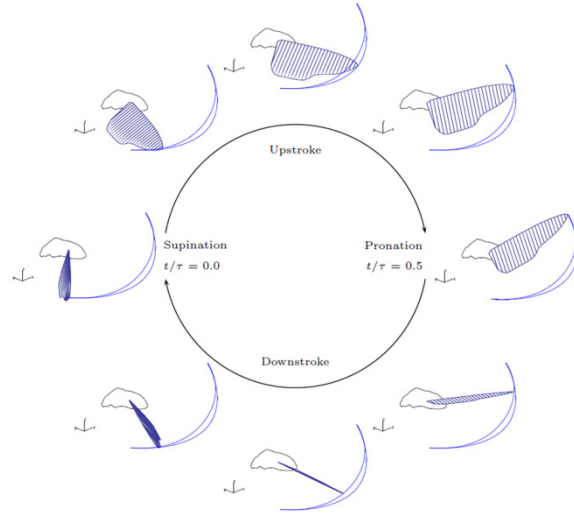
(a)
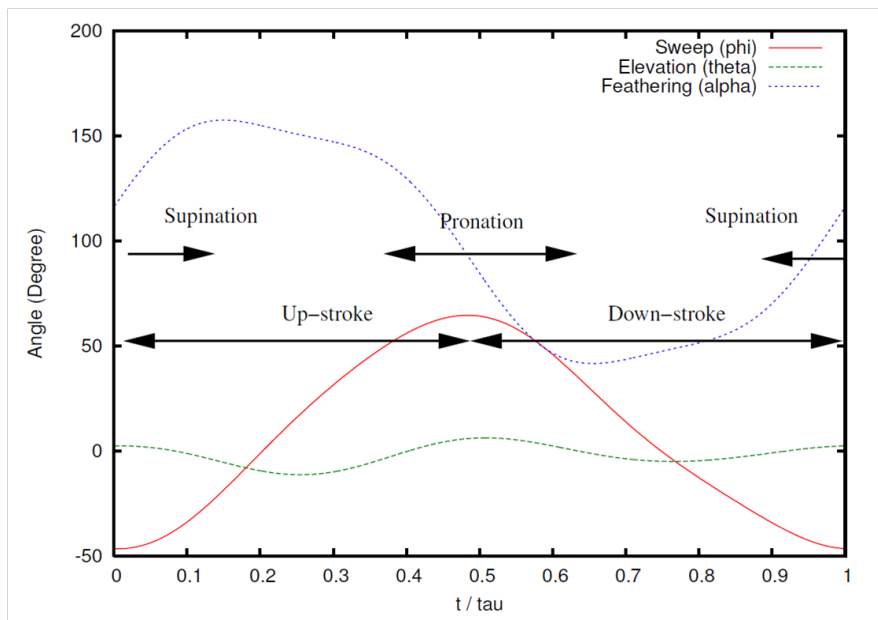
(b)

Figure 70: Graphical depiction of a hawkmoth wing's flapping kinematics during hover (a) with plot of wing sweep, elevation, and feathering angles throughout a single wing-beat cycle (b). Note that the "wing" here is a composite overlay of the fore and hind wing. Smooth kinematic data derived from Liu [62, 61] and Aono [5] based on experimental data of Willmott and Ellington [112,113]. Graphic attributed to [66].

4.3   Experimental Methodology

This section discusses the experimental methodology employed to directly compare the expressions of a hawkmoth's forewing flapping in air and vacuum. It starts by explaining the motivation for the wing kinematics employed by the study and then presents brief overviews of the major components of the experimental apparatus to include a discussion of the motion capture hardware.

4.3.1   Equipment

4.3.1.1 Wing Flapping Mechanism   The decision on which wing flapping kinematics to impart to the wing was carefully considered from multiple vantage points. First, to match every detail of the kinematic parameters as defined in Figure 70 would be a significant undertaking. The MAV research community has been pursuing programmable kinematic mechanisms but the state-of-the-art has not yet arrived so the reality of trying to mimic detailed motion was quickly abandoned. Second, as discussed in the previous section, the kinematics of insects even within the same species and sometimes the same insect specimen, can be all over the map so that tying the research to the way one "bug" behaved during one study did not seem overly necessary or useful. Third, and more pragmatically, in the very early stages of developing a research vector and when the research was heading in a very different direction a flapping mechanism was developed and was therefore already available. By simply changing the mechanism's four-bar parameters and inventing a way to mount the wing it could easily be suited for this purpose as well. Finally, and most importantly, since the research was largely aimed at providing another point for comparison to the results by C&D, by

departing significantly from their imposed kinematics might invite scrutiny if the results turned out to conflict with their findings. With all of these considerations in mind, it was decided that only the sweep kinematic (ϕ) of Figure 70 would be approximated.

Before getting to the specifics of the mechanism, it is important to also understand that when insect wing kinematics are experimentally determined as described in section 4.2.3, the measured kinematics are the *outputs* of the kinematic inputs imparted at the base of the wing. Because an insect's wing is flexible and its response to forcing largely passive, it is a difficult problem to know what kinematic *input* is required to yield a specific kinematic *output*. Rather than iterating on an iterative design-build-test-assess process in hopes of better matching W&E's kinematic data, a more subjective approach was taken. Because the wing has inertia and is inherently flexible its response will be in the opposite sense of the imparted kinematic at the beginning of both the upstroke and downstroke. Shortly thereafter, the elastic energy in the wing is released and the wing springs back in the direction of the imparted kinematic, potentially even overtaking it. So at times the wing's response (output) will appear to be leading its kinematic input while at others times it may appear to lag. The degree to which the wing leads or lags its kinematic input is a function of the balance between the inertial, elastic, and aerodynamic forces acting on it that are implicitly a function of its geometry and material/structural properties as well as the nature of the kinematics imparted on it. Without knowing all of these coupled responses in a priori, there is no way of knowing how this lead/lag behavior will manifest. With this complexity in mind the kinematic input was chosen so that it would "undershoot" and "lead" the kinematic trace provided by W&E. The actual rigid body wing sweep kinematic that was imposed at the wing's base is shown in

Figure 72, denoted as the "AFIT Mechanism" and is compared with both W&E and the sinusoidal input used by C&D. A schematic of the four-bar mechanism that produces the motion of the AFIT mechanism is shown in Figure 72. The next step in the process was to fabricate the new mechanism with these four-bar parameters.
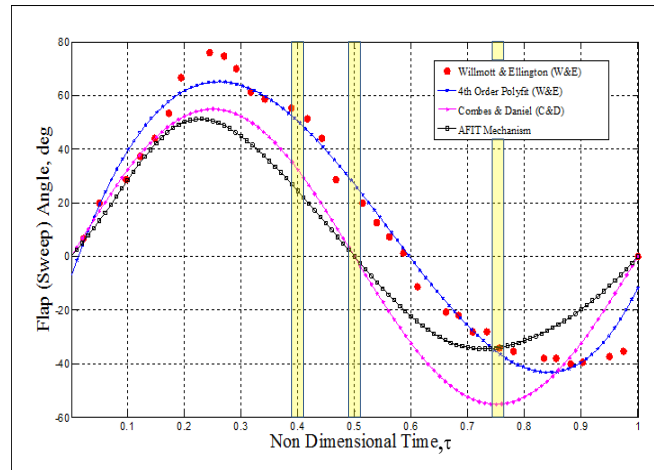
Figure 71: Comparison of the flapping (sweep) kinematic of the custom made flapping mechanism (AFIT) with that of the actual hawkmoth wing in flight (26 Hz) as recorded by Willmott & Ellington [112,113] and the approximate harmonic kinematic used by Combes and Daniel [14].
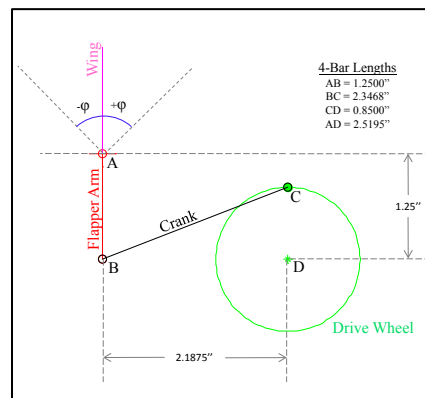
Figure 72: A schematic of the 4-bar mechanism with the relevant dimensions annotated. Points A and D are the centers-of-rotation of the wing and drive wheel respectively, and are fixed to ground to constrain translation.

Figure 73:   The 3D printer used to fabricate the major parts for the flapping mechanism.

The major components of the mechanism were designed in *SolidWorks* and printed on a 3D printer as shown in Figure 73.   A rendering of the three dimensional model of the mechanism is shown in Figure 74 and detailed drawings of each component of are provided for reference in Appendix C.   The flapper/rocker utilized the same insulating foam and sandwiching approach for wing clamping and was designed so that it could be conveniently mounted directly to the shaker head and used in system identification testing.   A small, electric, hobby class R/C motor (Figure 75) was used to drive the mechanism.   The drive disk was mounted to the motor shaft through the use of an adaptor (Figure 76) typically used for mounting propellers to hobby class R/C aircraft.
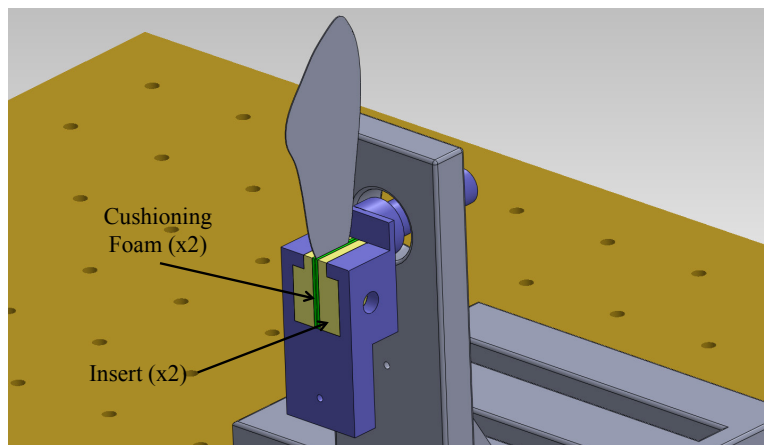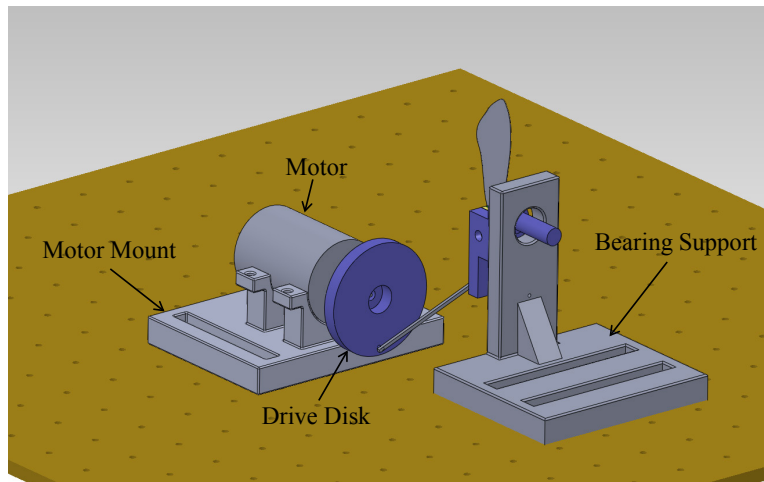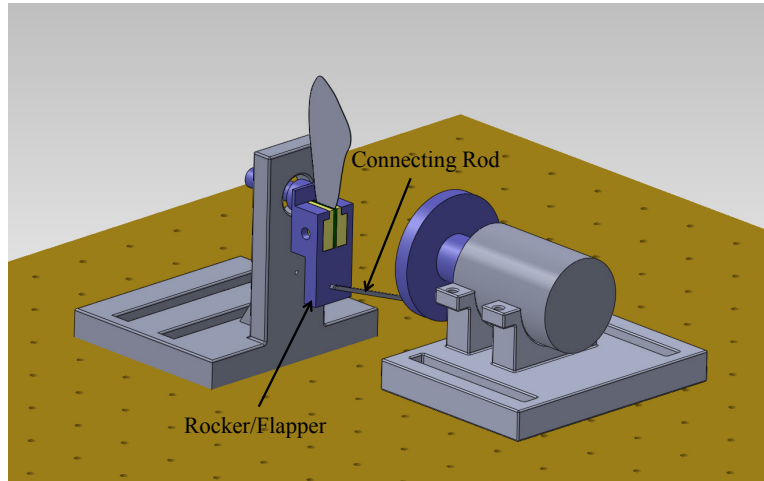
Figure 74:   Front and rear isometric views of the flapping mechanism (top, middle) and a close-up view of the flapper/rocker.

Figure 75: The *Titan 550* hobby-class electric car motor used to power the flapping mechanism. Specifications: 14.4V, 23-turn, fan-cooled. Dimensions: 3.07 inches end-to-end; 1.46 inch can diameter; 0.125 inch shaft diameter.

Figure 76: Rear (collet) and front (thread & nut) views of the self-centering, collet-type adaptor used for attaching the drive wheel to electric motor shaft. The collet side of the adaptor attaches directly to the motor shaft. The drive wheel slides over the threaded end and is held in place with the washer and nut.

4.3.1.2 Motion Capture To capture the wing's expression at specified positions in its wingbeat cycle stroboscopic photography and state-of-the-art photogrammetric software (*PhotoModeler Scanner*) were employed. Motion capture techniques and a version of the *PhotoModeler* had been used in previous research at AFIT [17,81] but none had utilized stroboscopic motion capture techniques nor the new

155

dense surface modeling algorithm used for extracting surfaces of three dimensional objects captured from different vantage points by multiple images.

The components of the motion capture system are shown in Figure 77. A Nikon D80 digital SLR camera with a 50mm fixed focal length lens was used to capture images of the flapping wing whose motion was "frozen" by strobe lights that were triggered at the same frequency as the flapping mechanism. The strobes were triggered when a small piece of reflective tape, affixed to the mechanism's drive disk, passed by the projected beam of an appropriately positioned and stationary infrared emitter/sensor. The phaser-type strobe lights allowed for their triggering at a specified time (or phase) relative to the passing of the reflective marker (Figure 81F), thus providing full control over freezing the wing at any given "position" in the wingbeat cycle. Two strobe lights were utilized in the arrangement. One was placed on the chamber's top acrylic pane and pointed into the chamber to provide ambient and diffuse lighting from above. The other was held and actively position by an assistant to cast light directly on the wing specimen and to avoid any shadows while digital images were taken with the camera from multiple angles.

Figure 77: Only three components were needed to capture and record the expression of the wing. From left to right are the phaser-strobe light, infrared emitter/sensor, and digital SLR camera. Captured images were subsequently processed by the commercially available *PhotoModeler* software to extract 3-D wing expressions.

To maximize the accuracy of *PhotoModeler's* dense surface modeling algorithm, the use of a "calibrated" camera and "coded markers" were employed as recommended. Due to subtle manufacturing variations the optical parameters of every camera lens are unique to it, slightly skewing and distorting the rays of lights that pass through it. Of course this is generally not a problem unless high fidelity photogrammetric measurements are to be gleaned from the images. To calibrate the camera, 12 pictures of the calibration grid (Figure 78) are taken and subsequently processed by *PhotoModeler* for use in image processing. Three images are taken from each side of the grid by either rotating the grid or moving around the grid while it lays on a table or floor. Pictures are taken with the camera held in landscape, right portrait, and left portrait orientations. Coded targets (Figure 79) were affixed to the mechanism and to the bottom of the vacuum chamber to aid PhotoModeler in auto referencing common point across images and for improving overall accuracy of the 3D point clouds it produces.

4.3.1.3 Integrated Apparatus   The flapping mechanism was placed within the same vacuum chamber (Figure 24) used for system identification testing and firmly secured with screws to the base plate piloted with threaded screw holes (Figure 99, Appendix D). The entire experimental apparatus is shown in Figure 80, with a close up view of the mounted physical mechanism shown in Figure 81.
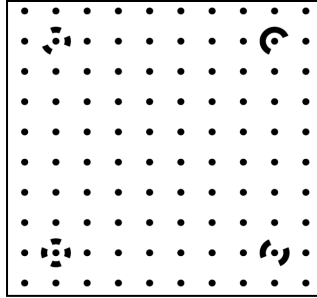
Figure 78: A calibration grid used to calibrate the digital camera for photogrammetric analysis performed with the *PhotoModler* software. A 12x12 inch grid like this was photographed for calibration.
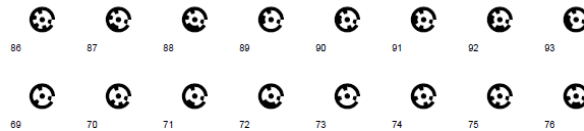
Figure 79: Coded targets used to correlate and reference objects across multiple images using the *PhotoModeler* software tool. Nearly 100 markers were affixed to the mechanism and chamber to maximize point cloud accuracy.
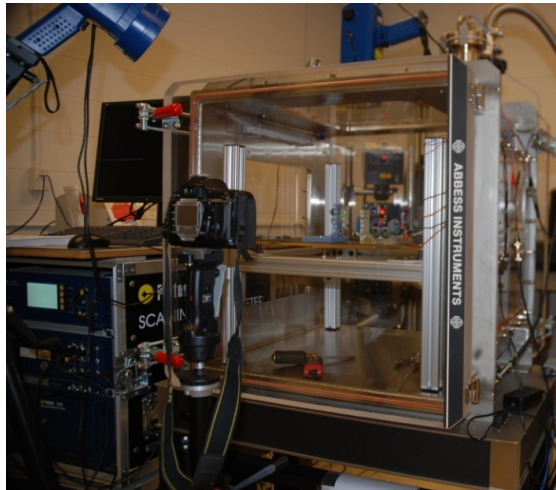
Figure 80: View of the entire aero-structural sensitivity testing apparatus. It consisted of a transparent vacuum chamber, standard digital SLR camera, two phaser strobe lights (blue colored devices) with infrared emitter/sensor, and a flapping mechanism (see close-up in Figure 81). Virtually no changes in setup between system ID and aeroelastic testing were required. The laser vibrometers heads can actually be seen through the chamber on close inspection.
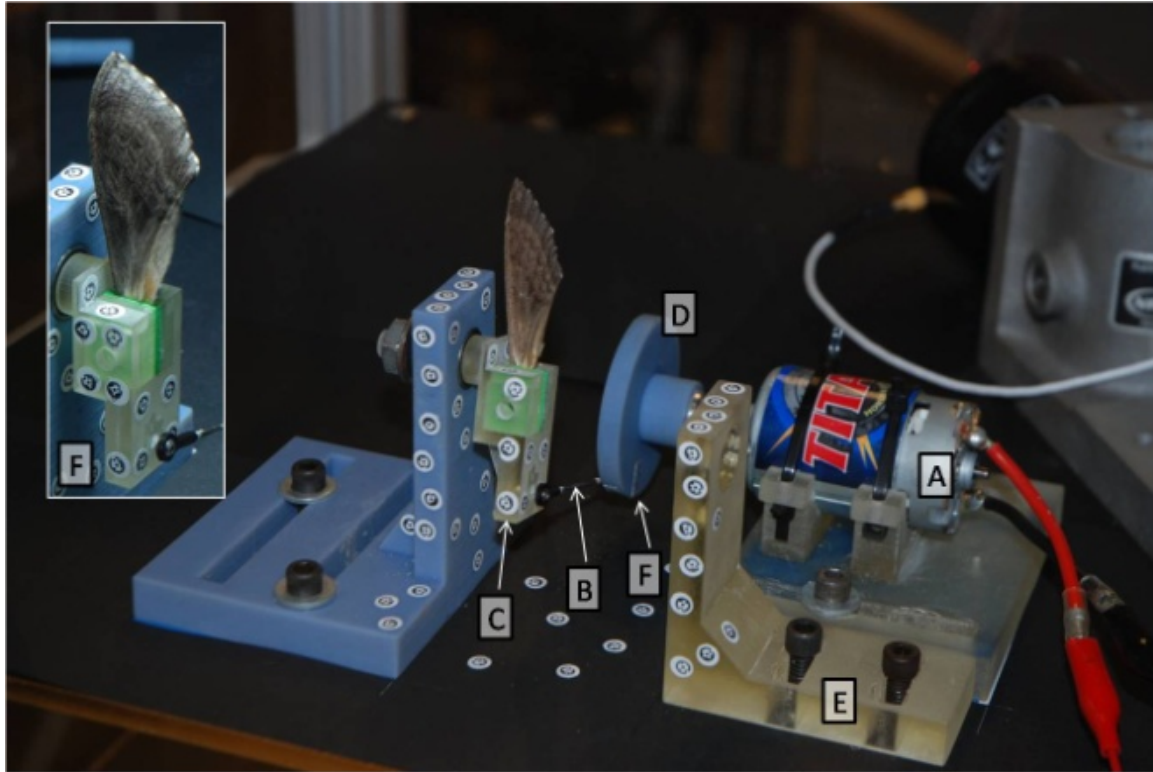
Figure 81: A close-up view of the flapping mechanism used in the aero-structural sensitivity test. The DC hobby car motor (A) is connected to an adjustable external power supply for controlling flapping frequency. With the exception of the motor and metal crank (B) that connects the flapper arm (C) with the drive disk (D) all components are made of rapid prototype plastic and were printed on a 3-D printer. Small coded markers are affixed to the mechanism and surroundings to provide photogrammetric references. The L-bracket (E) is utilized for the sole purpose of adding additional markers to the scene. An infrared emitter/sensor (Figure 77) triggers a set of strobe lights each time a small piece of reflective tape (F), attached to the drive disk, passes by the emitter. Note the presence of the green foam within the flapper arm illustrated in the graphical inlay (F). The final variant of the wing clamp employing a "sandwiching" method was "built-in" to the mechanism's flapper/rocker arm.

4.3.2   Procedure

Extreme and careful consideration was given to the relative camera positions for individual photos, the position of coded markers in the scene, lighting, and overall image quality. Poor image quality, camera positions, or calibration errors necessarily implied failure in reconstructing the wing's 3-D expression from the series of images taken during test. Prior to final wing testing a trial and error approach on a series of test wings was undertaken in order to achieve the best possible arrangement of strobe lighting and camera positions as well as the camera parameters (aperture, exposure, shutter speed, etc.). This process took over a month of full time lab work to perfect. Once perfected, actual testing and image capture took just a few minutes that would produce sub-millimeter accuracy of resulting point clouds.

Just before the "official" aero-structural sensitivity test commenced, system identification and CT scanning of a liberated hawkmoth wing (Moth ID = 54, Appendix B) was accomplished as described in Chapter III. Approximately 40 minutes later, the rocker arm with wing already inserted was attached to the flapping mechanism previously firmly mounted in the vacuum chamber. The doors of the chamber were closed and the mechanism brought up to 25 Hz flapping frequency. The ambient room lighting was dimmed and strobe lights activated. The phase of the synchronized strobes' was adjusted to freeze the wing in one of three pre-determined position of the wingbeat cycle (τ = 0.4, 0.5, 0.75). At each position no less than six photos (Figure 82) were taken of the flapping, but stroboscopically frozen wing. Once all images were collected for one position, the phase of the strobes was adjusted and the process repeated for the next position. After all positions were digitally photographed in air (765 Torr), the flapper

was turned off until the chamber was drawn down to vacuum (300mTorr). The same process for each position recorded in air was completed again under vacuum conditions.

Before terminating the test, the vacuum's venting valve was slightly opened allowing the pressure to slowly rise in the chamber. With the wing still flapping at 25 Hz and the position of the wing still frozen with the strobes ($\tau = 0.4$) the wing's expression was observed to change dramatically, indicating that the wing was beginning to be loaded by aerodynamic forces and in fact deforming. This single observation was literally breathtaking, proving that wing expression was clearly – and dramatically – affected by fluid dynamic forces. With the chamber pressure nearing ambient, the vent valve was closed again and the chamber drawn down to a "soft" vacuum of 100 Torr. This
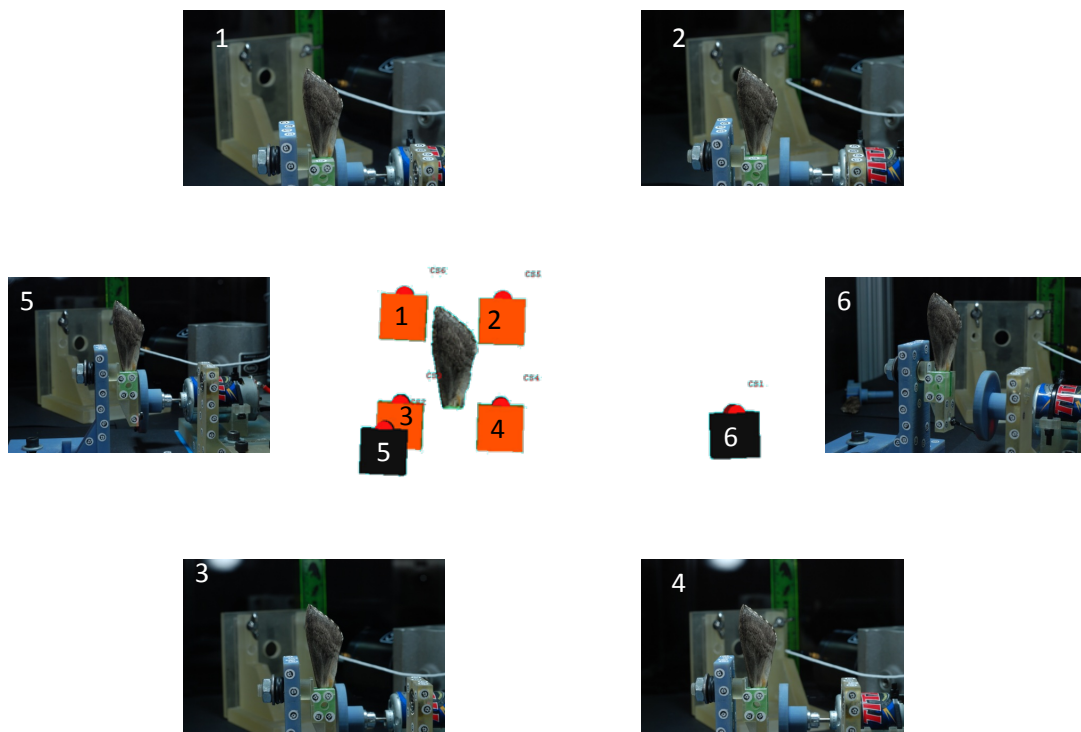
Figure 82: Sample images from one motion capture sequence. The quality of the images is remarkable considering they were taken under stroboscopic conditions.

intermediate pressure was selected in order to capture wing expression at a chamber air density of approximately 13% which was close to the equivalent air density of 15% that C&D had tested at. Again, images were taken as before and the test completed.

The sets of recorded images were analyzed using the *PhotoModeler* dense surface modeling *(*DSM) algorithm which produces point clouds (over 200,000 points on the wing surface) that approximate the surfaces of objects contained across multiple images. The process is part automated and part user interactive. The details of the algorithm are beyond the scope of this paper but can be attained at the company's website [196] where they have many useful links to technical papers on the subject. It is worth pointing out that not all objects lend themselves to the methodology. Objects that do not have a mottled or contrasting surface finish are not good candidates. Luckily, the hawkmoth wing is highly mottled with large contrast across the wing and is ideally suited for DSM methodology.

4.4   Experimental Results

Simply stated, dramatic differences were evident between the expressions of the forewings of a hawkmoth flapped in air and in vacuum. Figure 83 through Figure 86 say it better than any summary could (additional images are shown in Appendix E). In viewing these figures consider that the small arrows at the bottom right of each image are oriented to point in the direction of the wing's trailing edge. Small numbers are also included near the arrows. The best way to review the images is sequentially. Imagine the wings to be rotating along a vertical axis in the plane of the paper. In referring to them consider the age-old adage that "a picture is worth a thousand words." Clearly, by

162
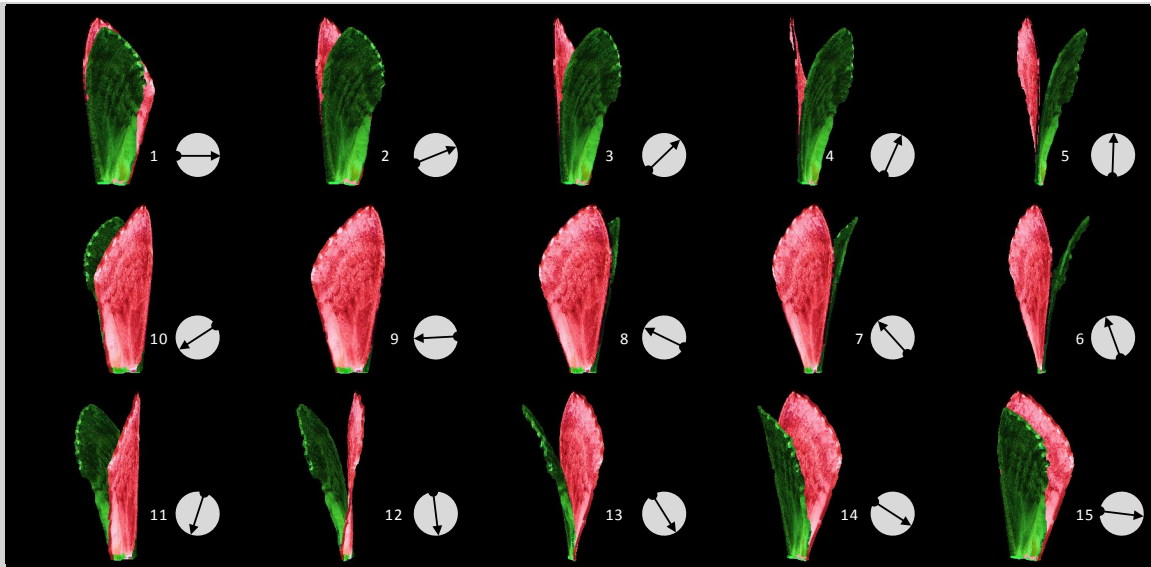
Figure 83: (25 Hz, $\phi = 27°$, Downstroke, $\tau = 0.4$, Air (red),Vacuum (green)). Each wing image is a point cloud consisting of over 200,000 points.
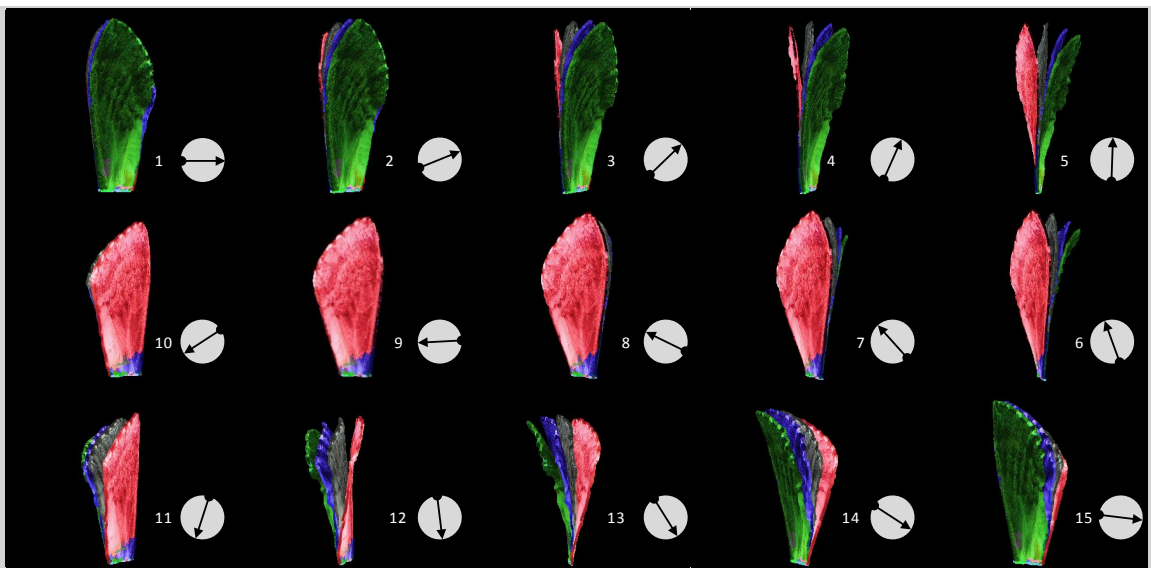
Figure 84: (25 Hz, $\phi = 27°$, Downstroke, $\tau = 0.4$, Air (red), Vacuum (green), 100 Torr (blue), Rigid (grey)). Each wing image is a point cloud consisting of over 200,000 points.
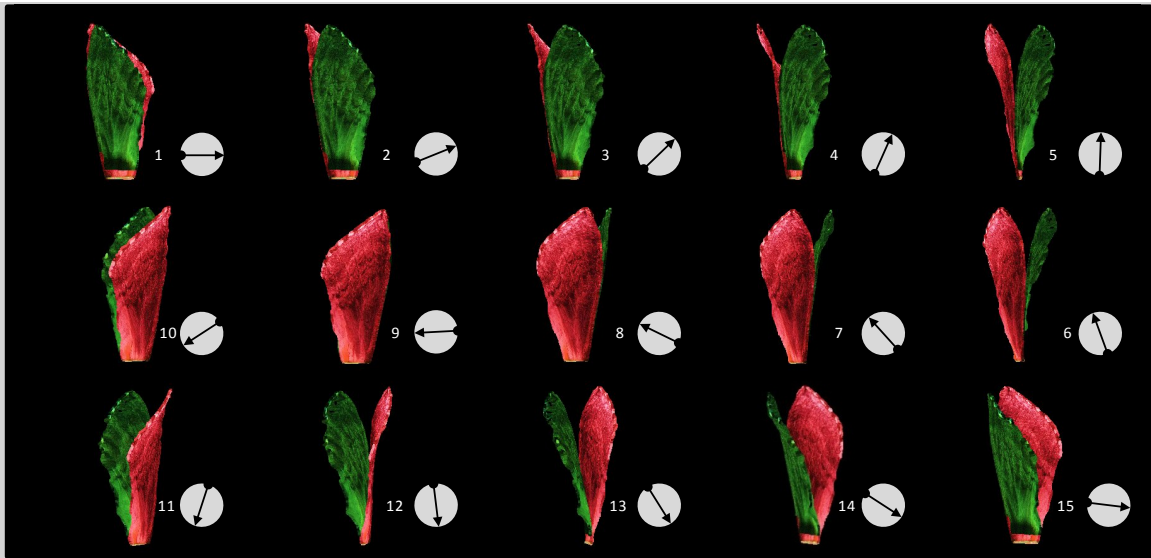
Figure 85: (25 Hz, $\phi = 0°$, Downstroke, $\tau = 0.5$, Air (red), Vacuum (green)). Each wing image is a point cloud consisting of over 200,000 points.
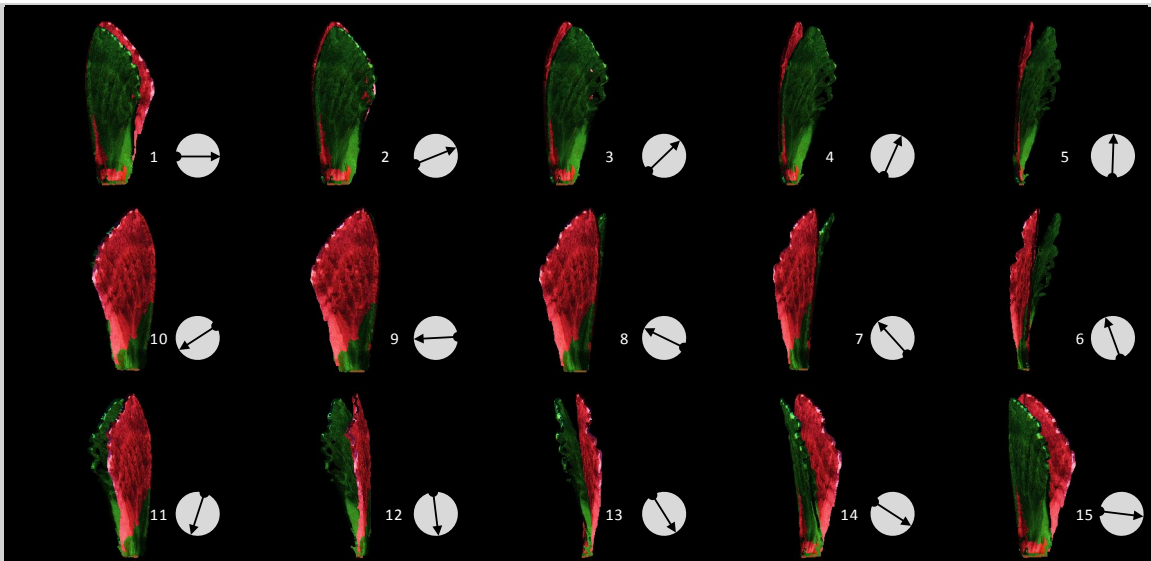
Figure 86: (25 Hz, $\phi = -34°$, Upstroke, $\tau = 0.76$, Air (red), Vacuum (green)). Each wing image is a point cloud consisting of over 200,000 points.

comparing the flapping wing's shape in air (shaded red/pink) with that in vacuum (shaded green) the differences are profoundly evident. Because the wing posture is truly a three dimensional, full-field phenomenon, only a 3-D view/model of the expressed wing can provide the reader with a true appreciation for the dramatic differences that these images attempt to illustrate.

While one cannot hope to communicate the complex nature of the wing's expression with a single number, Figure 87 shows a comparison of the sweep angles between a rigid wing undergoing pure rigid body flapping kinematics (RBK) as applied to the actual wing in this study, with that of the deformed flapping wing in air (765 Torr) and vacuum (300 mTorr). By referring to Figure 87 the wing acting in vacuum appears to "lead" the kinematic input at 0° and 27° sweep angles during its downstroke (DS). The likely scenario for this observation is that the wing is actually "snapping" back from its sweep reversal at $\tau \approx 0.2$ as strain energy in the deformed wing is released. As this potential energy is converted to kinetic energy, the wing's momentum catapults it back toward the rigid body kinematic (RBK) input. With virtually no air resistance to impede its motion, the wing must have enough momentum to "carry it" past the RBK input now acting to retard the motion of the catapulting wing, effectively decelerating it and causing it to flex in the direction of prescribed motion. To look at the images seems almost counterintuitive; yet on close examination the physics seem to make perfect sense. In the case of the wing acting in air at these same sweep angles, the air works in part to extract kinetic energy from the wing and limit/dampen its response while also setting up a flow field around the wing that prescribes a pressure field acting over its surface and contributing to the wing's resulting expression.
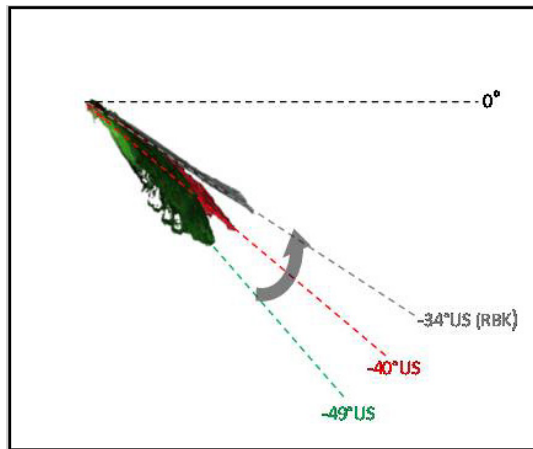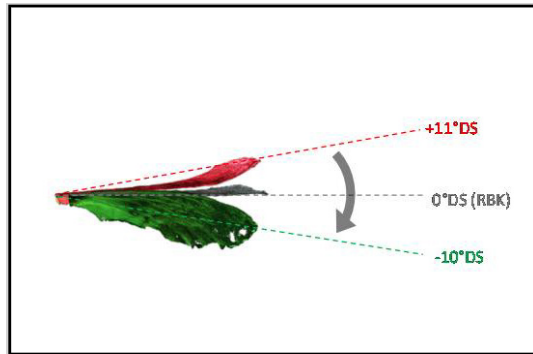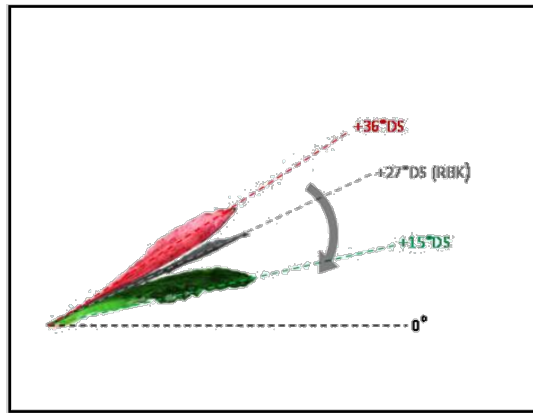
Figure 87   The differences between the wing expressions of the hawkmoth's forewing in air (red/pink) and vacuum (green) at the respective position in the wingbeat cycle. The grey wing labeled "RBK" (rigid body kinematic) is the position that a fictitious rigid wing would take for the given kinematics. Its slight, but apparent expression is due to the hawkmoth's natural wing having camber at rest; not due to applied loading.

The goal of this portion of the research was essentially to determine if significant differences existed in the expressions of a flapping hawkmoth forewing in air and vacuum in order to corroborate or refute the findings by C&D. Ultimately the evidence found herein runs counter to their findings. Clearly both conclusions cannot be right. To judge which conclusion is more credible consider the differences in methodologies employed. The current approach improves upon C&D's experiment in two ways. First, the affects of a surrounding fluid medium on the wing were eliminated by drawing down chamber pressure to 300 mTorr (0.0004 atm, 0.006 psi). Second, while C&D's approach tracked the motion of only three discrete points on the wing, the current method was able to capture nearly the entire field of wing expression. While these wing expressions were only investigated at three separate positions in the wingbeat cycle for archival purposes, the wing's expression was observed in the laboratory to be very sensitive to the presence of the surrounding air throughout the entire wingbeat cycle and Figure 83 through Figure 86 corroborating that observation. The conclusion of this research is that *the expression of the hawkmoth's forewing is determined by inertial __and__ fluid dynamic forces that act upon it during flapping.*

V.   Conclusion

A theory is something nobody believes, except the person who made it. An experiment is something everybody believes, except the person who made it.

Albert Einstein [53]

5.1   Structural Dynamics

The intent of the structural dynamic portion of this research was to develop a robust methodology for performing structural dynamic testing (system identification) on an insect wing and to present the finding for a hawkmoth forewing. To that end the research was successful. Furthermore, the goal was also to reveal the underlying eigenstructure of an insect wing; essentially for the first time ever. To that end the research was also successful.

But as important, or even more so, return for a moment to what motivated the search for the eigenstructure in the first place. It stemmed from asking the initial question of *what is truly common among flying insects.* At that point there was truly no expectation that the eigenstructure itself might actually be that feature. The results however would appear to suggest just that. Eigenstructure appears to be a common trait, at least among the insects tested in this research. And, the apparent small variability observed in the hawkmoth results alone seems to support the notion that it *may* be an important trait for flight of these agile fliers. Considering the connection between a passive structure's eigenstructure and its response to forcing, it is exceedingly hard to

conceive of it not being important for the flight of flapping-wing insects. Indeed it is the wing structure that responds to and acts upon the airflow so how could its underlying structural dynamic nature not be important?

There are certainly other features of insect wings, like roughness or small corrugations to name just two, not to mention the kinematics of the wing stroke that affect aerodynamics. But, to draw an admittedly imperfect analogy, the eigenstructure is to the flapping insect wing what the underlying wing structure is to the fixed-wing airfoil. It sets up the instantaneous wing shape and, along with rigid body wing kinematics and freestream conditions, the local airflow features about the wing that taken together determine aerodynamic response. Nobody would argue that seemingly negligible features of the wing (fixed or flapping) cannot produce, enhance, or degrade flow phenomenology that could have appreciable or even dominant roles on the wing's overall aerodynamic response; aerodynamic theory is clear on that. But the aircraft designer does not throw out the contribution of the airfoil to achieving desired fixed-wing aerodynamics; good designs start with the airfoil. Perhaps the eigenstructure will prove to be a starting point for small flapping-wing designs of the future.

One of the major questions from the totality of the system identification results of this study is why? Why should these very diverse creatures, having wildly different scale, planform, venation pattern, and even wingbeat frequency and kinematics, be so similar in their underlying eigenstructure? Is there something about these modeshapes that have made them successful adaptations for flight? Perhaps a "golden" design rule? How many other insects share these modeshapes? Are they all required for flight or just a subset? How important are the modal ratios and what happens when they're upset? It

is too early to answer any of these. Hopefully the findings and insights presented by this research will motivate future research to consider how the eigenstructure presented herein and hopefully still to be revealed in other insects, might benefit flight and even answer some of the questions posed above in the process.

5.2 Aero-Structural Sensitivity

The objective of this portion of the research was ultimately to determine if a hawkmoth's wing expression is affected by the fluid dynamic forces that act on it. The answer turns out to be a resounding "yes". Wing expression is clearly a coupled response between inertial-elastic and aero-elastic forces. The conclusion reached here obviously conflicts with results by Combes and Daniel [14] (C&D) which up until now had been the only noteworthy experimental data available on the subject. But the equipment and methodology employed by the current research was far superior to theirs and the results should therefore be more reliable. The downside to the conclusion here is that unlike C&D's conclusion, it underscores the need for a coupled aero-structural model to analyze the aerodynamics of flapping wings. In truth, that has always been most aerodynamicists intuitive sense anyway, but C&D's conclusion, albeit now tenuous, did provide some glimmer of hope that there could be an easier way out.

5.3 Contributions

There are five contributions that this research provides the broader flapping-wing MAV research community. The first is that an experimental framework for the systematic extraction of the structural dynamic parameters of an insect wing has been

developed. Future researchers may leverage the experimental methodologies fine tuned by this research to extract the modal parameters from countless other inset wings in order to compile a database of modal parameters that can be used for anchoring future bioinspired engineered and computational wing models. Second, for the first time ever, the eigenstructure of an actual natural insect wing has been elucidated to the point that it can be helpful to guiding researchers or designers who would use the hawkmoth as a biological inspiration for their computational or engineered wing models. The data presented herein is essentially the first entry of the database just mentioned, and waiting to be populated. From this baseline, parametric studies can begin to be undertaken that shift the insect wing's modal parameters away from those determined by this research to begin to understand the effects that they have on flight. Third, the new, first time finding of a shared underlying structural dynamic commonality between different species of insect should serve as a catalyst for further study and may very well point to a universal design rule or "sweet spot" for flexible flapping wing flight. Fourth, the results herein support the notion that the hawkmoth, while not operating on top of a wing resonance, is operating in close proximity and may (likely) be deriving benefit (150% to 230%) by it. The experimental evidence found by this research appears to be the most compelling evidence to date that supports the resonance hypothesis. And finally, this research has evened the score on the "Aeroelastic Debate". The results herein are so compelling that there should be no question that the expression of the hawkmoth's forewing is affected by fluid dynamic and inertial forces alike. It is unlikely that any other large insect whose wings express appreciably during flight would somehow act differently.

Appendix A

MODEL EV-30

Part Number 1008

This unique device is a dual PZT crystal sandwich transducer designed to excite or induce mechanical vibrations into test pieces at frequencies as high as several hundred kilohertz. While designed principally for holographic non-destructive testing of turbine blades, thin wall castings, blowers, and other devices, the Ev-30 should find wide spread applicatiions in other areas where low displacement, high frequency and low cost are factors.

The shaker can now be electrically connected to any low power audio oscillator providing 30 volts into a typical load of 600 ohms. examples of this type of power supply are the HP-200AB and HP-201C. For holographic applications, drive voltages from several volts to twenty volts provides adequate excitation for most vibration analysis experiments.

SPECIFICATIONS
Axial Deflection: 0.12µm per 100 volts input, minimum
Maximum Loading: 100 lb (220.5 kg)
Transducer Configuration: dual PZT crystal sandwich
Maximum input voltage: 2000 volts (ACpp or DC)
Operating frequency: DC to 150 kHz
Safe continuous output power: 30 watts
Input cable length: 10 ft (3.305 m) HV coaxial cable with flying leads
Shaker mounting plate: (1) centered 1/4-20 tapped hole and (4) 1/4 inch clearance holes on 3 inch diagonals
Overall height: 4.125 inch (10.48 cm)
Weight: 2 lb (0.907 kg)
Construction: nickel plated steel base and pole pieces with insulating protective housing

Figure 88: Specifications of the shaker head used to excite the wing modes during for system identification testing [56].

Appendix B

Wing Specimen Dimensional, Mass, and Modal Data as Measured in the Lab

Table 8:   Hawkmoth mass and handling data.

Wing ID	Moth ID	Moth Age	RtWing (0) LtWing(1)	Test Date			Time In Cooler		Time Out Cooler		Total Moth Mass	Pre-Test Wing Mass	Post-Test Wing Mass			Avg Test Temp	Avg Test RH
[##]	[##]	[Days]	[0 - 1]	[yyyy]	[mm]	[dd]	[hr]	[min]	[hr]	[min]	[gr]	[gr]	[gr]	[hr]	[min]	[°F]	[%]
01	01	3.5	0	2009	05	01	14	54	15	15	2.3039	0.0353	0.0344	15	54	70	65
02	01	3.5	1	2009	05	01	14	54	15	56	2.3039	0.0345	0.0338	16	30	70	65
03	02	3.5	0	2009	05	04	11	38	12	15	2.4189	0.0442	0.0431	12	45	70	24
04	02	3.5	1	2009	05	04	11	38	12	48	2.4189	0.0449	0.0434	13	13	69	24
05	03	3.5	0	2009	05	04	12	48	13	15	2.1139	0.0397	0.0385	13	42	70	24
06	03	3.5	1	2009	05	04	12	48	13	44	2.1139	0.0382	0.0372	14	05	71	24
07	04	1	0	2009	05	04	21	21	21	48	3.2460	0.1272	0.1231	22	32	69	37
08	04	1	1	2009	05	04	21	21	22	35	3.2460	0.1407	0.1361	23	01	70	40
09	05	3.5	0	2009	05	06	23	37	00	16	1.9230	0.0373	0.0360	00	41	69	38
10	05	3.5	1	2009	05	06	23	37	00	41	1.9230	0.0410	0.0386	01	09	69	38
11	06	3.5	0	2009	05	06	00	51	01	11	2.2025	0.0422	0.0400	01	33	70	44
12	06	3.5	1	2009	05	06	00	51	01	33	2.2025	0.0391	0.0384	01	58	70	44
13	07	3.5	0	2009	05	06	01	37	02	00	2.4871	0.0434	0.0415	02	22	69	44
14	07	3.5	1	2009	05	06	01	37	02	23	2.4871	0.0440	0.0422	02	47	69	44
15	08	3.5	0	2009	05	06	02	25	02	48	2.0870	0.0370	0.0365	03	09	70	45
16	08	3.5	1	2009	05	06	02	25	03	09	2.0870	0.0350	0.0343	03	34	70	45
17	09	3.5	0	2009	05	06	03	14	03	35	2.4868	0.0446	0.0420	04	01	70	45
18	09	3.5	1	2009	05	06	03	14	04	02	2.4868	0.0434	0.0421	04	26	70	45
19	10	2	1	2009	05	06	04	10	04	27	1.9791	0.0451	0.0443	04	50	70	45
20	11	2	0	2009	05	06	04	38	04	52	2.5612	0.0425	0.0406	05	13	70	45
21	11	2	1	2009	05	06	04	38	05	13	2.5612	0.0423	0.0417	05	31	70	45
22	12	5	0	2009	05	15	08	45	09	10	2.0810	0.0427	0.0417	09	40	71	41
23	12	5	1	2009	05	15	08	45	09	44	2.0810	0.0425	0.0412	10	16	71	41
24	13	5	0	2009	05	15	10	40	11	30	1.7750	0.0344	0.0337	11	53	74	43
25	13	5	1	2009	05	15	10	40	11	54	1.7750	0.0386	0.0372	12	58	74	43
26	14	4	0	2009	05	15	13	04	13	17	2.2523	0.0468	0.0460	13	47	75	47
27	14	4	1	2009	05	15	13	04	15	06	2.2523	0.0454	0.0437	15	45	74	45
28	15	5	0	2009	05	15	22	25	22	47	1.9767	0.0385	0.0377	23	17	76	58
29	15	5	1	2009	05	15	22	25	23	17	1.9767	0.0401	0.0396	23	49	76	58
30	16	5	0	2009	05	16	20	15	20	46	2.2440	0.0440	0.0425	21	19	73	33
31	16	5	1	2009	05	16	20	15	21	19	2.2440	0.0466	0.0460	21	44	73	33
32	17	5	0	2009	05	16	20	54	21	45	2.0206	0.0397	0.0390	22	08	73	73
33	17	5	1	2009	05	16	20	54	22	08	2.0206	0.0414	0.0405	22	32	73	73
34	18	5	0	2009	05	16	22	15	22	33	2.6273	0.0495	0.0487	23	02	73	28
35	18	5	1	2009	05	16	22	15	23	03	2.6273	0.0479	0.0462	23	29	73	28
36	19	5	0	2009	05	17	20	18	20	35	1.9931	0.0416	0.0403	21	00	71	17
37	19	5	1	2009	05	17	20	18	21	01	1.9931	0.0401	0.0394	21	22	71	17
38	20	5	0	2009	05	17	20	45	21	23	2.0498	0.0422	0.0417	21	47	71	18
39	20	5	1	2009	05	17	20	45	21	46	2.0498	0.0415	0.0410	22	09	71	18
40	21	5	0	2009	05	17	21	33	22	10	2.4577	0.0439	0.0434	22	28	71	19
41	21	5	1	2009	05	17	21	33	22	29	2.4577	0.0450	0.0440	22	49	71	19
42	22	4	0	2009	05	18	21	40	22	11	2.1943	0.0375	0.0367	22	32	71	20
43	23	5	0	2009	09	10	21	58	22	24	1.9369	0.0412	0.0373	00	45	NaN	NaN
44	23	5	1	2009	09	10	21	58	23	25	1.9369	0.0402	0.0379	00	45	NaN	NaN
45	24	6	0	2009	09	11	22	38	22	59	2.0633	0.0433	0.0399	23	50	NaN	NaN
46	24	6	1	2009	09	11	22	38	23	50	2.0633	0.0425	0.0384	00	30	NaN	NaN
47	25	6	0	2009	09	11	00	30	00	54	2.1746	0.0458	0.0431	01	43	NaN	NaN
48	25	6	1	2009	09	11	00	30	01	43	2.1746	0.0443	0.0404	02	35	NaN	NaN
49	26	5	0	2009	09	12	21	21	21	45	2.4748	0.0492	0.046	22	53	NaN	NaN
50	26	5	1	2009	09	12	21	21	22	54	2.4748	0.0476	0.046	23	45	NaN	NaN
51	27	5	0	2009	09	12	23	21	23	43	2.4106	0.0453	0.0431	00	46	NaN	NaN
52	27	5	1	2009	09	12	23	21	00	43	2.4106	0.0451	0.0416	02	12	NaN	NaN
53	28	7	1	2009	10	13	10	25	10	58	2.0335	0.0435	NaN	NaN	NaN	NaN	NaN
54	29	6	1	2009	10	26	08	35	08	44	2.4574	0.0439	NaN	NaN	NaN	NaN	NaN
55	30	NaN	1	2009	09	30	Nan	NaN	NaN	NaN	0.4712	0.0207	NaN	NaN	NaN	NaN	NaN
56	31	NaN	1	2009	09	30	NaN	NaN	NaN	NaN	0.3456	0.0181	NaN	NaN	NaN	NaN	NaN
57	32	NaN	1	2009	10	13	Nan	NaN	NaN	NaN	0.0975	0.0012	NaN	NaN	NaN	NaN	NaN
58	33	NaN	1	2009	10	18	Nan	NaN	NaN	NaN	0.8631	0.0010	NaN	NaN	NaN	NaN	NaN

NOTES

- Moth ID 30 = Monarch

- Moth ID 31 = Swallow Tail

- Moth ID 32 = Skipper

- Moth ID 33 = Bumblebee

- Moth ID 54 = Final Hawkmoth Wing Tested only in Vaccum; Specimen used in Aeroelastic flapping study as well.

- Moth ID 4 = Moth that was inadvetently dropped so tested early and noted to have hemolymph still in wing veins; excluded from stat rollup

- Moths Listed as 3.5 days old are 3 to 5 days old
- Butterfly Age was Unknown
- NaN are either data not taken or computation not possible due to missing data dependency

Table 9:   Hawkmoth wing specimen modal frequencies.

Wing ID	Moth ID	Moth Age	RtWing (0) LtWing(1)	Flapping (Air)		Torsion (Air)		Saddle (Air)		2-Saddle (Air)		Flapping (Vac)		Torsion (Vac)		Saddle (Vac)		2-Saddle (Vac)	
				Freq	Dmp	Freq	Dmp	Freq	Dmp	Freq	Dmp	Freq	Dmp	Freq	Dmp	Freq	Dmp	Freq	Dmp
[##]	[##]	[Days]	[0 - 1]	[Hz]	[%]	[Hz]	[%]	[Hz]	[%]	[Hz]	[%]	[Hz]	[%]	[Hz]	[%]	[Hz]	[%]	[Hz]	[%]
01	01	3.5	0	60	5.0	85	5.0	107	5.0	142	5.0	NaN	NaN	NaN	NaN	NaN	NaN	NaN	NaN
02	01	3.5	1	59	5.4	87	5.0	104	5.8	153	5.0	NaN	NaN	NaN	NaN	NaN	NaN	NaN	NaN
03	02	3.5	0	59	5.4	80	5.0	100	5.4	126	5.0	NaN	NaN	NaN	NaN	NaN	NaN	NaN	NaN
04	02	3.5	1	58	5.0	81	5.0	100	5.0	132	5.4	NaN	NaN	NaN	NaN	NaN	NaN	NaN	NaN
05	03	3.5	0	53	5.3	79	4.6	100	5.0	138	5.3	NaN	NaN	NaN	NaN	NaN	NaN	NaN	NaN
06	03	3.5	1	54	5.3	79	5.0	98	5.3	133	5.0	NaN	NaN	NaN	NaN	NaN	NaN	NaN	NaN
07	04	1	0	23	8.0	32	8.5	43	8.5	62	9.0	NaN	NaN	NaN	NaN	NaN	NaN	NaN	NaN
08	04	1	1	22	8.0	34	8.0	43	8.0	NaN	NaN	NaN	NaN	NaN	NaN	NaN	NaN	NaN	NaN
09	05	3.5	0	60	5.0	83	5.0	110	5.0	142	5.0	NaN	NaN	NaN	NaN	NaN	NaN	NaN	NaN
10	05	3.5	1	58	5.0	NaN	NaN	103	5.0	135	5.0	NaN	NaN	NaN	NaN	NaN	NaN	NaN	NaN
11	06	3.5	0	63	5.0	86	5.0	109	5.0	151	6.0	NaN	NaN	NaN	NaN	NaN	NaN	NaN	NaN
12	06	3.5	1	60	5.0	91	4.0	125	5.0	163	5.0	NaN	NaN	NaN	NaN	NaN	NaN	NaN	NaN
13	07	3.5	0	60	5.7	78	5.7	102	5.4	129	4.2	NaN	NaN	NaN	NaN	NaN	NaN	NaN	NaN
14	07	3.5	1	65	5.0	82	5.0	107	5.4	129	4.0	NaN	NaN	NaN	NaN	NaN	NaN	NaN	NaN
15	08	3.5	0	65	5.0	92	5.0	123	5.0	161	5.0	NaN	NaN	NaN	NaN	NaN	NaN	NaN	NaN
16	08	3.5	1	60	5.0	90	5.0	110	5.5	150	5.5	NaN	NaN	NaN	NaN	NaN	NaN	NaN	NaN
17	09	3.5	0	58	4.8	85	5.0	106	5.5	135	5.5	NaN	NaN	NaN	NaN	NaN	NaN	NaN	NaN
18	09	3.5	1	57	5.0	84	5.0	114	5.0	135	5.0	NaN	NaN	NaN	NaN	NaN	NaN	NaN	NaN
19	10	2	1	50	5.0	NaN	NaN	88	5.0	144	5.0	NaN	NaN	NaN	NaN	NaN	NaN	NaN	NaN
20	11	2	0	67	4.4	96	5.0	135	5.0	170	5.0	NaN	NaN	NaN	NaN	NaN	NaN	NaN	NaN
21	11	2	1	59	5.0	86	5.0	110	5.0	136	6.0	NaN	NaN	NaN	NaN	NaN	NaN	NaN	NaN
22	12	5	0	59	5.0	85	5.0	108	5.0	145	5.0	NaN	NaN	NaN	NaN	NaN	NaN	NaN	NaN
23	12	5	1	54	5.0	87	5.0	126	5.0	151	5.0	NaN	NaN	NaN	NaN	NaN	NaN	NaN	NaN
24	13	5	0	60	5.0	91	4.0	143	5.0	179	5.0	NaN	NaN	NaN	NaN	NaN	NaN	NaN	NaN
25	13	5	1	56	5.0	79	5.0	106	5.0	146	5.0	NaN	NaN	NaN	NaN	NaN	NaN	NaN	NaN
26	14	4	0	50	5.5	70	5.5	88	5.5	124	5.5	NaN	NaN	NaN	NaN	NaN	NaN	NaN	NaN
27	14	4	1	49	5.8	68	5.0	87	5.3	124	5.7	NaN	NaN	NaN	NaN	NaN	NaN	NaN	NaN
28	15	5	0	59	5.5	NaN	NaN	118	5.0	160	5.7	NaN	NaN	NaN	NaN	NaN	NaN	NaN	NaN
29	15	5	1	63	5.0	90	5.0	120	5.0	155	5.0	NaN	NaN	NaN	NaN	NaN	NaN	NaN	NaN
30	16	5	0	55	5.0	NaN	NaN	100	5.0	140	5.0	NaN	NaN	NaN	NaN	NaN	NaN	NaN	NaN
31	16	5	1	57	5.0	79	5.0	104	5.0	134	5.0	NaN	NaN	NaN	NaN	NaN	NaN	NaN	NaN
32	17	5	0	54	6.0	80	5.0	106	6.0	147	6.0	NaN	NaN	NaN	NaN	NaN	NaN	NaN	NaN
33	17	5	1	52	5.5	77	6.0	95	5.0	130	6.0	NaN	NaN	NaN	NaN	NaN	NaN	NaN	NaN
34	18	5	0	57	4.6	75	5.0	98	5.0	132	5.0	NaN	NaN	NaN	NaN	NaN	NaN	NaN	NaN
35	18	5	1	54	4.8	76	5.0	97	5.0	136	5.0	NaN	NaN	NaN	NaN	NaN	NaN	NaN	NaN
36	19	5	0	68	5.0	104	5.0	131	5.0	173	5.0	NaN	NaN	NaN	NaN	NaN	NaN	NaN	NaN
37	19	5	1	68	5.0	90	5.0	123	5.0	165	5.0	NaN	NaN	NaN	NaN	NaN	NaN	NaN	NaN
38	20	5	0	53	5.0	NaN	NaN	100	5.0	136	5.0	NaN	NaN	NaN	NaN	NaN	NaN	NaN	NaN
39	20	5	1	52	5.0	NaN	NaN	95	5.0	125	5.0	NaN	NaN	NaN	NaN	NaN	NaN	NaN	NaN
40	21	5	0	59	5.5	78	6.0	102	5.0	129	5.0	NaN	NaN	NaN	NaN	NaN	NaN	NaN	NaN
41	21	5	1	56	5.0	NaN	NaN	105	5.0	143	5.0	NaN	NaN	NaN	NaN	NaN	NaN	NaN	NaN
42	22	4	0	60	4.5	84	5.0	115	5.0	139	4.5	NaN	NaN	NaN	NaN	NaN	NaN	NaN	NaN
43	23	5	0	63	5.0	95	5.0	126	5.0	158	5.0	89	2.5	119	2.0	158	3.0	192	3.0
44	23	5	1	61	5.0	93	5.0	111	5.0	140	5.0	83	2.5	NaN	NaN	137	3.0	165	3.0
45	24	6	0	59	5.0	84	5.0	114	5.0	152	5.0	80	3.0	NaN	NaN	136	3.0	177	4.0
46	24	6	1	62	5.0	87	5.0	109	5.0	164	5.0	88	3.0	109	3.0	132	3.0	NaN	NaN
47	25	6	0	59	5.0	82	5.0	107	5.0	139	5.0	82	3.0	NaN	NaN	135	3.5	170	3.5
48	25	6	1	60	5.0	87	5.0	118	5.0	149	5.0	85	3.0	NaN	NaN	151	3.0	185	3.5
49	26	5	0	53	5.0	74	5.0	87	5.0	115	5.0	73	3.5	97	3.5	107	3.5	135	3.5
50	26	5	1	60	5.0	NaN	NaN	103	5.0	133	5.0	82	3.0	100	2.0	125	3.5	154	3.5
51	27	5	0	63	4.0	NaN	NaN	112	5.0	140	4.0	88	3.0	NaN	NaN	136	2.0	163	2.5
52	27	5	1	58	5.0	75	5.0	95	5.0	119	5.0	81	3.0	98	3.0	117	3.5	145	4.0
53	28	7	1	65	5.0	83	5.0	114	5.0	155	5.0	97	3.0	NaN	NaN	160	3.0	203	3.0
54	29	6	1	NaN	NaN	NaN	NaN	NaN	NaN	NaN	NaN	86	3.0	106	3.0	158	3.0	185	3.0
55	30	NaN	1	41	5.0	60	5.0	75	5.0	95	5.0	61	2.5	83	2.5	98	2.5	118	2.5
56	31	NaN	1	41	5.0	59	5.0	88	5.0	104	5.0	NaN	NaN	NaN	NaN	NaN	NaN	NaN	NaN
57	32	NaN	1	300	3.0	450	3.0	539	3.0	774	3.0	446	1.5	550	1.5	720	1.5	1050	1.5
58	33	NaN	1	145	4.0	348	4.0	693	4.0	845	4.0	171	2.0	390	2.0	NaN	NaN	908	2.0

Table 10:   Hawkmoth wing dimensional parameters.

Wing ID	Moth ID	Moth Age	RtWing (0) LtWing(1)	Area	L	b	C_tip	AR(L)	AR(b)	C_avg(L)	C_avg(b)
[##]	[##]	[Days]	[0 - 1]	[in²]	[in]	[in]	[in]	[in]	[in]	[in]	[in]
01	01	3.5	0	1.021	1.79541	1.793	1.068	3.157197	3.148726	0.56867225	0.5694367
02	01	3.5	1	1.039	1.788027	1.785	1.042	3.077037	3.066627	0.58108738	0.58207283
03	02	3.5	0	1.111	1.937437	1.915	1.16	3.378633	3.300833	0.57343809	0.58015666
04	02	3.5	1	1.194	1.94519	1.94	1.167	3.168982	3.152094	0.6138218	0.61546392
05	03	3.5	0	1.452	2.238708	2.222	1.282	3.451662	3.400333	0.64858842	0.65346535
06	03	3.5	1	1.146	1.895473	1.876	1.101	3.135093	3.071009	0.60459851	0.6108742
07	04	1	0	1.195	1.878773	1.867	1.06	2.953798	2.916895	0.63605333	0.64006427
08	04	1	1	1.197	1.943031	1.943	1.048	3.154027	3.153926	0.61604777	0.61605764
09	05	3.5	0	1.086	1.856033	1.856	1.112	3.17206	3.171948	0.58511903	0.58512931
10	05	3.5	1	1.161	1.961957	1.941	1.132	3.315484	3.245031	0.59175596	0.59814529
11	06	3.5	0	1.114	1.894481	1.884	1.12	3.221775	3.186226	0.58802395	0.59129512
12	06	3.5	1	1.087	1.792786	1.791	1.081	2.956836	2.950948	0.60631894	0.60692351
13	07	3.5	0	1.173	1.900958	1.886	1.121	3.080682	3.032392	0.61705741	0.62195122
14	07	3.5	1	1.211	1.904848	1.894	1.133	2.996239	2.96221	0.63574634	0.63938754
15	08	3.5	0	1.047	1.833804	1.826	1.049	3.211879	3.1846	0.57094434	0.57338445
16	08	3.5	1	1.039	1.736035	1.736	1.011	2.90069	2.900574	0.59849029	0.5985023
17	09	3.5	0	1.23	1.978632	1.969	1.162	3.182915	3.152001	0.62164151	0.62468258
18	09	3.5	1	1.189	1.919427	1.918	1.113	3.09857	3.093965	0.6194557	0.61991658
19	10	2	1	1.275	2.015182	2.004	1.148	3.185067	3.149816	0.63269708	0.63622754
20	11	2	0	1.113	1.822384	1.799	1.137	2.983901	2.907818	0.61073859	0.61867704
21	11	2	1	1.155	1.860421	1.843	1.123	2.99668	2.940822	0.62082734	0.6266956
22	12	5	0	1.152	1.945999	1.932	1.113	3.287251	3.240125	0.59198379	0.59627329
23	12	5	1	1.096	1.868194	1.862	1.114	3.184442	3.163361	0.58666291	0.58861439
24	13	5	0	1.069	1.816327	1.811	1.079	3.086101	3.068027	0.58855057	0.59028161
25	13	5	1	1.148	1.972513	1.972	1.113	3.389206	3.387443	0.58199859	0.5821501
26	14	4	0	1.254	2.121239	2.116	1.174	3.588243	3.570539	0.5911638	0.5926276
27	14	4	1	1.308	2.051165	2.051	1.163	3.216573	3.216056	0.63768645	0.63773769
28	15	5	0	1.194	1.970078	1.928	1.112	3.250594	3.113219	0.60606724	0.61929461
29	15	5	1	1.222	1.959278	1.959	1.153	3.141383	3.140492	0.62369916	0.62378765
30	16	5	0	1.222	1.964365	1.953	1.132	3.157717	3.121284	0.62208397	0.62570405
31	16	5	1	1.329	2.061612	2.054	1.199	3.198078	3.174504	0.64464111	0.64703019
32	17	5	0	1.217	1.989705	1.955	1.147	3.25302	3.14053	0.61164854	0.62250639
33	17	5	1	1.175	1.951901	1.941	1.119	3.242483	3.206367	0.60197729	0.60535806
34	18	5	0	1.415	2.11916	2.119	1.239	3.173736	3.173259	0.66771755	0.66776782
35	18	5	1	1.345	2.037497	2.037	1.203	3.086538	3.085033	0.66012367	0.66028473
36	19	5	0	1.284	1.996916	1.993	1.141	3.105665	3.093496	0.64299145	0.64425489
37	19	5	1	1.229	1.941157	1.94	1.154	3.06598	3.062327	0.63312769	0.63350515
38	20	5	0	1.298	2.031211	2.024	1.198	3.178596	3.156068	0.63902774	0.64130435
39	20	5	1	1.272	1.967391	1.958	1.163	3.042947	3.013965	0.64654148	0.64964249
40	21	5	0	1.194	1.940789	1.919	1.056	3.154657	3.084222	0.61521379	0.62219906
41	21	5	1	1.27	2.004551	2	1.122	3.163957	3.149606	0.63355832	0.635
42	22	4	0	1.174	1.863978	1.853	1.14	2.959466	2.92471	0.62983585	0.63356719
43	23	5	0	1.227	2.005026	1.989	1.116	3.27639	3.224222	0.61196208	0.61689291
44	23	5	1	NaN	NaN	NaN	NaN	NaN	NaN	NaN	NaN
45	24	6	0	1.232	2.02835	2.027	1.066	3.339452	3.335007	0.60739015	0.60779477
46	24	6	1	1.211	2.004182	1.99	1.149	3.316882	3.270107	0.60423665	0.60854271
47	25	6	0	1.309	2.109696	2.096	1.197	3.400165	3.356162	0.62046863	0.6245229
48	25	6	1	1.258	2.065984	2.063	1.215	3.392917	3.383123	0.60891081	0.60979157
49	26	5	0	1.314	2.117104	2.117	1.122	3.411058	3.410722	0.62065912	0.62068966
50	26	5	1	1.367	2.065791	2.064	1.157	3.121794	3.116383	0.66173203	0.6623062
51	27	5	0	1.368	2.072029	2.069	1.141	3.138381	3.129211	0.66022236	0.66118898
52	27	5	1	1.373	2.097266	2.091	1.125	3.203587	3.184473	0.65466181	0.65662363
53	28	7	1	NaN	NaN	NaN	NaN	NaN	NaN	NaN	NaN
54	29	6	1	1.286	2.0092	2.007	1.14	3.139102	3.132231	0.64005572	0.64075735
55	30	NaN	1	1.523	2.023718	2.013	1.377	2.689056	2.660649	0.75257535	0.75658222
56	31	NaN	1	1.165	1.844823	1.843	1.204	2.92135	2.915579	0.6314968	0.63212154
57	32	NaN	1	0.129	0.665466	0.651	0.344	3.432907	3.285279	0.19384912	0.19815668
58	33	NaN	1	0.093	0.574008	0.574	0.275	3.542849	3.542753	0.16201869	0.16202091

NOTES:

Aspect Ratio
AR(L) = L^2/Area
AR(b) = b^2/Area

Mean Chord
C_avg(L) = Area/L
C_avg(b) = Area/b

176

Appendix C

Engineering Drawings of Flapping Mechanism Components

Figure 89: Rocker arm. With a wing specimen sandwiched between the foam-lined inserts and pushed into the rectangular void, the rocker served as both a clamp and the central component of the flapping mechanism during aero-inertial-elastic testing.
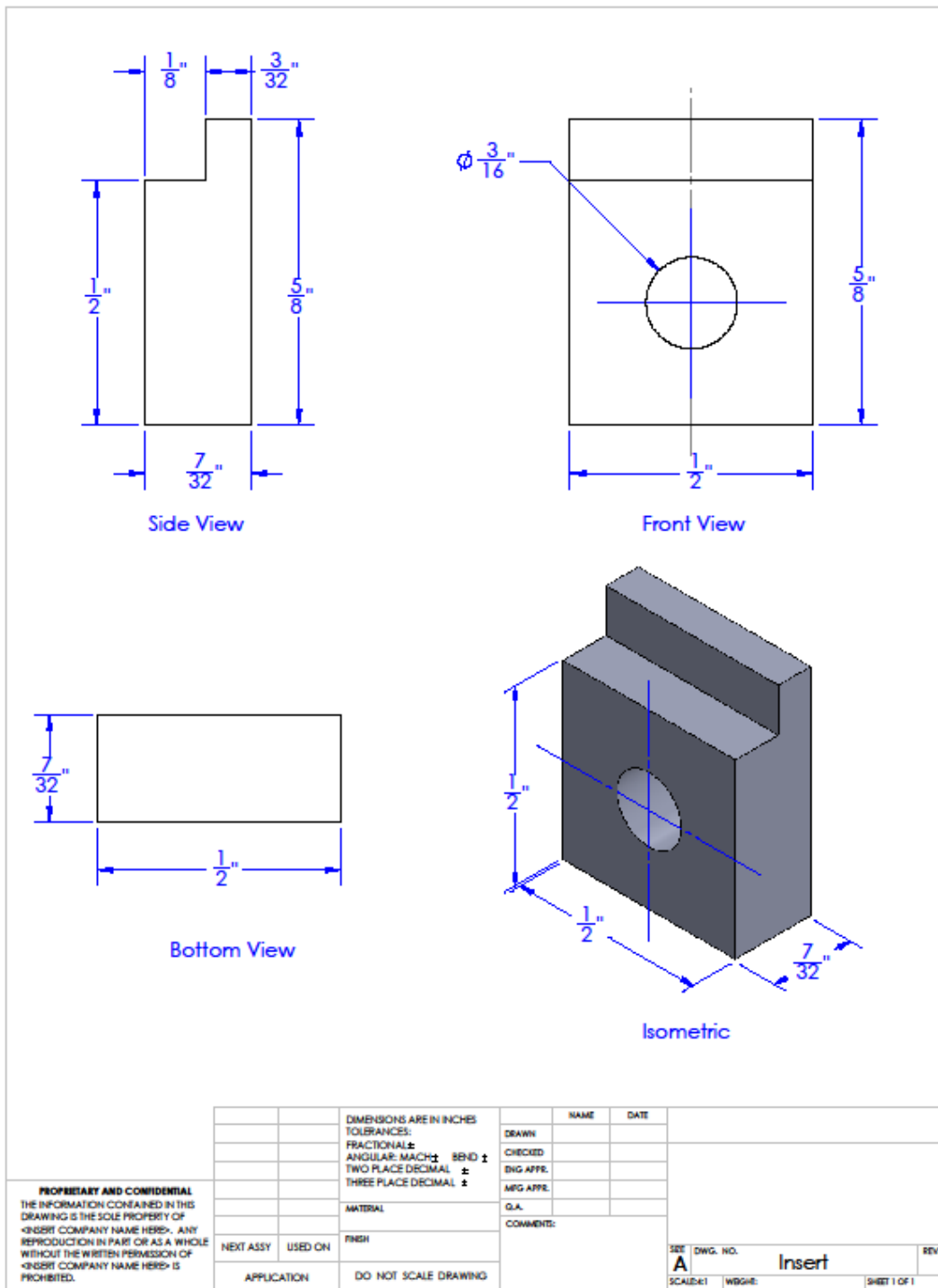
Figure 90: Insert. Hobby foam was adhered to the rear face of the insert. Two foam-lined inserts were then used to "sandwich" the wing specimen and subsequently inserted into the rocker assembly.
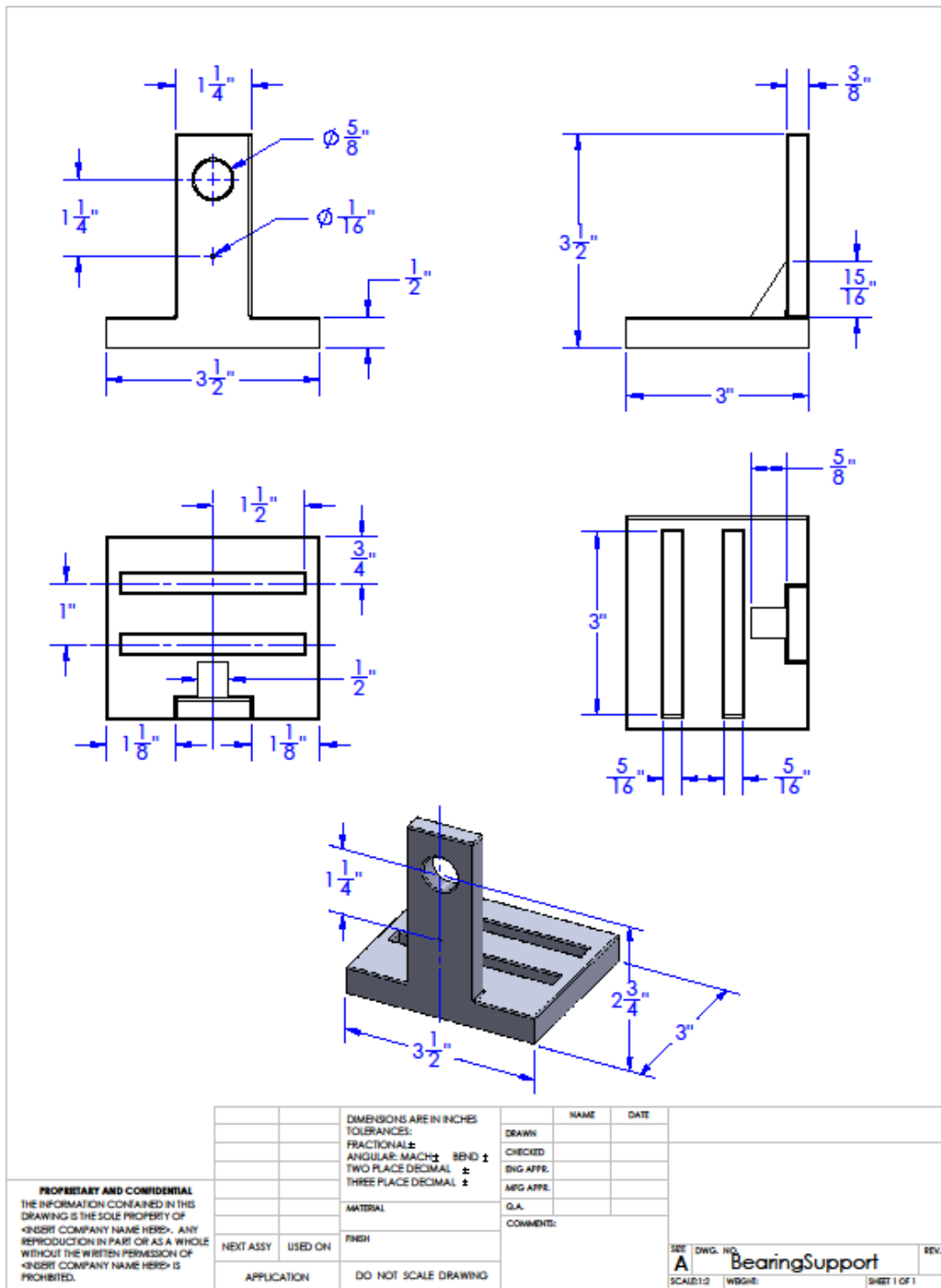
Figure 91: Bearing support. A small skateboard wheel bearing was press fitted into the hole on the upright member. The cylindrical boss of the rocker was then inserted through the bearing. A metallic lock washer and threaded nut were used to secure the rocker to the bearing support. The 3D printer material used for fabrication was both soft and strong enough so that the nut was able to thread the boss.
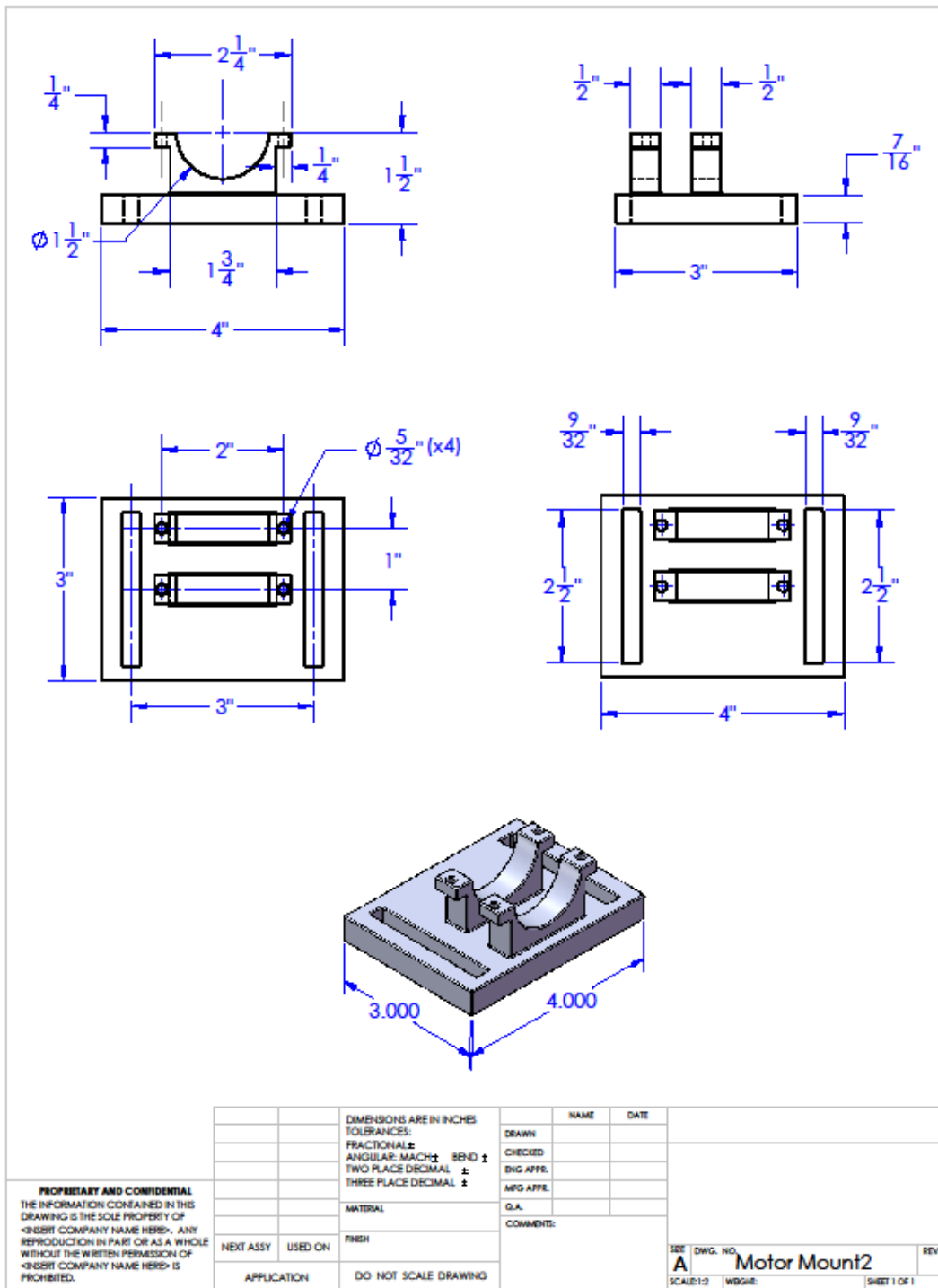
Figure 92: Motor mount. A small, hobby-class, electric car motor (Figure 75) was secured to the motor mount using plastic zip ties that were laced through the small circular holes on each side of the semicircle seats and over the cylindrical chassis of the motor.
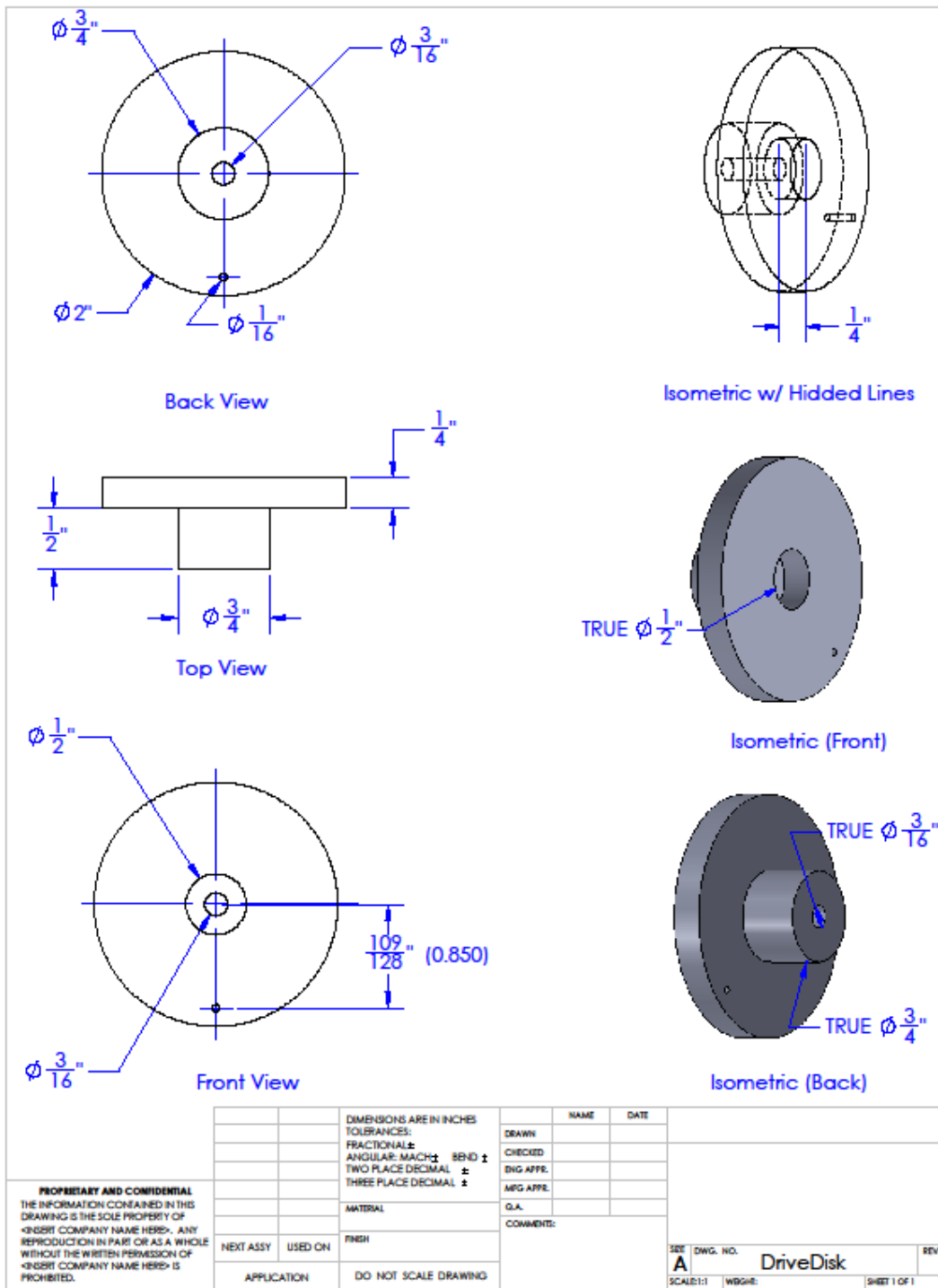
Figure 93: The flapping mechanism's drive disk. The drive disk was attached to the motor by way of a small threaded adaptor (Figure 76) typically used for securing the propeller to the motor shaft of small hobby-class R/C aircraft.

Appendix D

Engineering Drawing of Vacuum Chamber

QF 63 FLANGE (EXTEND TUBE FOR CLEARANCE)

2.000 THK CLEAR ACRYLIC WINDOW
TYP 3 PLC

LED LIGHT BAR TYP EA. SIDE

.250 COLD ROLLED CARBON STEEL PLATE
ON (9) .750 DIA TEFLON PADS

1.000

2.500

3.625

4.500

15.000

24.500

17.250

15.000

4.500

2.500

FRONT VIEW
DOOR REMOVED

Figure 94: Front view of the vacuum chamber.

184
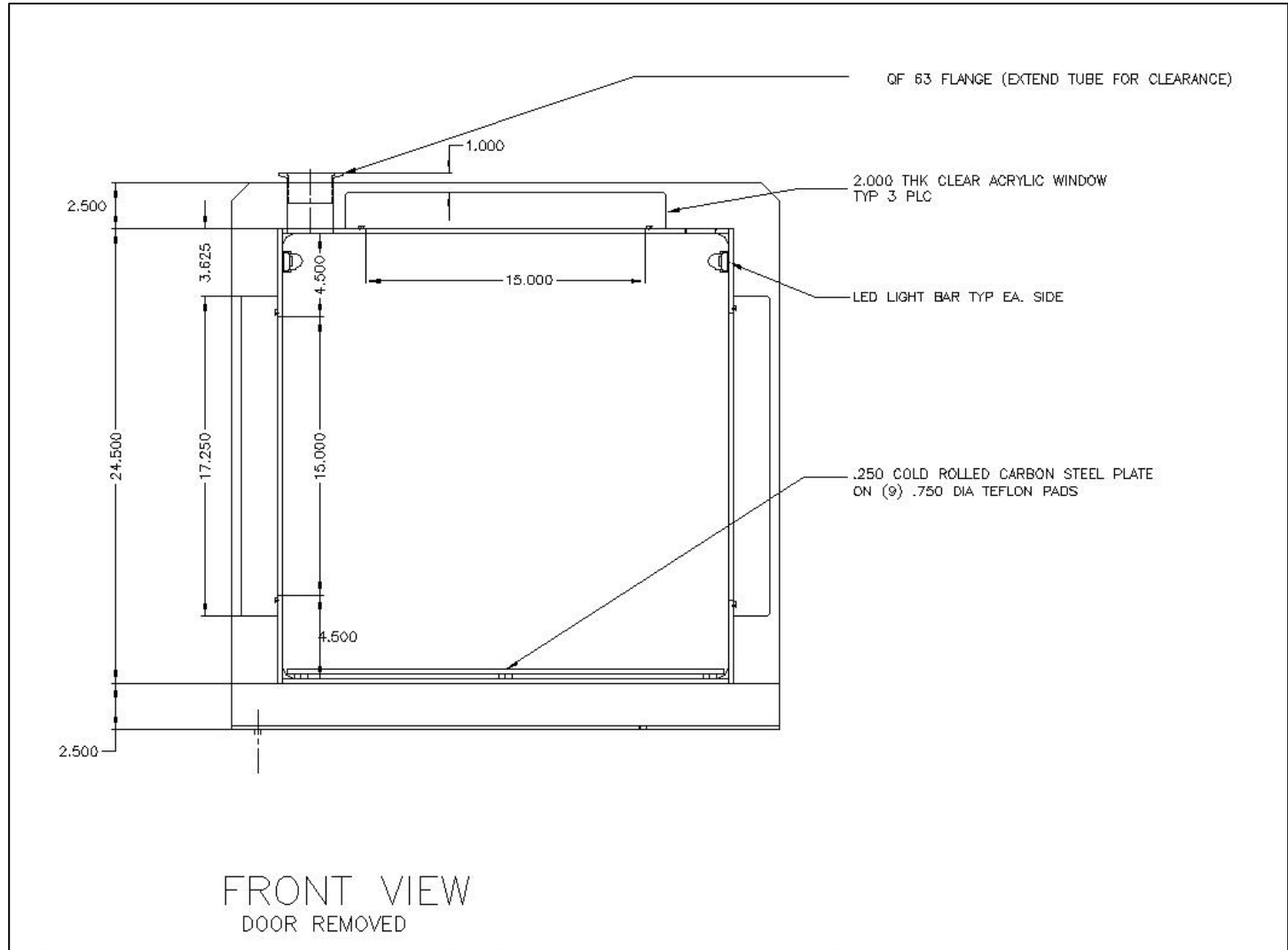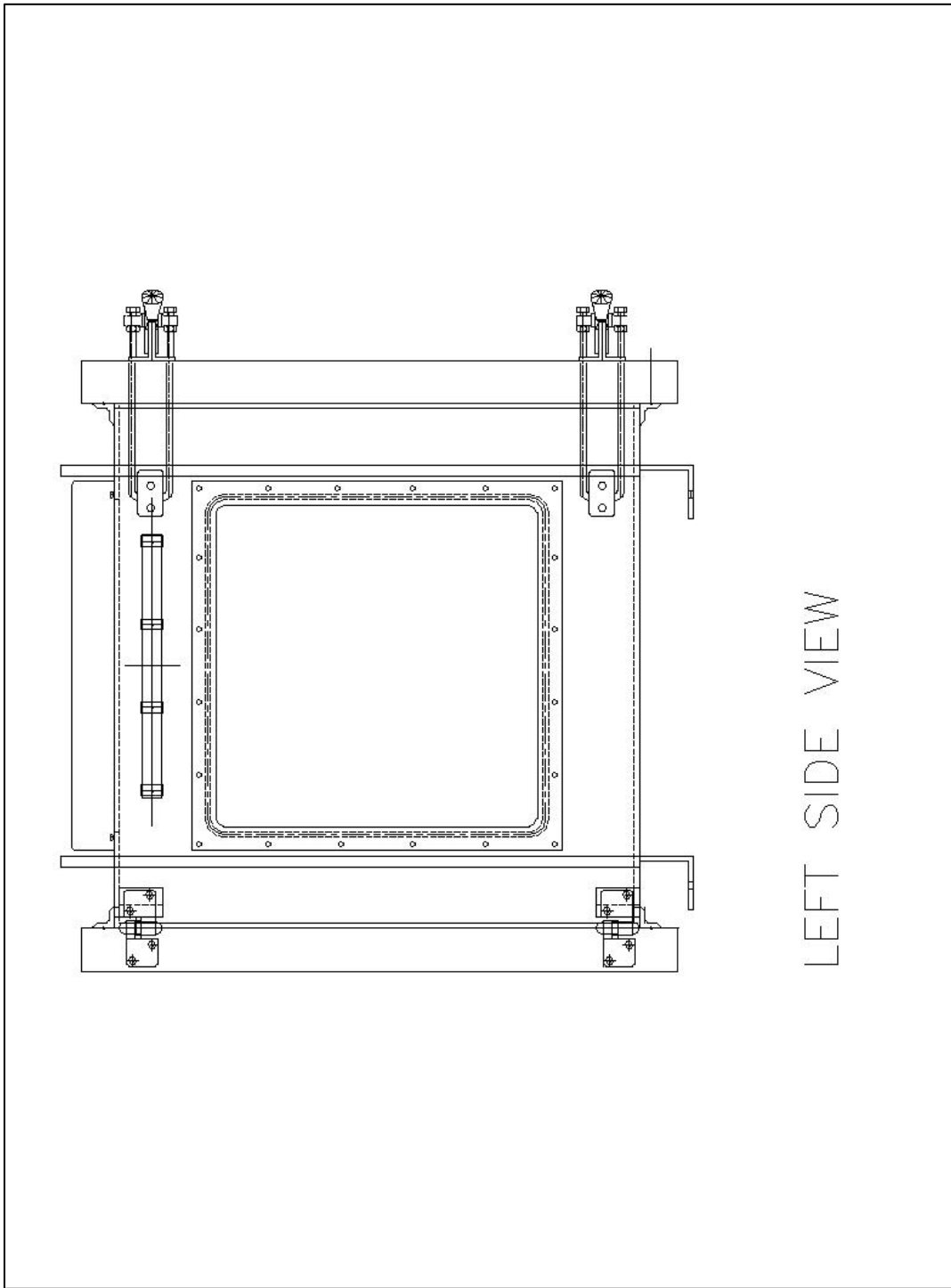
Figure 95: Left side view of the vacuum chamber.

Figure 96: Right side view of the vacuum chamber.

186
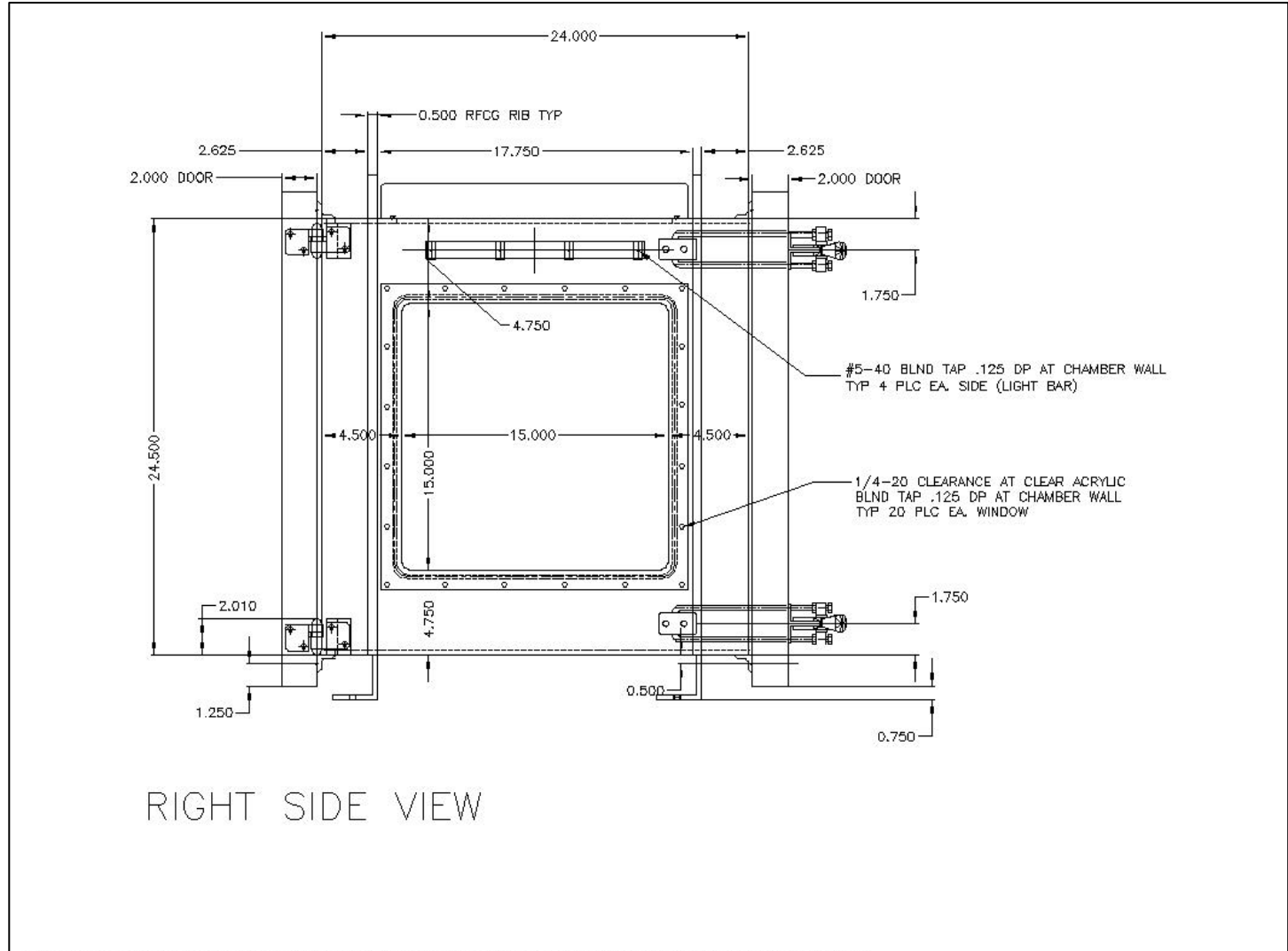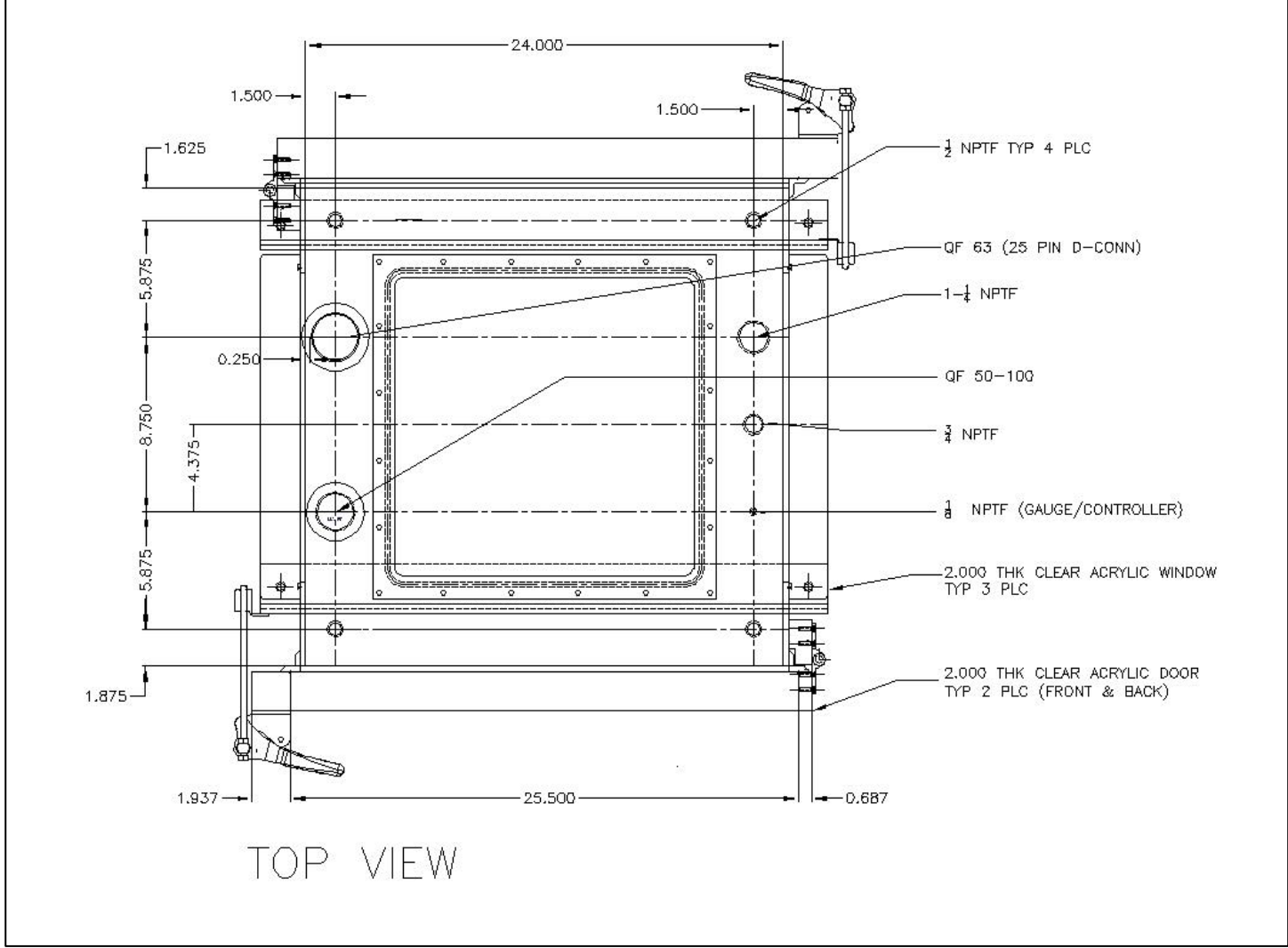
Figure 97: Top view of the vacuum chamber.
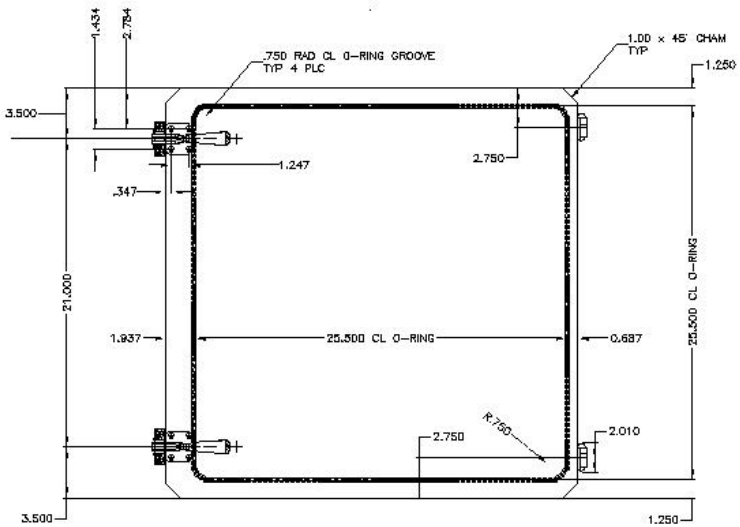
24 INCH CLEAR ACRYLIC DOOR

"O" RING GROOVE
CROSS SECTION
SCALE: 1:1
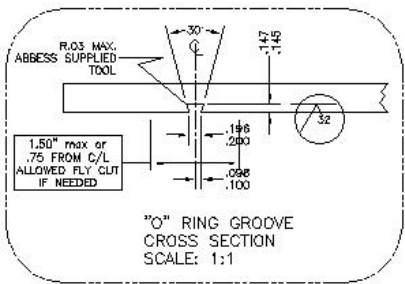
NOTES:
1. MATERIAL: CELL CAST ACRYLIC 2" THICK
2. REMOVE BURRS AND SHARP EDGES
3. TREATMENT: PROTECT FROM DAMAGE TO SURFACES
4. FINISH: 64 OR BETTER

Figure 98: Acrylic door. Hinged acrylic doors were attached to the front and back sides of the chamber. The large panes permitted maximum visibility for enabling more convenient laser vibrometry and photogrammetric measurements as well as more ready chamber access.

188

17.500

.250 CHFR

17.500

1/4-20 TAP THRU TYP 289 PLC

.250 X .750 DIA TEFLON PAD
1/4-20 CNTRBR TYP 9 PLC

TRAY MATERIAL= .250 COLD ROLLED CARBON STEEL

TOP VIEW MAGN PL
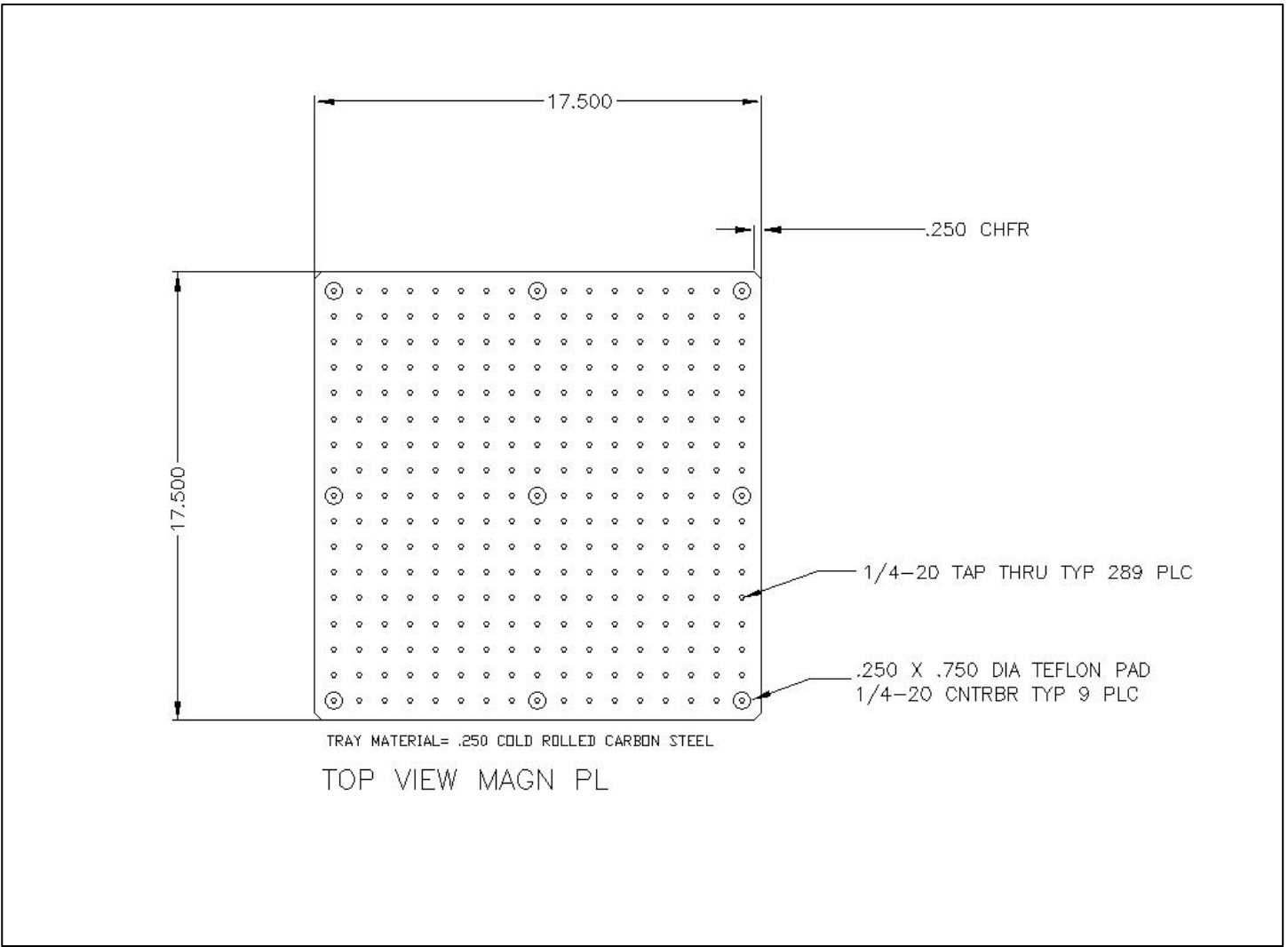
Figure 99: Magnetic base plate. The plate permitted maximum flexibility in positioning the shaker head that was horizontally mounted to an optical mount with a permanent magnet in its base. The threaded holes distributed on 1-inch centers enabled easy fastening of the motor and bearing support mounts

189

Appendix E

Supplemental Views of Wing Expressions
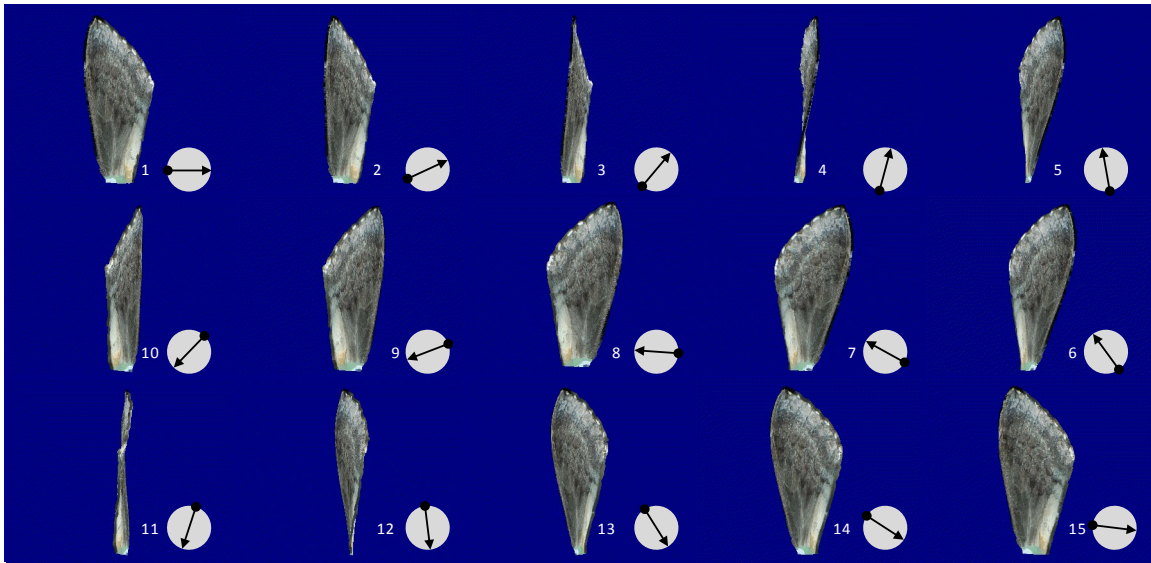
Figure 100: (25 Hz, $\phi = 27°$, Downstroke, $\tau = 0.4$, Air)
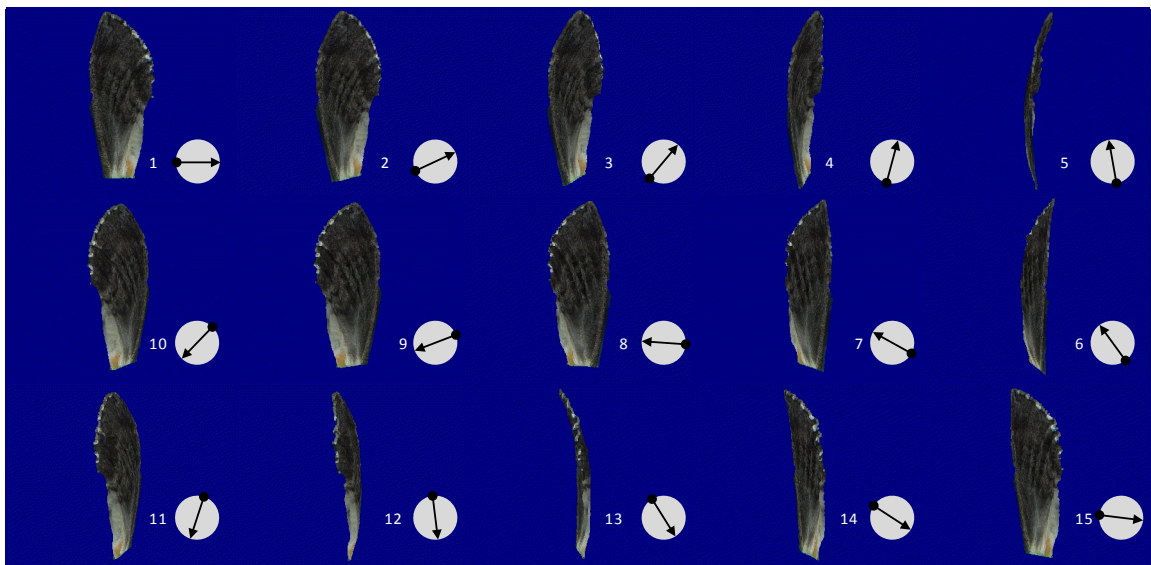
Figure 101: (25 Hz, $\phi = 27°$, Downstroke, $\tau = 0.4$, Vacuum)
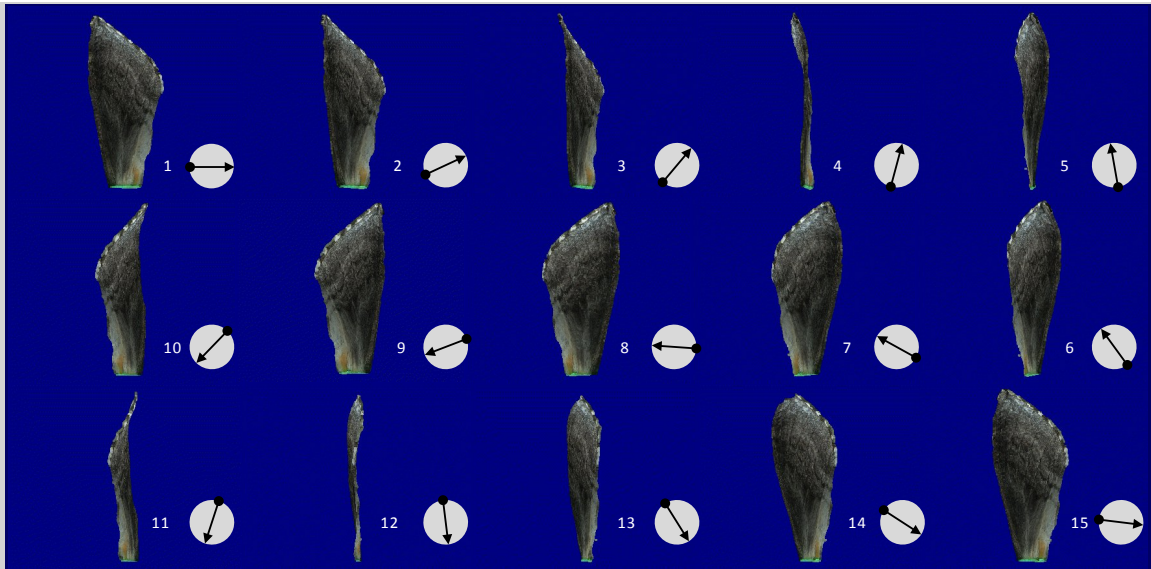
Figure 102: (25 Hz, $\phi = 0°$, Downstroke, $\tau = 0.5$, Air)
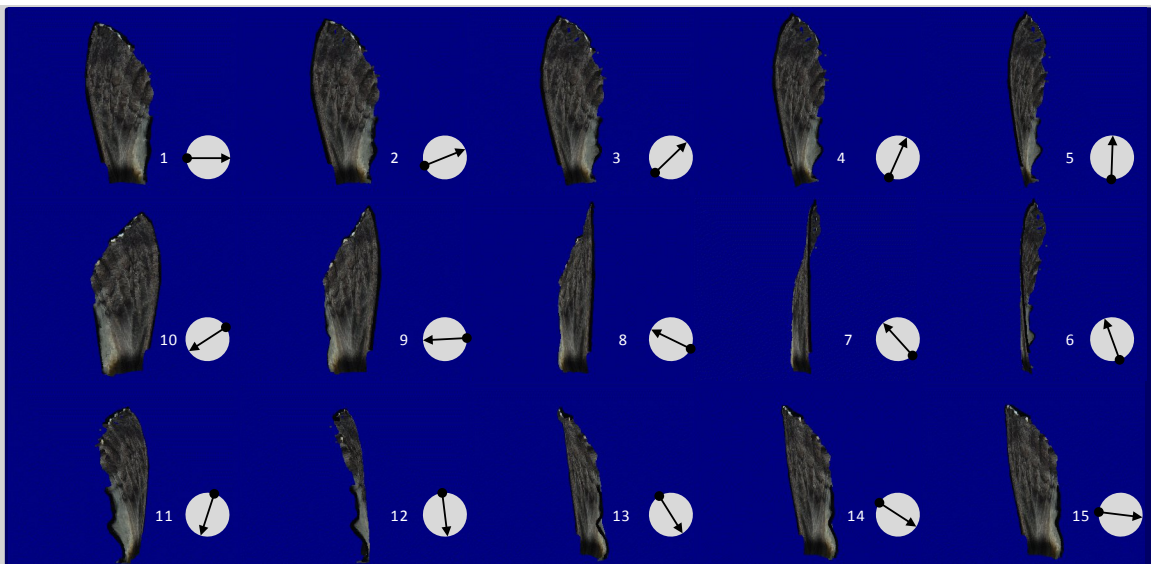
Figure 103: (25 Hz, $\phi = 0°$, Downstroke, $\tau = 0.5$, Vacuum)
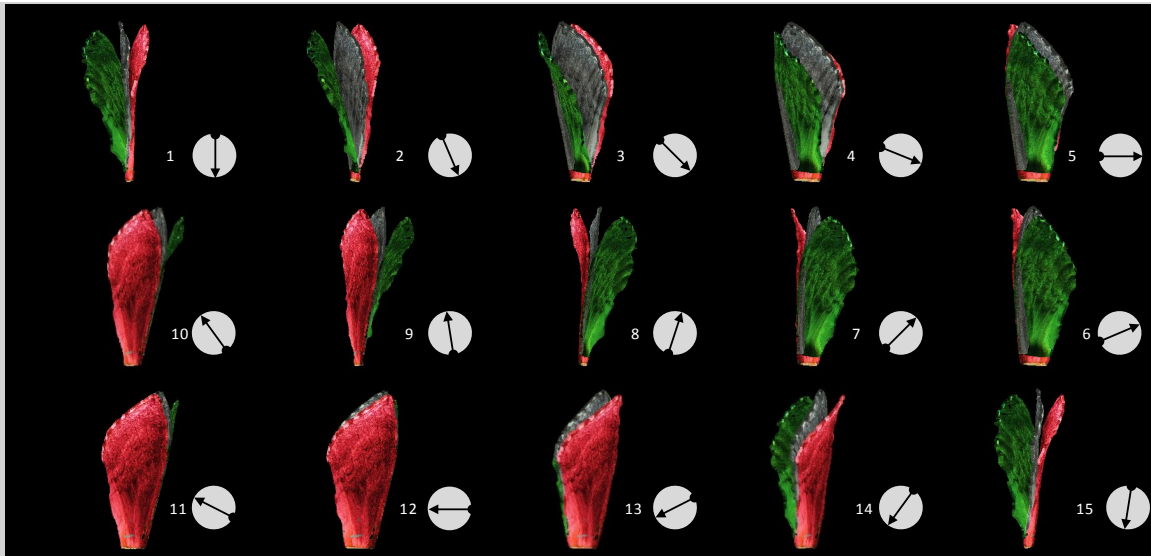
Figure 104: (25 Hz, $\phi = 0°$, Downstroke, $\tau = 0.5$, Air (red), Vacuum (green), Rigid (grey))
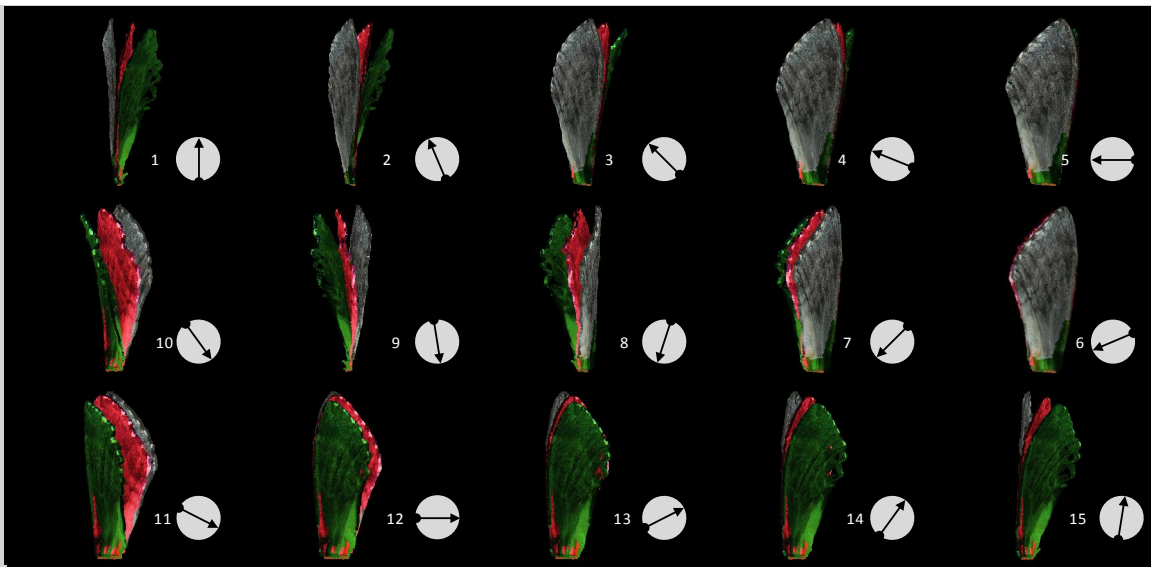
Figure 105: (25 Hz, $\phi = -34°$, Upstroke, $\tau = 0.76$, Air (red), Vacuum (green), Rigid (grey))

193

Bibliography

1. Abbott, I.H., von Doenhoff, A.E., <u>Theory of Wing Sections</u>, Dover Publications, New York, 1949.

2. AIAA Publications, Online Database, Accessed February 2008, http://www.aiaa.org.

3. Air Force Instruction, AFI 11-502, Volume 1, 26 Apr 2012.

4. Anderson, M.L., *Design and Control of Micro Air Vehicles*, Dissertation, AFIT/DS/ENY/11-12, Air Force Institute of Technology, Air University, Wright Patterson AFB, Ohio, September 2011.

5. Anderson, M.L., Sladek, N.J., and Cobb, R.G., "Design, Fabrication, and Testing of an Insect-Sized MAV Wing Flapping Mechanism," AIAA-2011-0549, Orlando, FL, January 2011.

6. Aono, H., Shyy, W., and Liu, H., "Vortex Dynamics in Near Wake of a Hovering hawkmoth," 46th AIAA Aerospace Sciences Meeting and Exhibit, 2008.

7. Bodanis, D., <u>The Secret Garden: Dawn to Dusk in the Astonishing Hidden World of the Garden</u>, Simon & Schuster, New York, 1992.

8. Brackenberry, J., <u>Insects in Flight</u>, Sterling Publications, Portland, OR, 1995.

9. Bumiller, E., Shanker, T., "War Evolves With Drones, Some Tiny as Bugs", New York Times, June 19, 2011.

10. Caffarilla, Nicholas, April 2011, Creative Commons Attribution-Share Alike 3.0, Accessed December 2013, en.wikipedia.org/wiki/Insect_wing.

11. Calico, R. A.March, J., "Active Control Of Helicopter Blade Flapping", *AIAA Guidance, Navigation and Control Conference*, AIAA-1985-1963, August 1985.

12. Chen, J.S., Chen, J. Y., Chou, Y.F., "On the Natural Frequencies and Mode Shapes of Dragonfly Wings", *Journal of Sound and Vibration*, Vol. 313, 643–654, 2008.

13. Clough, B.T, "UAV Swarming? So what are those swarms, what are the implications, and how do we handle them?", AFRL Tech Report, AFRL-VA-WP-TP-2002-308, April 2002.

14. Combes, S. A., & Daniel, T. L., "Into Thin Air: Contributions Of Aerodynamic and Inertial-Elastic Forces To Wing Bending In the Hawkmoth Manduca Sexta", *Journal of Experimental Biology, 206*, 2999-3006, 2003.

15. Cook, R.D., Malkus, D.S., Plesha,M.E., and Witt, R.J., <u>Concept and Applications of Finite Element Analysis, 4th Ed.</u>, John Wiley & Sons, New Jersey, 2002.

16. Crary, S.B., Ananthasuresh, G.K. and Kota, S., "Prospects for microflight using micromechanisms", *Proceedings of the International Symposium on Theory of Machines and Mechanisms, International Federation of Theory of Machines and*

Mechanisms-Japan Council, Nagoya, Japan, September 24-26, 1992, pp. 273-276.

17. Curtis, D.H., Reeder, M.F., Svanberg, C.E., and Cobb, R.G., "Flapping-wing Micro Air Vehicle Bench Test Set-up," *Proceedings of the 47th AIAA Aerospace Sciences Meeting Including The New Horizons Forum and Aerospace Exposition,* Orlando, FL, Jan. 2009.

18. Dalton, S., Borne on the Wind, Readers Digest Press, New York, 1975.

19. Darwin, C., The Descent of Man, John Murray Publishing, London, 1871.

20. Dawson, D., *Repeatable Manufacture of Wings For Flapping-Wing Micro Air Vehicles Using Microelectromechanical System (Mems) Fabrication Techniques*, MS Thesis, AFIT/GAE/ENY/11-M06, Air Force Institute of Technology, Air University, Wright Patterson AFB, Ohio, March 2011.

21. DeLuca, A.M., *Experimental Investigation into the Aerodynamic Performance of Both Rigid and Flexible Wing Structured Micro Air Vehicles*, MS Thesis, AFIT/GAE/ENY/04-M06, Air Force Institute of Technology, Air University, Wright Patterson AFB, Ohio, March 2004.

22. DeLuca, A.M., Reeder, M.F., Freeman J., and Ol, M.V., "Flexible- and Rigid-Wing Micro Air Vehicle: Lift and Drag Comparison", *Journal of Aircraft*, Vol. 43, No. 2, 572-575, 2006.

23. Dickinson, M., "Solving the Mystery of Insect Flight", *Scientific America*, Vol. 284, No. 6, 48-57, 2001.

24. Dickson, W. B., Straw, A. D., Poelma, C., & Dickinson, M. H., "An Integrative Model of Insect Flight Control", *44th AIAA Aerospace Sciences Meeting*, AIAA-2006-34, 2006.

25. DOD Publication, *National Defense Budget Estimates for FY 2013*, Office of the Undersecretary for Defense, March 2012.

26. DOD Publication, *Unmanned Aircraft System Airspace Integration Plan*, v2.0, March 2011.

27. DOD Publication, *Unmanned Aircraft Systems Roadmap 2005-2030,* August 2005

28. DOD Publication, *Unmanned Systems Integrated Roadmap FY2011-2036, 2011*

29. Dudley, R., *The Biomechanics of Insect Flight: Form, Function, Evolution*, Princeton University Press, Princeton, New Jersey, 2000, Chaps 1-2.

30. Ellington, C.P., "The Aerodynamics of Hovering Insect Flight. I. The Quasi-Steady Analysis", *Phil. Trans. R. Soc. Lond. B*, 305, 1-15, February 1984.

31. Ellington, C.P., "The Aerodynamics of Hovering Insect Flight. II. Morphological Parameters", *Phil. Trans. R. Soc. Lond.,* 305, 17-40, February 1984.

32. Ellington, C.P., "The Aerodynamics of Hovering Insect Flight. III. Kinematics", *Phil. Trans. R. Soc. Lond. B*, 305, 41-78, February 1984.

33. Ellington, C.P., "The Aerodynamics of Hovering Insect Flight. IV. Aerodynamic Mechanisms", *Phil. Trans. R. Soc. Lond. B*, 305, 79-113, February1984.

34. Ellington, C.P., "The Aerodynamics of Hovering Insect Flight. V. A Vortex Theory", *Phil. Trans. R. Soc. Lond. B*, 305, 115-144, February1984.

35. Ellington, C.P., "The Aerodynamics of Hovering Insect Flight. VI. Lift and Power Requirements", *Phil. Trans. R. Soc. Lond. B*, 305, 145-181, February1984.

36. Ellington, C.P., "The Novel Aerodynamics of Insect Flight: Applications To Micro-Air Vehicles", *Journal of Experimental Biology, 202*, 3439-3448, 1999.

37. Eos Systems Incorporated, Company Website, http://www.photomodeler.com.

38. Feynman, R.P., "The Development of the Space-Time View of Quantum Elctrodynamics", *Nobel Lectures*, Physics 1963-1970, Elsevier Publishing Company, Amsterdam, 1972.

39. Flynn, A.M., "Gnat robots (and how they will change robotics)", *Proceedings of the IEEE MicroRobots and Teleoperators Workshop*, New York, 1987.

40. Gamble, B.J., *Experimental Analysis of Propeller Interactions with a Flexible Wing Micro-Air Vehicle*, MS Thesis, AFIT/GAE/ENY/06-M10, Air Force Institute of Technology, Air University, Wright Patterson AFB, Ohio, March 2006.

41. Gaonkar, G. H., Hohenemser, K. H., "Comparison Of Two Stochastic Models For Threshold Crossing Studies Of Rotor Blade Flapping Vibrations", *12th Structures, Structural Dynamics And Materials Conference*, AIAA-1971-389, April 1971.

42. Gaonkar, G. H.Hohenemser, K. H., "Flapping Response Of Lifting Rotor Blades To Atmospheric Turbulence", *AIAA and American Helicopter Society VTOL Research, Design, and Operations Meeting,* AIAA-1969-206, February 1969.

43. Gaonkar, G.H., "A Study Of Lifting Rotor Flapping Response Peak Distribution In Atmospheric Turbulence", *Journal of Aircraft*, Vol. 11, No. 2, 104-111, 1974.

44. Gaonkar, G.H., Hohenemser, K.H., "Flapping Response Of Lifting Rotor Blades To Atmospheric Turbulence", *Journal of Aircraft*, Vol. 6, No. 6, 496-503, 1969

45. Gaonkar, G.H., Hohenemser, K.H., Yin, S.K., "Random Gust Response Statistics For Coupled Torsion-Flapping Rotor Blade Vibrations", *Journal of Aircraft*, Vol. 9, No.10, 726-729, 1972.

46. Gogulapati, A., Friedmann, P.P., Shyy, W., "Nonlinear Aeroelastic Effects in Flapping Wing Micro Air Vehicles", *49th AIAA/ASME/ASCE/AHS/ASC Structures, Structural Dynamics, and Materials Conference,* AIAA-2008-1817, 2008.

47. Hauck, D.J., "Pandora's Box Opened Wide: UAVs Carrying Genetic Weapons", Air War College, Air University, Maxwell AFB, November 2005.

48. Heathcote, S., Wang, Z., and Gursul, I., "Effect of spanwise flexibility on flapping-wing propulsion", Journal of Fluids and Structures, Vol. 24, No. 2, 183-199, 2008.

49. Hedgcock, C., University of Arizona, Department of Neuroscience, Date unknown, permission granted February 2013.

50. Hedrick, T.L., "Software techniques for two- and three-dimensional kinematic measurements of biological and biomimetic systems", *Journal of Bioinspiration & Biomimetics*, Vol. 3, No.3, 2008.

51. Higgs, Travis J., *Modeling, Stability, and Control of a Rotatable Tail on a Micro Air Vehicle*, MS Thesis, AFIT/GAE/ENY/06-05, Air Force Institute of Technology, Air University, Wright Patterson AFB, Ohio, December 2005.

52. Hohenemser, K.H., Crews, S.T., "Unsteady Wake Effects On Progressing/ Regressing Forced Rotor Flapping Modes", *2nd AIAA Atmospheric Flight Mechanics Conference*, AIAA-1972-957, September 1972.

53. Holton, G., <u>The Advancement of Science and its Burdens</u>, Cambridge University, New York, 1986.

54. Huber, A.F., "Death by a Thousand Cuts: Micro-Air Vehicles in the Service of Air Force Missions", Air War College, Maxwell AFB, July 2002.

55. Hundley, R.O., Gritton, E.C., "Future Technology-Driven Revolutions in Military Operations," Briefing by the RAND National Defense Research Institute, December 1992.

56. Jodon Incorporated., Company Website, Accessed October 2009, http://www.jodon.com.

57. Johnson,W., "A Perturbation Solution of Helicopter Rotor Flapping Stability", *Journal of Aircraft*, Vol. 10, No. 5, 257-258, 1973.

58. Keaton, M., Aerovironment Project Manager, DAPRA Nano Air Vehicle (Hummingbird) Program, Personal Communication, May, 2011.

59. Kim, J.H., Park, C.Y., Jun, S.M., Parker, G., Yoon, K.J., Chung, D.K., "An instrumented flight test of flapping micro air vehicles using a tracking system", *18th International Conference on Composite Materials*, Korea, 2011.

60. Lehmann, F.O. & Dickinson, M. H., "The changes in power requirements and muscle efficiency during elevated force production in the fruit fly Drosophila melanogaster", *Journal of Experimental Biology*, 200, 1133-1143, 1997.

61. Liu, H. and Kawachi, K., "A Numerical Study of Insect Flight", *Journal of Computational Physics*, 146, 124–156, 1998.

62. Liu, H., Ellington, C. P., Kawachi, K., van den Berg, C., and Willmott, A.P., "A Computational Fluid Dynamic Study of Wawkmoth Hovering," *Journal of Experimental Biology*, 201, 461-477, 1998.

63. Madhani, A, "Air Force plans to pull out big (uh, little) guns", Chicago Tribune September 14, 2008.

64. Mark, R.E., Habeger, C.C., Borch, J., Lyne, M.B., <u>Handbook of Physical Testing of Paper</u>, Volume 1, Second Edition, Dekker Pubs, New York, 2002.

65. Marshall, S.A., <u>Insects, Their Natural History and Diversity</u>, Firefly Books Ltd., New York, 2006.

66. McClung, Aaron., *Influence of Structural Flexibility on Flapping-Wing Propulsion*, Dissertation, AFIT/DS/ENY/09-J01, Air Force Institute of Technology, Air University, Wright Patterson AFB, Ohio, June 2009

67. McMichael, J.M., and Francis, M.S., "Micro Air Vehicles – Toward a New Dimension in Flight", *Unmanned Systems*, Vol. 15, No. 3, pp. 8-17, 1997.

68. Meirovitch, L., <u>Fundamental of Vibrations</u>, McGraw Hill, New York, 2001.

69. Mendoza, L., *Damage Considerations of a Flexible Micro Air Vehicle Wing Using 3-D Laser Vibrometry*, MS Thesis, AFIT/GAE/ENY/07-J13 Air Force Institute of Technology, Air University, Wright Patterson AFB, Ohio, March 2007.

70. Mengesha, T.E., Vallance, R.R., Barraja, M., and Mittal, R., "Parametric Structural Modeling of Insect Wings," *Bioinspiration and Biomimetics*, v4, no. 3, 2009.

71. Michelson, I., "Flapping Propulsion Wake Analysis", *AIAA Journal,* Vol. 1, No. 11, 1963.

72. Michelson, R.C. & Reece, S., "Update on Flapping-wing Micro Air Vehicle Research", 13th *Bristol International RPV Conference*, 1998.

73. Movie Archive, The Daniel Lab, University of Washington, Accessed February 2008, http://faculty.washington.edu/danielt/movies.html.

74. Mueller, T.J., <u>Fixed and Flapping-wing Aerodynamics for Micro Air Vehicle Applications, Volume 1</u>, Progress in Astronautics and Astronautics, AIAA, Virginia, 2001.

75. National Aeronautics and Space Administration, Education Outreach Website, Accessed January, 2013, http://wright.nasa.gov/overview.htm

76. Norberg, U.M. and Rayner, J.M.V., "Ecological Morphology and Flight in Bats (Mammalia; Chiroptera): Wing Adaptations, Flight Performance, Foraging Strategy and Echolocation", *Phil. Trans. R. Soc. Lond. B*, 316, 335-427, September 1987.

77. Norris, A.G., Palazotto, A.N., Cobb, R.G., "Structural Dynamic Characterization of an Insect Wing: Toward the Development of Bug Sized Flapping Micro Air Vehicles", *51st AIAA/ASME/ASCE/AHS/ASC Structures, Structural Dynamics, and Materials Conference,* Orlando, FL, AIAA-2010-2790, April 2010.

78. O'hara, R.P., and Palazotto, A.N., "The morphological characterization of the forewing of the Manduca Sexta species for the application of biomimetic flapping wing micro air vehicles", *Bioinspiration & Biomimetics*, 7, 046011, October 2012.

79. O'hara, Ryan, *The Characterization of Material Properties and Structural Dynamics of the Manduca Sexta Forewing for Application to Flapping Wing Micro Air Vehicle Design,* Dissertation, AFIT/DS/ENY/12-06, Air Force Institute of Technology, Air University, Wright Patterson AFB, Ohio, September 2012.

80. Penn State University Libraries Website, "Conducting a Literature Review", www.libraries.psu.edu/instruction/infolit/lst301h/condlitsearchrev.htm, February 2008.

81. Pitcher, N.A., *A Static Aeroelastic Analysis of a Flexible Wing Mini Unmanned Aerial Vehicle*, MS Thesis, AFIT/GAE/ENY/08-M23, Air Force Institute of Technology, Air University, Wright Patterson AFB, Ohio, March 2008.

82. Pitcher, N.A., and R.C. Maple, "A Static Aeroelastic Analysis of a Flexible Wing Mini Unmanned Aerial Vehicle," *38th AIAA Fluid Dynamics Conference and Exhibit, Seattle, WA,* AIAA-2008-4057, June 2008.

83. Planck,M., Scientific Autobiography and Other Papers, Philosophical Library, New York, 1949.

84. Polytec Corporation, Company Website, http://www.polytec.com.

85. Polytec Corporation, Theory Manual: Polytec Scanning Vibrometer, v8.5.

86. Puster, Robert, April 2005, Creative Commons Attribution 2.0, http://en.wikipedia.org, February 2010.

87. Ramsey, Derek, July 2007, Creative Commons Attribution 2.0, http://en.wikipedia.org, February 2010.

88. Raney, D. L., & Waszak, M. R., "Biologically Inspired Micro-Flight Research", SAE Transactions, Vol. 120, 2003, pp. 598-610.

89. Raney, D., & Slominski, E., "Mechanization And Control Concepts For Biologically Inspired Micro Aerial Vehicles", *AIAA Guidance, Navigation, and Control Conference and Exhibit,* AIAA-2003-5345, 2003.

90. Shang, J.K., Combes, S.A., Finio, B.M., and Wood, R.J., "Artificial insect wings of diverse morphology for flapping-wing micro air vehicles", *Bioinspiration and Biomimetics*, 4, 1-7, 2009.

91. Sims, T.W., *A Structural Dynamic Analysis of a Manduca Sexta Forewing*, MS Thesis, AFIT/GAE/ENY/10-M22, Air Force Institute of Technology, Air University, Wright Patterson AFB, Ohio, March 2010.

92. Sims,T., Palazotto, A., Norris, A., "A Structural Dynamic Analysis of a Manduca Sexta Forewing", International Journal of Micro Air Vehicles, vol. 4, no. 3, 119-140, 2010.

93. Singer, P.W., <u>Wired for War</u>, Penguin Express, London, 2009.

94. Smithsonian, National Air and Space Museum, Government Website, January, 2013, http://airandspace.si.edu/wrightbrothers/index_full.cfm

95. Sreetharan, P., Whitney, J.P., Strauss, M., and Wood, R.J., "Monolithic fabrication of millimeter-scale machines", *Journal of Micromechanics & Microengineering*, 22, 055027, 2012.

96. Stults J. A., *Computational Aeroelastic Analysis of Micro Air Vehicle with Experimentally Determined Modes*, MS thesis, AFIT/GAE/ENY/05, Air Force Institute of Technology, Air University, Wright Patterson AFB, Ohio, March, 2005.

97. Sun, M. & Tang, J., "Lift and power requirements of hovering flight in Drosophila virilis", *Journal of Experimental Biology,* 205, 2413-2427, 2002.

98. Sunada, S., Zeng, L., and Kawachi, K., "The Relationship Between Dragonfly Wing Structure and Torsional Deformation", *Journal of Theoretical Biology*, 193, 39-45, 1998.

99. Svanberg, C. E., *Biometric Micro Air Vehicle Testing Development and Small Scale Flapping-wing Analysis*, MS Thesis, AFIT/GAE/ENY/08-M27, Air Force Institute of Technology, Air University, Wright Patterson AFB, Ohio, March 2008.

100. Tanaka, H., and Wood, R.J., "Fabrication of corrugated artificial insect wings using laser micro-machined molds", *Journal of Micromechanics and Microengineering*, 20, 7, 2010.

101. Thomas,C., Milton Contact Ltd., 2001. Permission granted February 2013.

102. Toal, Anne, June 2006, Creative Commons Attribution 2.0, http://en.wikipedia.org, February 2010.

103. Tobias, A.P., *Experimental Methods to Characterize Nonlinear Vibration of Flapping-Wing Micro Air Vehicles*, MS Thesis, AFIT/GAE/ENY/07-M23, Air Force Institute of Technology, Air University, Wright Patterson AFB, Ohio, March 2007.

104. Tubbs, T.B., *Biological Investigation of the Stimulated Flapping Motions of the Moth, Manduca Sexta*, AFIT/GSS/ENY/11-M04, Air Force Institute of Technology, Air University, Wright Patterson AFB, Ohio, March 2011.

105. University of Cambridge, Department of Engineering, Materials Group Website, http://www-materials.eng.cam.ac.uk/mpsite/interactive_charts/default.html, June 2009.

106. Vibrant Technology, Company Website, http://www.vibetech.com.

107. Wakeling, J. M. & Ellington, C. P., "Dragonfly Flight. III. Lift and Power Requirements", *Journal of Experimental Biology,* 200, 583-600, 1997.

108.   Walker, R.L., *Finite Element Solution: Nonlinear Flapping Beams for Use with Micro Air Vehicle Applications*, MS Thesis, AFIT/GAE/ENY/07-M26, Air Force Institute of Technology, Air University, Wright Patterson AFB, Ohio, March 2008.

109.   Wan, F. Y. M., "Effect Of Spanwise Load-Correlation On Rotor Blade Flapping", *15th ASME, and SAE, Structures, Structural Dynamics and Materials Conference*, AIAA-1974-418, April, 1974.

110.   Wilkin, P. J. & Williams, M. H., "Comparison of the Aerodynamic Forces on a Flying Sphingid Moth with Those Predicted by Quasi-Steady Theory", *Physiological. Zoology*, 66, 1015-1044, 1993.

111.   Willis, M., Personal Communications, July, 2009.

112.   Willmott, A. P. and Ellington, C. P., "The mechanics of flight in the hawkmoth Manduca Sexta I. Kinematics of hovering and forward flight", *Journal of Experimental Biology*, 200, 2705-2722, 1997.

113.   Willmott, A. P. and Ellington, C. P., "The mechanics of flight in the hawkmoth Manduca Sexta II. Aerodynamic consequences of kinematic and morphological variation", *Journal of Experimental Biology*, Vol. 200, 2723-2745, 1997.

114.   Wooton, R.J., "Functional Morphology of Insect Wings", *Annual Review of Entomology*, 37, 113-140, 1992.

115.   Zanker, J. M. & Gotz, K. G., "The Wing Beat of Drosophila Melanogaster. II. Dynamics", *Phil. Trans. R. Soc. Lond. B*, 327, 19-44, 1990.

116.   Zeng, L., Matsumoto, H., Sunada, S., Ohnuki, T., Kawachi, K., "Two-dimensional, non-contact measurement of the natural frequencies of dragonfly wings using quadrant position sensor", *Optical Engineering*, Vol. 34, Issue 4, 1226-1231, April 1995.

Vita

Lieutenant Colonel Norris is a graduate of Cal Poly where he earned his BS and MS degrees in Aerospace Engineering in 1994 and 1997 respectively. He commissioned as a Distinguished Graduate from AFROTC, Cal State San Bernardino, in 1997. Throughout his career he has served in a variety of technical roles.

During his first tour at the AFRL he served as an Aerospace Engineer studying flow field distortion associated with flush and serpentine inlet technologies as well as the hammer shock phenomena associated with supersonic jet aircraft engine stall. He worked alongside Boeing's Phantom Works to perform CFD on the X-45 UCAV and then served as a test engineer for wind tunnel weapons separations testing at AEDC. His experience with UCAV propelled him to Deputy the AFRL's UCAV Office where he was responsible for building technology transition plans and laying the foundation to transition the program to what would eventually become J-UCAS.

Following his lab time, he led the Delta IV Propulsion Team for the EELV SPO at Los Angeles AFB. He and his team completed final developmental testing and enabled first operations of the RS-68 mainstage rocket engine, the United States' first LOX-Hydrogen engine since SSME developed nearly 30 years earlier. In 2003 his team was named the JANNAF Propulsion Team of the Year and he was recognized as the Air Force's Outstanding Junior Engineer of the Year. He was subsequently promoted to Chief Engineer for the Delta IV "Heavy Demo" mission where he oversaw launch assurance activities and served as the "on-console" Chief Systems Engineer for day-of-launch operations. Following mission success of the first 3-body liquid rocket in American history, he was appointed as Delta IV's first Chief, Systems Engineering Branch in 2006.

After completion of doctoral studies at AFIT (Oct 06 - Oct 09), Lieutenant Colonel Norris was assigned to the AFRL's Munitions Directorate at Eglin AFB where he served for a year as Deputy, Strategic Planning and Assessments Division overseeing execution of two JUONs. He was later selected by the AFRL/CC to serve as Chief Engineer for the AFRL MAV Program where he led an IPT to develop a plan to build and test an operational-ready MAV platform by 2015. Despite the success of developing an executable plan enthusiastically endorsed by the AFRL/CC, the program was cancelled due to budget constraints. Lieutenant Colonel Norris is currently serving in the Munitions Directorate as Deputy, Weapons Engagement Division where he leads nearly 200 civilian and contractor employees and over 30 military to develop weapons technologies that will enable the Air Force's 5th and 6th generation aircraft

REPORT DOCUMENTATION PAGE			*Form Approved* *OMB No. 0704–0188*
The public reporting burden for this collection of information is estimated to average 1 hour per response, including the time for reviewing instructions, searching existing data sources, gathering and maintaining the data needed, and completing and reviewing the collection of information. Send comments regarding this burden estimate or any other aspect of this collection of information, including suggestions for reducing this burden to Department of Defense, Washington Headquarters Services, Directorate for Information Operations and Reports (0704–0188), 1215 Jefferson Davis Highway, Suite 1204, Arlington, VA 22202–4302. Respondents should be aware that notwithstanding any other provision of law, no person shall be subject to any penalty for failing to comply with a collection of information if it does not display a currently valid OMB control number. PLEASE DO NOT RETURN YOUR FORM TO THE ABOVE ADDRESS.			

1. REPORT DATE (DD–MM–YYYY) 21-03-2013	2. REPORT TYPE Doctoral Dissertation	3. DATES COVERED *(From — To)* Dec 2008 – Feb 2013	

4. TITLE AND SUBTITLE Experimental Characterization of the Structural Dynamics and Aero-Structural Sensitivity of a Hawkmoth Wing Toward the Development of Design Rules for Flapping-Wing Micro Air Vehicles	5a. CONTRACT NUMBER
	5b. GRANT NUMBER
	5c. PROGRAM ELEMENT NUMBER
6. AUTHOR(S) Norris, Aaron, G., Lieutenant Colonel, USAF	5d. PROJECT NUMBER 09-719
	5e. TASK NUMBER
	5f. WORK UNIT NUMBER

7. PERFORMING ORGANIZATION NAME(S) AND ADDRESS(ES) Air Force Institute of Technology Graduate School of Engineering and Management (AFIT/ENY) 2950 Hobson Way WPAFB OH 45433-7765	8. PERFORMING ORGANIZATION REPORT NUMBER AFIT-ENY-DS-13-M-40
9. SPONSORING / MONITORING AGENCY NAME(S) AND ADDRESS(ES) Dr. Douglas Smith Air Force Office of Scientific Research 875 N. Randolph Street Arlington, VA, 22203 DSN: 426-6202	10. SPONSOR/MONITOR'S ACRONYM(S) AFRL/AFOSR
	11. SPONSOR/MONITOR'S REPORT NUMBER(S)

12. DISTRIBUTION / AVAILABILITY STATEMENT   APPROVED FOR PUBLIC RELEASE; DISTRIBUTION UNLIMITED

13. SUPPLEMENTARY NOTES   This material is declared a work of the U.S. Government and is not subject to copyright protection in the United States.

14. ABSTRACT

A case is made for why the structures discipline must take on a more central role in the research and design of flapping-wing micro-air-vehicles, especially if research trends continue toward bio-inspired, insect-sized flexible wing designs. In making the case, the eigenstructure of the wing emerges as a key structural metric for consideration. But with virtually no structural dynamic data available for actual insect wings, both engineered and computational wing models that have been inspired by biological analogs have no structural truth models to which they can be anchored. An experimental framework is therefore developed herein for performing system identification testing on the wings of insects. This framework is then utilized to characterize the structural dynamics of the forewing of a large sample of hawkmoth (Manduca Sexta) for future design and research consideration. The research also weighs-in on a decade-long debate as to the relative contributions that the inertial and fluid dynamic forces acting on a flapping insect wing have on its deformation (expression) during flight. Ultimately the findings proves that both affect wing expression significantly, casting serious doubt on the long-standing and most frequently cited research that indicates fluid dynamic forces have minimal or negligible effect.

15. SUBJECT TERMS   Micro Air Vehicles; MAV; Bio-inspired; Flapping-Wing; Structural Dynamics; Inertial-elastic

16. SECURITY CLASSIFICATION OF: U			17. LIMITATION OF ABSTRACT	18. NUMBER OF PAGES	19a. NAME OF RESPONSIBLE PERSON Dr. Anthony N. Palazotto, AFIT/ENY
a. REPORT U	b. ABSTRACT U	c. THIS PAGE U	UU	227	19b. TELEPHONE NUMBER (Include Area Code) (937)255-3636, ext 4599

Standard Form 298 (Rev. 8–98)
Prescribed by ANSI Std. Z39.18